THE UNIVERSITY
of EDINBURGH

Amyloid-β and chronic cerebral hypoperfusion in the early pathogenesis of Alzheimer's disease

Natalia Salvadores Bersezio

Doctor of Philosophy

University of Edinburgh

2015

Declaration

I declare that this thesis comprises my own work and has not been submitted previously for any degree. The work comprising this thesis was carried out by myself, except where acknowledged in the text. All sources of data and information have been referenced.

Natalia Salvadores Bersezio

Abstract

Alzheimer's disease (AD) is a severe age-related neurodegenerative disorder and is the most common form of dementia. Although the pathogenesis of AD remains unknown, the deterioration of the cerebrovascular system constitutes a risk factor associated with the development of the disease. Notably, brain hypoperfusion, a feature of healthy ageing brain and AD, occurs prior to the onset of cognitive decline in AD and correlates with the severity of dementia. Although there is a clear link between hypoperfusion and cognitive alterations in AD, a causal relationship remains to be established. It was hypothesised that chronic cerebral hypoperfusion leads to the accumulation of parenchymal and vascular amyloid-β (Aβ), triggering the development of vascular lesion (microinfarcts (MIs) and haemorrhages) and altering the neurovascular unit (NVU) integrity. Second to this, it was hypothesised that reductions in Aβ levels by immunotherapy targeted to amyloid in young mice, reduce amyloid levels, and prevent vascular lesions improving cognitive performance. Three studies were conducted to test these hypotheses.

In the first study, the aim was to characterise age-dependent changes in amyloid-related pathology in a transgenic mouse model (Tg-SwDI). The temporal amyloid precursor protein (APP) expression, accumulation of parenchymal and cerebrovascular Aβ and Aβ-related microglial and astrocytic activation in the cortex, hippocampus and thalamus of the Tg-SwDI mice at 3, 6 and 9 months of age was compared to wild-type controls. Significantly higher APP expression ($p < 0.05$), as well as Aβ aggregation ($p < 0.001$) as the animals aged was found in the Tg-SwDI mice in all the brain regions analysed, which was accompanied by extensive and progressive activation of microglial ($p < 0.001$) and astrocytic ($p < 0.01$) cells. These data provided a basis to design the next studies, as it was planned to induce hypoperfusion in these mice before significant Aβ deposition occurs.

In the second study, the aim was to investigate the effect of hypoperfusion on Aβ dynamics and subsequently, to study the contribution of hypoperfusion and Aβ pathology to the development of MIs and haemorrhages, and to the potential

alteration of astrocyte and tight junction (TJ) integrity. To address this, mild chronic cerebral hypoperfusion was induced in Tg-SwDI and wild-type mice by bilateral common carotid stenosis for 1 and 3 months. A significant increase in soluble Aβ40/42 levels was initially found after 1 month of hypoperfusion in the parenchyma (Aβ40, $p = 0.0239$; Aβ42 $p = 0.0198$) in parallel with elevated APP levels and APP proteolytic cleavage products ($p < 0.05$). Thereafter, following 3 months, a significant increase in insoluble Aβ40/42 levels was determined in the parenchyma (Aβ40, $p = 0.0024$; Aβ42 $p = 0.008$) and vasculature (Aβ40, $p = 0.0046$; Aβ42 $p = 0.0118$) of Tg-SwDI mice. There was no change in the levels of Aβ co-localised to vessels following 1 month of hypoperfusion; however Aβ levels were significantly increased in cerebral vessels after 3 months ($p = 0.0483$). The proportion of Aβ containing vessels was significantly higher in the small vessels of the hypoperfused animals compared to sham mice ($p < 0.05$). MIs associated with microglial proliferation were present in the Tg-SwDI mice and the burden was exacerbated by hypoperfusion at 1 and 3 months ($p < 0.05$). Significantly higher levels of NADPH Oxidase-2 (NOX2) were found in the transgenic mice compared to the wild-type controls at both time-points analysed ($p < 0.05$), and this was exacerbated after 1 month of hypoperfusion in the Tg-SwDI mice ($p < 0.05$). There was a positive correlation between NOX2 and soluble parenchymal Aβ levels ($r = 0.6643$, $p = 0.0019$). A minimal effect on the development of haemorrhages at these time-points was observed. In parallel to this, astrocyte activation was significantly higher in the Tg-SwDI mice compared to the wild-type controls at both time-points studied ($p < 0.05$); however, no effect of hypoperfusion was observed. Also, significantly higher levels of aquaporin-4 (AQP4) in the Tg-SwDI mice compared to the wild-type controls following 1 month of hypoperfusion were found ($p < 0.001$). There was a positive correlation between AQP4 and soluble parenchymal Aβ levels ($r = 0.4735$, $p = 0.0095$). Claudin-5 levels were significantly higher in the Tg-SwDI mice compared to the wild-type controls at both time-points analysed ($p < 0.0001$), and this was exacerbated following 1 month of hypoperfusion in the transgenic model ($p < 0.05$). A positive correlation between claudin-5 and vascular Aβ levels was observed ($r = 0.6113$, $p = 0.0004$). Together, these data suggest a synergistic contribution of

amyloid and hypoperfusion pathologies to the tissue damage and implicate a role of oxidative stress and inflammation.

In the third study, the aim was to determine the effects of passive amyloid immunisation on Aβ levels, development of MIs and haemorrhages and behavioural performance in the Tg-SwDI mice. To address this, the mice underwent weekly intraperitoneal injections with either 3D6 or 10D5 antibodies during 3 months. Although there were no significant changes between control and 10D5/3D6 treated mice in amyloid levels, appearance of MIs and cognitive performance, it was noted that there was a trend towards a reduction in amyloid levels and MI area in the 10D5/3D6 treated mice compared to the control animals. Furthermore, there was no evidence of microhaemorrhages in response to the immunisation. These results demonstrate that Aβ immunotherapy with the antibodies 3D6 and 10D5 may potentially decrease parenchymal and vascular amyloid accumulation, reducing the appearance of MIs and notably without triggering the development of microhaemorrhages.

Collectively, the findings presented in the current thesis demonstrate that chronic cerebral hypoperfusion increases parenchymal and vascular Aβ levels and point towards a mechanism in which the cascade of events including inflammation and oxidative stress, triggered synergistically by hypoperfusion and Aβ, resulted in the widespread development of MIs and NVU changes which may further induce the alteration of cognition networks. A mixed therapy, aimed at improving cerebrovascular health and targeting the accumulation of Aβ, represents a promising strategy to prevent neurodegenerative processes and further cognitive decline in AD.

Acknowledgements

Firstly, I would like to express my gratitude to my supervisor Prof. Karen Horsburgh for giving me the opportunity to work in her lab and guiding me throughout these past 3 years.

I would also like to thank all those past and present members of the lab including Fiona Scott for her technical support and kindness, Phil Holland and Luke Searcy for their help and advice and Jess Duncombe for creating a nice environment in the lab. A special mention goes to my friend Yasmina Manso for her amazing support and encouragement, all those useful and entertaining conversations, and most importantly for all that jamón that she brought me from Spain.

My deepest gratitude goes to my family for giving me their unconditional love and support always. A special thanks to my beloved daughter Matilda, for accompanying me and keeping me awake with her little kicks while I was writing up this thesis. A big thank you to my mom for travelling, braving the cold and taking care of Matilda so I could finish writing up.

No words can express the gratitude I have for my husband Mario for being by my side and giving me all his love, care, understanding and support not only during our time doing the PhD, but during our whole journey.

Finally, I would like to thank AXA research fund, the Scottish Overseas Research students Award Scheme, the Charles Darwin Postgraduate Research Scholarship and the Chilean National Commission for Scientific and Technological Research (CONICYT) for funding the scholarships that allowed me to do this PhD.

Table of Contents

List of Figures

List of Tables

List of Abbreviations

Aβ	Amyloid-β
AD	Alzheimer's disease
ANOVA	Analysis of variance
APP	Amyloid precursor protein
apoE4	ε4 allele of the apolipoprotein E gene
AQP4	Aquaporin-4
ARIA	Amyloid related imaging abnormalities
BACE	β-secretase
BBB	Blood brain barrier
BCAS	Bilateral common carotid arteries stenosis
BCCAO	Bilateral common carotid arteries occlusion
CAA	Cerebral amyloid angiopathy
CBF	Cerebral blood flow
CNS	Central nervous system
CTF	Carboxyl terminal fragments
ELISA	Enzyme-linked immunosorbent assay
GFAP	Glial fibrillary acidic protein
H&E	Haematoxylin and eosin
HIF1	Hypoxia inducible factor 1
KDa	Kilodalton
LRP-1	Lipoprotein receptor-related protein 1
MCAO	Occlusion of the middle cerebral artery
MI	Microinfarct
NOX2	NADPH Oxidase-2
NFTs	Neurofibrillary tangles
NVU	Neurovascular unit
OEF	Oxygen extraction factor
PB	Phosphate buffer
PBS	Phosphate buffered saline
PFA	Paraformaldehyde

PS	Presenilin
PVDF	Polyvinylidene fluoride
RCT	Randomised controlled trial
ROS	Reactive oxygen species
RT	Room temperature
Scara1	Scavenger receptor A
SMA	Smooth muscle actin
TB	Tris buffer
TJ	Tight junction
VaD	Vascular dementia
VRF	Vascular risk factor

Chapter 1. Introduction.

1.1 Alzheimer's disease.

1.1.1. Overview.

Alzheimer's disease (AD) is a devastating progressive neurodegenerative disorder and constitutes the most frequent form of dementia accounting for 60-80% of all cases (Alzheimer's Association, 2014). With an increasing prevalence, AD, first described in 1906 by the German psychiatrist Alois Alzheimer (Alzheimer, 1907; Devi and Quitschke, 1999), represents the most important neurodegenerative disease in the elderly population. It is estimated that 5.2 million Americans were affected by the disease in 2014, of which > 96% are above age 65. In the UK, 505,813 persons were affected by the disease in 2014. A number of prevalent cases of more than 35 million across the world is currently estimated and it is predicted that this number will triple by 2050 (Wimo and Prince, 2010; Huang and Mucke, 2012, Alzheimer's Association, 2014). AD constitutes a major emotional and financial burden to carers and society as patients require constant and extensive care. Thus, considering the worldwide population ageing, this disease has become an enormous challenge to public health.

Clinically, AD is generally characterised by a progressive memory loss, with episodic memory impairment being the most relevant, constituting one of the earliest signs of the disease (Gold and Budson, 2008). The memory alterations are followed by the deterioration of other cognitive functions; in more advanced stages of the disease, behavioural changes such as depression and language difficulties are noticeable (Weintraub et al., 2012). Currently, there is a lack of a sensitive, early diagnosis to identify the patients before they display the clinical symptoms and the disease can only be confirmed by examination of *post-mortem* brains (Urbanelli et al., 2009).

1.1.2. Neuropathology.

The neuropathological hallmarks of the disease include the accumulation of two types of misfolded proteins: intraneuronal deposits of hyperphosphorylated micro-tubule-associated tau protein called neurofibrillary tangles (NFTs) and amyloid-β (Aβ) aggregates in brain parenchyma and in the blood vessel walls (Terry, 1994; Trojanowski and Lee, 2000). The distribution of NFTs follows a typical pattern of lesions, being accumulated early in the entorhinal cortex, followed by hippocampal accumulation and then association cortex. This consistent temporal distribution constitutes the basis of the Braak and Braak staging system for AD diagnosis (Braak and Braak, 1991). Although NFT accumulation is highly associated with neuronal and synapse loss, the causative role of these aggregates in neuronal cell death remains ill understood (Serrano-Pozzo et al., 2011). Nevertheless, a high correlation has been found between the degree of NFTs and the severity of dementia in AD (Arriagada et al., 1992; Bierer et al., 1995). Different degrees of Aβ aggregation may lead to a variety of Aβ structures in the AD brain and two types of assemblies are most commonly observed: diffuse plaques, which are also a common feature of the normal ageing brain with no evidence of associated cognitive alterations (Morris et al., 1996), and the dense-core plaques which are formed by a central mass of fibrillar Aβ with radial filaments that are surrounded by degenerating neurites and are associated with microglial and astrocyte activation (Serrano-Pozzo et al., 2011). In contrast to the NFTs, the temporal distribution pattern of Aβ plaques is less consistent, however they are mostly observed in the isocortex. Although the evidence has failed to demonstrate a correlation between plaque extent and cognitive alterations in AD (Arriagada et al., 1992; Giannakopoulos et al., 2003), more recent studies have attributed these alterations to different Aβ structures rather than amyloid plaques (see section 1.1.5). Although vascular amyloid accumulation can be found in the normal ageing brain, it is highly prevalent in the AD brain and constitutes another pathological feature of the disease (see section 1.1.7).

Atrophy of the brain as the result of neuronal cell death and widespread synaptic loss also represents a typical observation in AD. The regional distribution of cerebral

atrophy can be determined *in vivo* by using imaging approaches such as magnetic resonance imaging (MRI) or by *post-mortem* histological analysis. Differential topographic patterns of atrophy are associated with different diseases and extensive involvement of the temporal lobe, predominantly in the hippocampus and entorhinal cortex, have been observed in the early stages of AD (Braak and Braak, 1991). Indeed, high resolution MRI has been shown to be useful to study the progression of the disease and predict further cognitive decline in AD (de Leon et al., 1993; Rusinek et al., 2003; Desikan et al., 2009).

1.1.3. Amyloid-β metabolism.

Aβ peptide is derived from the proteolytic cleavage of the amyloid precursor protein (APP). APP is a single transmembrane protein with three major isoforms generated from alternative splicing and defined by the number of amino-acids they contain (695, 751 and 770) (Chasseigneaux and Allinquant, 2012). APP is ubiquitous, however APP695 is highly expressed in neuronal cells and low expression of this isoform is found in other type of cells (Haass et al., 1991). The biological function of this protein remains unclear, however *in vitro* and *in vivo* studies have demonstrated that APP and the soluble fragments released during its processing including Aβ, are implicated in several processes including the development of the nervous system, gene regulation, cell adhesion, synaptic plasticity, axonal transport and synaptogenesis (Gralle and Ferreira, 2007; Chasseigneaux and Allinquant, 2012).

APP can be metabolised by two different pathways, undergoing different proteolytic cleavages in each of them. Cleavage by α-secretase produces the soluble APP α (sAPPα) and an 83 amino acid long C-terminal fragment. In the alternative or amyloidogenic pathway, sequential cleavage of APP by β and γ-secretases generates the soluble APP β (sAPPβ), the APP intracellular domain (AISD) and the full length, 4kDa Aβ protein (Figure 1.1) (Hartmann et al., 1997). γ-secretase can cut at various sites within the APP, leading to the formation of Aβ peptides fluctuating from 38 to 43 amino-acids, although the most common forms are Aβ40 and Aβ42, which under normal physiological conditions are found in an Aβ42:Aβ40 ratio of ~1:9 in the brain (Pauwels et al., 2012).

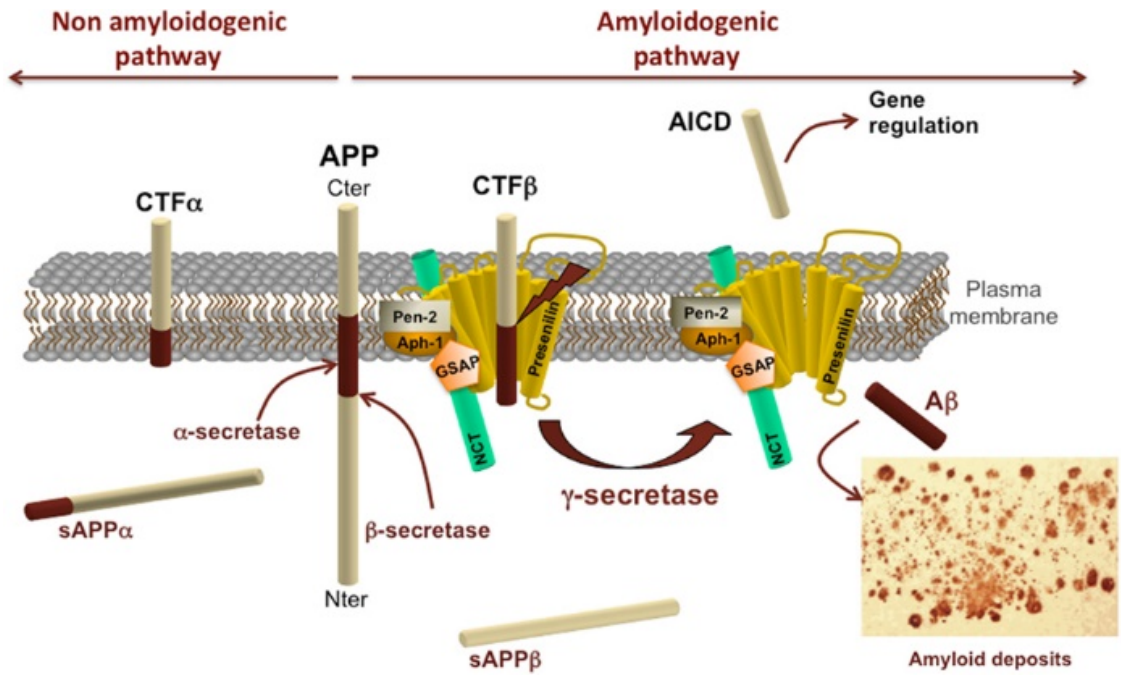

Figure 1.1. Schematic representation of APP processing. APP is cleaved via two alternative pathways. In the non-amyloidogenic pathway, cleavage by α secretase releases the sAPPα. In the amyloidogenic pathway cleavage by β and γ secretases releases Aβ (image taken from Vingtdeux et al., 2012).

Increases in total Aβ levels or changes in the Aβ42:Aβ40 ratio are associated with the pathogenesis of AD (Pauwels et al., 2012). *In vitro* studies have shown that Aβ is able to spontaneously bind to another monomer to rapidly form aggregates, hence in AD brains, as well as in cerebrospinal fluid from AD patients, it is possible to find a range of Aβ species including monomers, oligomers, proto-fibrils and fibrils. Aβ42, which is more susceptible to self-aggregation into fibrils and more cytotoxic, is the main peptide found in extracellular deposits in the brain whilst Aβ40 is mostly found in vascular aggregates (Jarrett et al., 1993; Younkin, 1995; Dahlgren et al., 2002).

In healthy brains, Aβ is effectively metabolised with little accumulation and the maintenance of normal brain levels of Aβ depends on the correct balance between its production and elimination. There are several pathways through which Aβ is cleared from the brain. These include cellular uptake through different receptors such as the microglial scavenger receptor A-1 (scara1) and degradation (Li et al., 2012), clearance along the interstitial fluid drainage pathway (Weller et al., 2008), lipoprotein receptor-related protein (LRP) and receptor for advanced glycation endproducts (RAGE) mediated flux across the blood brain barrier (BBB) (Zlokovic, 2004), and through proteolytic degradation by Aβ-degrading enzymes (Iwata et al., 2001; Farris et al., 2003) (Figure 1.2).

1.1.4. Risk factors.

There are two different forms of the disease. The early onset (< 65 years) autosomal-dominant familial Alzheimer's (FAD) is rare and represents less than 5% of the cases. This form of the disease is caused by mutations in the APP gene, or mutations in the presenilin 1 (PS1) 1 or presenilin 2 (PS2) (which are the catalytic subunits of the γ-secretase) genes, leading to altered Aβ metabolism and increased deposition of the protein, representing the major known genetic risk factor for AD (Goate et al., 1991; Citron et al., 1992; Hendriks et al., 1992; Mullan et al., 1992; Suzuki et al., 1994a; Harvey et al., 2003).

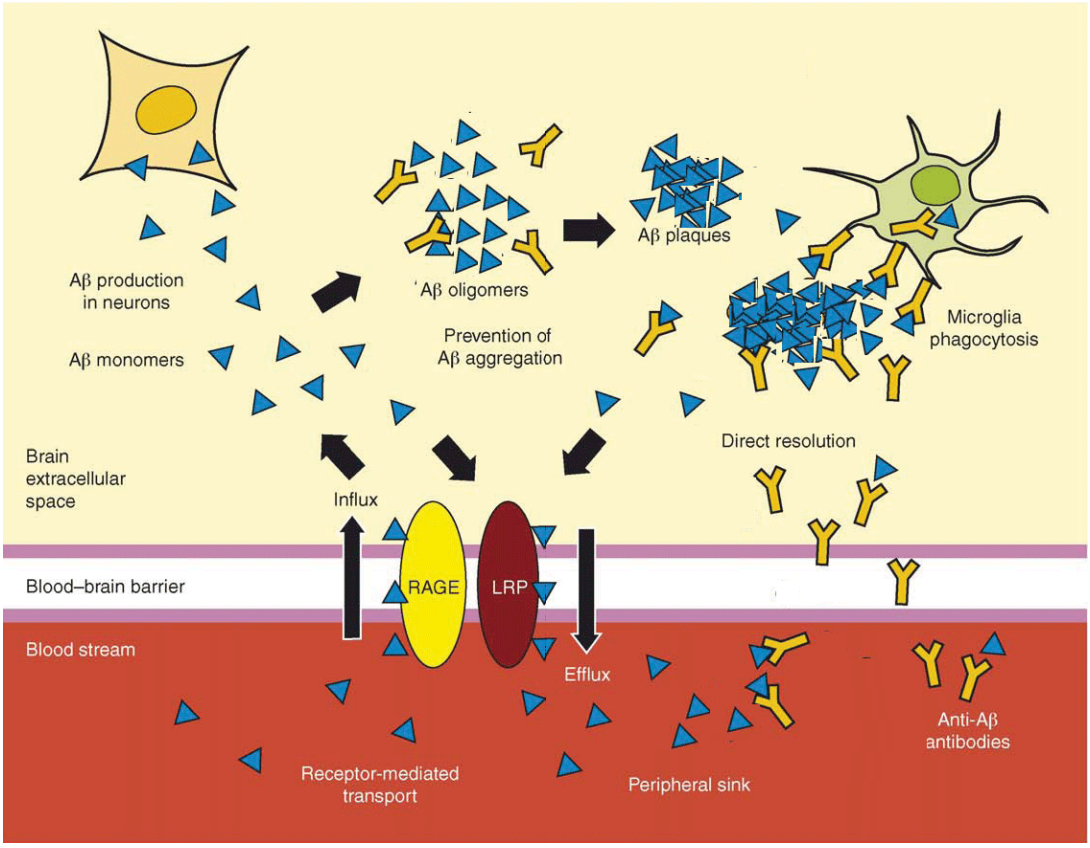

Figure 1.2. Mechanisms of Aβ clearance. The maintenance of normal brain levels of Aβ depends on the correct balance between its production and elimination. The different clearance pathways by which Aβ is eliminated from the brain are illustrated in the figure, which shows Aβ clearance following amyloid immunotherapy (image taken from Wang et al., 2006).

The most common form of the disease is the sporadic late onset (>65 years) AD, the cause of which remains unknown, probably due to the multifactorial nature of the disease; however it has been related to several risk factors. Ageing is the most important known risk factor for sporadic AD and notably, the risk doubles every 5 years after the age of 65 years (Qiu et al., 2009). The major genetic risk factor recognised to be associated with the late onset AD is the presence of the ε4 allele of the apolipoprotein E gene (apoE4), which increases the risk by three times in heterozygotes and by 15 times in homozygotes (Farrer et al., 1997). It is estimated that 40-60% of people affected with the disease display at least one copy of the ε4 allele (Hauser and Ryan, 2013). Although the underlying mechanism behind this higher susceptibility remains currently unclear, immunohistochemistry studies have shown that brains from patients expressing apoE4 protein present enhanced amounts of Aβ aggregates compared to patients lacking the protein, particularly Aβ40 deposits in brain parenchyma and microvessels (Rebeck et al., 1993; Schmechel et al., 1993; Greenberg et al., 1995; Gearing et al., 1996) suggesting that the presence of the apoE4 genotype might be associated with increased Aβ deposition or altered clearance of the protein.

More recent studies have revealed an association between mutations in the triggering receptor expressed on myeloid cells 2 (TREM2) and a significant increase in the risk of AD, with an odds ratio (OR) > 3 (Guerreiro et al., 2013; Jonsson et al., 2013). TREM2 is involved in microglial signalling and plays an important role in phagocytosis activation as well as suppressing cytokine production and inflammation (Takahashi et al., 2005). Although the percentage of the population affected by these mutations is unknown, it has been reported that a single mutation in the gene that encodes this receptor predisposes to AD, which strongly supports a role for inflammation in AD. Mutations in TREM2 may possibly not be directly related with the onset of AD; however it might enhance the susceptibility to the disease progression by triggering alterations in microglial function. Interestingly, a study performed in aged APP23 transgenic mice showed upregulation of TREM2 in amyloid plaque-associated microglia compared to plaque-free tissue, which provides evidence of the involvement of this receptor in microglia-Aβ interaction.

Furthermore, there is a positive correlation between TREM2 expression and Aβ phagocytosis (Frank et al., 2008; Melchior et al., 2010). Thus, mutations in this receptor may lead to altered Aβ uptake by microglia. In the other hand, given the anti-inflammatory function of TREM2, mutations in this protein may also contribute to the progression of AD pathology by promoting neuroinflammation.

Although TREM2 has been the only gene found to be linked with increased risk of AD following the associations between the ε4 allele of the apoE gene and the disease, enormous efforts have been made to find further genetic association. Thus, the International Genomics of Alzheimer's Project has been created and large genetic screens are ongoing (Guerreiro and Hardy, 2014). The most relevant susceptibility loci identified by genome-wide association studies include the bridging integrator 1, phosphatidylinositol binding clathrin assembly protein, clusterin and complement component receptor 1, among others (Lambert et al., 2013). Environmental factors including head injury, diabetes, low educational level and vascular risk factors (VRFs) have also been suggested to play a role in the development of the disease (Rosendorff et al., 2007; Van Den Heuvel et al., 2007; Sharp and Gatz, 2011; Milone, 2012). However although several risk factors have been associated with the pathophysiology of sporadic AD, the exact cause of the disease remains unrevealed probably due to the heterogeneous nature of the disease where ageing in concert with susceptibility genes and environmental factors combine in complex interactions that lead to the development and progression of the disease.

1.1.5. Amyloid hypothesis of Alzheimer's disease.

Aβ peptide was first isolated and characterised from human leptomeningeal arteries 3 decades ago (Glenner and Wong, 1984). Following this discovery, the protein was identified as the main component of senile plaques in brain tissue from AD patients and aged individuals with Down's syndrome (DS) (Masters et al., 1985). Subsequently, it was demonstrated that Aβ is generated from the proteolytic cleavage of APP and the APP gene was first cloned and mapped to a locus on chromosome 21 (Kang et al., 1987). DS patients, who carry an extra copy of this chromosome,

manifest early onset dementia and exhibit neuropathological features of AD (Millan Sanchez et al., 2012). Similar to what occurs in patients affected by mutations in APP, PS 1 or PS 2, trisomy of chromosome 21 leads to altered Aβ metabolism and an increased Aβ42:Aβ40 ratio (Teller et al., 1996). Furthermore, there is evidence showing an association between mutations in the PS gene and increased DS offspring, which has been suggested to be related with chromosome missegregation due to mitosis alterations (Geller and Potter, 1999; Lucarelli et al., 2004).

Later, the identification of the mutations in the APP gene causing a familial form of the disease (Levi et al., 1990; Van Broeckhoven et al., 1990; Fernandez-Madrid et al., 1991; Goate et al., 1991; Naruse et al., 1991; Hendriks et al., 1992; Mullan et al., 1992), led to the amyloid cascade hypothesis of AD. This was first proposed in 1991 (Hardy and Allsop, 1991) and states that Aβ peptide is the central player in AD pathogenesis and that aggregation and deposition of this protein in brain directly induce synaptic injury in addition to inflammation and oxidative damage leading to widespread cell death and finally dementia. According to this hypothesis, all other neuropathological hallmarks of the disease such as NFTs are the consequence of Aβ deposition, which is the result of an imbalance between Aβ production and clearance (Selkoe, 1991; Hardy and Higgins, 1992).

Although the amyloid cascade hypothesis has been the focus of AD research since it was first proposed in the early 1990s and has proven useful to understand the progression and pathogenesis of the disease, there are concerns regarding some aspects of this hypothesis. One of the criticisms is that many transgenic mouse models showing substantial Aβ accumulation and neuropil abnormalities do not have extensive neuronal loss (Irizarry et al., 1997). Moreover, transgenic mice that undergo Aβ accumulation have shown cognitive alterations before Aβ deposition in the brain (Hsiao et al., 1996). Similarly, spatial learning deficits occur independently of plaques in Aβ overexpressing mice (Koistinaho et al., 2001). Finally, the main objection of the hypothesis is the lack of a strong correlation between the degree of dementia and the burden of Aβ deposits in the brain of AD patients (Terry et al., 1991).

However, these studies are based on immunohistochemical analyses where smaller, oligomeric Aβ species are undetected and importantly, biochemical studies have revealed a good correlation between the load of these soluble species and the degree of neurodegeneration (Lue et al., 1999; McLean et al., 1999). Indeed, recent findings support the oligomer hypothesis of AD, which states that soluble Aβ oligomers are the main etiologic agent that participates in the initiation of the neurodegenerative process in AD, by triggering a cascade of pathogenic events involving inflammation and oxidative injury (Klein et al., 2004; Glabe and Kayed, 2006; Haass and Selkoe, 2007).

Over the years since the amyloid cascade hypothesis was first proposed it has been refined to incorporate an increasing awareness of the mechanisms by which Aβ leads to the development of the disease. The amyloid hypothesis has also been updated to include vascular dysfunction which was incorporated as an additional component to further explain the pathophysiology of AD (Hardy, 2009). The rationale behind this will be explained further in the next section.

1.1.6. Vascular hypothesis of Alzheimer's disease.

Although the pathogenesis of AD remains unknown, VRFs including ageing, hypertension, diabetes, stroke, atherosclerosis and heart failure, lead to the deterioration of the cerebrovascular system, which constitutes a risk factor associated with the development of the disease (Breteler, 2000; Kalaria and Ince, 2000; De la Torre, 2002; de Leeuw et al., 2006; van Norden et al., 2012; Muresanu et al., 2014). Indeed, cerebrovascular pathology can be found in almost all cases of AD examined *post-mortem*. These lesions include cerebral amyloid angiopathy (CAA) (see section 1.1.7), haemorrhage, endothelial and vascular smooth muscle deterioration, infarction, and white matter (WM) alterations related to small vessel disease (Vinters, 1987; Kalaria, 1996). BBB damage due to microvascular alterations is also present in AD brains. These alterations include reduced endothelial mitochondrial content, increased vessel diameter, disruption of the basement membranes, reduced total microvascular density, pericyte degeneration and astrocyte end-feet swelling

(Zlokovic, 2008). All the pathologies above mentioned may disrupt the integrity of the cerebral blood vessels leading to reduced brain perfusion (Attems and Jellinger, 2014). Furthermore, reduced cerebral blood flow (CBF), a feature of healthy ageing brain and AD, occurs prior to the onset of cognitive decline in AD (Alsop et al., 2010; Chao et al., 2010) and correlates with the severity of dementia (Johnson et al., 1998; Huang et al., 2002; Yoon et al., 2012) (see section 1.2).

Vascular dementia (VaD), also called vascular cognitive impairment (VCI), represents the second most common cause of dementia in the elderly after AD. It is thought to be caused by cerebrovascular alterations that lead to reduced CBF, which can contribute to cognitive decline by altering neuronal networks related to memory, cognition and behaviour (Jellinger, 2007). Several VRFs have been related to the development and progression of the disease (Battistin and Cagnin, 2010).

Importantly, neuropathological studies have demonstrated that a considerable proportion of patients who meet the clinical criteria for VaD also present with coexisting AD pathology (Kosunen et al., 1996). Hence, the concept of mixed dementia, referring to the conditions where cognitive decline can be attributed to both cerebrovascular alterations and AD related pathology, has emerged (Jellinger, 2007). Indeed, a study using a sensitive imaging technique to detect brain amyloid, revealed that about 30% of VaD diagnosed patients showed significant Aβ deposition (Lee et al., 2011a). The clinical and pathological resemblances between these two presumably different diseases (Kalaria and Ballard, 1999), as well as compelling evidence demonstrating that VRFs are associated with increased risk of AD, have contributed to the development of the vascular hypothesis of AD, first proposed in 1993. This hypothesis was built on the idea that during ageing, different factors can induce progressive structural alterations to the microvasculature, resulting in chronic cerebral hypoperfusion that alters the normal supply of nutrients such as oxygen and glucose, critical to the correct functioning of the brain, eventually leading to ischemic brain damage and triggering AD pathology (de la Torre and Mussivand, 1993).

Intervention trials aimed at treating hypertension have shown reduced risk of developing dementia (Forette et al., 1998; Forette et al., 2002; Tzourio et al., 2003); however, other studies have failed to replicate those trials (Applegate et al., 1994; Shepherd et al., 2002). In addition, it was demonstrated that multicomponent vascular care using pharmacological treatment for hypercholesterolemia and hypertension as well as non-pharmacological interventions such as exercise and dietary advice, slowed the progression of WM alterations in AD patients with cerebrovascular lesions (Richard et al., 2010). However, the same group showed in an earlier study, that a similar treatment did not slow cognitive decline in this type of patients (Richard et al., 2009). It can be possible that the damage induced by VRFs starts to occur years before the appearance of the symptoms and eventually becomes irreversible.

1.1.7. Cerebral amyloid angiopathy, a convergence point for both theories.

CAA, defined as Aβ deposition in cerebral blood vessels (Figure 1.3), can occur both sporadically and hereditarily. CAA has a prevalence of 90-100% in AD diagnosed patients and is present in about 30% of non-demented elderly (Attems, 2005; Love et al, 2009; Weller et al, 2009). CAA has been classified into two different types based on the presence or absence of capillary Aβ, both showing different pathological, morphological and genetic features. CAA-type 1, which is most frequently found in AD cases and is strongly associated with apoE4, shows Aβ aggregation in capillaries whereas CAA-type 2 does not and is only present in bigger blood vessels (Attems and Jellinger, 2004; Thal et al., 2008).

Different theories for the pathogenesis of CAA have been developed. One of them suggested that the source of vascular amyloid was blood (Glenner et al., 1984). Another proposed source was vascular smooth muscle cells (Wisniewski and Weigel, 1994). However, cerebral capillaries which lack smooth muscle cells also present Aβ accumulation (Herzig et al., 2006). In contrast, increasing evidence suggests that vascular amyloid has a neuronal origin, followed by drainage along the perivascular lymphatic fluid where, under pathologic conditions, it starts to accumulate in the

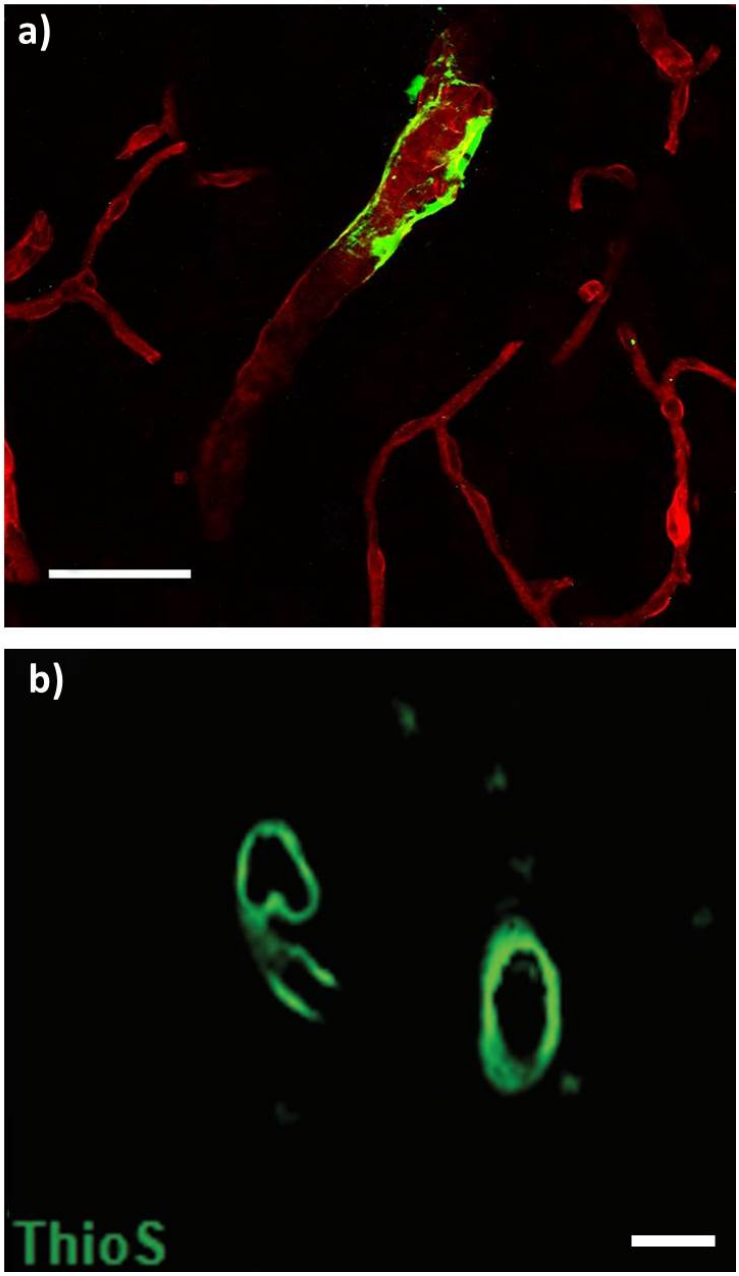

Figure 1.3. Cerebral amyloid angiopathy. Image shows a blood vessel (immunostained with anti-collagen IV, red) covered by Aβ (stained with 6E10 antibody, green) (Scale bar = 30 μm). The tissue sample corresponds to Tg-SwDI mouse brain (a). Thioflavin S staining of human brain tissue from an AD case showing vascular amyloid (Scale bar = 100 μm) (image adapted from Hultman et al., 2013) (b).

vessel walls (Weller et al., 1998; Burgermeister et al., 2000; Van Dorpe et al., 2000; Herzig et al., 2004; Jucker, 2006; Weller et al., 2008; Vidal et al., 2009). Indeed, CAA can be observed in transgenic mouse models overexpressing human Aβ only in neurons (Calhoun et al., 1999).

Several animal and human studies have demonstrated the association of CAA with structural and functional alterations of the cerebrovasculature such as thickening or thinning of the tunica media depending on the stage of the CAA, fibrinoid necrosis, microaneurysm and dilatation of arteries, which leads to the disruption of vascular function and contributes to cognitive impairment (Maeda et al., 1993; Zekry et al., 2003; Auriel and Greenberg, 2012).

A number of mechanisms by which CAA may have an impact on cognition have been proposed. It has been suggested that blockage of perivascular drainage pathways due to accumulation of vascular Aβ may alter the clearance of metabolites from the brain as well as induce impaired transport of nutrients across the BBB (Weller et al., 2008; Carrano et al., 2012; Hartz et al., 2012) triggering altered brain homeostasis that leads to cognitive alterations. Moreover, alteration of CBF due to CAA related capillary occlusion has been demonstrated in transgenic mouse models and AD patients (Thal et al., 2009) and notably, reduced cerebral perfusion has been linked with microinfarction (Shibata et al., 2004) which may also contribute to cognitive decline (Damasceno, 2012). Additionally, severe CAA has been associated with neuronal loss (Zarow et al., 1999).

Interestingly, cerebral microbleeds (Figure 1.4), which occur as a consequence of vascular damage, are closely linked to vascular amyloid deposition (Greenberg et al., 2009; Schrag et al., 2010) and have been proposed as a potential connection between the amyloid and vascular hypotheses of AD. In the proposed model, cerebrovascular pathology and Aβ may synergistically contribute to cause AD through the development of these lesions (Cordonnier and van der Flier, 2011).

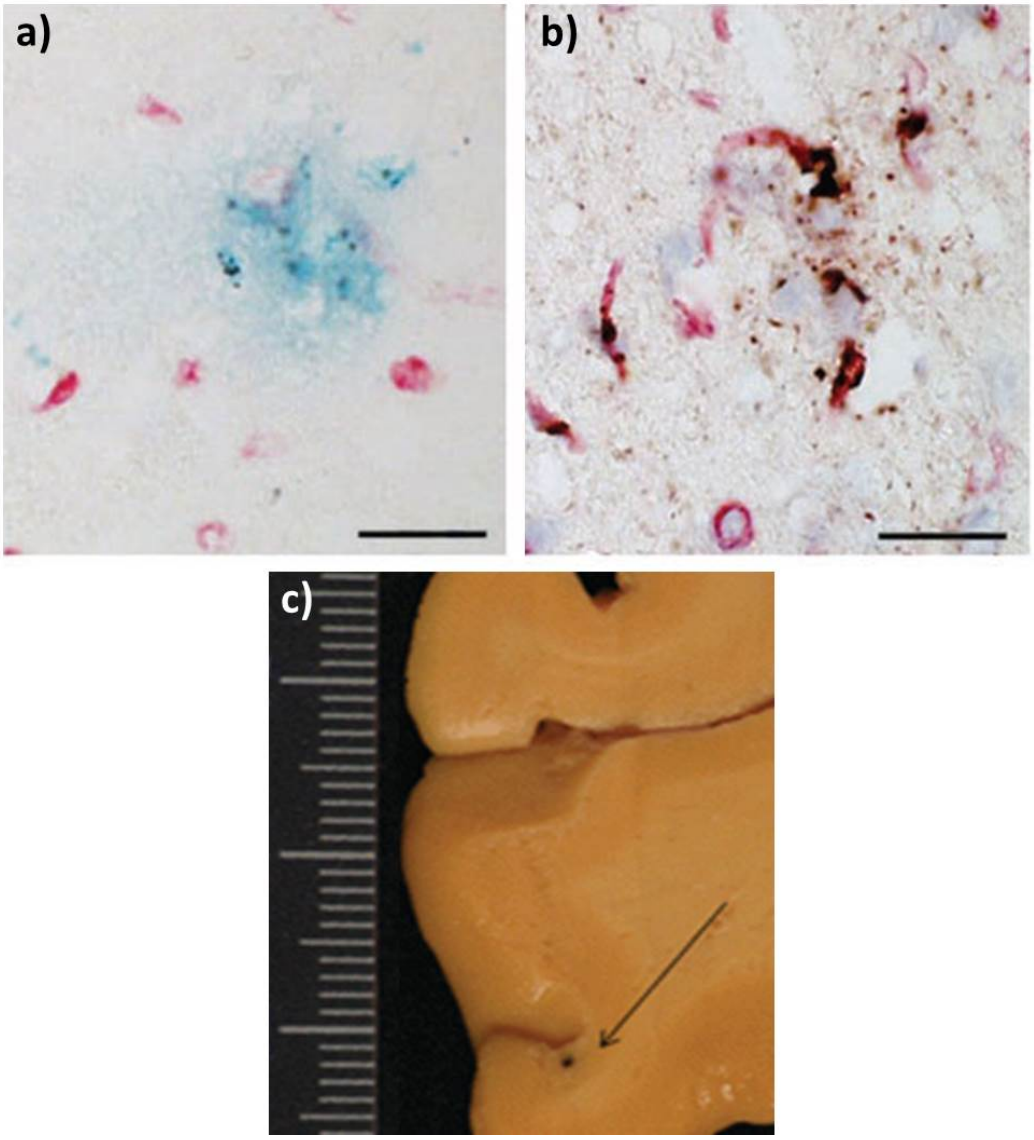

Figure 1.4. Cerebral microbleeds. Prussian blue staining of Tg-SwDI mouse brain tissue showing a microbleed (a) and adjacent double immunostained section showing CAA at the same site (b) (Scale bars = 50 μm) (images taken from Davis et al., 2004). Human brain tissue from an AD case showing a microbleed (see arrow) (image taken from Cordonier and van der Flier, 2011) (c).

1.1.8. Transgenic mouse models of AD.

Numerous mammalian species including cat, sheep, goat, dog and monkey have been reported to develop neurodegenerative features similar to those found in human ageing and AD (Braak et al., 1994; Heuer et al., 2012; Vite and Head, 2014). Rodents constitute excellent research models and some of the advantages that they present include short generation time and small size that allows an easy handling, housekeeping and testing. However, to date only one rodent has been shown to display some of the pathological hallmarks of AD (Inestrosa et al., 2005). Hence, the lack of neuropathology markers of the disease in rodent brains and the finding of AD-related genes, have provided the basis for the creation of transgenic mouse models. Although FAD only represents less than 5% of the cases, the disease shares evident resemblances with the sporadic form of the disease including its pathology.

A number of transgenic mouse lines have been created in order to recapitulate the key neuropathological hallmarks of AD. The first mouse model, named PDAPP, was generated in 1995. These mice express high levels of human APP containing the V171F mutation under the control of the platelet derived growth factor-β promoter, and show progressive accumulation of Aβ, neuronal loss and inflammation (Games et al., 1995). Later, several models expressing the human APP harbouring FAD mutations have been produced using similar approaches to those used to produce the PDAPP including the Tg2576, one of the most commonly used models (Hsiao et al., 1996). Another of these models is the Tg-SwDI. This line expresses the human APP gene with the Swedish, Dutch and Iowa mutations, under the control of the mouse Thy-1.2 promoter (Figure 1.5). The Swedish mutation has been described to enhance the production and secretion of Aβ due to increased β-secretase (BACE) activity (Mullan et al., 1992; Cole and Vassar, 2007). Both, Dutch and Iowa mutations are associated with development of cerebrovascular amyloid deposition (Van Broeckhoven et al., 1990; Grabowski et al., 2001). Thus, robust age-dependent accumulation of Aβ in the parenchyma and predominantly in the wall of cerebral vessels is the pathological hallmark of this mouse model (Davis et al., 2004). Despite the fact that Tg-SwDI mice do not reproduce the full spectrum of AD pathology, this

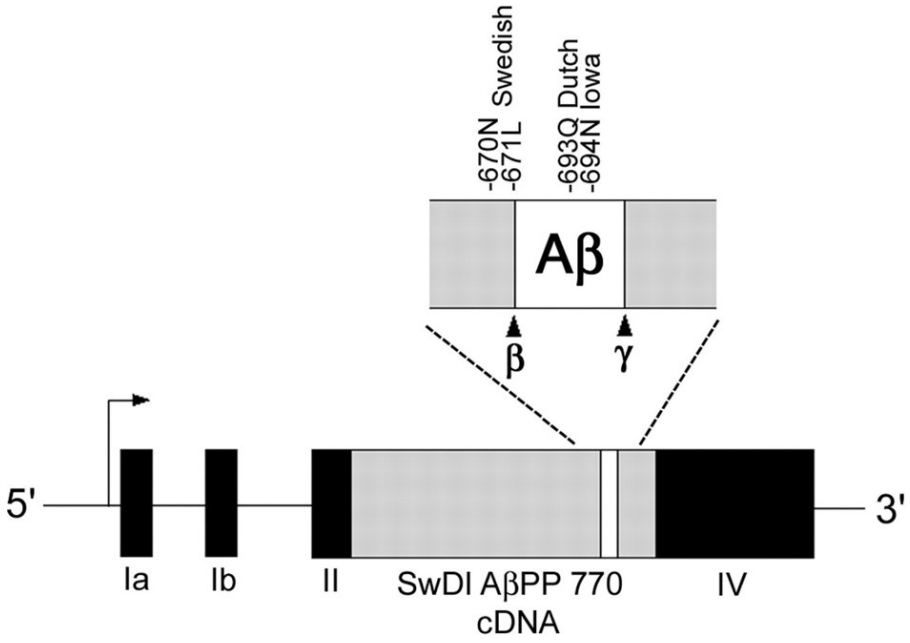

Figure 1.5. Schematic representation of the transgenic construct used to generate the Tg-SwDI mouse model. The figure shows the 9-kilobase construct carrying the 770 isoform of the human APP gene, harbouring the Swedish K670N/M671L, Dutch E693Q and Iowa D694N mutations, under the control of the mouse Thy-1.2 promoter (image taken from Davis et al., 2004).

model is particularly relevant for the study of different aspects related to Aβ deposition particularly CAA. Therefore, this mouse line has been used to study mechanisms relevant to human AD and it has also been useful in the development of new therapeutic approaches (Vasilevko et al., 2007; Goñi et al., 2013). This line was used to conduct the investigation exposed in the present thesis and the characterisation of the model is presented in the chapter 3. Moreover, mouse models expressing the mutated PS1 or PS2, which exhibit enhanced production of Aβ42 species have also been generated, although they do not develop amyloid plaques (Duff et al., 1996). However, these mice undergo neurodegeneration despite the lack of plaques (Chui et al., 1999). Furthermore, a triple transgenic model (3xTgAD), expressing mutated PS1, APP and tau proteins, was shown to develop age-dependant synaptic dysfunction before the accumulation of amyloid plaques and NFTs (Oddo et al., 2003).

As mentioned above, AD is a multifactorial disorder with multiple components contributing to the onset and progression of the disease, therefore an ideal model should include the full spectrum of clinicopathological hallmarks of the disease which includes deposition of tau and Aβ in the brain, neuronal and synapse loss, inflammation, oxidative stress, cerebrovascular damage, memory loss and behavioural alterations (Vinters, 1987; Terry, 1994; Kalaria, 1996; Trojanowski and Lee, 2000; Wilkinson and Landreth, 2006; Gold and Budson, 2008; Serrano-Pozzo et al., 2011; Weintraub et al., 2012). Yet, despite their undoubted value, the main caveat of the transgenic models is that they usually display only some very specific aspects of the disease (Elder et al., 2010) therefore the study of the interaction between all of these components becomes difficult. Nevertheless, they have been extremely valuable to understand the contribution of each of these elements and the different facets of the disease in isolation. Hence, the development of these models constitute one of the most important research tools in the field and has been critical in the understanding of the pathophysiology of the disease as well as in the preclinical testing of potential treatments (Schenk et al., 1999; Schroeter et al., 2008; Elder et al., 2010). The selection criteria of a model, depends on the specific questions to be addressed in the particular study. A summary of commonly used transgenic mouse models is listed in Table 1.1.

Table 1.1. Examples of transgenic mouse models of Alzheimer's disease.

Name	Gene	Mutation	Promoter	Protein aggregation	Cognitive deficit (mo)	Reference
Tg-SwDI	APP	Swedish, Dutch, Iowa	Thy-1	Aβ Parenchyma, CAA	3	Davis et al., 2004
PDAPP	APP	Indiana	PDGF-β	Aβ Parenchyma	3	Games et al., 1995 Rockenstein et al., 1995
J20	APP	Swedish, Indiana	PDGF-β	Aβ Parenchyma	4	Mucke et al., 2000
Tg-2576	APP	Swedish	HamPrP	Aβ Parenchyma, CAA	10	Hsiao et al., 1996
APP23	APP	Swedish	Thy-1	Aβ Parenchyma, CAA	3	Sturchler-Pierrat et al., 1997
Tg-CRND8	APP	Swedish, Indiana	HamPrP	Aβ Parenchyma, CAA	3	Chishti et al., 2001
5XFAD	APP/PSEN1	Swedish, London, Florida/M146L,L28V	Thy-1/Thy-1	Parenchyma	6	Oakley et al., 2006
APPswe/ PSEN1dE9	APP/PSEN1	Swedish/dE9	MoPrP/MoPrP	Parenchyma	12	Jankowsky et al., 2001 Jankowsky et al., 2004
PS-APP	APP/PSEN1	Swedish/M146L	HamPrP/PDGF-β	Aβ Parenchyma, CAA	5	Holcomb et al., 1998
3xTg	APP/PSEN1/Tau	Swedish/M146V/ P30IL	PS1/Thy-1	Aβ Parenchyma, Tau tangles	4	Oddo et al., 2003
Htau	Tau	Wild-type	hTau	Tau Tangles	12	Polydoro et al., 2009
APPswe-Tau	APP/Tau	Swedish/P30IL	HamPrP/MoPrP/ Thy-1	Aβ Parenchyma, Tau tangles	Motor deficit	Lewis et al., 2001

1.1.9. Alzheimer's disease therapies.

AD progresses as a complicated mixture of numerous genetic and environmental factors, therefore the exact etiopathogenesis of the disease is ill understood (see section 1.1.4). For this reason, the search for a treatment or cure has been extremely complicated. However, considering the increasing frequency of the disease as the worldwide population ages and the social and economic burden that this implies, the development of an effective intervention for AD represents a critical clinical need (Wimo et al., 2010).

The only approved drugs that are currently available, which are limited to modestly improve symptoms, target cholinergic and glutamatergic neurotransmission and were developed based on the cholinergic hypothesis of AD, which states that the disease is caused by reduced synthesis of acetylcholine (Francis et al., 1999). These include an N-methyl-D-aspartate receptor antagonist and four cholinesterase inhibitors; yet, their neuroprotective activity is still under discussion (Mangialasche et al., 2010; Howard et al., 2012; Hyde et al., 2013).

Current therapies are only limited to delay the progression of symptoms, but do not have effective disease modifying effects (Lannfelt et al., 2014). However, different strategies designed to inhibit the progression of the disease have been tested in clinical trials. The primary targets of these therapies include: metabolic dysfunction, tau and Aβ (Citron, 2010). A comprehensive review of the clinical trials carried out from 2002 to 2012 by Cummings and colleagues revealed that 413 trials were performed, 36.6% of which tested drugs intended to improve cognition, 35.1% using disease modifying molecules and 18% corresponded to immunotherapies. The overall outcomes were dramatic, with a 99.6% failure rate for approval (Cummings et al., 2014).

Approaches targeting tau have been recently started to be tested in animal models as a potential treatment for AD. In 2007, the first report on tau immunotherapy in mice was published (Asuni et al., 2007). The study demonstrated that injection of a

phosphorylated tau epitope in P301L mice, which develop NFTs, amyotrophy and motor alterations, reduced the aggregation of the protein and improved the behavioural performance. Subsequently, active and passive immunisation studies performed in different tau mutant transgenic mouse models have shown similar results, where decreased tau pathology and reversed cognitive deficits have been demonstrated (Boimel et al., 2010; Boutajangout et al., 2010; Bi et al., 2011, Boutajangout et al., 2011; Chai et al., 2011; Troquier et al., 2012; d'Abramo et al., 2013; Castillo-Carranza et al., 2014). Additionally, Methylthioninium (MT) is a diaminophenothiazine that has been shown to prevent tau aggregation *in vitro* and dissolve paired helical filaments from AD brain tissue (Wischik et al., 1996). The results of the first phase 2 clinical trial of MT in patients with mild to moderate AD, revealing the minimum safe and effective dose of the drug, have recently been published and suggest that MT could have therapeutic utility in AD (Wischik et al., 2015).

Supported by compelling evidence involving Aβ in the pathogenesis of AD (Selkoe, 1991; Hardy and Higgins, 1992), AD drug development has based primarily on the amyloid hypothesis, and the majority of randomised controlled trials (RCTs) have been designed to target this protein. These include drugs that reduce Aβ production, drugs that prevent Aβ aggregation and drugs aimed at promoting the clearance of the protein (Mangialasche et al., 2010). In the first group, drugs designed to inhibit or modulate β and γ-secretases have been tested in several clinical trials. One of these compounds, Tarenflurbil, was demonstrate to reduce Aβ42 production and prevent cognitive alterations in transgenic mouse lines of AD (Eriksen et al., 2003; Kukar et al., 2007). More interestingly, in a phase II RCT Tarenflurbil was proven to be safe and effective in terms of global function in patients with mild to moderate AD (Wilcock et al., 2008). However, the treatment failed to show efficacy in a phase III trial (Green et al., 2009). Another phase III RCT was ended due to the adverse side effects induced by the γ-secretase inhibitor Semagacestat, which triggered worsening of cognitive decline (Schor, 2011). By inhibiting γ-secretase, many other substrates for the enzyme such as Notch are affected therefore the treatment might disturb several vital pathways (Barten et al., 2006). Following a comprehensive analysis of

the data from the trial with Semagacestat, Bart De Strooper suggested that better understanding of the basic biology of secretases would allow to successfully using them as a pharmacological target for the treatment of AD (De Strooper, 2014). Among the drugs that enhance Aβ clearance, Aβ immunotherapy constitutes one of the most promising strategies (Panza et al., 2012; Li et al., 2013; Sarazin et al., 2013).

1.1.10. Aβ immunotherapy.

In 1996 it was first demonstrated that anti-Aβ antibodies could prevent the aggregation of Aβ and inhibit fibril formation *in vitro* (Solomon et al., 1996; Solomon et al., 1997). Later, in 1999 the first report showing decreased amyloid pathology *in vivo* following active immunisation of PDAPP mice with synthetic Aβ42 aggregates was published (Schenk et al., 1999). These results were encouraging as suggested that Aβ immunotherapy could represent the first disease modifying strategy to treat humans with AD.

AN1792 was the first active immunotherapy strategy tested in humans, using the full length Aβ42 as immunogen; however, it was discontinued in phase II due to the development of meningoencephalitis in a subset of AD patients (Gilman et al., 2005). Although, despite the adverse secondary effects, decreased Aβ deposition was found in the brains of treated patients (Nicoll et al., 2003) and long-term follow-up of the interrupted study revealed reduced cognitive decline in patients with antibody response to the treatment (Holmes et al., 2008; Vellas et al., 2009). Hence, numerous preclinical studies of active immunotherapy started to be developed and demonstrated reduction of Aβ levels and improvement of cognitive abilities following immunisation in transgenic mouse models of AD (Janus et al., 2000; Lemere et al., 2000; Weiner et al., 2000; Maier et al., 2006; Lemere and Masliah, 2010; Panza et al., 2012). However, several Aβ peptide antigens failed to stimulate Aβ clearance, due to impairment of the antibodies to cross the BBB (Vasilevko et al., 2007).

In 2000 the first passive Aβ immunotherapy experiments were performed in transgenic mice. The results demonstrated that 10D5 and 3D6 antibodies, specific for n-terminal epitopes of Aβ, were able to enter the brain following systemic administration, and trigger Aβ clearance through Fc receptor-mediated microglial phagocytosis (Bard et al., 2000). Subsequently, several preclinical studies were performed and showed that antibodies against different epitopes of Aβ were able to reduce Aβ levels and improve cognitive abilities (DeMattos et al., 2001; Dodart et al., 2002; Bard et al., 2003; Hartman et al., 2005; Spires-Jones et al., 2009; Lemere and Masliah, 2010). However, the high incidence of secondary effects including the development of haemorrhages in transgenic models following passive immunisation (Pfeifer et al., 2002b; Wilcock et al., 2004; Racke et al., 2005; Wilcock et al., 2006; Burbach et al., 2007; Karlnoski et al., 2008; Schroeter et al., 2008), provided some reason of caution. Bapineuzumab, which constitutes the humanised form of the 3D6 antibody, was the first antibody tested in humans. The treatment showed reduced Aβ load, however it was associated with high incidence of amyloid related imaging abnormalities, and the program was terminated in phase III due to failure of the treatment to reach clinical endpoint (Panza et al., 2011; Tayeb et al., 2013). Solanezumab, another antibody designed to target monomeric Aβ, failed to meet clinical endpoint in two phase III trials, yet encouraging results were found in a subgroup of mild AD patients, which showed slowed cognitive decline (Carlson et al., 2011; Tayeb et al., 2013), therefore a third phase III study was started in mild AD patients.

In addition, second generation active immunotherapies and new anti-Aβ antibodies are currently being tested in patients at very early stages of the disease (Panza et al., 2014). A summary of active and passive immunotherapy clinical trials are shown in Tables 1.2 and 1.3 respectively.

Interestingly, several findings have suggested that tau is implicated in Aβ-related neurodegeneration (Rapoport et al., 2002; Santacruz et al., 2005; Roberson et al., 2007). Furthermore, it was demonstrated that Aβ immunotherapy influenced tau pathology in AD patients actively immunised with AN1792, where reduced levels of

Table 1.2. Examples of completed and ongoing randomised clinical trials for active Aβ immunotherapy (taken from Schneider et al., 2014).

[140]	
ıort peptides mimicking native Aβ. AD02 and ıase 1 in mild–moderate AD, ≈76 individuals, [141] wo phase 2 RCTs in ≈520 subjects with early or rate and prodromal AD over 24 months (results ɛd)	*AD02* (Affiris/GSK): Phase 2 RCT in 300 individuals with early AD (18 months); additionally, extended follow-up of subjects who participated in the phase I RCT is ongoing (total follow-up of 2 years) *AD03* (Affiris): an RCT is ongoing to follow-up subjects who participated in the phase I RCT

Table 1.3. Examples of completed and ongoing randomised clinical trials for passive Aβ immunotherapy (taken from Schneider et al., 2014).

Bapineuzumab: mainly targets fibrillar forms of Aβ. Two phase 3 RCTs in mild–moderate AD, ≈ 2400 subjects, did not report clinical benefits after 18 months. Two other phase 3 RCTs interrupted based on the latter results [142] *Solanezumab*: mainly targets soluble, monomeric Aβ. Two phase 3 RCTs in mild–moderate AD, ≈ 2050 subjects, did not show benefits in the primary outcomes after 18 months. Questionable benefit reported in mild AD [143]	*Solanezumab* is in a phase 2/3 RCT in older adults with positive Aβ PET scans and without cognitive impairment (2 + 3 years, ≈ 1500 participants); and a phase 3 trial of mild AD, with ≈2100 participants
Gantenerumab: mainly targets Aβ plaques. 4-week phase 1 RCT in 18 patients with mild–moderate AD, reduction in brain Aβ; high doses showed adverse effects (ARIA-E) [144] *Crenezumab*: mainly targets monomeric or oligomeric forms of Aß *BAN2401*: monoclonal antibody against Aβ oligomers, phase 2a, 60 AD participants (completed)	*Gantenerumab*: in a phase 2/3 RCT in prodromal AD, 2 years, ≈770 participants *Crenezumab*: phase 2 in mild–moderate AD, 2 years, ≈ 375 participants; phase 2/3 RCT in *PS 1* mutation carriers with normal cognition, 5 years, ≈300 participants *BAN2401*: an 18-month phase 2 RCT in 800 participants with MCI due to AD or mild AD, NCT01767311
Ponezumab PF-04360365: phase 2 RCT, 175 participants, completed in 2011 (not published; development discontinued)	*B11B 037*: phase 2 RCT in prodromal and early AD, 160 participants (NCT01677572)
IVIG polyclonal antibodies including anti-Aβ antibodies: 6 months, phase 2 RCT in 24 participants with mild–moderate AD reported cognitive improvement [145]; 6-month, phase 2 RCT in 58 with mild–moderate AD showed no effect on cognition or AD biomarkers [146] 18-month, phase 3 RCT in mild–moderate AD (≈390 subjects) showed no significant effect [147]	*IVIG*: phase 2 RCT in aMCI, 2 years, ≈50 participants

tau aggregates in neuronal processes were observed (Boche et al., 2010). However, the treatment did not affect NFTs that were accumulated in the neuronal cell bodies. Hence, the authors suggest that this could explain the persistent cognitive decline in the patients after the treatment. It was recently reported that the mechanism by which Aβ immunotherapy alters tau aggregation involves reduced expression of GSK-3β, a kinase implicated in tau phosphorylation (Amin et al., 2014).

In conclusion, encouraging clinical trials are currently ongoing, yet more efficiently designed trials are needed. The trials have arguably been conducted late and when there is extensive pathology and degeneration. AD is a multifactorial disease, therefore increased collaboration between basic and clinical researchers, with the aim of better understanding of the complex interacting networks influencing the onset and progression of the disease is required, as therapeutic strategies aiming at modifying several targets rather that one, might probably take the AD drug development field closer to the design of a successful treatment (Mangialasche et al., 2010; Schneider et al., 2014).

1.2. Links between chronic cerebral hypoperfusion and AD.

1.2.1. Cerebral blood flow.

The brain is totally dependent on an uninterrupted blood supply to function. The regulation of CBF, to deliver oxygen and glucose to meet the metabolic demand of specific brain regions, known as functional hyperaemia, is determined by local brain activity (Ainslie and Tftrailszeng, 2010). This regulation of CBF supply is carried out by the highly co-ordinated communication between different brain cells comprising the neurovascular unit (NVU) (Lok et al., 2007). Under physiological conditions, functional hyperaemia depends on cerebral perfusion pressure (CPP) and cerebrovascular resistance (CVR), thus, any fluctuations in CPP would be compensated by changes in CVR to maintain that way a relatively constant CBF, a process known as autoregulation (Aaslid et al., 1989). This mechanism of autoregulatory vasodilation is dependent on several elements including neurogenic,

myogenic, endothelial-derived, chemical and hormonal factors (Farkas and Luiten, 2001).

In humans, CBF in an adult is about 60 ml of blood per 100 grams of brain tissue per minute. However, it is estimated that CBF drops with age, in a rate of about 0.5% per year, with a decrease of about 20% between ages of 20 to 60 years (Leenders et al., 1990; Zou et al., 2009; Chen et al., 2011a).

1.2.2. Cerebral hypoperfusion.

Normally, the oxygen extraction fraction (OEF), defined as the proportion of oxygen extracted from the circulation by the brain is 40% (Leenders et al., 1990). When the capacity of autoregulatory vasodilation fails to maintain the CBF on the normal range, the OEF increases to maintain the metabolic rate of oxygen, a phenomenon termed misery perfusion, also known as cerebral hypoperfusion (Baron et al., 1981). When severe interruption of blood perfusion occurs due to blockage of a vessel, OEF reaches its limit, leading to an imbalance between blood supply and metabolic activity of the brain, this process is known as ischemia and results in regional neuronal damage. Chronic, modest reduction of CBF can alter brain function and has been involved in the development of dementia (Farkas et al., 2007).

Several VRFs have been associated with the onset of chronic brain hypoperfusion including aging, stroke, diabetes, hypertension, heart failure, coronary artery disease, atherosclerosis, smoking and alcoholism (de la Torre, 2002; Qiu et al., 2003; Novak et al., 2006; Beason-Held et al., 2007; Singh-Manoux et al., 2009). It has been hypothesised that VRFs may lead to endothelial cell dysfunction, resulting in nitric oxide (NO) uncoupling, which may alter the dynamic regulation of CBF and as consequence lead to chronic cerebral hypoperfusion. Indeed, oxidative stress induced by hypertension can alter endothelial cell release of NO leading to decreased CBF. Similarly, diabetes can contribute to CBF alterations by inducing endothelial cell damage and endothelin-1 mediated altered NO production, which impairs normal vasodilation (de la Torre, 2012).

1.2.3. Cerebral hypoperfusion in the early stages of AD.

Neuroimaging studies have revealed regional cerebral hypoperfusion within the temporo-parietal cortex of AD patients (Prohovnik et al., 1988; Hirao et al., 2005; Matsuda, 2007). The reduced CBF is evident in the early stages of the disease (Franceschi et al., 1995; Ishibashi et al., 1998) suggesting a primary role in the development of dementia. It is hypothesised that during normal ageing, VRFs lead to the deterioration of the cerebrovascular system, resulting in reduced CBF, which can contribute to neurodegeneration and have an impact on cognitive decline (see section 1.1.6) (O'Brien et al., 2003; de la Torre, 2004). Notably, epidemiological data demonstrate that all risk factors for AD have shown to induce hypoperfusion (de la Torre, 2000a). Moreover, several neuropsychological and imaging studies looking at the relationship between stroke and dementia have demonstrated an increased incidence of dementia in people who had cerebral infarcts compared to those with no such lesions (Kokmen et al., 1996; Vermeer et al., 2003; Hachinski, 2011; Tolppanen et al., 2013). Interestingly, circulating Aβ levels are elevated in ischemic stroke patients and immunohistochemical analysis has shown association between Aβ deposition and hypoxic/ischemic lesions (Jendroska et al., 1995; Lee et al., 2005; Qi et al., 2007).

The reduction in cerebral perfusion precedes the onset of cognitive decline in AD, correlates with the severity of dementia (Kalaria and Ince, 2000) and evidence from longitudinal epidemiological and neuroimaging studies (Ruitenberg et al., 2005; Fernando et al., 2006; Farkas et al., 2007) suggests that underlying chronic cerebral hypoperfusion contributes to cognitive decline. Furthermore, the use of imaging techniques to detect changes in brain perfusion has permitted the prediction of individuals who will undergo cognitive decline (Alsop et al., 2010). Mild cognitive impairment (MCI), which is thought to be the transition between normal ageing and dementia (Morris and Cummings, 2005), is characterised by reduced perfusion compared to healthy controls; however this reduction has been demonstrated to be more significant in AD patients, which has allowed to predict the conversion from MCI to dementia (Johnson et al., 2005; Chao et al., 2010).

Cerebral hypoperfusion in AD is thought to be linked with both structural and functional alterations that may culminate with irreversible brain damage. However due to the co-existence of reduced CBF with a spectrum of pathology including amyloid plaques, CAA, tau aggregates, atrophy and microinfarcts (MIs), the role of hypoperfusion on the onset and progression of AD is not clear and whether reduced CBF is a cause or consequence of the disease is still debated (Mazza et al., 2011). However, the investigation of experimentally induced chronic cerebral hypoperfusion in animal models has revealed similar structural, metabolic, biochemical and cognitive alterations to those observed in AD brains (Kalaria, 2000; de la Torre, 2008), including microvascular damage, altered protein synthesis, oxidative stress, inflammation, altered Aβ production, tau hyperphosphorylation, axon-glial disruption, WM lesions, cerebral infarction and memory impairment (de la Torre et al., 1992a; De Jong et al., 1999; Shibata et al., 2004; Coltman et al., 2011; Reimer et al., 2011; Liu and Zhang, 2012; Okamoto et al., 2012; Zhao et al; 2014). Based on the differential effects of reduced CBF in animal models depending on the age at which they underwent hypoperfusion, and also on the synergistic effect of age and severity of hypoperfusion on the associated alterations (de la Torre et al., 1992b; de la Torre et al., 1997; Pappas et al., 1997), the critically attained threshold of cerebral hypoperfusion hypothesis of AD was proposed. This hypothesis suggests that the combination of advanced ageing with the manifestation of VRFs might result in reduced cerebral perfusion that reaches a critical threshold, which can culminate with structural capillary damage and altered microcirculation patterns in the brain, and would impair the normal supply of oxygen and glucose, leading to the progressive breakdown of metabolic pathways. This cascade of events, that would require many years to develop before clinical symptoms can be detected, is suggested to eventually trigger the pathology that characterises AD (de la Torre, 1999; de la Torre, 2000b).

Substantive evidence supports the impact of cardiovascular risk factors on the development of dementia, and offers the possibility to use them as therapeutic targets for the prevention and intervention of the progression of cognitive decline (de la Torre, 2012). Indeed, treatment of heart failure has shown to improve CBF and

cognitive performance (Zuccalà et al., 2005). However, although treatment using antihypertensive drugs has been demonstrated to prevent or delay cognitive deterioration and dementia (Forette et al., 1998; Forette et al., 2002; Tzourio et al., 2003; Cherubini et al., 2010; Kitagawa, 2010), some studies have not been able to reproduce these results (Applegate et al., 1994; Shepherd et al., 2002). Moreover, a recent study revealed a poor correlation between VRFs including hypertension and the development of cerebral WM hyperintensities (Wardlaw et al., 2014). In addition, although multicomponent pharmacological strategies targeting hypercholesterolemia and hypertension have been shown to reduce WM alterations in AD patients, no changes in cognitive performance following this treatment were demonstrated (Richard et al., 2009; Richard et al., 2010). Hence, the early identification of VRFs, before symptoms arise, is crucial to stop the progression of underlying disease (Solomon et al., 2009).

In summary, chronic cerebral hypoperfusion constitutes a self-perpetuating condition, and when cognitive decline is irreversible, a cure for AD seems improbable. However, if VRFs are identified in time during clinical examination, early intervention could prevent further cerebrovascular deterioration, altered metabolism and reduced cerebral perfusion that precede cognitive deterioration.

1.2.4. Animal models of cerebral hypoperfusion.

The study of the effect of chronic cerebral hypoperfusion on cognitive alterations in AD patients is complicated by the existence of multiple factors that may lead to reduced CBF and the heterogeneous nature of the pathology. Thus, several animal models of brain hypoperfusion have been developed in order to reconstruct this pathological condition and explore in isolation its impact on the onset of cognitive decline in ageing and AD. Due to economical and ethical acceptability issues, most hypoperfusion experiments have been established in rodents.

Transient or permanent occlusion of the middle cerebral artery (MCAO) constitute common methods developed to model focal cerebral ischemia (Tamura et al., 1981.

Longa et al., 1989). Neuropathological assessment following this type of injury demonstrates localised areas of ischemic brain damage including cortical and basal ganglia infarction. A well characterised model of cerebral hypoperfusion, used mainly in rats, correspond to the bilateral occlusion of the common carotid arteries (BCCAO) or two vessel occlusion, which can be performed transiently or permanently. This procedure has been shown to induce metabolic alterations, progressive neuronal loss especially in the hippocampus, widespread WM injury and cognitive disturbances (Wakita et al., 2002; Ohtaki et al., 2006; Farkas et al., 2007).

Another model of cerebral hypoperfusion, which produces a less severe neuropathological outcome, has also been established by using microcoils in order to induce bilateral common carotid arteries stenosis (BCAS) (Figure 2.1) (Kurumatani et al., 1998; Shibata et al., 2004). Microcoils of different diameters lead to different degrees of CBF reduction (Figure 1.6). In general, WM lesions with severity that is inversely proportional to the diameter of the microcoil can be observed, and working memory deficits can be detected following placement of a 0.18 mm coil (Shibata et al., 2007; Coltman et al., 2011).

With the purpose of understanding the underlying mechanisms by which chronic cerebral hypoperfusion can influence the aetiology of AD, the models described above have been applied to study changes associated with Aβ metabolism.

In models in which CBF is severely reduced, including global and focal ischemia, there is evidence demonstrating that Aβ production and deposition can be promoted (Pluta et al., 1998; Popa-Wagner et al., 1998; Pluta., 2000; Wang et al., 2010). Indeed, studies of short term transient MCAO in rats, have shown increased APP levels surrounding the infarcted areas (Stephenson et al., 1992; Yam et al., 1997; Nihashi et al., 2001). However, in another study, long term follow up of rats subjected to transient MCAO, which also showed elevated APP along with increased Aβ levels at early time points, demonstrated that in some areas of the brain this was only a temporal change (van Groen et al., 2005). Similarly, APP upregulation and Aβ accumulation have also been observed following BCCAO (Kalaria et al., 1993).

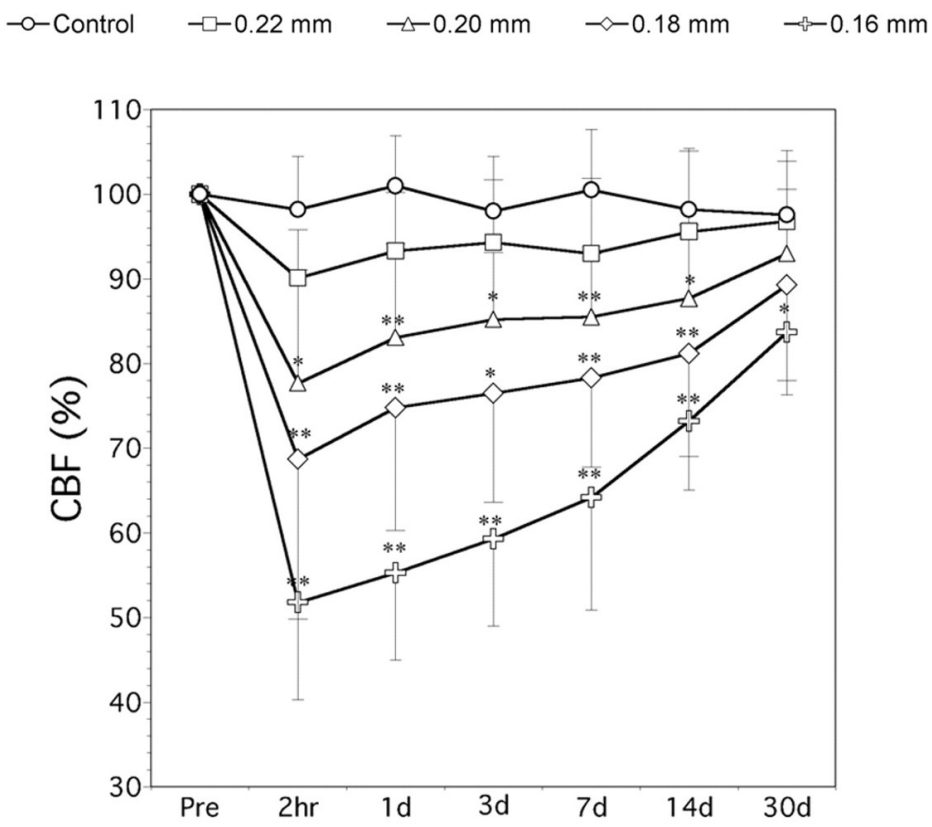

Figure 1.6. Cerebral blood flow values following bilateral carotid arteries stenosis (BCAS). Microcoils of different diameters lead to different degrees of CBF reduction (image taken from Shibata et al., 2004).

Studies aimed at investigating the molecular mechanisms underlying the increased levels of Aβ following focal ischemic insults or chronic hypoperfusion, have revealed enhanced APP processing associated with increased BACE activity and altered expression of Aβ degrading enzymes (Hiltunen et al., 2009). Notably, the enhanced expression of BACE and increased Aβ levels have shown positive correlation with cognitive impairment (Zhiyou et al., 2009).

Furthermore, these models of ischemic insults or hypoperfusion have also been studied in transgenic mouse lines of AD, with similar results. For instance, 3xTg-AD mice exposed to MCAO showed increased amyloid levels associated with enhanced BACE expression (Koike et al., 2010). By using the same experimental stroke model, APPswe/PS1dE9 mice showed acute and transient Aβ aggregation into plaques and CAA near to the infarcted area, however no changes in APP, PSEN1 or Aβ degrading enzymes were observed and the authors suggest that stroke may potentially alter clearance pathways (Garcia-Alloza et al., 2011).

Additionally, APP23 mice exposed to hypoxia exhibited increased amyloid deposition, which was associated with hypoxia inducible factor 1α (HIF1α)-mediated BACE1 upregulation, that enhanced amyloidogenic APP cleavage. However, no changes in APP levels were observed in this study (Sun et al., 2006; Zhang et al., 2007). Interestingly, BCAS has shown to induce increased amyloid deposition, WM alterations and astrocyte proliferation in APPSwInd mice (Kitaguchi et al., 2009); however, in a different study, the same group has latter found suppression of Aβ deposition but increased soluble Aβ and neuronal loss following surgery, which was associated with memory impairment. Thus, the authors proposed that soluble rather than insoluble Aβ species might have had an influence on the cognitive alterations found (Yamada et al., 2011). Additionally, enhanced CAA and MIs have also been observed following chronic cerebral hypoperfusion in Tg-SwDI mice (Okamoto et al., 2012).

1.3. Neurovascular unit dysfunction in the aetiology of AD.

1.3.1. Neurovascular unit structure and function.

During the last decade, the study of the cerebrovasculature has been expanded to several types of cells, which are closely associated with the endothelium to form the NVU (Abbott et al., 2006). The close interaction between these cells, allows the dynamic response of the microcirculation to the energy demands of the brain via neurovascular coupling, to maintain the normal function of the central nervous system (CNS) (del Zoppo and Mabuchi, 2003).

The NVU is structurally formed by a monolayer of endothelial cells lining the microvasculature, which are connected and sealed by the tight junctions (TJs) and delineated by the basal lamina. Surrounding the endothelium are the pericyte processes, which are attached to the basement membrane. Astrocytic end-feet encase most of the capillary wall and extend their processes to be in direct contact with neuronal terminals, allowing neurovascular communication. Circulating immune cells are also part of this functional structure and include microglia and perivascular macrophages, which participate in the immune response at the NVU (Figure 1.7) (Neuwelt et al., 2011; Zlokovic, 2011). The principal functions of the NVU complex include the CBF regulation in response to neuronal activation, the dynamic regulation of the BBB permeability to maintain brain homeostasis, neurovascular remodelling and immune response (Ohtsuki and Terasaki, 2007; Newelt et al., 2011).

Neurovascular coupling is largely mediated by astrocytes, which react in response to changes in neuronal metabolism, influencing CBF to provide the correct nutrient supply, which occurs under normal physiological or pathological conditions (Volterra and Meldolesi, 2005). It has been shown that one of the mechanisms by which the regulation of CBF occurs, is through cerebrovascular dilation or constriction elicited by vasoactive molecules released by the astrocytic end-feet in response to calcium signalling that propagates along the astrocyte projections; this response depends on the regional availability of oxygen (Mulligan and MacVica,

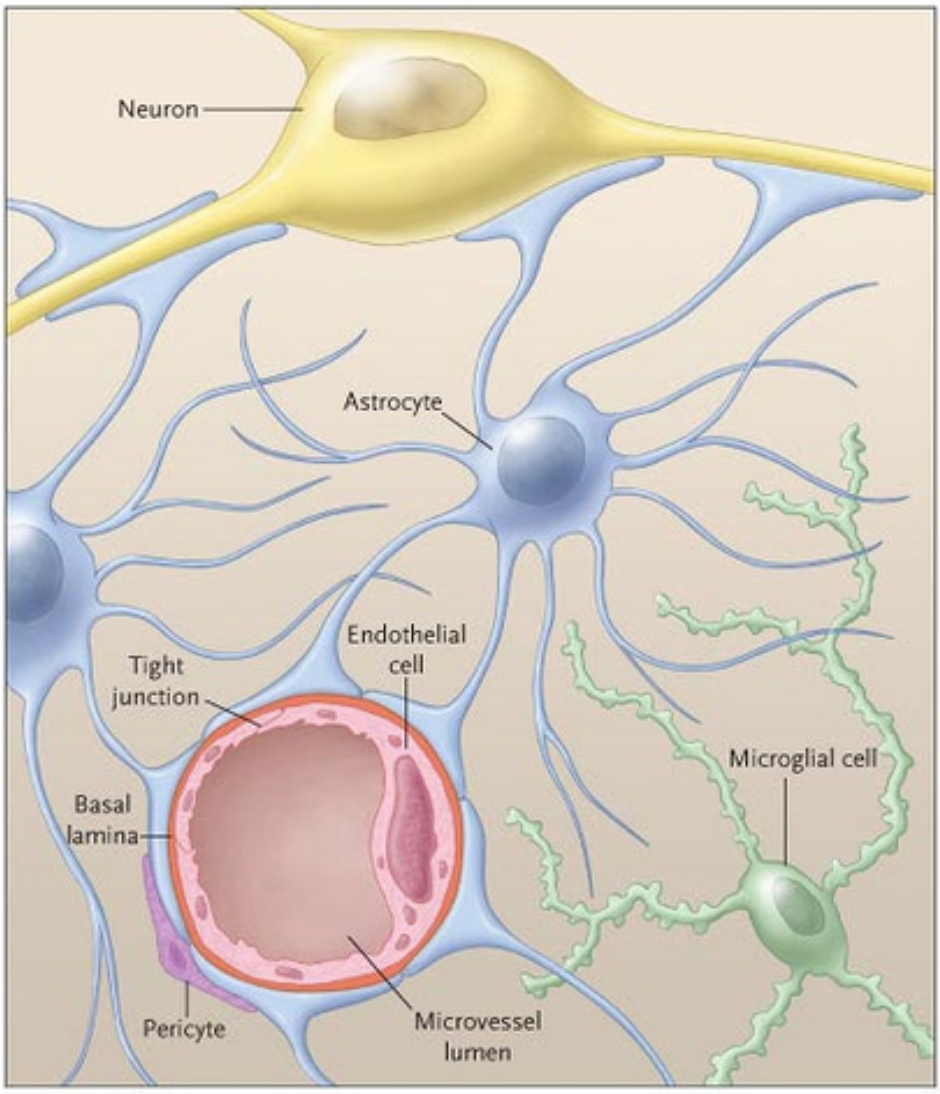

Figure 1.7. Cellular components of the neurovascular unit. The NVU corresponds to the structural and functional interaction between brain endothelial cells, pericytes, astrocytes, microglia and neurons (image taken from del Zoppo, 2006).

2004; Haydon and Carmignoto, 2006; Gordon et al., 2008). Interestingly, it has been proposed that the BBB transport of glucose, the major energy substrate for brain cells, can also be dynamically controlled depending on the regional glucose needs, through a mechanism similar to the neurovascular coupling. Thus, a phenomenon called neurobarrier coupling was proposed, in which neuronal activity influences BBB transport through astrocyte communication (Leybaert, 2005).

The BBB constitutes a key component of the NVU. It is a physical and metabolic barrier formed by microvascular endothelial cells, which are connected by the TJs (Figure 1.8), forming a highly specialised membrane that controls the transport of molecules between the brain and the circulation to maintain the microenvironment for the correct brain function. The main roles of the BBB include molecular trafficking, diffusion barrier, maintenance of ionic composition and protecting the brain from neurotoxins and pathogens (Abbott et al., 2010; Obermeier et al., 2013). Transmembrane proteins including claudins and occludins, which are anchored to the endothelium, constitute the highly selective intercellular TJs that are necessary to restrict paracellular diffusion of hydrophilic molecules across the BBB (Ballabh et al., 2004).

The mechanism that regulates the permeability of the BBB is highly dependent on all the components of the NVU, which interact to establish and maintain the barrier properties. For instance, pericytes participate in the differentiation of endothelial cells and can modulate capillary permeability (Bandopadhyay et al., 2001; Hurtado-Alvarado et al., 2014). Furthermore, astrocytic end-feet (Figure 1.8), which envelop the capillaries, are highly polarised structures due to the high expression of the water channel aquaporin-4 (AQP4) and the potassium channel Kir4.1, which regulate the ionic and osmotic balance. Importantly, numerous studies have demonstrated that astrocytes can improve the barrier properties of the BBB by enhancing enzymatic activity, upregulating transporters and enhancing barrier tightness by increasing TJ formation (Janzer and Raff, 1987; Tout et al., 1993; Hayashi et al., 1997; Lee et al., 2003; Alvarez et al., 2011b).

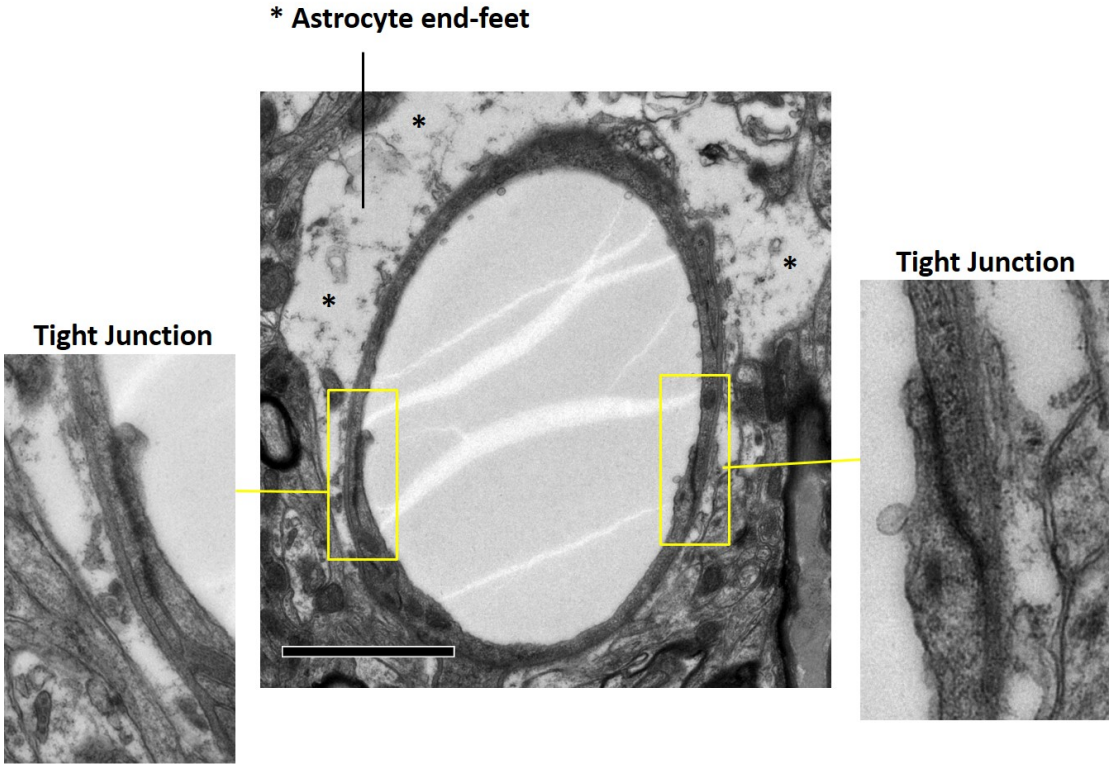

Figure 1.8. Electron micrograph of a mouse brain capillary. The image shows an astrocyte end-foot surrounding the capillary and tight junctions between endothelial cells (Scale bar = 1 μm) (Salvadores, unpublished)

1.3.2. Neurovascular unit and neurodegeneration.

When one component of the NVU fails, the dynamic crosstalk between its different elements can break down leading to dramatic consequences and eventually culminate with neurodegenerative processes. Interestingly, Bell and colleagues demonstrated progressive age-dependent vascular damage in pericyte-deficient mice, which led to cerebral hypoperfusion and BBB breakdown that preceded neuronal loss and cognitive alterations (Bell et al., 2010). This study emphasises the importance of the NVU in the process of neurodegeneration.

The pathophysiology of the NVU has been linked with the aetiology of several neurological disorders such as amyotrophic lateral sclerosis, Parkinson's disease, multiple sclerosis and AD (Waubant, 2006; Chung et al., 2010; Zlokovic, 2011; Garbuzova-Davis and Sanberg, 2014). A common event in these diseases is BBB disruption due to TJ alterations (Zlokovic, 2008; Henkel et al., 2009; Alvarez et al., 2011a), which has been shown to be associated with altered vascular-associated matrix metalloproteinases (MMPs) activity (Yang et al., 2007).

In vitro studies have shown increased expression levels of MMPs in astrocytes treated with Aβ (Deb et al., 2003). Furthermore, intracerebral injection of Aβ induced MMP-9 activation in mice and interestingly, the amyloid-induced cognitive decline was improved in MMP-9 knockout mice (Mizoguchi et al., 2009). Immunohistochemical examination of *post-mortem* AD brains has demonstrated enhanced expression of MMPs (Leake et al., 2000; Asahina et al., 2001) and elevated MMP-9 levels have also been demonstrated in biological fluids of AD patients including plasma and cerebrospinal fluid (Lorenzl et al., 2003; Horstmann et al., 2010).

There is evidence that uncontrolled activity MMPs, which are able to degrade basement membrane and TJ proteins, might play a crucial role in neurodegenerative processes, by increasing the permeability of the BBB leading to haemorrhage and cell death (Cheng et al., 2006; Yang et al., 2007; Rosenberg, 2009). Additionally,

altered Aβ clearance due to BBB damage may lead to amyloid accumulation which can enhance neurovascular dysfunction through the development of CAA (Bell and Zlokovic, 2009). Consequently, the development of chronic inflammatory response and oxidative stress may contribute to the neurovascular damage (Stanimirovic and Friedman, 2012).

Notably, there is evidence of cell-cell signalling between the components of the NVU, in an attempt of reorganisation and remodelling, following brain injury (Iadecola, 2004; del Zoppo, 2009). However, this adaptive response triggered in order to induce recovery, can be either disturbed or perpetuated and promote worsening of the damage. For instance, it has been shown that activation of HIF-1 following hypoxic injury, induces the expression of several genes that can promote cell survival and tissue adaptation by increasing the blood supply and oxygen delivery, yet the enhanced BBB permeability may consequently trigger changes in brain ionic and osmotic homeostasis that can lead to oxidative stress and promote damage. Moreover, HIF-1 can also trigger inflammatory responses and angiogenesis which can contribute to perpetuate cerebral deterioration. These cascade of events can lead to dramatic structural and functional changes in the NVU, including BBB leakage, edema and altered neurovascular coupling (Semenza, 2011; Stanimirovic and Friedman, 2012; Chen et al., 2013).

1.4. Thesis hypothesis and aims.

Together, the evidence presented above suggests a possible mechanism in which, as the result of chronic cerebral hypoperfusion, increased Aβ deposition could be implicated in the pathogenesis of AD by inducing neurovascular damage and downstream cognitive impairment. Nevertheless, there are several gaps regarding the pathways that are initiated by hypoperfusion and culminate with degenerative processes that may lead to cognitive decline in AD (Figure 1.9).

At the outset of the thesis, it was hypothesised that chronic cerebral hypoperfusion leads to the accumulation of parenchymal and vascular Aβ, triggering the

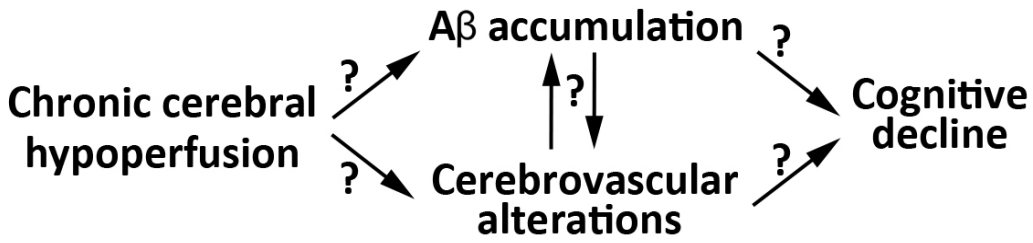

Figure 1.9. Events linking chronic cerebral hypoperfusion with cognitive decline. Diagram shows the gaps between the different events that are initiated by chronic cerebral hypoperfusion and culminate with degenerative processes that may lead to cognitive decline in AD.

development of MIs and haemorrhages and altering the NVU integrity. Second to this, it was hypothesised that Aβ immunotherapy decrease amyloid levels and reduce degenerative processes (MI and haemorrhages) improving cognitive performance.

The specific aims were as follows:

1. To characterise the temporal APP expression, accumulation of parenchymal and cerebrovascular Aβ and Aβ-related microglial and astrocytic activation that the Tg-SwDI model exhibits, in order to provide a basis to design the next studies.

2. To determine parenchymal and cerebrovascular Aβ levels in response to chronic cerebral hypoperfusion. A further aim was to investigate the effects of hypoperfusion and Aβ pathology on the development of MIs and haemorrhages and the potential alteration of astrocyte and tight junction integrity.

3. To determine the effects of passive immunisation with both 10D5 and 3D6 antibodies on Aβ40/42 levels in the parenchyma and cerebrovasculature of the Tg-SwDI mice. A further aim was to determine whether treatment with these antibodies induces changes in the appearance of MIs and haemorrhages and whether the treatment is associated with improved cognitive performance.

Chapter 2. Materials and Methods.

2.1. Animals.

Transgenic mutant mice Tg-SwDI, that overexpress human APP, harbouring the Swedish K670N/M671L, Dutch E693Q and Iowa D694N mutations under the control of the Thy1 promoter, generated on a C57Bl/6J background (Davis et al., 2004), were purchased from Jackson Laboratories. They were subsequently bred in house. For the experiments presented on chapters 3 and 4, male homozygous animals were used. For the experiments presented on chapter 5, male heterozygous animals were used. Wild type mice (C57Bl/6J) were purchased in Charles River Laboratories and were used as comparative controls. The age of the animals for each study is specified in each chapter.

Mice were housed on a 12 hour light/dark cycle and had access to food and water *ad libitum*. All procedures were authorised under the project licence number 60/4350 held by Prof. Horsburgh, approved by the UK Home Office and the University of Edinburgh's Ethical Review Committee and adhered to regulations specified in the Animals (Scientific Procedures) Act (1986).

2.2. Chronic cerebral hypoperfusion.

Chronic cerebral hypoperfusion was induced as previously described (Reimer et al., 2011). Mice were initially anaesthetised with 5% isoflurane in oxygen and then maintained under 1.5% isoflurane. Microcoils (0.18 mm internal diameter; Sawane Spring Co. Japan) were applied permanently to both common carotid arteries (Figure 2.1) with a 30 minute interval between the insertion of the first and second microcoil. Sham animals underwent identical surgical interventions without application of the microcoils. Mice were randomly assigned to the hypoperfused or sham group. The recovery of the mice was closely monitored with weight and general health recorded regularly. Animals that lost more than 20% of their pre-surgical weight or had poor recovery were culled. The surgeon was blind to the genotype of the mice and the studies downstream of the surgery were conducted by a researcher blind to the

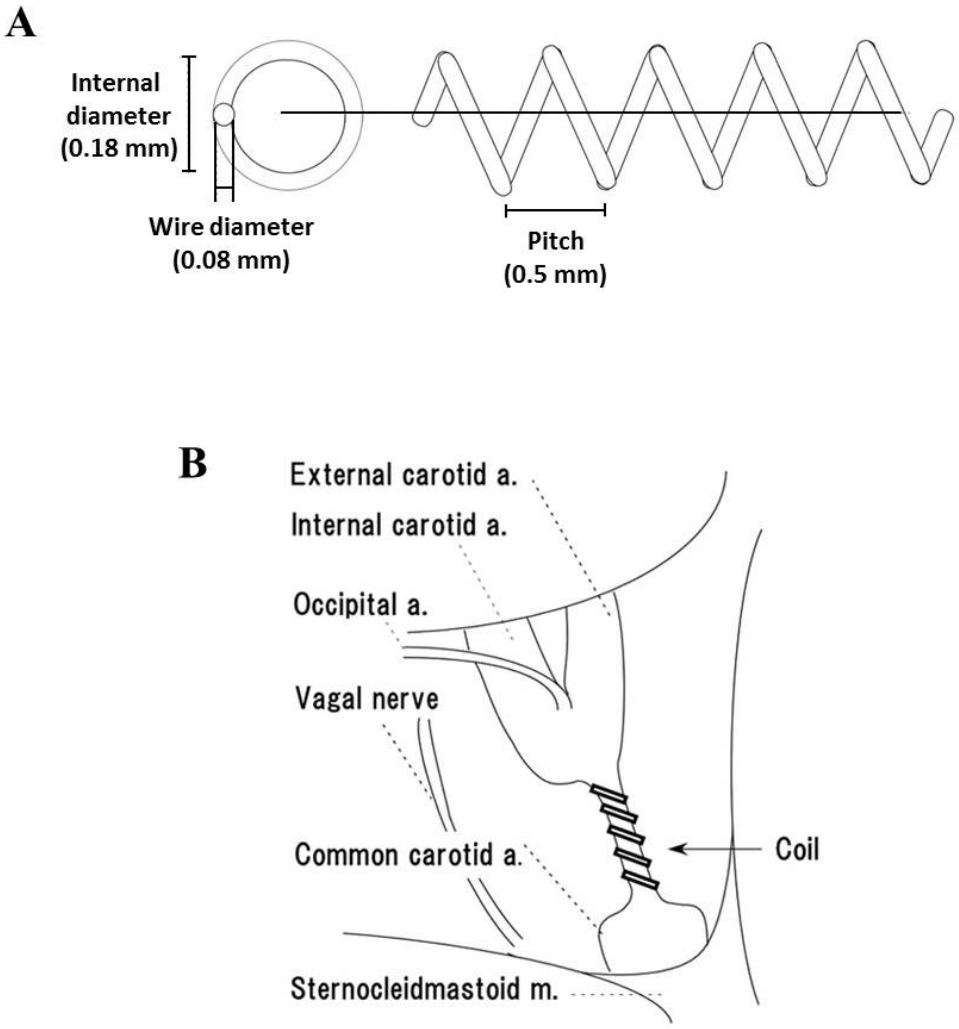

Figure 2.1. Bilateral common carotid artery stenosis. (**A**) Schematic diagram of microcoil. (**B**) Schematic diagram of microcoil in place around the common carotid arteries below the carotid bifurcation (Figure adapted from Shibata et al., 2004).

surgical intervention and genotype of the mice until the final data analysis. The surgery was carried out by Dr Philip Holland.

The expression of Thy1.2 promoter-driven genes has previously shown not to be affected by ischemic/hypoxic injury (McCarran and Goldberg, 2007; Underhill and Goldberg, 2007).

Mice were sacrificed 1 or 3 months after the surgery. Group sizes are listed in Table 2.1.

2.3. Administration of antibody for amyloid immunotherapy.

Mice were injected intraperitoneally weekly with either 10D5 (10 mg/kg), 3D6 (3 mg/kg) or vehicle (TYII-15) (10 mg/kg) during 12 weeks. The animals were injected in the morning and checked in the afternoon for any adverse signs during the whole experimental period and observations were recorded on recovery sheets. Adverse effects were not observed. Mice were randomly assigned to the vehicle or treatment group. The researcher was blind to the antibody that was being injected and the studies downstream of the treatment were conducted by a researcher blind to the treatment that the mice underwent until the final data analysis.

2.4. Transcardial perfusion.

Animals used for biochemical studies were saline perfused. Animals used for immunohistochemical studies were saline perfused followed by perfusion fixation as described below.

2.4.1. Saline perfusion.

Mice were deeply anesthetised under 5% isoflurane in an anaesthetic chamber. Subsequently, animals were removed from the chamber and a mask was used to maintain the anaesthesia at 2% during the procedure. A midline incision was made and the diaphragm exposed and cut to expose the heart. A needle was inserted into

Table 2.1. Cohort sizes used for biochemical and immunohistochemical analyses, following chronic cerebral hypoperfusion.

Cohort	Duration of hypoperfusion (months)	Tg-SwDI		Wild-Type	
		Sham	Hypo perfused	Sham	Hypo perfused
Biochemistry	1	10	9	8	6
Biochemistry	3	6	6	8	7
Immunohistochemistry	1	9	10	12	11
Immunohistochemistry	3	9	9	10	10

the left ventricle and clamped in place and a small incision was made in the right atrium to allow drainage of the blood. Mice were perfused with 20 ml of 0.9% heparinised phosphate buffered saline (PBS) (pH 7.4) at a rate of 2 ml/minute.

2.4.2. Perfusion fixation.

The surgical approach was as above (2.4.1). Mice were perfused firstly with 20 ml of saline buffer followed by perfusion of 20 ml of 4% paraformaldehyde (PFA) in 0.1 M phosphate buffer (PB) (pH = 7.4) to fix brain tissue.

2.5. Tissue processing for histopathology.

After perfusion, brains were removed from the skull, cut along the longitudinal fissure and both hemi-brains were post-fixed in 4% PFA at 4 °C prior to vibratome sectioning or paraffin embedding.

2.5.1. Processing for vibratome sections.

Following post-fixing for 24 hours in 4% PFA, the left hemibrain was then washed for 1 hour in PB and free-floating 30 μm thick sagittal sections were produced with a vibratome (Hydrax V50, Zeiss). Sections were collected and stored in cryoprotective medium (30% glycerol, 30% ethylene glycol in PB) at -20ºC until use for immunohistochemical studies.

2.5.2. Processing for paraffin embedding.

Following post-fixing for 48 hours in 4% PFA, the right hemibrain was washed for 1 hour in PB followed by automatic paraffin processing using a Tissue Tek VIP 2 (Sakura) tissue processor, as described in Table 2.2. Briefly, hemibrains were dehydrated by several incubations with increasing concentration of alcohol followed by a final incubation in xylene. Next, the tissue was incubated in paraffin wax until embedded into paraffin blocks. Sections of 6 μm thickness were produced with a

Table 2.2. Automatic processing for paraffin embedding.

Solution	Duration (hours)	Temperature (ºC)
70% Ethanol	1	35
90% Ethanol	1	35
100% Ethanol	1	35
100% Ethanol	1.5	35
100% Ethanol	2	35
100% Ethanol	1	35
Xylene	1	35
Xylene	1	35
Xylene	1	35
Paraffin wax TT 111	1	60
Paraffin wax TT 111	1	60
Paraffin wax TT 111	1	60
Paraffin wax TT 111	1	60

microtome (Leica RM2135) and mounted onto superfrost plus slides (VWR International) for histological or immunohistochemical studies. Specific details including orientation of the tissue sections are specified in the methods section of the corresponding chapter.

2.6. Immunohistochemistry.

For all immunohistochemistry experiments, previous assessment of the optimal concentration of each antibody was carried out by testing various dilutions. Negative controls, in which identical treatment was performed without addition of the primary antibody, were used in all the experiments to determine non-specific staining.

Primary and secondary antibodies used are listed in Table 2.3.

2.6.1. Fluorescent labelling.

Free-floating vibratome sections were rinsed in PBS followed by Tris buffer (TB) pH 7.6. Sections were mounted onto superfrost plus slides (VWR International) and left to air-dry at RT overnight.

Paraffinised tissue slices, were deparaffinised with heat (60 °C) for 30 minutes followed by incubation in xylene.

Either vibratome or paraffin tissue sections were re-hydrated through a series of alcohols (100%, 90% and 70% ethanol) and then equilibrated in PBS for 10 minutes.

Retrieval was performed by submerging slices in 10 mM citrate buffer (pH 6) and heated at 100 °C under pressure for 10 minutes. Subsequently, sections were rinsed in PBS and retrieval using 2 mM proteinase K, in buffer TE for 10 minutes at RT, was performed. Samples were then washed in PBS and blocked for 2 hours at RT with 20% normal serum 0.5% BSA followed by incubation with the primary antibody solution overnight at 4 °C. Samples were then washed in PBS and

Table 2.3. Antibodies used for immunohistochemistry.

Type of section	Primary antibody	Label	Source	Dilution	Secondary antibody	Source
Paraffin	6E10	AB	Sigma 39320	1:10000	Biotinylated anti-mouse	Vector BA2001
Paraffin	anti-APP	APP	Millipore MAB348	1:20000	biotinylated anti-mouse	Vector BA2001
Paraffin	anti-Iba1	Microglia	Menarini MP290	1:1000	biotinylated anti-rabbit	Vector BA1000
Paraffin	6E10	AB	Sigma 39320	1:1000	Dylight 488 anti-mouse	Millipore AP124JD
Paraffin	anti-GFAP	Astrocytes	Dako Z0334	1:5000	biotinylated anti-rabbit	Vector BA1000
Paraffin	anti-collagen IV	collagen IV	Fitzgerald 70R-CR013x	1:800	Cy3 anti-rabbit	Jackson 711165152
Vibratome	anti-SMA	SMA	Millipore CBL171	1:1000	alexa fluor 488	Invitrogen A11001
Vibratome	anti-collagen IV	collagen IV	Fitzgerald 70R-CR013x	1:800	alexa fluor 546	Invitrogen A11010
Vibratome	6E10	AB	Sigma 39320	1:1000	alexa fluor 488	Invitrogen A11001
Vibratome	anti-AQP4	AQP4	Millipore AB3594	1:50	sterptavidin 488 anti-rabbit	Invitrogen S11223

incubated with the secondary antibody solution for 2 hours at RT. Sections were washed with PBS followed by TB and left to air-dry at RT away from light. Finally, coverslips were mounted using Vectashield HardSet mounting medium and sections were stored at 4°C.

2.6.2. Immunoperoxidase labelling.

Tissue was deparaffinised with heat (60 °C) for 30 minutes followed by incubation in xylene. Samples were later incubated in 100% ethanol and then covered with 3% H_2O_2 for 30 minutes. Sections were rinsed with running water and citrate retrieval was performed by submerging slices in 10 mM citrate buffer (pH 6) and heated at 100 °C under pressure for 10 minutes. Subsequently, tissue sections were washed in PBS, blocked with 10% serum 0.5% BSA for 1 hour at RT and then incubated with the primary antibody overnight at 4 °C. Samples were washed in PBS and incubated with the secondary antibody solution for 1 hour at RT. Slides were washed in PBS followed by incubation with Vectastain Elite ABC reagent (Vector Labs). Sections were washed in PBS and incubated with diaminobenzidine solution (Vector Labs). Finally, tissue sections were rinsed with running water, dehydrated through a series of alcohols (70%, 90%, 100% ethanol) and incubated in xylene. Coverslips were mounted using DPX mounting medium (Thermo Fisher).

2.7. Histological detection of microinfarcts and haemorrhages.

2.7.1. Haematoxylin and eosin staining.

In order to determine the presence of MIs, sections were stained with haematoxylin and eosin (H&E) to visualise the presence of ischemic tissue damage. Paraffin sections were deparaffinised in an oven at 60°C for 30 minutes followed by incubation in xylene for 15 minutes. Samples were re-hydrated by incubation through a series of alcohols (100%, 90%, 70% ethanol) and running water. Sections were immersed in Shandon haematoxylin solution (Thermo Fisher) for 3 minutes and then rinsed briefly in running water. Differentiation of the staining was achieved by

incubation in acid alcohol solution (1% HCl in 70% ethanol) for 4 seconds and then sections were rinsed in running water for 2 minutes. Samples were immersed in Scott's tap water solution (2% MgSO4, 0.35% NaHCO3) for 2 minutes and then washed in running tap water for another 2 minutes. Slides were incubated in eosin Y (Thermo Fisher) solution for 2 minutes and then briefly rinsed in water. Sections were dehydrated by incubation through a series of alcohols (70%, 90%, 100% ethanol) followed by incubation in xylene. Finally, coverslips were mounted using DPX mounting medium (Thermo Fisher).

2.7.2. Prussian blue staining.

In order to detect the presence of haemorrhages, paraffin sections were deparaffinised in an oven at 60°C for 30 minutes followed by incubation in xylene for 15 minutes. Samples were re-hydrated by incubation through a series of alcohols (100%, 90%, 70% ethanol) and running water. Sections were immersed in Perls solution (2% potassium ferrocyanide, 2% hydrochloric acid) for 10 minutes and then rinsed in running water. Slides were counterstained using 0.1% nuclear fast red (Vector) for 5 minutes and washed in running water. Dehydration was performed by incubation through a series of alcohols (70%, 90%, 100% ethanol) followed by incubation in xylene. Finally, coverslips were mounted using DPX mounting medium (Thermo Fisher).

2.8. Analysis of immunohistochemistry.

Fluorescence labelled sections were analysed using a laser scanning confocal microscope (Zeiss LSM 510, Germany).

Images from Perls, H&E and immunoperoxidase labelled sections were acquired using a QImaging QICAM MicroPulisher 3.3 camera (QImaging, Surrey, BC, Canada) connected to an Olympus BX51 microscope (Olympus UK, Southendon-Sea, UK).

All measurements were carried out using Image J software (v1.42q). Specific details including brain region imaged and type of analysis performed are specified in the methods section of the corresponding chapter.

2.9. Generation of parenchymal and vessel enriched fractions.

Following saline perfusion, the brains were removed and cut along the midline. The right hemi-brain was stored at -80^{0}C until used for total protein extraction. The left hemi-brain was homogenised with a fit dounce homogeniser with 1 ml of PBS on ice, using 15 strokes. The homogenate was centrifuged at 250 x g for 10 minutes at 4^{0}C. The pellet was re-suspended in 3 ml of 17.5% ficoll (Sigma) and centrifuged at 3,200 x g for 25 minutes. The pellet (containing the vessel enriched fraction) was collected and the supernatant (containing the parenchymal fraction) was centrifuged again at 3,200 x g for 25 minutes. The pellets from both spins were re-suspended in 1 ml of 1% BSA in PBS and centrifuged at 2,000 x g for10 minutes. The pellet was washed with 1 ml of PBS and stored at -80^{0}C. The supernatant containing the parenchymal fraction was mixed with 6 ml of PBS and centrifuged at 3,200 x g for10 minutes. The supernatant was discarded and the pellet stored at -80^{0}C. Characterisation of the vessel enriched fraction was performed and shown in Figure 2.2. Immunostaining using antibodies against collagen IV and Aβ was performed to observe the presence of blood vessels and Aβ in aliquots from vessel enriched fractions, extracted from wild-type and Tg-SwDI mice. Western blot analysis of protein extracts from both parenchymal and vessel enriched fractions revealed significantly higher levels of vascular related proteins (smooth muscle actin (SMA) and occludin) in vessel enriched compared to parenchymal fractions.

2.10. Protein extraction and quantification.

2.10.1. Sequential protein extraction.

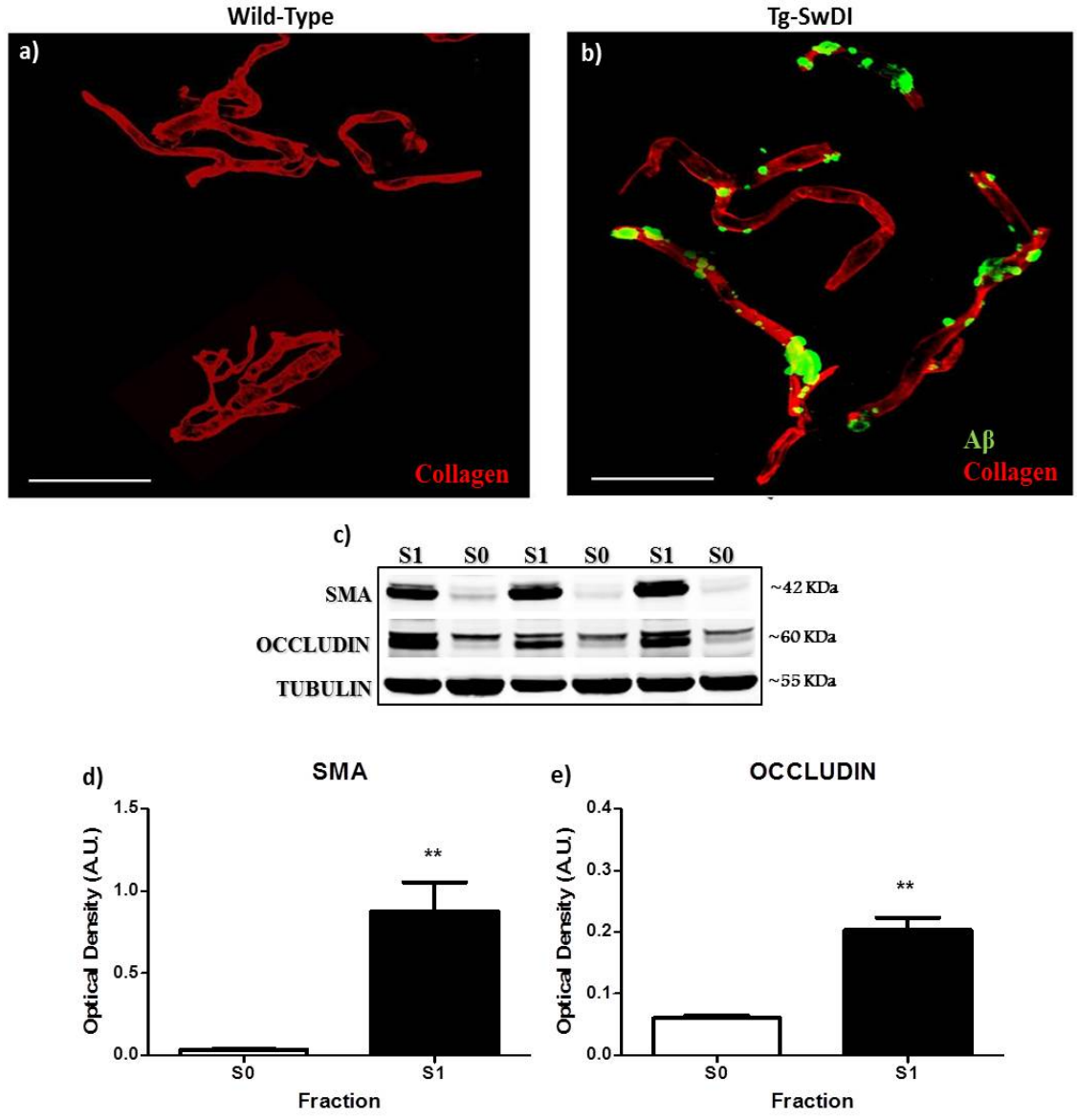

Figure 2.2. Characterisation of the vessel enriched fraction. Representative images showing aliquots from vessel enriched fractions, extracted from wild-type (a) and Tg-SwDI mice (b) immunostained with anti-collagen IV and anti-Aβ antibodies (scale bar = 40 μm). Western blot analysis of protein extracts from both parenchymal (SO) and vessel (S1) enriched fractions was used to determine the expression levels of SMA and occludin, represented in the graphs; tubulin was used as loading control. The data presented are the means ± S.E.M., $p < 0.05$ (c-e).

Sequential protein extraction was performed in order to obtain both soluble and insoluble protein fractions.

The tissue was homogenised with homogenisation buffer (20 mM tris base pH 7.4, 250 mM sucrose, 1 mM EDTA, 1 mM EGTA, 1X protease inhibitor cocktail [Calbiochem]) and centrifuged at 100,000 x g for 1 hour at 4^0C. The supernatant (containing the soluble protein fraction) was carefully transferred to a new tube and stored at -80^0C.

The pellet was resuspended and homogenised in guanidine buffer (5 M guanidne, 50 mM Tris/HCL) and mixed for 3 hours at room temperature (RT). The solution was diluted 1:10 with ice-cold reaction buffer (0.2 g/L KCL, 0.2 g/L KH_2PO_4, 8 g/L NaCl, 1.15 g/L Na_2HPO_4, 5% BSA, 0.03% tween 20, 1X protease inhibitor cocktail) and centrifuged at 16,000 x g for 20 minutes at 4^0C. The supernatant (containing the insoluble protein fraction) was stored at -80^0C.

2.10.2 Total protein extraction.

Total protein extraction was performed by homogenising the tissue in RIPA buffer (50 mM Tris, pH 7.5, 1% NP-40, 150 mM NaCl, 1 mM EDTA, 0.1% SDS, 0.5% sodium deoxycholate, 1X protease inhibitor cocktail), followed by sonication for 5 seconds at 10% amplitude (Branson digital sonifier). Samples were centrifuged at 5000 x g for 5 minutes and the supernatant was collected and stored at -80^0C.

2.10.3. Protein quantification.

Protein levels were quantified with the Pierce BCA Protein Assay Kit (Thermo Scientific). Manufacturer's instructions were used to perform the assay. Absorbance was read on a LT-4000 MS microplate reader (Labtech, East Sussex, UK).

2.11. Enzyme-linked immunosorbent assay (ELISA).

For all ELISA experiments, previous assessment of the optimal sample dilution was carried out by testing various dilutions in order to obtain absorbance values within the range of the standard curve. Levels of Aβ1-40, Aβ1-42, Scara1, AQP4 and NADPH Oxidase-2 (NOX2) were assessed using ELISA. In all experiments, manufacturer's instructions were used to perform the assays. Details of antibodies used are detailed in Table 2.4. Specific details including type of sample used and kit's source, are specified in the methods section of the corresponding chapter.

2.12. Western blotting.

APP, APP-CTF's, LRP, GFAP and claudin-5 levels were determined by using western blot. Details of antibodies used are detailed in Table 2.5. The type of sample used is specified in the methods section of the corresponding chapter.

Samples were prepared by mixing the protein extracts with 1X NuPAGE loading buffer (Invitrogen) and 1% NuPAGE reducing agent (Invitrogen) followed by incubation at 70˚C for 10 minutes in a water bath. Samples and molecular weight marker (Li-Cor, Cambridge, UK) were loaded and fractionated by electrophoresis using 4–12% sodium dodecyl sulphate polyacrylamide gels (Invitrogen) in MES running buffer (Invitrogen) at 100V. Subsequently, proteins were electroblotted at 30V for 1.5 hours on to polyvinylidene fluoride (PVDF) membranes (Hybond-P, GE Healthcare) using a XCell II Blot Module (Invitrogen). PVDF membranes were incubated with agitation in blocking buffer (Li-Cor) for 1 hour at RT, followed by incubation overnight at 4 ˚C with the primary antibody, which was diluted in a solution containing blocking buffer and 0.1% tween-20. Membranes were washed 3 times in PBS 0.1% tween-20, during 10 minutes each wash. Subsequently, membranes were incubated with the secondary antibody during 45 minutes and washed as previously described with a final wash for 5 minutes in distilled water. Membranes were air-dried and stored away from light. The immunoreactive bands were visualised using the Odyssey Infrared Imaging System (LiCor Biosciences, Lincoln, NE, USA) and densitometric analysis of the scans was performed by using the odyssey software (version 3.0; Li-Cor, Cambridge, UK).

Table 2.4. Antibodies used for ELISA.

Antibody	Target	Source
anti- Aβ1-40	Amyloid-β 1-40	Invitrogen
anti- Aβ1-42	Amyloid-β 1-42	Invitrogen
anti- Scara1	Scavenger receptor A	Cusabio
anti- AQP4	Aquaporin-4	Invitrogen
anti- NOX2	NADPH Oxidase-2	Cusabio

Table 2.5. Primary antibodies used for western blotting.

Antibody	Label	Species raised in	Clone	Source	Dilution
anti-APP	APP	Mouse	Monoclonal	Millipore, MAB348	1:1000
anti-APP-CTF's	APP-CTF's	Rabbit	Polyclonal	Calbiochem, 171610	1:1000
anti-LRP1	LRP1	Rabbit	Monoclonal	Abcam, ab92544	1:20000
anti-GFAP	Astrocytes	Rabbit	Polyclonal	Dako, ZO334	1:5000
anti-claudin-5	claudin-5	Rabbit	Monoclonal	Invitrogen,35-2500	1:1000

2.13. Barnes maze.

Spatial learning memory was assessed by using the Barnes maze (Figure 2.3). The maze consists of a 91.5 cm diameter, 115 cm height circular white platform (San Diego Instruments) with 20 circular holes around the perimeter of the platform. A small, dark escape chamber is attached to one of the holes. Visual cues including different shaped and coloured objects hanging in plain sight of the animals are placed around the maze to optimise cognitive performance. The platform is brightly lit by overhead lighting. A 10.5 cm diameter cylinder is used to retain the animals on the platform before the trial begins. A camera fixed above the maze was used to track the movement patterns of the animals by using the ANY-maze video tracking Software (v4.99).

The aim of the Barnes maze is to measure the ability of the animals to learn and remember the location of the escape chamber using the configuration of the cues.

2.13.1. Acclimation phase.

Prior to the beginning of the experiment, the mice were acclimated to the holding room and the maze room over a period of three days. During this phase, the animals were kept outside the maze room during one hour and then taken into the room. Mice were placed into the holding cylinder during ten seconds and then brought back to their home cage.

The animals were handled by the same experimenter throughout the study.

2.13.2. Habituation phase.

One day after the acclimation phase, mice were kept outside the maze room during one hour and then taken into the room as they were introduced to the maze.

Figure 2.3. Assessment of spatial learning and memory performance using the Barnes maze. Photograph showing the Barnes maze and the extra-maze cues.

Animals were allowed to freely explore the maze during three minutes, whilst aversive white noise was being played. After conclusion of the three minutes, if the mice stayed on the surface of the table, they were trained to enter to the escape chamber by being gently guided into the box and allowing them to stay inside for one minute with the white noise off.

To avoid the use of olfactory cues to find the escape box, the surface of the maze and the box were cleaned with a 70% ethanol solution between animals.

2.13.3. Spatial acquisition phase.

The training was performed over a period of five days, where two trials per day were ran. The mice were kept outside the maze room during one hour and then taken into the room to start the test. Animals were placed into the holding cylinder during ten seconds and the white noise started to play. The cylinder was lifted and the mice were given three minutes to find the escape box. After conclusion of the three minutes, if the mice did not find the exit hole, they were trained to enter to the escape chamber by being gently guided into the box and allowing them to stay inside for one minute with the white noise off.

The escape box was located in the same position of the maze for each animal throughout the training phase; however it was shifted 90 degrees between each mouse to avoid the use of olfactory cues in order to find the escape chamber. Also, the surface of the maze and the escape box were cleaned with a 70% ethanol solution.

Animals were divided into two groups. After every animal from the first group completed the first trial, the second trial was performed after one hour inter-trial interval.

2.13.4. Probe trial.

48 hours after the last training trial, the probe trial was conducted. The mice were kept outside the maze room during one hour and then taken into the room to start the test. Animals were placed into the holding cylinder during ten seconds and the white noise started to play. The cylinder was lifted and the mice were given 90 seconds to freely explore the maze with the escape box removed. The surface of the maze was cleaned between each mouse.

2.13.5. Measurements.

During the training (spatial acquisition) phase, the latency to escape (time required by the mouse to enter the escape box) and primary latency (time required by the mouse to explore the escape box regardless of whether they entered) were directly measured by the tracking software. The number of errors, defined as the exploration of incorrect holes, was recorded and quantified manually by the experimenter observing via the computer screen. Total errors (number of errors made before entering the escape box) and primary errors (number of errors made prior to the initial contact with the escape hole) were recorded. During the probe trial, the percentage of time spent in each quadrant was directly measured by the tracking software. The number of total and primary errors were recorded and quantified manually by the experimenter.

This test was carried out in collaboration with Dr Luke Searcy, who set up the maze and participated in the experimental procedure.

2.14. Statistical analysis.

All statistical analyses were performed using Graph Pad Prism 5.0 software (La Jolla, CA, USA). For experiments with two samples, a two-tailed un-paired Student's t-test was applied. For experiments with more than two samples, a one-way ANOVA

test was applied. For experiments with more than two samples but two variables, a two-way ANOVA test was applied. Bonferroni test was used as a post hoc-test.

Data are presented as the mean ± standard error of the mean. Unless otherwise indicated, a probability (p) value of < 0.05 was considered to be statistically significant.

Details of the statistical analysis performed for each result are specified in each chapter.

Chapter 3. Characterisation of the Tg-SwDI mouse model.

3.1. Introduction.

Several transgenic lines have been developed in an attempt to generate models that mimic specific aspects of human AD and they constitute a potent tool for the research in AD field; the Tg-SwDI is one of these models. This mouse line expresses a 9-kilobase construct carrying the 770 isoform of the human neuronal APP gene, harbouring the Swedish K670N/M671L and vasculotropic Dutch E693Q and Iowa D694N mutations, under the control of the mouse Thy-1.2 promoter (Figure 1.5), which drives the gene expression specifically in the brain. A report describing this model was published in 2004 by Davis and colleagues, where age-dependant Aβ accumulation, primarily in the cerebral microvasculature of these mice is demonstrated. Diffuse plaque-like structures in the parenchyma are also described to occur (Davis et al., 2004). These mice present astrogliosis and microglial activation, which is associated with vascular amyloid (Miao et al., 2005). Functional and structural deterioration of the cerebrovasculature has been detected in this model starting at 3 months of age (Park et al., 2013; Park et al., 2014).

Vascular accumulation of Aβ has been associated with the development of cerebral haemorrhages (Vonsattel et al., 1991) and microinfarction (Okamoto et al., 2009; Soontornniyomkij et al., 2010), which are a common histopathological finding in *post-mortem* studies of AD patients and may contribute to the cognitive decline (Ellis et al., 1996; Cordonier and van der Flier, 2011; van Rooden et al., 2014). Indeed, these type of cerebral lesions are also present in the Tg-SwDI mice and are a focus of the work presented in the chapter 4 of the present thesis, where the effect of chronic cerebral hypoperfusion on Aβ accumulation, and subsequent contribution to the development of these lesions was investigated. Interestingly, Tg-SwDI mice have shown to undergo cognitive alterations including learning and memory deficits detected in the Barnes maze task, which correlate with subicular accumulation of Aβ in the microvasculature (Xu et al., 2007). However, the contribution of haemorrhages and MIs to the cognitive impairment in these mice is unknown. This is studied in the chapter 5 of this thesis, where the effect of reducing amyloid load, on the

development of MIs and haemorrhages and potential behavioural improvement in the Tg-SwDI mice were investigated.

Although the model has previously been characterised (Davis et al., 2004), the rederivation of mice and subsequent breeding can often lead to changes from the original phenotype. Thus it was deemed important to characterise the amyloid and Aβ-related pathology with increasing age. Since it was planned to induce the hypoperfusion in these mice before significant Aβ deposition is observed it was also important to define when the onset of amyloid accumulation was initiated.

3.1.1. Hypothesis and aim of study.

It was hypothesised that the Tg-SwDI model undergoes increasing parenchymal and vascular Aβ accumulation associated with inflammation over time.

The aim of this study was to characterise the temporal APP expression, accumulation of parenchymal and cerebrovascular Aβ and Aβ-related microglial and astrocytic activation that the Tg-SwDI model exhibits, compared to wild-type animals, in order to provide a basis to design the next studies.

3.2. Methods.

3.2.1. Animals.

3 groups of 3, 6 and 9 months old male Tg-SwDI mice were used. Male wild-type (C57Bl/6J) mice were used as comparative controls. Animal numbers were as follows:

3 months, n = 8 wild-type and 8 Tg-SwDI; 6 months, n = 10 wild-type and 10 Tg-SwDI and 9 months, n = 15 wild-type and 15 Tg-SwDI.

The researcher was blind to the genotype of the mice until the final data analysis.

3.2.2. Perfusion and tissue processing.

Animals underwent saline perfusion followed by perfusion fixation as described in section 2.4.2. Brains were processed for paraffin embedding and coronal sections were produced as described in section 2.5.2.

3.2.3. Immunohistochemistry.

Immunohistochemistry was carried out as described in section 2.6. Tissue sections at anatomical level corresponding to -1.70 mm from bregma (Franklin and Paxinos, 1997) were used. APP expression, Aβ deposition, microglial activation and astrogliosis were conducted using immunoperoxidase labelling. Vascular Aβ accumulation was performed using fluorescent labelling.

3.2.4. Image analysis.

For the analysis of APP expression, Aβ deposition, microglial activation and astrogliosis, one image from the cortex, one from the hippocampus and one from the thalamus were acquired as described in section 2.8, at 4x magnification. Quantitative

measurement of the staining was assessed by measuring the percentage of the stained area compared to the total area.

For the analysis of vascular Aβ, four images of the thalamus per brain were acquired as described in section 2.8 with a 40x objective at a 1024 x 1024 pixel resolution. Colocalisation analysis between blood vessels and Aβ was done by calculating the ratio between the area occupied by colocalising pixels and the percentage of collagen IV (red channel) stained area.

3.2.5. Statistical analysis.

The data was analysed for statistical significance using two-way analysis of variance (ANOVA) (with age and genotype as factors) followed by the Bonferroni post-test.

Results from vascular Aβ measurements were analysed for statistical significance using unpaired t-test with $p < 0.05$.

For the association analysis, the Pearson correlation coefficient was determined.

3.3. Results.

3.3.1. Temporal expression of APP in Tg-SwDI mouse brain.

In order to visualise the expression of APP, immunostaining was performed using an antibody that recognises an epitope within amino acids 66-81 of APP (N-terminus) and therefore binds to both murine and human APP. This protein is normally concentrated in neurons and this was observed in both Tg-SwDI and wild-type mice, however the staining was much more evident in the tissue sections from transgenic animals (Figure 3.1). As shown in Figure 3.2, the expression of the protein increased as the animal aged in all the brain regions analysed. As comparison, representative images from 9 months old wild-type mice are shown (Figure 3.2, j-l).

The image analysis showed that APP immunostaining was significantly higher in the Tg-SwDI mice when compared to wild-type controls starting at 6 months of age in the cortex and hippocampus and by 9 months in the thalamus (Figure 3.3).

These results indicate that the Tg-SwDI model presents an age-dependent increase in APP expression levels in the brain.

3.3.2. Amyloid-β deposition.

In order to study Aβ deposition in the Tg-SwDI mouse brain, immunostaining was conducted using the antibody 6E10, epitope of which is situated within amino acids 3-8 of Aβ and therefore recognises all isoforms of the protein.

As shown in Figure 3.4, there was a progressive and robust accumulation of Aβ in cortex, hippocampus and thalamus of the transgenic animals. The accumulation of the protein increased as the animal aged, showing extensive aggregation by 9 months, markedly in the thalamus (Figure 3.4, i). Aβ plaque-like deposits started to appear at 6 months of age and they became more evident by 9 months, were many

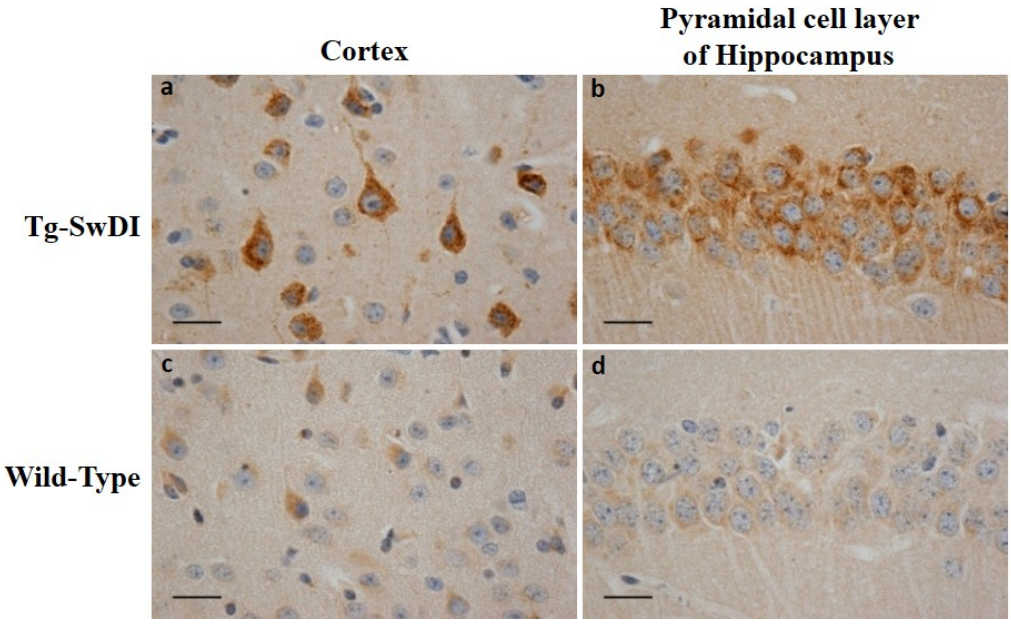

Figure 3.1. Amyloid precursor protein expression in the Tg-SwDI model. Tissue sections from 9 months old transgenic and wild type animals were immunostained with a marker of APP. Representative images taken in the cortex (a, c) and hippocampus (b, d) are shown (scale bar = 20 μm).

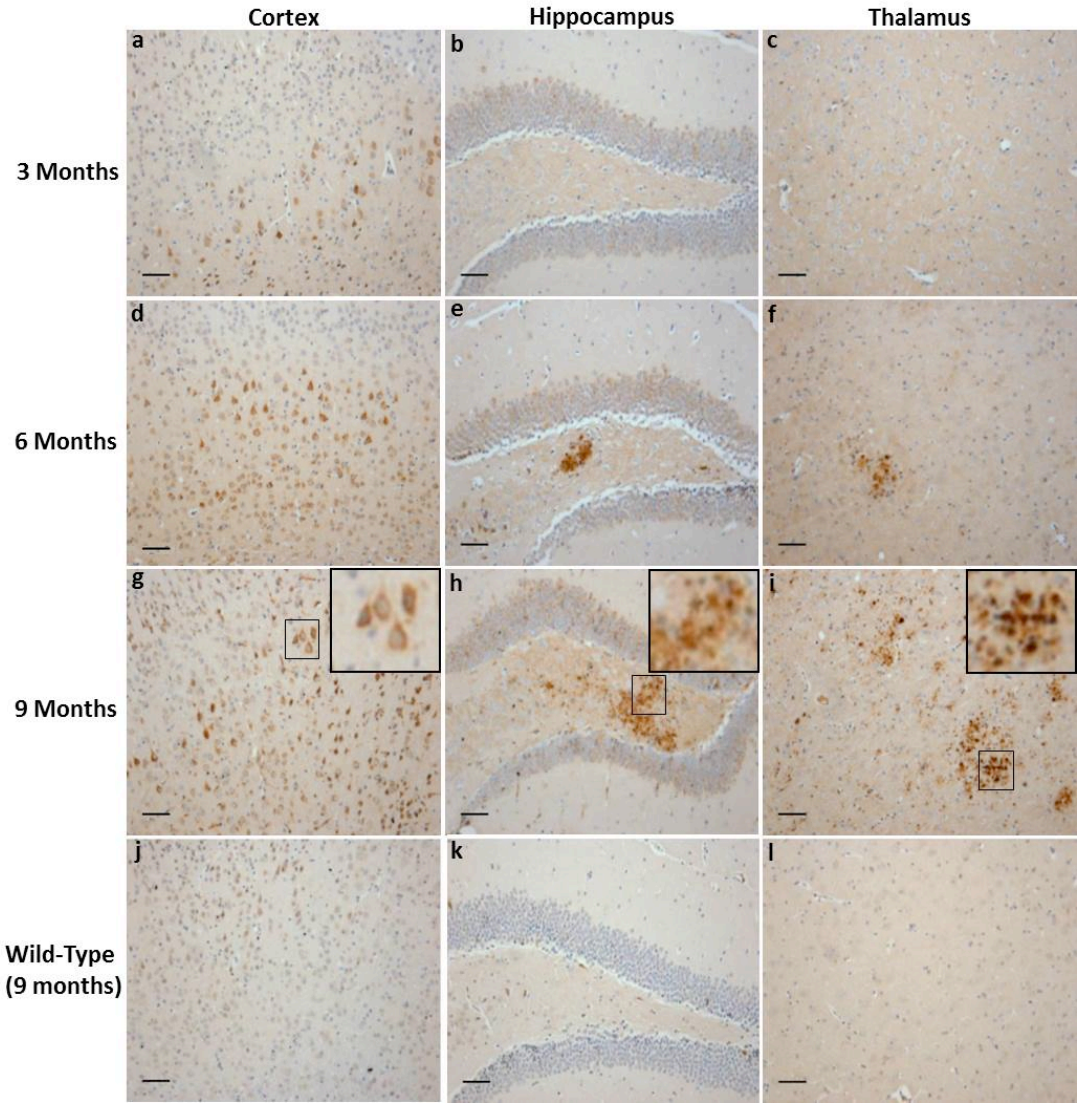

Figure 3.2. Temporal expression of APP in the Tg-SwDI model. Transgenic and wild type animals were sacrificed at 3, 6 and 9 months of age and histological analysis of the cortex (a, d, g, j), hippocampus (b, e, h, k) and thalamus (c, f, i, l) was performed. Sections were immunostained and APP was visualised using a marker that recognises both human and murine APP (scale bar = 50 μm).

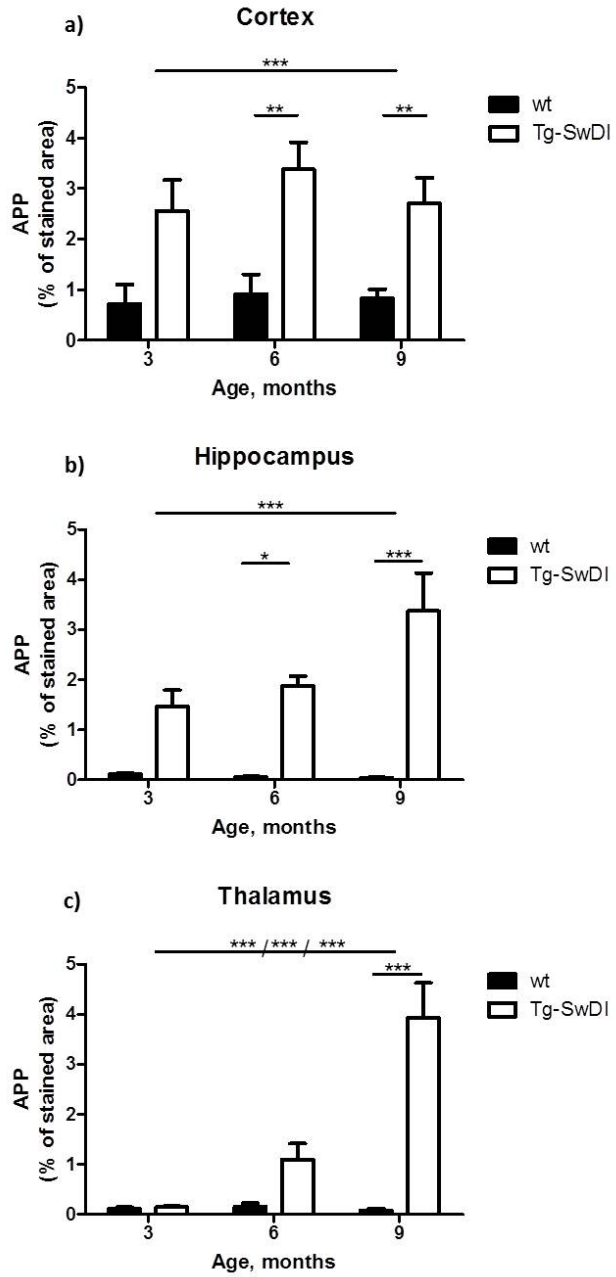

Figure 3.3. APP expression increases over time in the transgenic mouse model Tg-SwDI. Quantitative analysis of APP immunostaining was assessed by measuring the percentage of stained area, represented in the graphs. The data presented are the means ± S.E.M.; two-way ANOVA: cortex: significant effect of genotype ($F_{(1,57)}$ = 28.49, ***p < 0.0001), Bonferroni post-test (**p < 0.01) (a); hippocampus: significant effect of genotype ($F_{(1,58)}$ = 31.23, ***p < 0.0001), Bonferroni post-test (*p < 0.05; ***p < 0.001) (b); thalamus: significant effect of age ($F_{(2,58)}$ = 11.96, ***p < 0.0001), significant effect of genotype ($F_{(1,58)}$ = 20.47, ***p < 0.0001), significant interaction ($F_{(2,58)}$ = 11.30, ***p < 0.0001), Bonferroni post-test (***p < 0.001) (c).

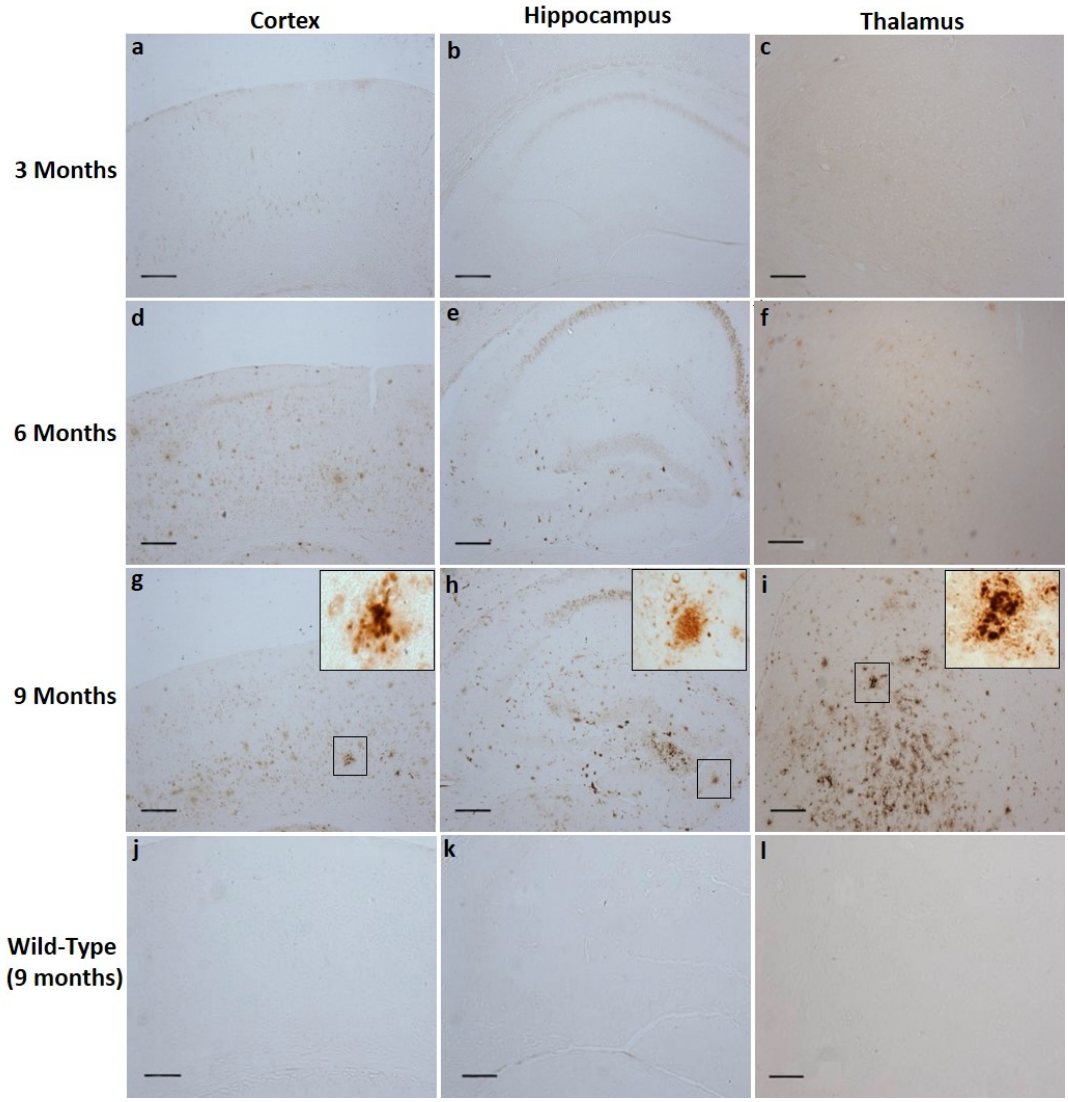

Figure 3.4. Temporal Aβ deposition in the transgenic mouse model Tg-SwDI. Transgenic and wild type animals were sacrificed at 3, 6 and 9 months of age and histological analysis of the cortex (a, d, g, j), hippocampus (b, e, h, k) and thalamus (c, f, i, l) was performed. Sections were immunostained and amyloid was visualised using the specific marker 6E10 (Scale bar= 200 μm).

diffuse aggregates were present in all the brain regions analysed, as shown at higher magnification (Figure 3.4, insets).

As expected, amyloid aggregation was absent in wild-type controls; representative images from 9 month old wild-type mice are shown (Figure 3.4, j-l).

The image analysis showed that Aβ deposition was significantly higher in the Tg-SwDI mice when compared to wild-type controls starting at 6 months of age in the cortex and hippocampus and by 9 months in the thalamus (Figure 3.5).

This result indicates that the Tg-SwDI model presents an age-dependent increase in Aβ deposition in the brain.

3.3.3. Microglia activation.

Microglia constitutes the principal cell component of the active immune defence in the CNS. An inflammatory response has been associated with amyloid deposition and particularly to CAA in transgenic mouse models and in AD patients (Morgan et al., 2005; Chung et al., 2011; Zabel et al., 2013; Baron et al., 2014).

In order to determine whether this mouse line undergoes microglial activation, an immunohistochemical study was conducted using the antibody Iba1, which recognises the ionized calcium-binding adaptor molecule 1, a protein that is upregulated during the activation of microglia (Ito et al., 1998).

As shown in Figure 3.6, microglial activation increased in the Tg-SwDI model as the animal aged in all the brain regions analysed. In comparison, there was minimal microglia in wild-type mice compared to Tg-SwDI mice at the same ages. Representative images of microglia from 9 month old wild-type mice are shown to illustrate this marked difference (Figure 3.6, j-l).

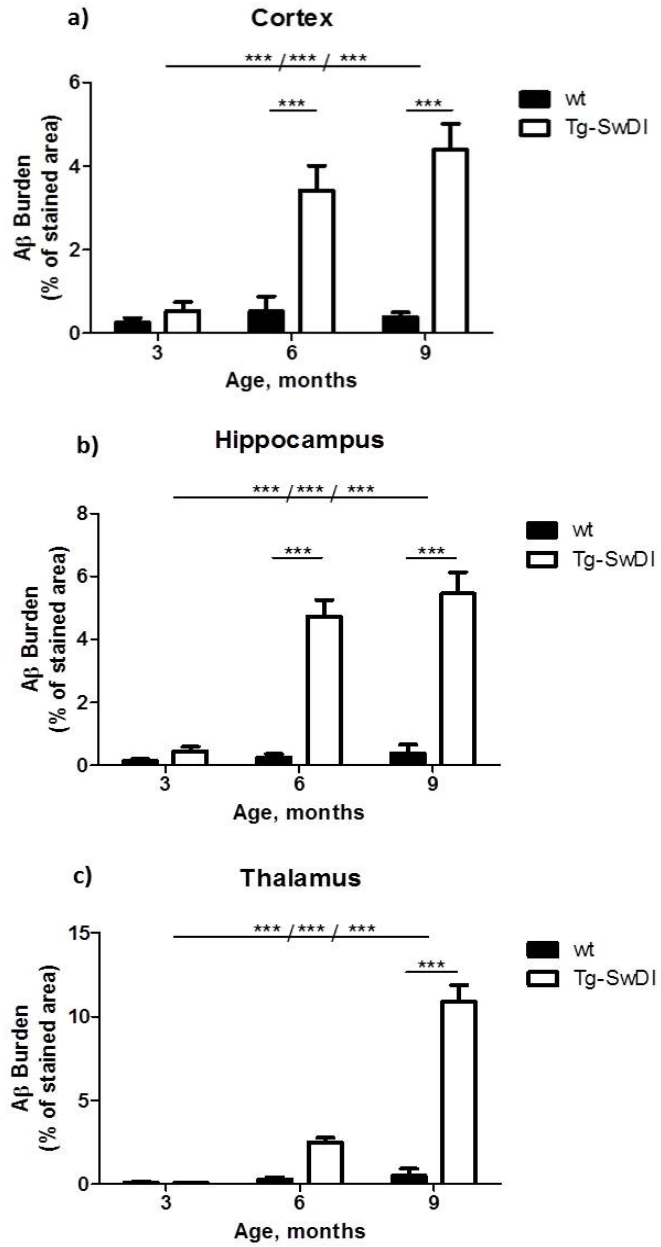

Figure 3.5. Aβ deposition increases over time in the transgenic mouse model Tg-SwDI. Quantitative analysis of Aβ deposition was assessed by measuring the percentage of stained area, represented in the graphs. The data presented are the means ± S.E.M.; two-way ANOVA: cortex: significant effect of age ($F_{(2,58)} = 10.59$, ***p = 0.0001), significant effect of genotype ($F_{(1,58)} = 43.15$, ***p < 0.0001), significant interaction ($F_{(2,58)} = 9.040$, ***p = 0.0004), Bonferroni post-test (***p < 0.001) (a); hippocampus: significant effect of age ($F_{(2,56)} = 16.80$, ***p < 0.0001), significant effect of genotype ($F_{(1,56)} = 73.33$, ***p < 0.0001), significant interaction ($F_{(2,56)} = 14.07$, ***p < 0.0001), Bonferroni post-test (***p < 0.001) (b); thalamus: significant effect of age ($F_{(2,58)} = 50.91$, ***p < 0.0001), significant effect of genotype ($F_{(1,58)} = 67.87$, ***p < 0.0001), significant interaction ($F_{(2,58)} = 44.52$, ***p < 0.0001), Bonferroni post-test (***p < 0.001) (c).

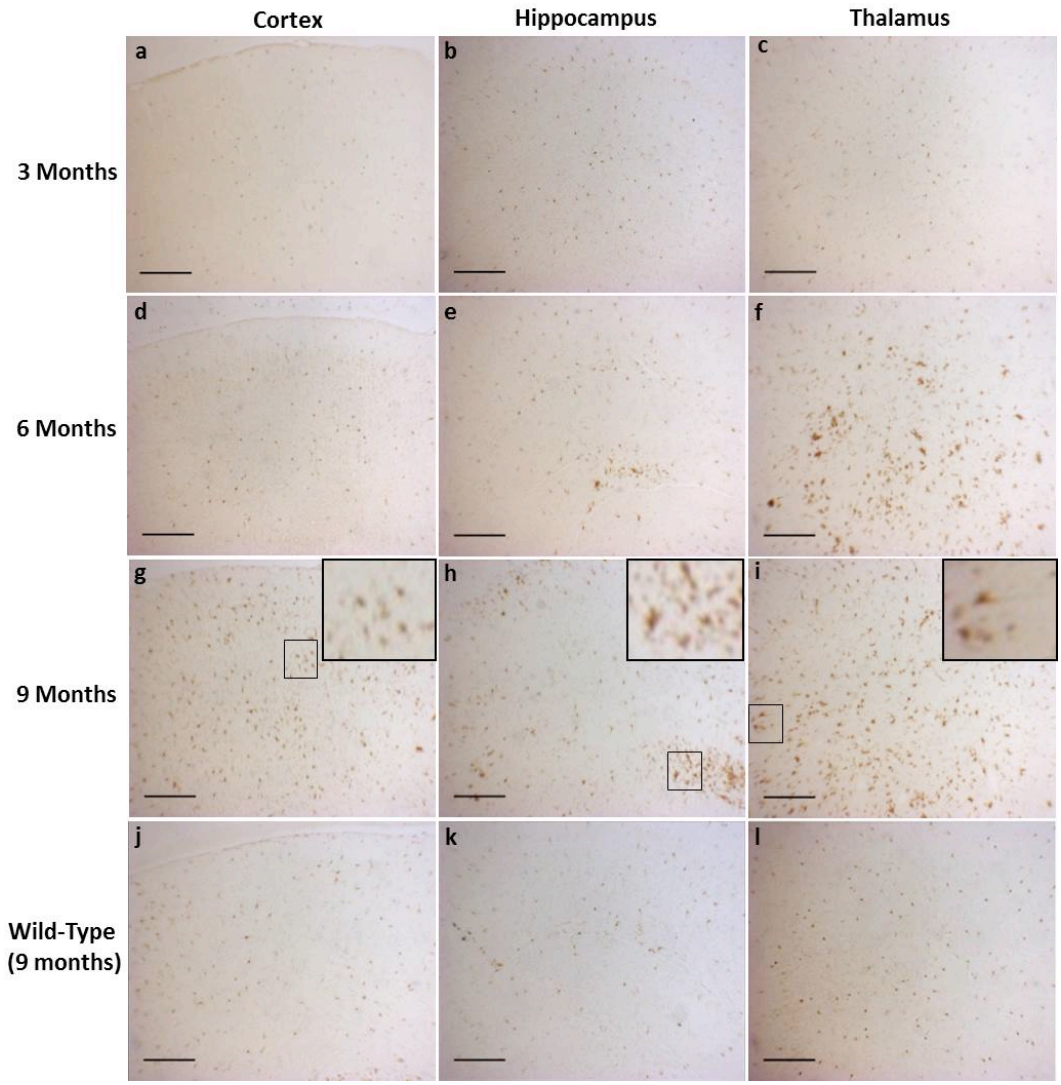

Figure 3.6. Temporal increase of microglial activation in the transgenic mouse model Tg-SwDI. Transgenic and wild type animals were sacrificed at 3, 6 and 9 months of age and histological analysis of the cortex (a, d, g, j), hippocampus (b, e, h, k) and thalamus (c, f, i, l) was performed. Sections were immunostained and microglia was visualised using the specific marker Iba1 (Scale bar= 200 μm).

Quantitative measurement of percentage area stained with Iba1 revealed that microglial activation was significant only by 9 months of age in cortex and hippocampus of the transgenic animals when compared to the wild-type controls (Figure 3.7, a and b, respectively), whereas in the thalamus extensive and significant activation of microglial cells was found by 6 months (Figure 3.7, c). Note that this pattern of activation follows the load of amyloid across the different brain regions.

Furthermore, comparison of the results obtained from both Aβ and Iba1 immunostaining analyses revealed a positive correlation between both proteins (Figure 3.8), suggesting that amyloid accumulation in this model is associated to the initiation of an inflammatory process.

3.3.4. Astrocyte activation.

In order to determine astrocyte reactivity in the Tg-SwDI model, immunostaining was conducted using a marker that recognises the glial fibrillary acidic protein (GFAP), an intermediate filament protein that is highly expressed in astrocytes and upregulated during astrogliosis, therefore used to study astrocyte activation.

As shown in Figure 3.9, there was strong astrocyte activation in cortex, hippocampus and thalamus of the transgenic animals. GFAP upregulation was progressive in the cortex and thalamus and was markedly high in young mice in the hippocampus. As comparison, representative images from 9 months old wild-type mice are shown (Figure 3.9, j-l). The image analysis showed that GFAP immunostaining was significantly higher in the Tg-SwDI mice when compared to wild-type controls starting at 6 months of age in the cortex and thalamus and as early as 3 months in the hippocampus (Figure 3.10).

This result indicates that the Tg-SwDI model presents age-dependent increased astrogliosis.

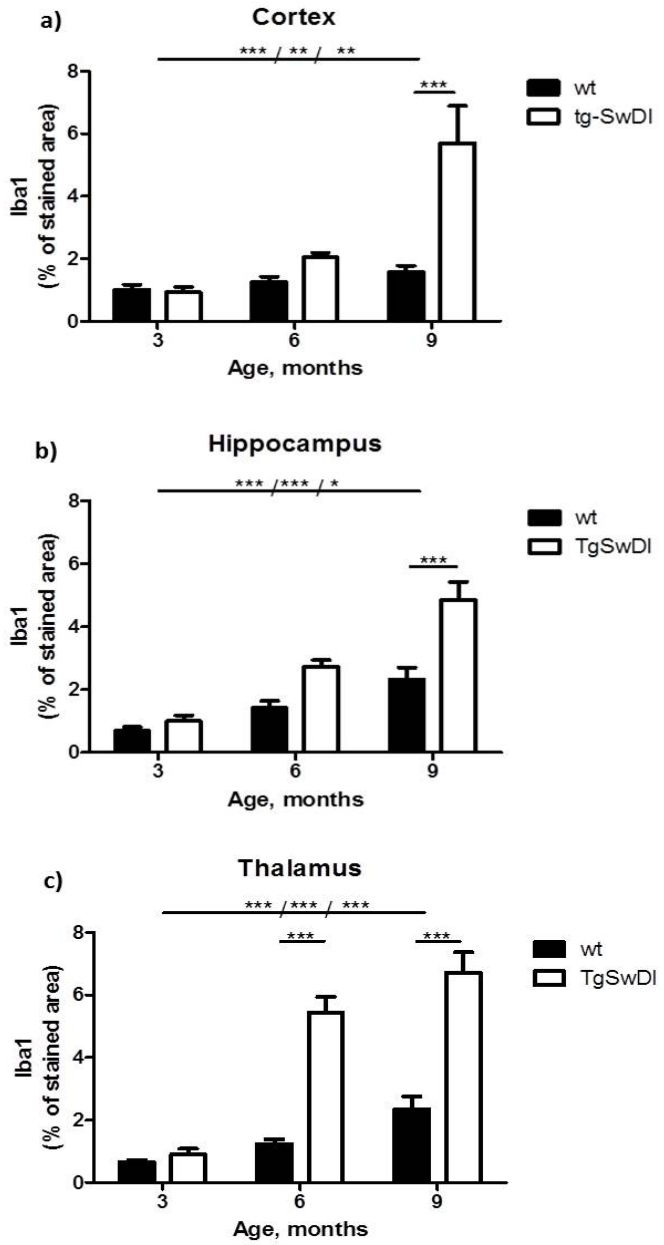

Figure 3.7. Microglial activation increases over time in the transgenic mouse model Tg-SwDI. Quantitative analysis of Iba1 signal was assessed by measuring the percentage of stained area, represented in the graphs. The data presented are the means ± S.E.M.; two-way ANOVA: cortex: significant effect of age ($F_{(2,58)}$ = 9.332, ***p = 0.0003), significant effect of genotype ($F_{(1,58)}$ = 8.358, **p = 0.0054), significant interaction ($F_{(2,58)}$ = 5.998, **p = 0.0043), Bonferroni post-test (***p < 0.001) (a); hippocampus: significant effect of age ($F_{(2,57)}$ = 26.12, ***p < 0.0001), significant effect of genotype ($F_{(1,57)}$ = 19.17, ***p < 0.0001), significant interaction ($F_{(2,57)}$ = 4.333, *p = 0.0177), Bonferroni post-test (***p < 0.001) (b); thalamus: significant effect of age ($F_{(2,58)}$ = 31.32, ***p < 0.0001), significant effect of genotype ($F_{(1,58)}$ = 56.99, ***p < 0.0001), significant interaction ($F_{(2,58)}$ = 10.71, ***p = 0.0001), Bonferroni post-test (***p < 0.001) (c).

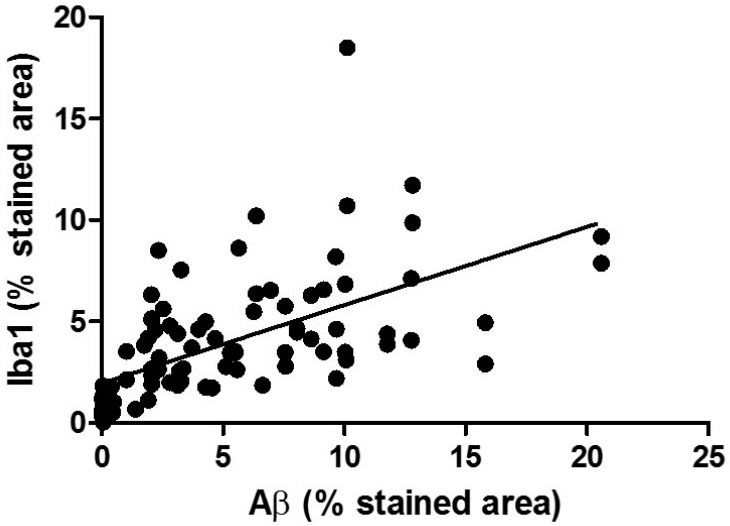

Figure 3.8. Aβ deposition correlates with increased microglial activation. Pearson correlation: Scatter plot shows a positive correlation between percentage of Iba1 stained area and percentage of Aβ stained area, Pearson correlation test: r = 0.3630, ***p < 0.0001.

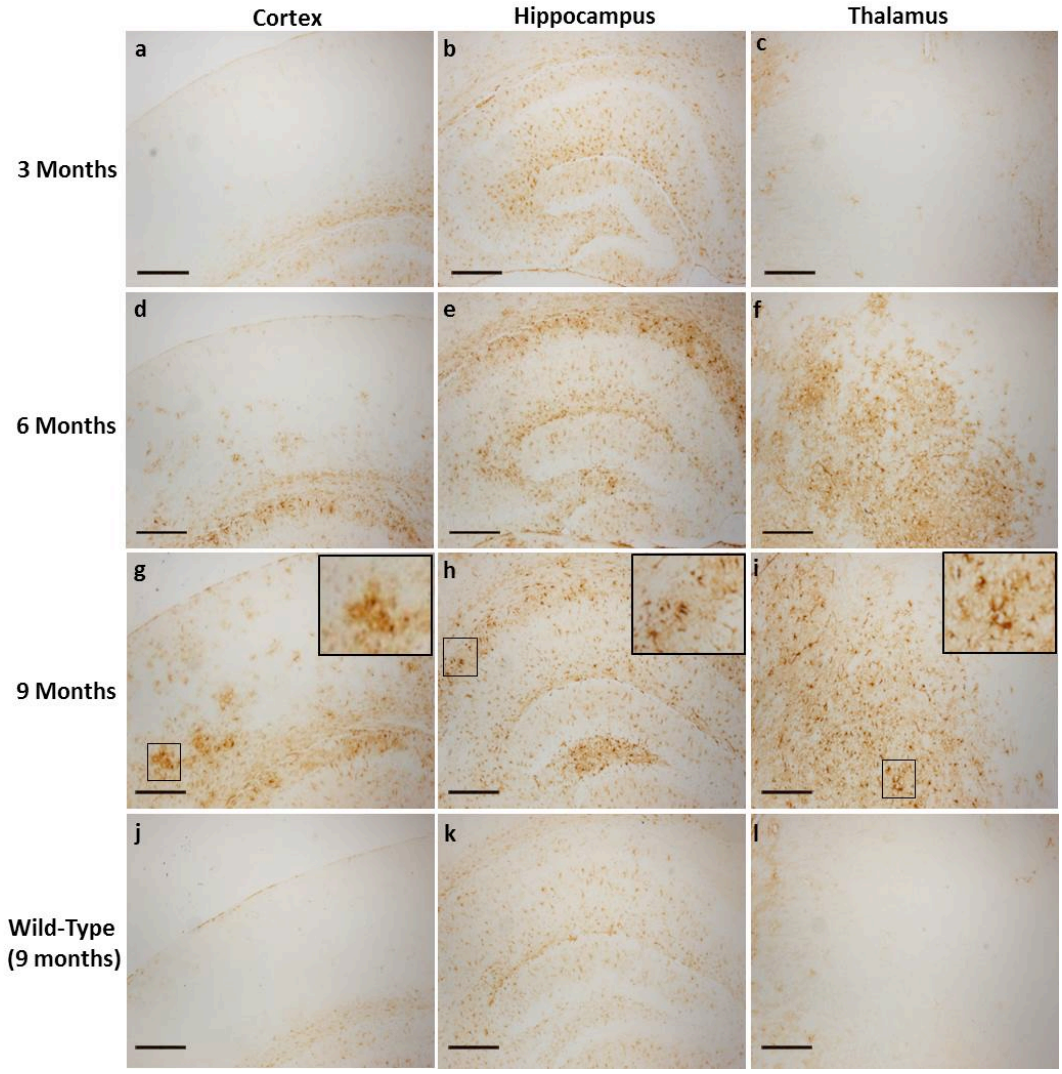

Figure 3.9. Temporal increase of astrocyte activation in the transgenic mouse model Tg-SwDI. Transgenic and wild type animals were sacrificed at 3, 6 and 9 months of age and histological analysis of the cortex (a, d, g, j), hippocampus (b, e, h, k) and thalamus (c, f, i, l) was performed. Sections were immunostained and astrocytes were visualised using a specific marker of GFAP (Scale bar= 200 μm).

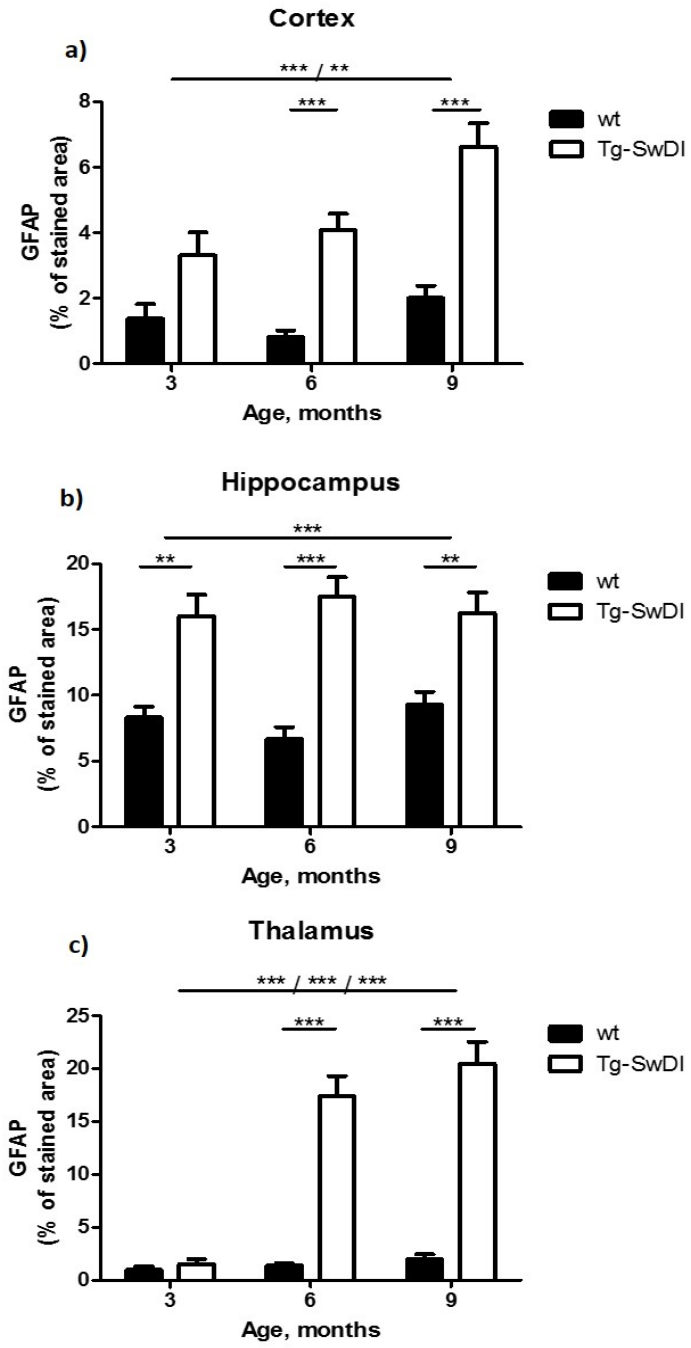

Figure 3.10. Astrocyte activation increases over time in the transgenic mouse model Tg-SwDI. Quantitative analysis of GFAP signal was assessed by measuring the percentage of stained area, represented in the graphs. The data presented are the means ± S.E.M.; two-way ANOVA: cortex: significant effect of age ($F_{(2,52)} = 7.469$, **p = 0.0014), significant effect of genotype ($F_{(1,52)} = 46.43$, ***p < 0.0001), Bonferroni post-test (***p < 0.001) (a); hippocampus: significant effect of genotype ($F_{(1,52)} = 53.72$, ***p < 0.0001), Bonferroni post-test (**p < 0.01; ***p < 0.001) (b); thalamus: significant effect of age ($F_{(2,52)} = 21.94$, ***p < 0.0001), significant effect of genotype ($F_{(1,52)} = 85.31$, ***p < 0.0001), significant interaction ($F_{(2,52)} = 18.40$, ***p < 0.0001), Bonferroni post-test (***p < 0.001) (c).

3.3.5. Cerebral amyloid angiopathy.

In order to temporally characterise the accumulation of Aβ in the cerebral vasculature of Tg-SwDI mice, colocalisation analysis of Aβ with blood vessels was performed in the thalamus, which has been described to be one of the brain areas showing higher levels of CAA in this model (Davis et al., 2004).

As shown in Figure 3.11, the vessels (red channel) were visualised with a specific marker of collagen IV, a type of collagen found in the basement membrane carrying out a structural function within the vasculature. The antibody 6E10 was used to visualise Aβ (green channel).

Quantitative analysis of the colocalisation of Aβ with vessels as an index of vascular Aβ revealed that the load of vascular Aβ was significantly increased as the animals aged, as well as the number of amyloid containing vessels (Figure 3.11, d and e respectively), suggesting that Aβ deposition increases and distributes uniformly in the vasculature of the Tg-SwDI model over time.

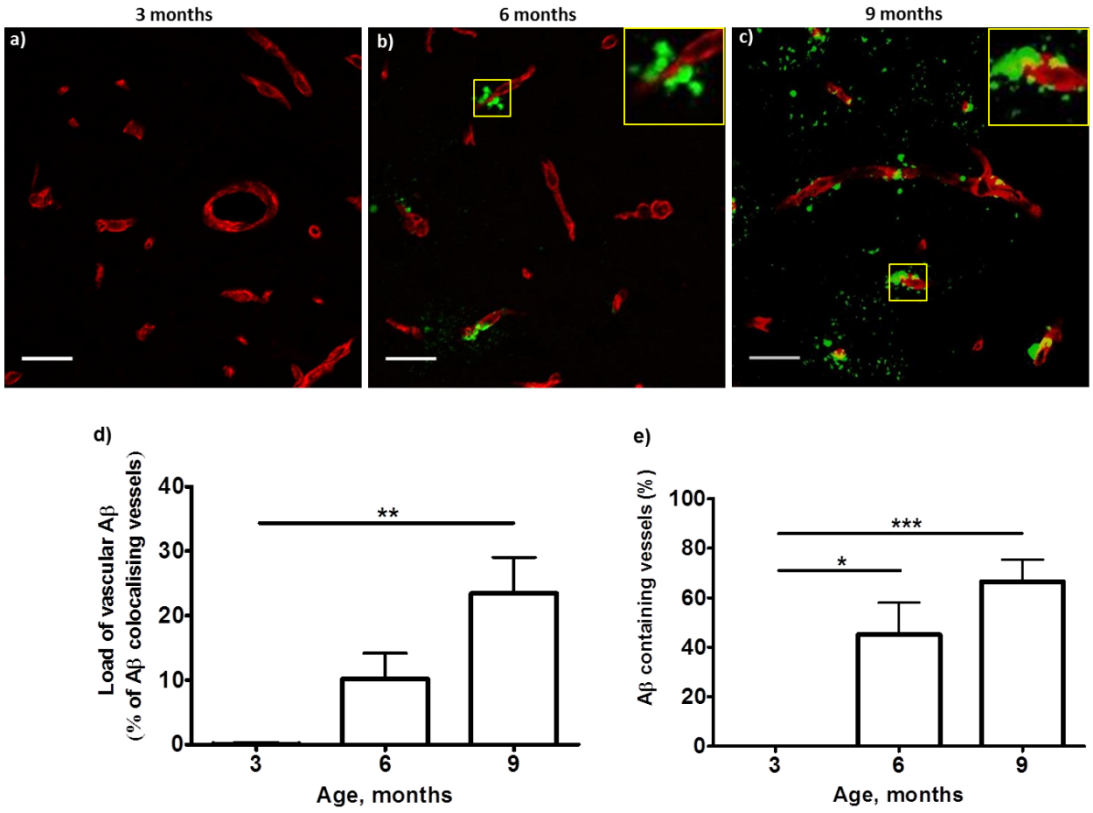

Figure 3.11. Vascular Aβ increases over time in the transgenic mouse model Tg-SwDI. Double immunostaining was performed using anti-collagen IV (vessels) and 6E10 (Aβ). Colocalisation analysis of the merged images was made by calculating the proportion of vessels (red channel) colocalising with Aβ (green channel) (d). The proportion of Aβ containing vessels was quantified and represented in the graph (e). The data presented are the means ± S.E.M., one-way ANOVA: $p < 0.05$, n= 32 (scale bar= 30 μm).

3.4. Discussion.

The aim of this study was to temporally characterise the Aβ and Aβ-related pathology in the Tg-SwDI mouse model. Increasing APP expression was found as well as Aβ aggregation as the animals aged in the cortex, hippocampus and thalamus, which was accompanied by extensive and progressive activation of microglial and astrocytic cells.

3.4.1. APP expression and Aβ accumulation.

The results from this study, in agreement with the original publication describing the Tg-SwDI model (David et al., 2004) show an age-dependent regional accumulation of amyloid predominantly in the thalamus. Furthermore, in agreement with the results obtained from Van Nostrand group, vascular amyloid is particularly prominent in the model (Davis et al., 2004). However, there are details in the temporal accumulation of amyloid and APP that differ from the results obtained by Davis and colleagues (Davis et al., 2004). For example, the authors of this paper observed that human APP expression levels were modest and lower compared to the endogenous mouse APP. In contrast, in the present study higher levels were observed in the transgenic mice when compared to the wild-type controls. One possible explanation for this difference, apart from the fact that different approaches were used to determine this (western blot in the published study and immunohistochemistry in the current study), is that the antibody used in the present study recognises both murine and human APP, which could be the reason why higher levels were observed in the Tg-SwDI animals. Moreover, an important difference between both studies that needs to be considered when comparing this data is that all the published analyses conducted by Van Nostrand group (Davis et al., 2004) were done in heterozygous Tg-SwDI mice and differently, the current study was performed using homozygous animals. This could be another explanation for the contrasting results between the two studies. Also, it is important to note that the authors observed that APP levels remained consistently low over time, and

differently, the results from the current study revealed a significant and progressive increase in the levels of the protein as the animals aged.

In parallel with the increasing APP levels, age-dependent progression of Aβ accumulation was observed. These findings are in line with those from Davis and colleagues who, despite the low levels of APP found, also demonstrated early onset and robust temporal accumulation of Aβ (Davis et al., 2004). Quantification of the regional accumulation of Aβ revealed that by 12 months, vascular accumulation was strong in the thalamus and subiculum. In agreement, the present study found higher accumulation of the protein in the thalamus compared to the cortex and hippocampus; consequently, quantitation of vascular Aβ was performed focusing only in this region. Again, similarly to what was described by the authors, age-dependent increase of amyloid associated to the cerebrovasculature was found in the present study.

3.4.2. Aβ-related inflammation.

Inflammation has been largely studied in relation to amyloid deposition and has been described to positively correlate, particularly with vascular Aβ (Akiyama et al., 2000; Mrak and Griffinbc, 2001; Patel et al., 2005, Zabel et al., 2013; Baron et al., 2014). Microglia and astrocytes are key players involved in the development of inflammation and both cells have been shown to be associated with microvascular amyloid deposits (Grabowski et al., 2001; Eng et al., 2004). Hence, a further aim of this study was to explore the Aβ-related microglial and astrocyte activation in the Tg-SwDI model.

The results obtained suggest that amyloid deposition occurred before microglial activation in cortex and hippocampus. In both regions there was significant Aβ deposition by 6 months of age but microglial activation was observed only by 9 months. In contrast, although amyloid deposition was significantly higher in the transgenic mice compared to controls by 9 months of age in the thalamus, microglial activation occurred earlier in this region, by 6 months. As mentioned above, vascular

Aβ deposition has been previously described to be higher in thalamus than other regions in the brain of this transgenic mouse line. Hence, it is possible that the regional difference of microglial activation observed in the present study may be related to the vascular Aβ deposition, which has been shown to be associated with a stronger immune response than parenchymal amyloid accumulation. Indeed, a previous study performed with homogenates of parenchymal and vessel enriched fractions extracted from human *post mortem* brains from AD patients with parenchymal and vascular Aβ and AD patients with only parenchymal amyloid, revealed higher expression levels of inflammatory markers in the samples from subjects that had CAA compared to those who presented only parenchymal amyloid. Moreover, inflammation was markedly associated with vessels containing amyloid compared to those that did not presented CAA (Zabel et al., 2013). The analysis of astrocyte activation in the present study revealed progressive astrogliosis over time in the transgenic mice compared to the wild-type controls. These results are in line with a study conducted by Miao and colleagues, where large number of reactive astrocytes and activated microglia were observed in the Tg-SwDI model. Furthermore, reduction of cerebrovascular amyloid, obtained by breeding Tg-SwDI mice with apoE knock-out mice, resulted in decreased number of microglia and astrocytes emphasising the link between CAA and inflammation (Miao et al., 2005).

Compelling evidence has demonstrated that microglial activation and astrogliosis are associated with increased production of pro-inflammatory cytokines, neurotoxins and ROS, which have been suggested to contribute to cognitive decline in AD (Combs et al., 2001; Mrak and Griffin, 2001; Streit, 2004). Interestingly, anti-inflammatory treatment with minocycline reduced the neuroinflammation and induced improvement of the behavioural performance in the Tg-SwDI model without changing Aβ levels (Fan et al., 2007). This evidence highlights the important role of inflammation in the mechanisms by which amyloid leads to cognitive alterations in the model. It is important to note that microglia and astrocytes play an important role at the NVU. In transgenic models of AD, the response of these cells is heterogeneous and can potentially be protective as well as detrimental. This is further discussed in the next chapter.

3.4.3. Neurovascular alterations.

Numerous transgenic mouse lines have been generated to recapitulate the main neuropathological futures of AD and have been widely used in the field. Although the creation of these mouse models is based on the genetic mutations that lead to the development of the disease, which constitute less than 5% of the cases, both familial and sporadic AD present markedly similar pathology. Since AD constitutes a multifactorial disorder, each model displaying particular hallmarks of the disease is useful to understand a very specific aspect of the pathology. The transgenic Tg-SwDI model, expressing the mutant human APP, mimics several features of the Dutch- and Iowa-type familial CAA, and integrates the early onset of Aβ accumulation with high association of the protein to the cerebrovasculature. Despite the fact that the Tg-SwDI model fails to recapitulate other features of AD pathology including NFTs and neuronal death, it provides a robust experimental paradigm for the *in vivo* study of different aspects related to Aβ deposition, in particular to CAA.

Furthermore, this mouse line is particularly interesting in the study of AD as notably, CAA is present in almost all cases of the disease. Several studies have demonstrated that vascular Aβ deposition induces structural alterations to the blood vessels such as loss of smooth muscle cells, detachment of the tunica media and fibrinoid necrosis (Maeda et al., 1993; Zekry et al., 2003; Auriel and Greenberg, 2012), leading to functional deterioration of the cerebrovascular system. A study conducted in young Tg-SwDI mice (3-4 months) revealed that these animals present impaired functional hyperaemia and endothelium-dependent responses, assessed by laser-Doppler flowmetry, even before displaying substantial vascular amyloid accumulation (Park et al., 2013). A more recent study published by the same group, looking at the functional correlates of vascular damage induced by CAA in the same model, demonstrated that the neurovascular dysfunction in these mice is age-dependant and occurs in parallel to the structural alteration of the cerebrovasculature. These alterations included fragmentation of smooth muscle cells and disrupted pericyte morphology. Thus, although it wasn't a focus of the present study, it would be expected, given the increasing load of vascular amyloid, that there would be both

structural and functional alterations to the vasculature in these mice. Importantly, early but not late treatment with the reactive oxygen species (ROS) scavenger Mn(III)tetrakis(4-benzoic acid)porphyrin Chloride, resulted in the complete rescue of the cerebrovascular dysfunction, implicating oxidative stress in the mechanisms of CAA-induced neurovascular dysfunction in these animals (Park et al., 2014).

3.4.4. Summary and conclusions.

In summary, the current study has shown the temporal APP expression, accumulation of parenchymal and cerebrovascular Aβ and Aβ-related microglial and astrocytic activation that the Tg-SwDI mice exhibit. Although this mouse line do not reproduce the full spectrum of human AD pathology, including neuronal loss and tau tangles, both being important hallmarks of the disease, the pathology that this mice present shares evident resemblances with the pathology of human AD brains. The most important similarities between the model and the human AD pathology include the presence of amyloid aggregates and the inflammation triggered by Aβ accumulation (McGeer et al,. 1989). Notably, CAA is one of the features of human AD brains (Attems, 2005) and as shown in the present study, the Tg-SwDI mice display early and robust accumulation of the protein in the vessel wall.

This model represents a useful tool for the next studies within this thesis, which were aimed at investigating the effects of chronic cerebral hypoperfusion on Aβ deposition in the parenchyma and the cerebrovasculature and subsequently, its contribution to the appearance of structural changes in the NVU and to the development of MIs and haemorrhages. The data presented in the current chapter were useful in providing a basis to design the following studies since by assessing Aβ deposition in the parenchyma and the cerebrovasculature at different (early and late) time points, insights into the temporal and regional accumulation of the protein, as well as the Aβ-related pathology, in the Tg-SwDI mice were gained. This allowed us to induce the chronic cerebral hypoperfusion before substantial amyloid accumulation was observed, and therefore we were able to examine whether the reduced CBF may exacerbate Aβ accumulation and cerebrovascular alterations in these mice.

Chapter 4. The Effect of mild chronic cerebral hypoperfusion on Aβ accumulation and its consequences on the neurovascular integrity.

4.1. Introduction

Misfolding, aggregation and accumulation of Aβ in brain parenchyma and blood vessel walls are major hallmarks of AD brains and constitute critical stages for the pathogenesis of the disease. Importantly, several studies have shown that cerebral hypoperfusion can modulate Aβ metabolism, but this is ill-defined with reports showing that hypoperfusion can both increase (Kitaguchi et al., 2009; Okamoto et al., 2012; ElAli et al., 2013) and suppress (Yamada et al., 2011) Aβ deposition. Although the mechanistic basis by which hypoperfusion alters Aβ metabolism has not yet been established, there is evidence that a severe reduction of CBF may induce increased APP expression and processing leading to enhanced generation of Aβ (Kalaria et al., 1993; Bennett et al., 2000; Shi et al., 2000; van Groen et al., 2005; Zhiyou et al., 2009). On the other hand, it has been suggested that cerebrovascular alterations leading to brain hypoperfusion can induce defective vascular Aβ clearance. Such alterations impair the efficient perivascular lymphatic drainage, triggering Aβ accumulation in the vessel walls with further blockage of the drainage pathways, leading to accumulation of the protein in the brain (Weller et al., 1998; Weller et al., 2008; Sagare et al., 2013). Thus, the pathways by which cerebral hypoperfusion is implicated in the pathogenesis of AD may be directly associated to the induction of accelerated accumulation of amyloid. However, the mechanistic basis by which this occurs remains unclear.

Cerebral microinfarction is a common histopathological finding in *post-mortem* studies of AD patients (Brundel et al., 2012; van Rooden et al., 2014) and has often been linked to CAA. However, the analysis of the association between CAA and the development of MIs remains inconclusive, with data showing positive (Olichney et al., 1995; Haglund et al., 2006; Okamoto et al., 2009; Soontornniyomkij et al., 2010) weak (van Rooden et al., 2014) and no correlation (Launer et al., 2008; Kövari et al., 2013) between these parameters, suggesting that vascular amyloid might play a role, but cannot be considered as the only contributor factor for the development of these lesions. Interestingly, microinfarction has been shown to occur in areas of brain hypoperfusion in AD patients and this has also been demonstrated in mouse models

of cerebral hypoperfusion (Suter et al., 2002; Shibata et al., 2004; Okamoto et al., 2012). Additionally, evidence has shown that vascular accumulation of Aβ constitutes the main cause of cerebral haemorrhage in the elderly (McCarron et al., 2000; Rosand et al., 2000; Charidimou et al., 2012) and there is a positive correlation between the severity of CAA and the presence of haemorrhages (Vonsattel et al., 1991).

Furthermore, dysfunction of the NVU occurs during normal ageing and has been proposed to contribute to the neurodegenerative process in AD (Iadecola, 2004; Zlokovic, 2011). Interestingly, cerebral hypoperfusion, which is also a future of the normal ageing brain, is associated with the altered activity of ion pumps at the BBB (Zlokovic, 2008). This altered activity at the BBB due to reduced blood flow may promote the accumulation of toxins in the brain (ElAli and Hermann, 2011) leading to a metabolically altered microenvironment that contribute to neurovascular dysfunction. This evidence supports some aspects of the vascular hypothesis of AD which states that, during ageing, VRFs alter the NVU leading to chronic cerebral hypoperfusion and BBB dysfunction contributing to cognitive decline (de la Torre and Mussivand, 1993). In addition, there is increasing experimental evidence showing alterations in specific structures of the NVU including astrocytes (Wilcock et al., 2009; Moftakhar et al., 2010; Merlini et al., 2011; Yang et al., 2011; Fukuda and Badaut, 2012) and TJs (Marco and Skaper, 2006; Hartz et al, 2012) triggered by the accumulation of Aβ.

Taken together, this evidence suggests that the mechanism by which VRFs can contribute to the development of AD may be through the alteration of the neurovasculature, in parallel with the induction of Aβ accumulation which may exacerbate those alterations and perpetuate neurovascular dysfunction. Nevertheless, the contribution of these factors in combination remains unclear.

4.1.1. Hypothesis and aim of study.

It was hypothesised that chronic cerebral hypoperfusion leads to the accumulation of parenchymal and vascular Aβ, triggering the development of MIs and haemorrhages and altering the NVU integrity.

The specific aims of this study were as follows:

1. To determine parenchymal and cerebrovascular Aβ levels in response to hypoperfusion, at two different time points post-surgery (1 and 3 months). A detailed examination of the isoforms and species of Aβ and type of blood vessel associated to its accumulation was carried out. If increased Aβ levels were to be found, a further aim was to determine the mechanism by which this happens. Therefore, the effect of hypoperfusion on APP and receptors involved in Aβ clearance (LRP and Scara1) were studied.

2. To investigate the effects of hypoperfusion and Aβ pathology on the development of MIs and haemorrhages, and the potential alteration of astrocyte and tight junction integrity. Furthermore, potential links between hypoperfusion, Aβ and NOX2 with the development of MIs were investigated.

4.2. Methods.

4.2.1. Animals and surgery.

Male, 3 months old Tg-SwDI and wild-type (C57Bl/6J) mice were used. One cohort was used for biochemical studies and a second cohort was used for immunohistochemical studies.

Animals underwent bilateral common carotid artery stenosis or sham surgery as previously described in section 2.2. Mice were sacrificed 1 or 3 months after the surgery. Group sizes are listed in Table 2.1.

4.2.2. Perfusion and tissue processing.

Animals used for immunohistochemical studies were saline perfused followed by perfusion fixation as described in section 2.4.2. The left hemi-brain was processed for vibratome cutting and sagittal sections were produced as described in section 2.5.1. The right hemi-brain was processed for paraffin embedding and sagittal sections were produced as described in section 2.5.2.

Animals used for biochemical studies were saline perfused as described in section 2.4.1. The left hemi-brain was used to generate parenchymal and vessel enriched fractions as described in section 2.9. The right hemi-brain was used to prepare total brain homogenates. Protein extraction and quantification were performed as described in section 2.10.

4.2.3. Immunohistochemistry.

Immunohistochemistry was carried out as described in section 2.6. Tissue sections at anatomical level corresponding to 1.92 mm from midline (Franklin and Paxinos, 1997) were used. Aβ, collagen IV, SMA and AQP4 immunostainings were

conducted using fluorescent labelling. Iba1 immunostaining was performed using immunoperoxidase labelling.

4.2.4. Histological detection of MIs and haemorrhages.

The detection of MIs was done by using H&E staining, which was performed as previously described in section 2.7.1. Haemorrhages were identified using Prussian blue staining as described in section 2.7.2. Tissue sections at anatomical level corresponding to 1.92 and 1.56 mm from midline (Franklin and Paxinos, 1997) were used.

4.2.5. Image analysis.

For the analyses of Aβ/collagen 4, SMA/collagen 4 and AQP4/collagen 4 immunostainings, four images of the thalamus per brain were acquired as described in section 2.8 with a 40x objective at a 1024 x 1024 pixel resolution. Parenchymal Aβ was determined by subtracting the percentage of stained area occupied by the colocalised pixels to the percentage of stained area of the green channel (Aβ). Colocalisation analysis between blood vessels and Aβ was done by calculating the Manders coefficient. To classify blood vessels into small or large, the width of the vessels containing or not SMA was measured using ImageJ. To determine the proportion of Aβ containing vessels, colocalisation analysis between vessels and Aβ was performed and the proportion of Aβ containing (small or large) vessels was quantified; each vessel branch was considered as a single vessel. Colocalisation analysis between blood vessels and AQP4 was performed by calculating the ratio between the area occupied by colocalising pixels and percentage of collagen IV (red channel) stained area.

For the study of MIs, two sections per brain were analysed and one image of the thalamus per section was acquired as described in section 2.8, at 10x magnification. MIs were defined as sharply delimited areas of tissue pallor that were accompanied

by microglial proliferation identified by Iba1 immunostaining in adjacent sections. The area covered by infarcted tissue was measured.

For the study of haemorrhages, two sections per brain were scanned. Haemorrhages were identified by the presence of ferric iron deposits on Perls stained sections. The presence or absence of haemorrhages in each mouse was recorded.

4.2.6. Enzyme-linked immunosorbent assay.

Levels of both Aβ40 and Aβ42 (Invitrogen) were determined in the soluble and insoluble protein fractions extracted from the parenchymal and the vessel enriched fractions. NOX2 (Cusabio), Scara1 (Cusabio) and AQP4 (Invitrogen) levels were assessed in total proteins extracted from brain homogenates. In all experiments, manufacturer's instructions were used to perform the assays.

4.2.7. Western blot.

Western blotting was performed as described in section 2.12. Total proteins extracted from brain homogenates were used to detect APP, APP-CTF's and GFAP. Protein extracts from vessel enriched fractions were used to detect LRP and claudin-5.

4.2.8. Statistical analysis.

The samples obtained from the two different time-points analysed (1 and 3 monhs) were used in independent assays, therefore the results obtained from the two different groups were statistically analysed independently.

Results from parenchymal and vascular Aβ measurements (Imaging and ELISA), APP, CTFs and LRP western blot assays and scara1 ELISA measurement, were analysed for statistical significance using unpaired t-test with $p < 0.05$.

For NOX2 and AQP4 ELISA measurements, GFAP and claudin-5 western blot assays, AQP4/collagen 4 colocalisation analysis and MIs study, statistical comparison was carried out using two-way ANOVA (with age and genotype as factors), followed by the Bonferroni post-test. For the association analyses, the Pearson correlation coefficient was determined.

4.3. Results.

4.3.1. Soluble Aβ levels are increased in response to cerebral hypoperfusion and precede fibrillar Aβ accumulation in the parenchyma.

In order to determine whether chronic cerebral hypoperfusion can increase Aβ accumulation in the parenchyma of Tg-SwDI mice, confocal microscopy was used to quantify Aβ deposition. However, no significant changes were observed between sham and hypoperfused groups following either 1 or 3 months (Figure 4.1). To further investigate whether chronic hypoperfusion may have an effect on the different pools of Aβ within the parenchyma, the levels of soluble and insoluble Aβ were quantified by ELISA. After 1 month of hypoperfusion, significantly increased levels of both Aβ40 and Aβ42 were found in the soluble protein fraction, when compared to the sham control. In contrast, the insoluble protein fraction remained unchanged. After 3 months of hypoperfusion, there were no significant changes between the sham and hypoperfused groups in the soluble fraction, however increased concentration of both Aβ40 and Aβ42 was observed in the insoluble fraction (Figure 4.2).

Although no changes were found by using the immunochemical approach, the ELISA constitutes a more sensitive detection method that allows the quantification of very low amounts of amyloid and therefore permitted the detection of the differences between the groups. These data suggest that hypoperfusion can modify Aβ metabolism, triggering an early increase of the protein followed by aggregation into insoluble fibrils in the parenchyma.

4.3.2. Delayed accumulation of vascular Aβ in response to cerebral hypoperfusion.

As shown in the previous chapter of the present thesis, Tg-SwDI mice exhibited minimal vascular accumulation of Aβ at 3 months of age. To examine whether chronic cerebral hypoperfusion may increase accumulation of Aβ in the

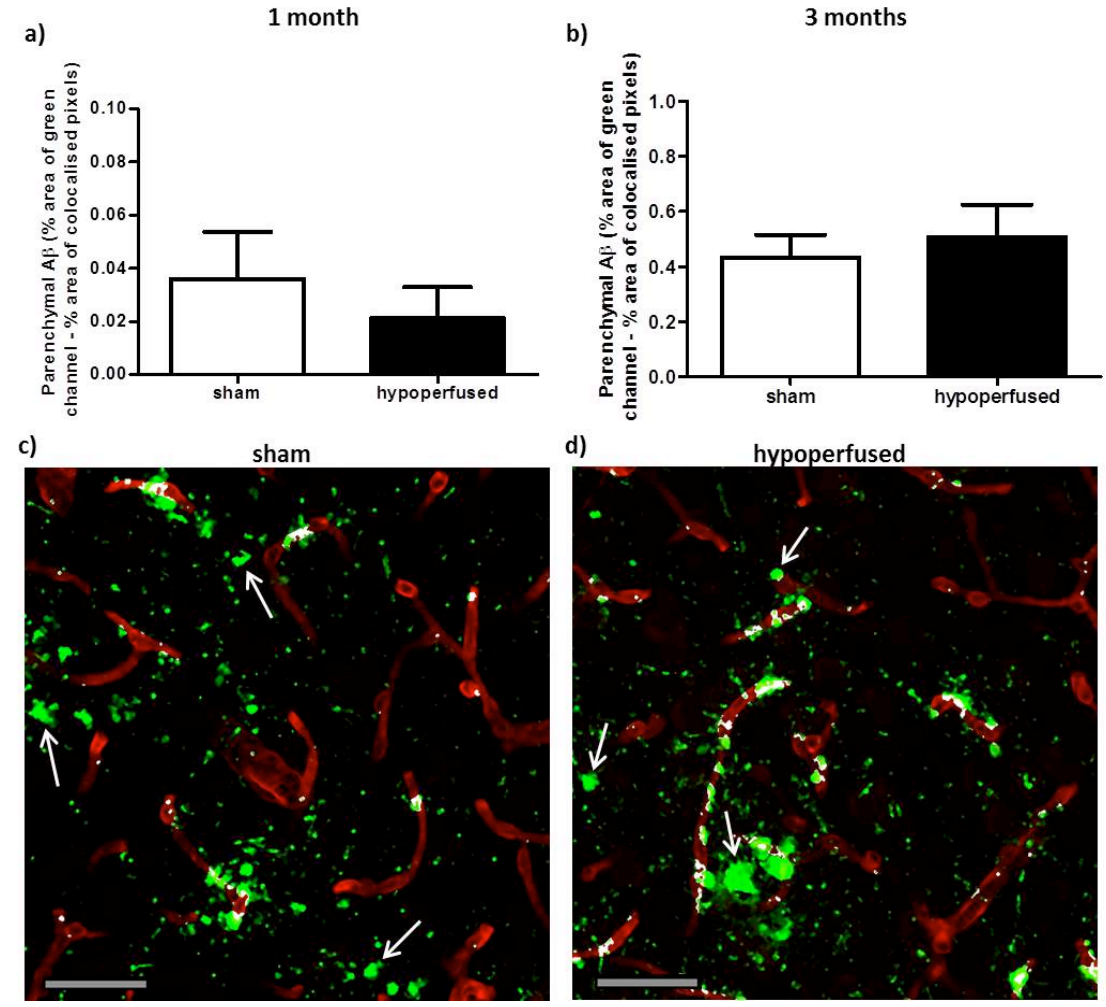

Figure 4.1. Parenchymal Aβ deposition following chronic cerebral hypoperfusion in Tg-SwDI mice. Double immunostaining was performed using markers of collagen (red) and Aβ (green). Parenchymal Aβ was determined using ImageJ, by subtracting the percentage of stained area occupied by the colocalised pixels (white area) to the percentage of stained area of the green channel. The result is represented in the graphs. The data presented are the means ± S.E.M. (unpaired t-test $p > 0.05$, 1 months n=19, 3 months n=18). Representative images from sham and 3 months hypoperfused mice are shown (scale bar = 50 μm).

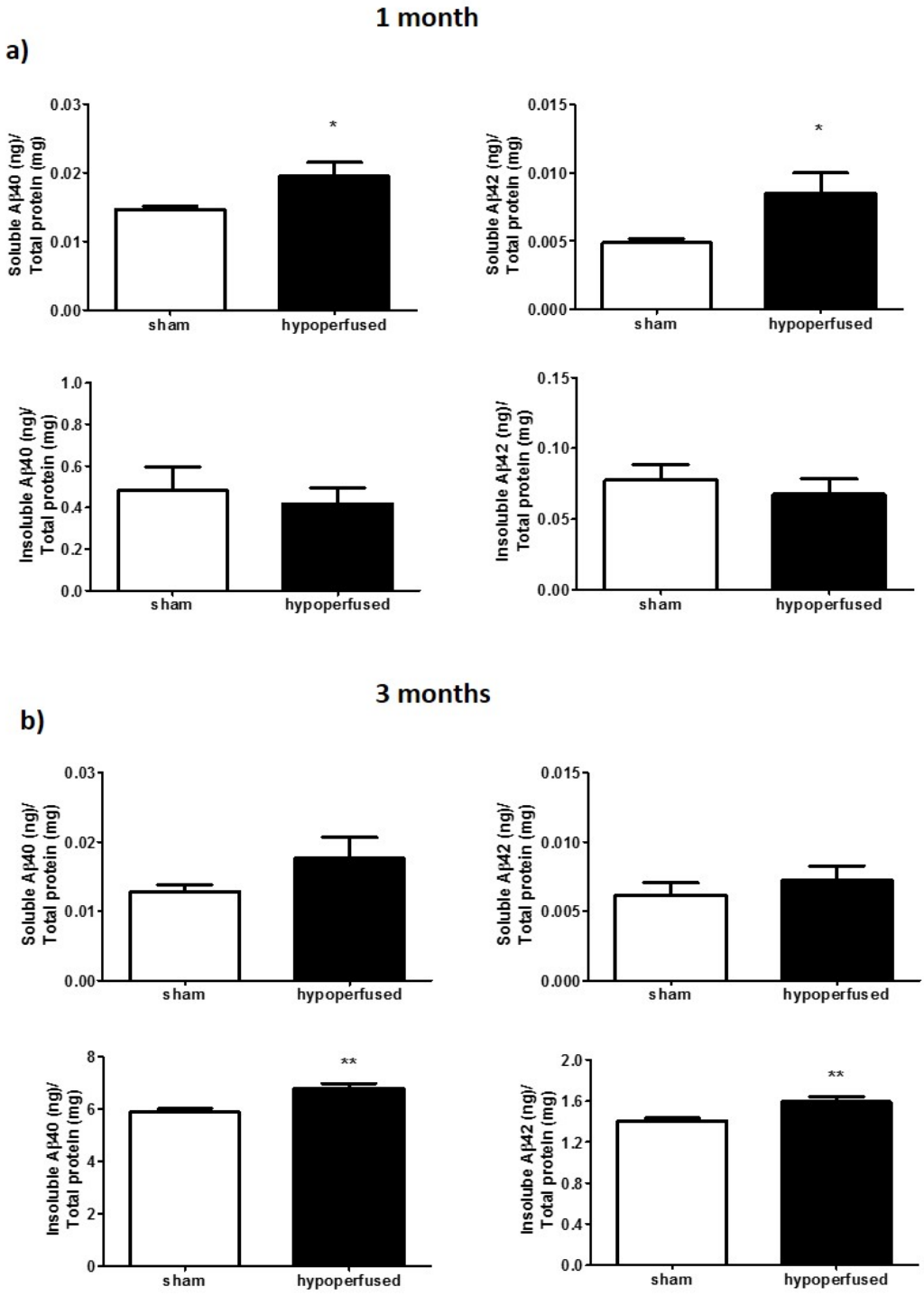

Figure 4.2. Chronic cerebral hypoperfusion induces early increase in soluble Aβ levels followed by fibrillar Aβ accumulation in the parenchyma of the transgenic mouse model Tg-SwDI. Tg-SwDI animals were sacrificed after 1 (a) and 3 (b) months of chronic cerebral hypoperfusion. Following sequential protein extraction, the levels of soluble and insoluble Aβ40/42 were quantified in the parenchymal fraction by ELISA. Graphs represent the levels of the protein normalised to total protein concentration. The data presented are the means ± S.E.M., *$p < 0.05$ (unpaired t-test, 1 months n=19, 3 months n=12).

cerebrovasculature of these mice, confocal microscopy was used to quantify Aβ colocalisation with the vasculature. After 1 month of hypoperfusion there were no changes in the levels of Aβ colocalised to vessels between sham and hypoperfused mice in the thalamus (Figure 4.3, a). Conversely, following 3 months of hypoperfusion, the levels of Aβ colocalised to vessels significantly increased in the hypoperfused animals, compared to the sham group (Figure 4.3, b-d, see arrows).

To further examine the pools of Aβ, ELISA measurement of protein extracts from the vessel enriched fraction was performed to determine quantitatively the levels of vascular Aβ40 and Aβ42. In agreement with the imaging analysis, no significant changes were observed between hypoperfused and sham animals after 1 month of hypoperfusion; however, following 3 months there was a significant increase in the levels of both Aβ40 and Aβ42 in the insoluble fraction of the hypoperfused group when compared to the sham animals (Figure 4.4).

Collectively, these results indicate that hypoperfusion promotes the build-up of fibrillar Aβ in the cerebrovasculature, process that is preceded by accumulation of the protein in the parenchyma.

4.3.3. Vascular Aβ deposition induced by chronic cerebral hypoperfusion occurs in small blood vessels.

To further explore whether the increased levels of vascular Aβ observed after 3 months of cerebral hypoperfusion were accumulating in small or large blood vessels, double immunostaining was used with a marker of collagen IV, to visualise all types of blood vessels and a marker of SMA, only present in larger vessels (Figure 4.5, a). In order to differentiate between the different types of vessels, image analysis of confocal micrographs was performed and vessels were classified into small (<6μm), corresponding to capillaries and large (>6μm), corresponding to bigger vessels including arterioles and arteries. Subsequently, the proportion of Aβ colocalising vessels (Figure 4.5, b) was calculated in each group. As represented in the graphs, the proportion of Aβ containing vessels was significantly higher in the

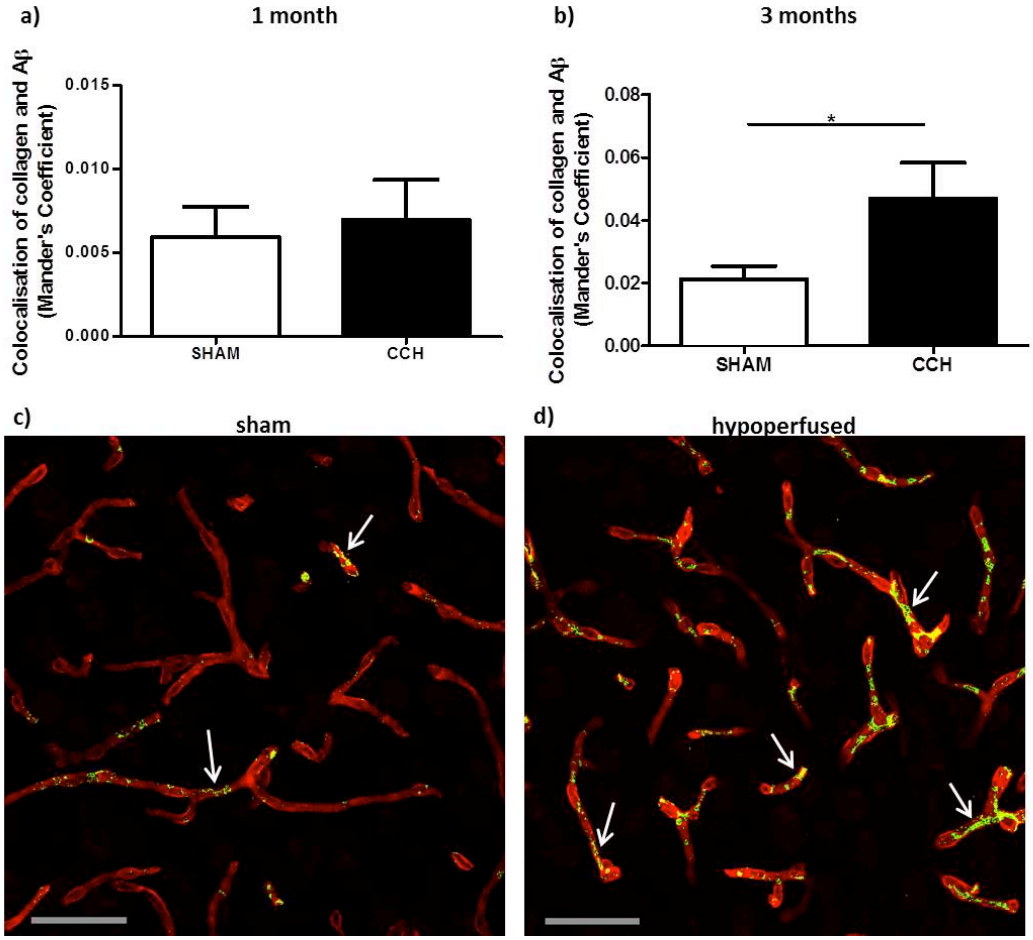

Figure 4.3. Chronic cerebral hypoperfusion accelerates Aβ/vasculature colocalisation in the transgenic mouse model Tg-SwDI. Double immunostaining was performed using markers of collagen (red) and Aβ (green). Colocalisation analysis of the merged images was made by calculating the Manders coefficient with ImageJ, represented in the graphs. The data presented are the means ± S.E.M., *$p < 0.05$ (unpaired t-test, 1 months n=19, 3 months n=18). Representative images from sham and 3 months hypoperfused mice, indicating Aβ/vasculature colocalisation are shown (scale bar = 50 μm).

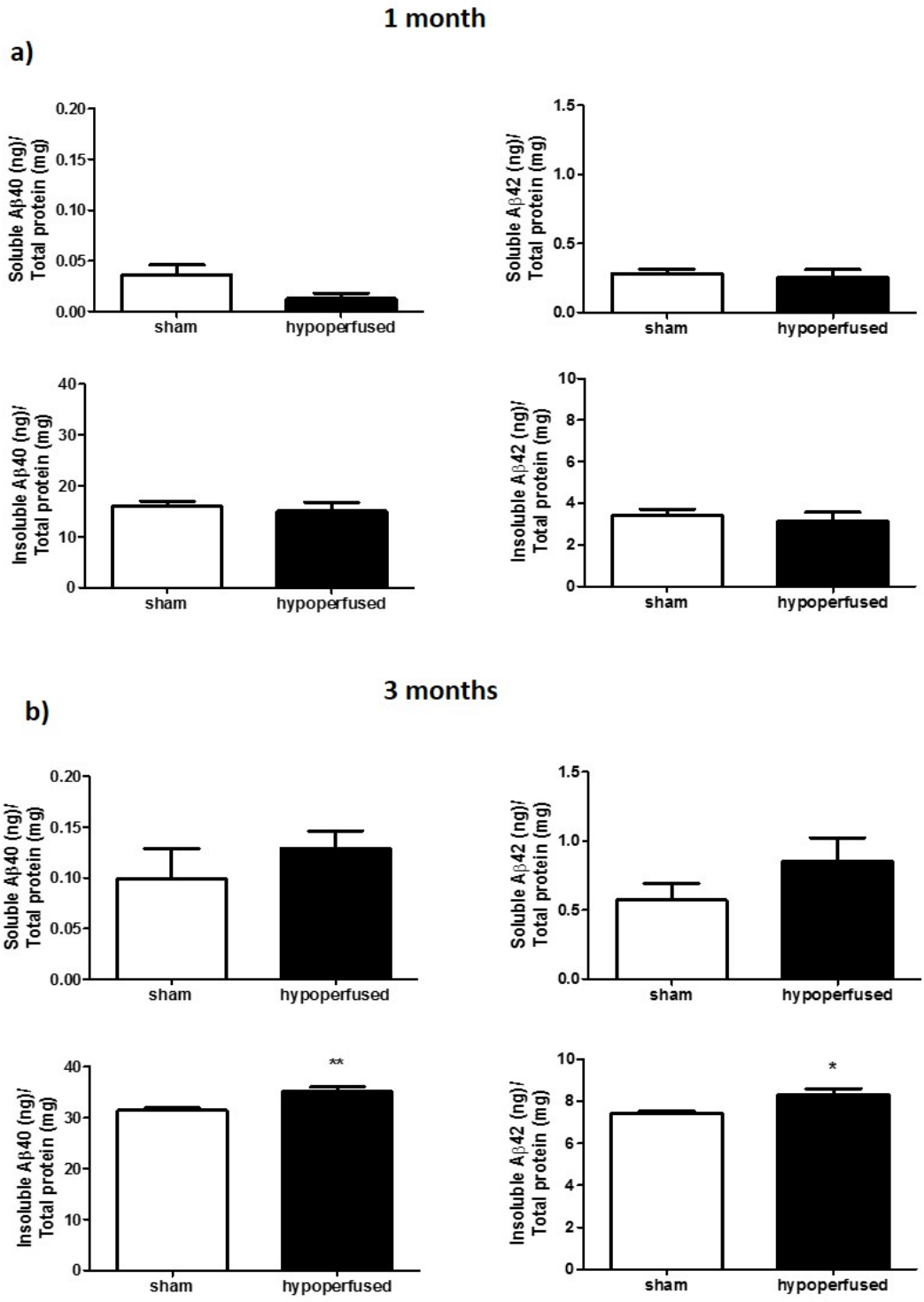

Figure 4.4. Chronic cerebral hypoperfusion accelerates vascular Aβ accumulation in the transgenic mouse model Tg-SwDI. Tg-SwDI animals were sacrificed after 1 (a) and 3 (b) months of chronic cerebral hypoperfusion. Blood vessel enriched fractions were generated, followed by sequential protein extraction. Subsequently, Aβ40/42 levels were quantified by ELISA. Graphs represent the levels of the protein normalised to total protein concentration. The data presented are the means ± S.E.M., *$p < 0.05$ (unpaired t-test, 1 months n=19, 3 months n=12).

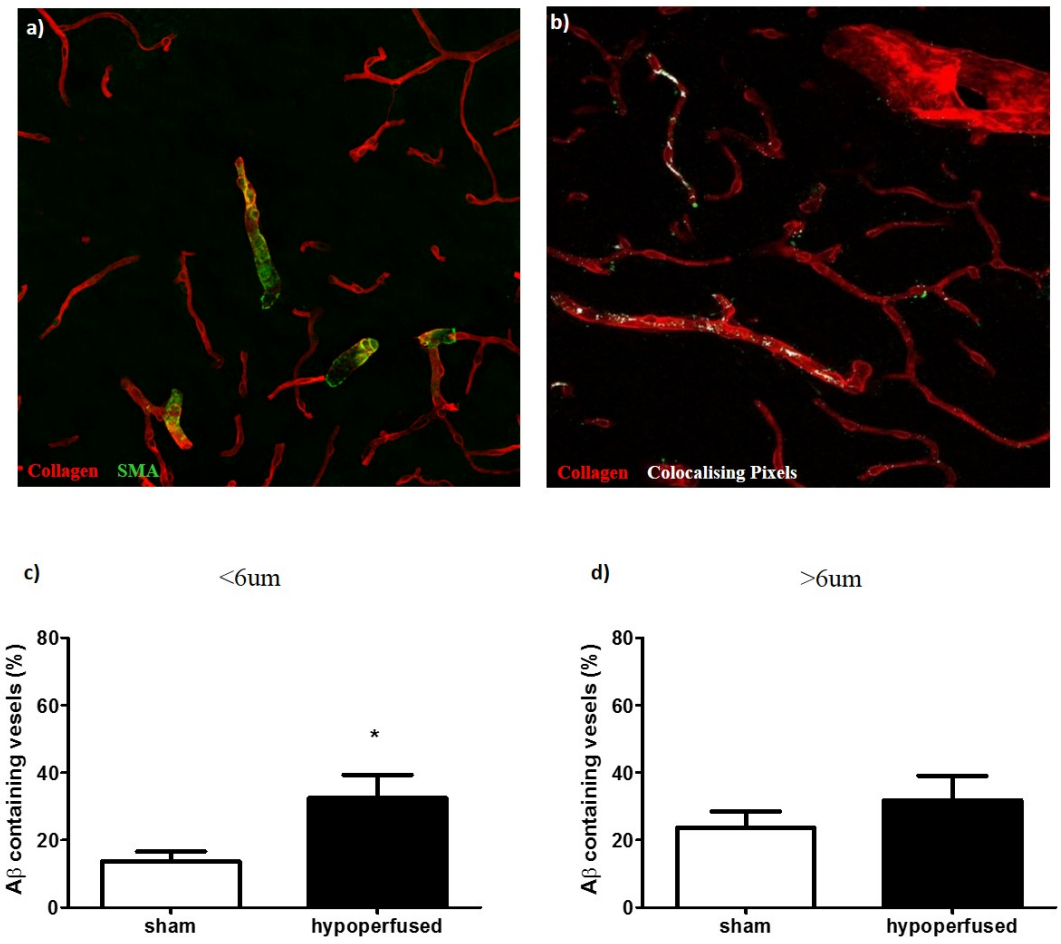

Figure 4.5. Vascular Aβ deposition induced by chronic cerebral hypoperfusion occurs in small blood vessels of Tg-SwDI mice. Double immunostaining was performed using markers collagen (red) and SMA (green) (a); subsequently, colocalisation analysis of the merged images was made with ImageJ (b). Graphs represent the proportion of Aβ containing vessels (c, d). The data presented are the means ± S.E.M., *$p < 0.05$ (unpaired t-test, 1 months n=19, 3 months n=18).

small vessels of the hypoperfused animals compared to sham mice (Figure 4.5, c) and not in the large vessels (Figure 4.5, d), suggesting that hypoperfusion triggered Aβ accumulation predominantly in the capillaries.

4.3.4. Chronic cerebral hypoperfusion increases APP levels and processing.

Based on the previous findings showing that cerebral hypoperfusion increased Aβ levels, a process that started in the parenchyma, followed by accumulation in the vasculature, it was next determined whether this process was mediated by increased APP production or processing. To this end, western blot analysis of brain protein extracts was performed using specific antibodies that recognise APP and its carboxyl terminal fragments (CTFs), produced after proteolytic cleavage by the specific enzymes BACE1 that generates the CTFβ, and α-secretase that results in the formation of the CTFα (Figure 4.6). Interestingly, the immunoblotting analysis revealed a significant increase in the levels of APP, CTFβ and CTFα in the hypoperfused animals following 1 month, when compared to the sham group (Figure 4.6, a, c-e). However, after 3 months of hypoperfusion no difference was observed between the two groups (Figure 4.6, b, f-h), suggesting that the increased Aβ levels observed, might be the result of enhanced APP synthesis and processing, triggered at early stages during chronic cerebral hypoperfusion.

4.3.5. LRP and scara1 levels are not affected by chronic cerebral hypoperfusion.

To further assess whether, along with the increased production and processing of APP, altered clearance of Aβ could have contributed to the accumulation of the protein induced by hypoperfusion at 3 months, the levels of LRP-1 and levels of scara1 were determined.

Immunoblots showed there were no significant changes in the levels of LRP following 1 or 3 months of hypoperfusion when compared to sham animals (Figure

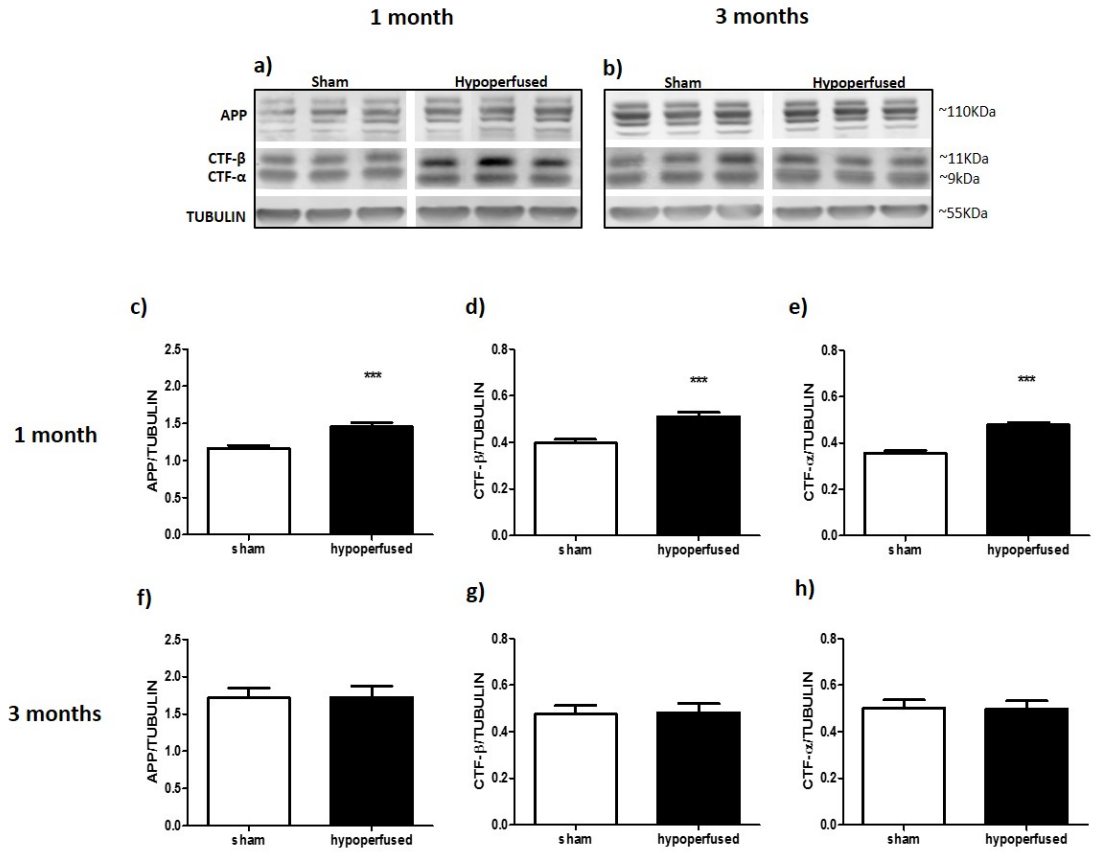

Figure 4.6. Chronic cerebral hypoperfusion increases APP levels and processing in the transgenic mouse model Tg-SwDI. Western blot analysis of brain protein extracts after 1 (a, c-e) and 3 (b, f-h) months of hypoperfusion was performed to determine the expression levels of APP, CTFβ and CTFα. Specific bands were quantified by densitometric analysis and expressed relative to total tubulin protein, represented in the graphs. The data presented are the means ± S.E.M., *p < 0.05 (unpaired t-test, 1 months n=19, 3 months n=12).

4.7). Similarly, ELISA quantitation of scara1 indicated that hypoperfusion did not alter the levels of the receptor (Figure 4.8).

These data suggests that the hypoperfusion-induced increase in Aβ levels observed in the Tg-SwDI mice was not mediated either by changes in vascular clearance through LRP or by altered macrophage clearance through scara1.

4.3.6. MIs, associated with microglial proliferation, are precipitated by chronic cerebral hypoperfusion.

The effect of both Aβ and chronic cerebral hypoperfusion, on the development of MIs, was examined by studying cerebral hypoperfusion in wild-type and Tg-SwDI mice following 1 and 3 months and comparing to sham mice (Figure 4.9). Histological examination of tissue sections using H&E staining was performed and the area covered by MIs was quantified.

Representative images showing normal (Figure 4.9, a) and infarcted (Figure 4.9, b) tissue are shown. Adjacent sections to those used for MI analysis were immunostained using Iba1 to investigate further evidence of microglial infiltration within the infarcted area. Microglial proliferation in the lesion area was evident in the hypoperfused tissue (Figure 4.9, d) compared to the control (Figure 4.9, c). There was no evidence of MIs in sham wild-type mice but small areas of infarcted tissue were observed in sham Tg-SwDI animals (Figure 4.9, e,f). However, after hypoperfusion there was an increase in MIs and this was exacerbated in Tg-SwDI mice. Following 1 month, no MIs were observed in the wild-type group; however, there was a significant increase in the infarcted area in Tg-SwDI hypoperfused (0.021 $mm^2 \pm 0.007$) compared to sham (0.0079 $mm^2 \pm 0.004$) mice. After 3 months, a small infarcted area was found in the wild-type hypoperfused animals (0.0026 $mm^2 \pm 0.02$), however it did not reach significance when compared to the sham controls. There were no MIs in sham mice. In contrast, there was a significant increase in the

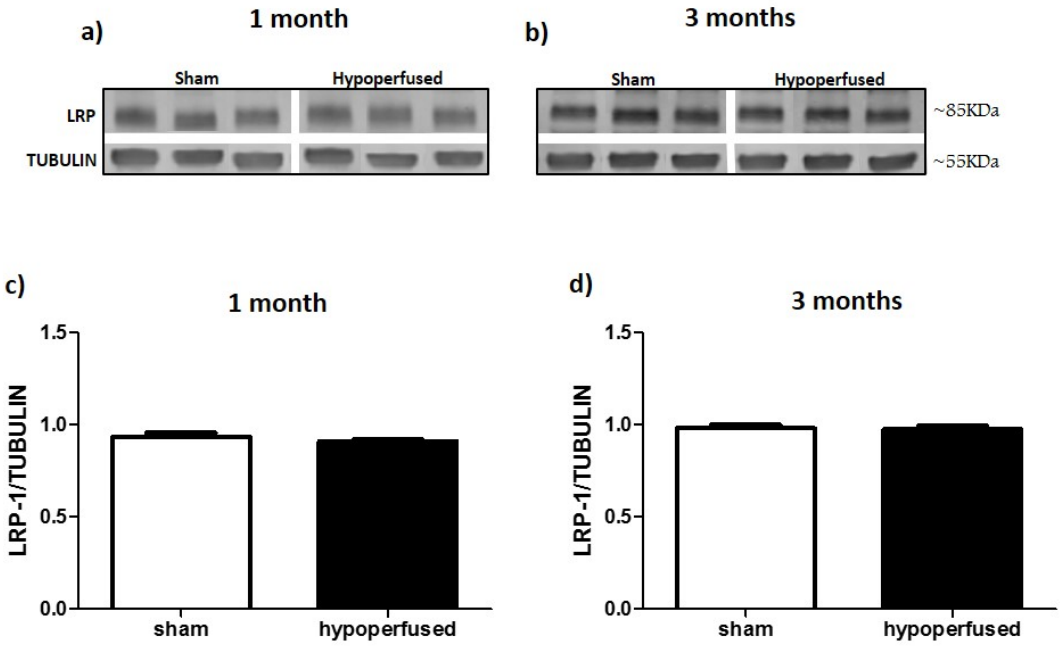

Figure 4.7. LRP levels are not affected by chronic cerebral hypoperfusion in the transgenic mouse model Tg-SwDI. Western blot analysis of proteins extracts from vessels enriched fractions after 1 (a, c) or 3 (b, d) months of hypoperfusion was performed to determine the expression levels of LRP in Tg-SwDI mice; specific bands were quantified by densitometric analysis and expressed relative to total tubulin protein, represented in the graphs. The data presented are the means ± S.E.M. (unpaired t-test, $p > 0.05$, 1 months n=19, 3 months n=12).

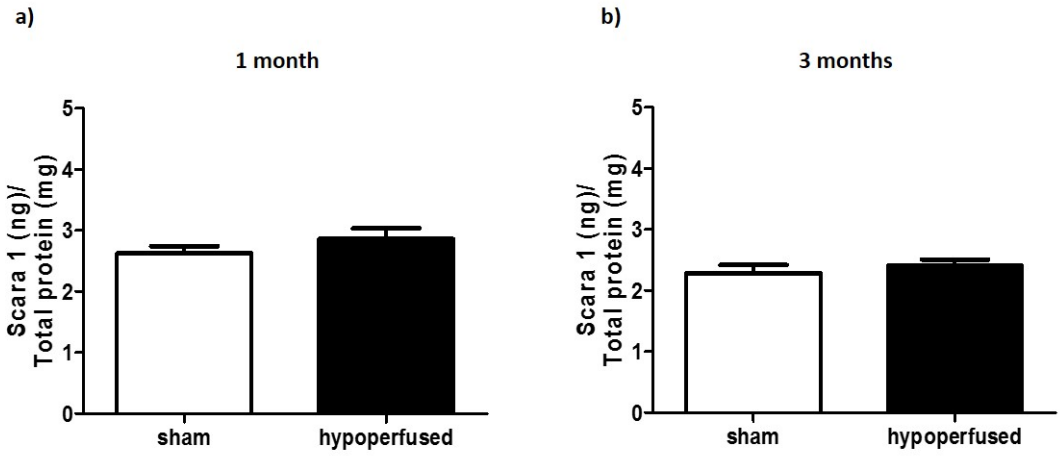

Figure 4.8. Scara1 levels are not affected by chronic cerebral hypoperfusion in the transgenic mouse model Tg-SwDI. Scara1 levels were quantified in protein extracts from brain homogenates using ELISA after 1 (a) and 3 (b) months of hypoperfusion; graphs represent the levels of the protein normalised to total protein concentration. The data presented are the means ± S.E.M. (unpaired t-test, $p > 0.05$, 1 months n=19, 3 months n=12).

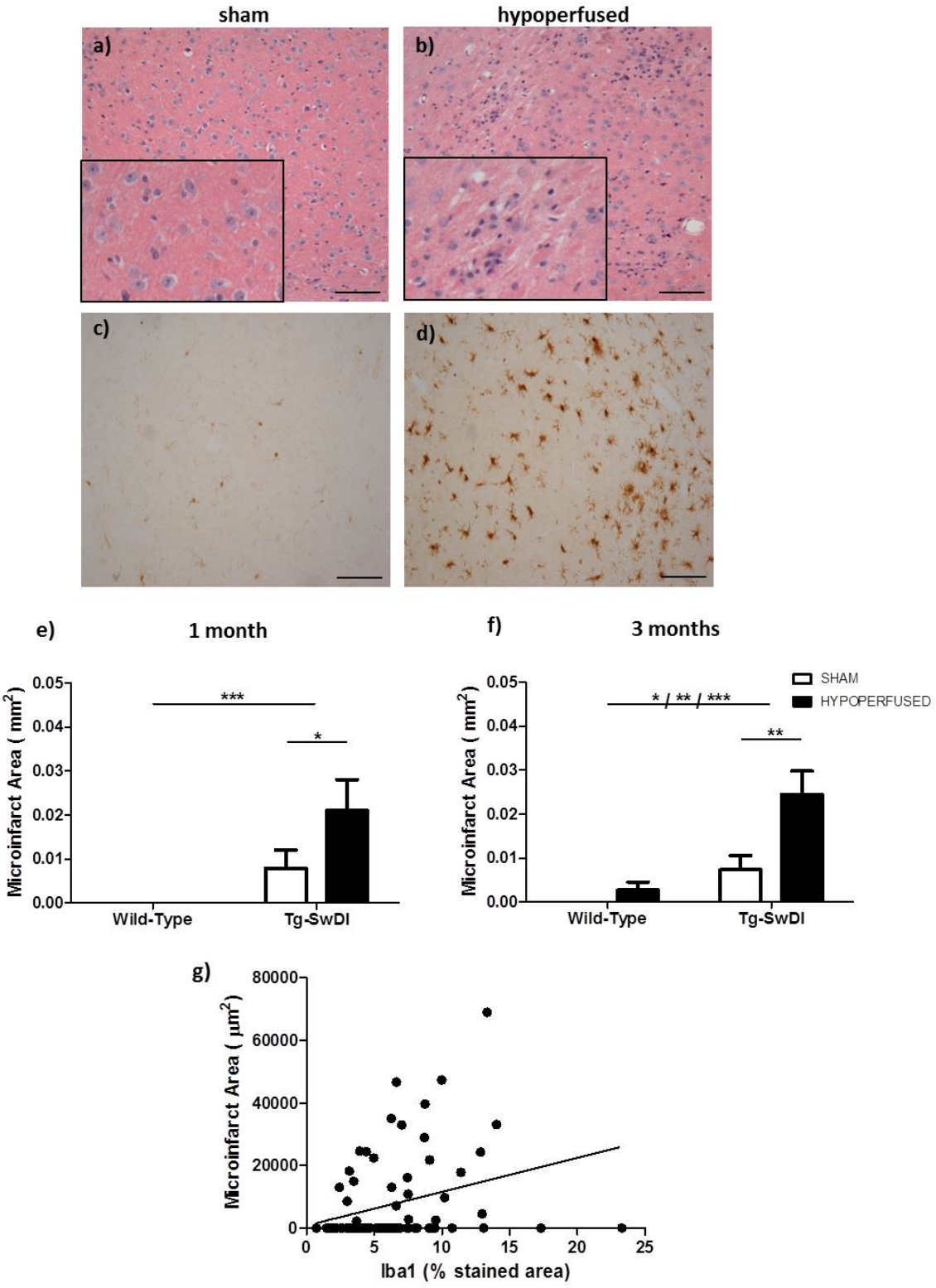
sham
hypoperfused
a)
b)
c)
d)
e)
1 month
f)
3 months
SHAM
HYPOPERFUSED
Microinfarct Area (mm2)
0.05
0.04
0.03
0.02
0.01
0.00
***
*
* / ** / ***
**
Wild-Type
Tg-SwDI
g)
Microinfarct Area (µm2)
80000
60000
40000
20000
0
0
5
10
15
20
25
Iba1 (% stained area)

Figure 4.9. Aβ promotes the development of MIs, which is exacerbated by chronic cerebral hypoperfusion and associated with microglial proliferation. Representative images showing normal (a) and infarcted (b) tissue using H&E staining; insets show a higher magnification of the image. Iba1 staining was used to visualise microglial proliferation (c, d) (scale bar = 100 μm). Histopathological analysis was performed using H&E staining in tissue sections from Tg-SwDI and wild-type animals following 1 (e) and 3 (f) months of hypoperfusion; the area covered by infarcted tissue was measured and is represented in the graphs. The data presented are the means ± S.E.M., two-way ANOVA: significant effect of genotype ($F_{(1,38)}$ = 14.52, ***p = 0.0005), Bonferroni post-test (*p < 0.05) (e); significant interaction ($F_{(1,34)}$ = 5.446, *p = 0.0257), significant effect of surgery ($F_{(1,34)}$ = 10.14, **p = 0.0031), significant effect of genotype ($F_{(1,34)}$ = 21.82, ***p < 0.0001), Bonferroni post-test (**p < 0.05) (f). Scatter plot shows a positive correlation between MI area and microglia burden, Pearson correlation: r = 0.3043, p = 0.0064 (g).

infarcted area in the Tg-SwDI hypoperfused (0.024 mm^2 ± 0.005) compared to sham (0.0073 mm^2 ± 0.003) mice. There was a positive correlation between the MI area and the microglia burden (Figure 4.9, g).

Together, these data indicate that MIs are present in Tg-SwDI mice and that the burden is exacerbated with chronic cerebral hypoperfusion.

Histopathological analysis revealed that there were no haemorrhages following 1 month of hypoperfusion. After 3 months of hypoperfusion, haemorrhages were detected in only one wild-type mouse, and in 3 Tg-SwDI mice (Figure 4.10). Thus, chronic hypoperfusion and presence of amyloid at these time-points had minimal effects on the development of haemorrhages.

4.3.7. Chronic cerebral hypoperfusion increases NOX2 levels in the transgenic mouse model Tg-SwDI.

In order to examine the effect of both Aβ and chronic cerebral hypoperfusion on the development of oxidative stress, ELISA measurement of brain protein extracts was assayed to determine the levels of NOX2 in wild-type and Tg-SwDI mice following hypoperfusion (Figure 4.11). Significantly higher levels of the protein were found in the transgenic mice compared to the wild-type controls at both time-points analysed, and this was exacerbated after 1 month of hypoperfusion in the Tg-SwDI mice.

Conversely, following 3 months, there were no significant changes between sham and hypoperfused animals. Interestingly, increased levels of NOX2 positively correlated with the levels of soluble parenchymal Aβ, and no correlation between NOX2 and vascular Aβ was found (Figure 4.11, c, d).

These data suggest that soluble amyloid may induce an oxidative response which is enhanced by cerebral hypoperfusion.

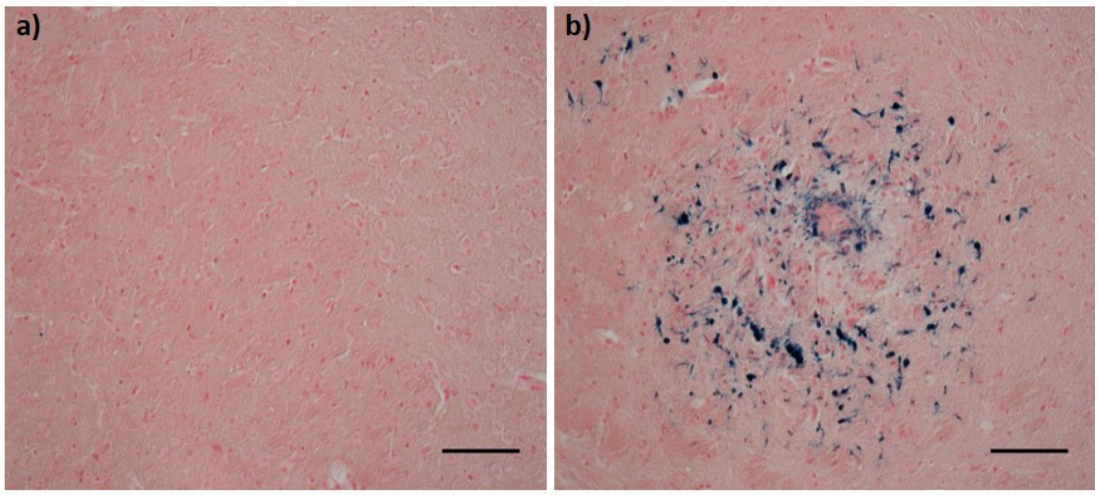

c)

	1 month		3 months	
	sham	hypoperfused	sham	hypoperfused
Wild-Type	0/12 (0%)	0/11 (0%)	0/10 (0%)	1/10 (10%)
Tg-SwDI	0/9 (0%)	0/10 (0%)	0/9 (0%)	3/9 (33%)

Figure 4.10. Proportion of mice with haemorrhages following chronic cerebral hypoperfusion. Histopathological analysis was performed using Perls staining in tissue sections from Tg-SwDI and wild-type animals following 1 and 3 months of hypoperfusion. Representative images showing normal (a) and haemorrhagic (b) tissue are shown (scale bar = 100 um). The number of mice with haemorrhages was determined and is indicated in the table.

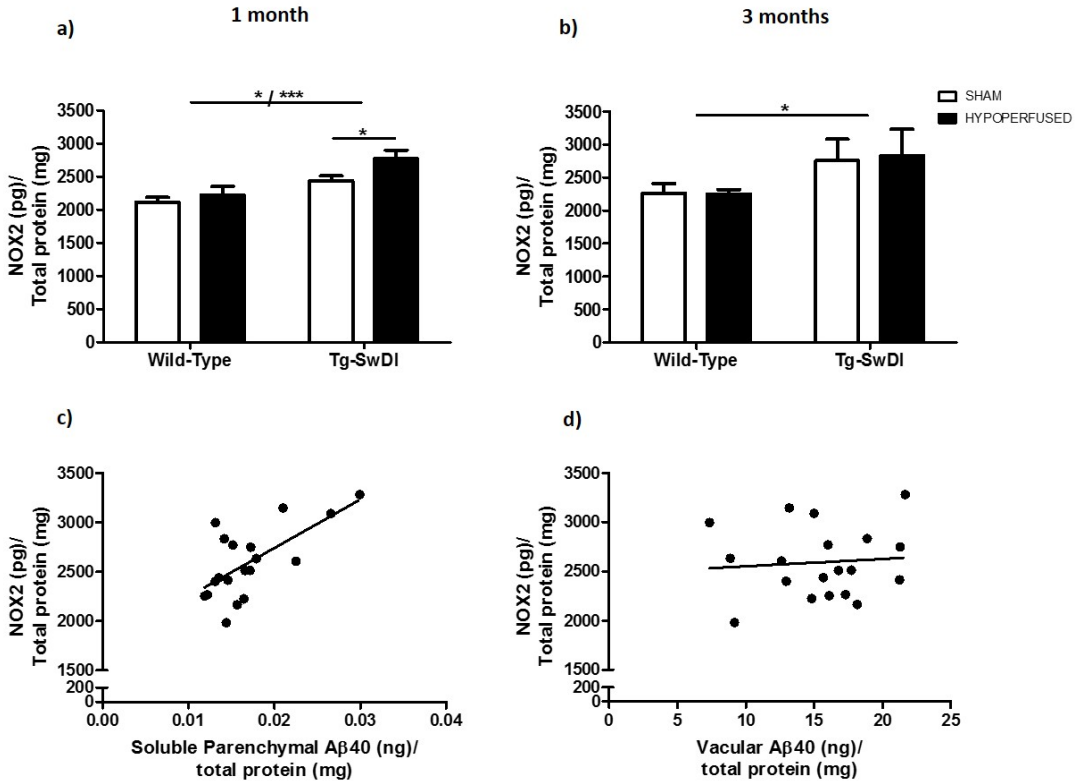

Figure 4.11. Aβ increases NOX2 levels, which is exacerbated by chronic cerebral hypoperfusion. NOX2 levels were quantified in protein extracts from brain homogenates using ELISA after 1 (a) and 3 (b) months of hypoperfusion. Graphs represent the levels of the protein normalised to total protein concentration. The data presented are the means ± S.E.M., two-way ANOVA: significant effect of surgery ($F_{(1,29)}$ = 4.288, *p = 0.0474), significant effect of genotype ($F_{(1,29)}$ = 16.79, ***p = 0.0003), Bonferroni post-test (*p < 0.05) (a); significant effect of genotype ($F_{(1,23)}$ = 4.719, *p = 0.0404) (b). Pearson correlation: Scatter plots show a positive correlation between NOX2 levels and soluble parenchymal Aβ40 levels, r = 0.6643, p = 0.0019 (c) and no correlation between NOX2 levels and vascular Aβ40 levels, r = 0.0853, p = 0.7284 (d).

4.3.8. Effect of both chronic cerebral hypoperfusion and Aβ on astrocyte integrity.

The effect of both brain hypoperfusion and amyloid on astrocyte activation was examined after chronic cerebral hypoperfusion in wild-type and Tg-SwDI mice following 1 and 3 months and compared to sham mice (Figure 4.12). Western blot was used to assess the total levels of reactive gliosis by quantifying GFAP levels. Significantly higher levels of GFAP were found in the Tg-SwDI mice compared to the wild-type controls. Although the levels of the protein were slightly increased in the transgenic hypoperfused mice and in the wild-type group after 3 months of hypoperfusion, this was not significantly different from the sham controls.

To further investigate the effects of Aβ and hypoperfusion on astrocytes, the next studies focussed on AQP4, an astrocyte end-foot marker. The measurement of total levels of AQP4 in brain protein extracts was performed using an ELISA (Figure 4.13). There were significantly higher levels of AQP4 in the Tg-SwDI mice compared to the wild-type controls following 1 month of hypoperfusion (Figure 4.13, a). In contrast, after 3 months, no significant changes where found between the groups (Figure 4.13, b).

Interestingly, association analyses showed a positive correlation between AQP4 levels and the levels of soluble parenchymal Aβ. However there was no correlation between AQP4 and vascular Aβ levels (Figure 4.13, c, d). Furthermore, a highly significant positive correlation between AQP4 and NOX2 levels was found (Figure 4.13, e).

Subsequently, in order to determine vascular AQP4 coverage, confocal microscopy was used to quantify AQP4 colocalisation with the vasculature (Figure 4.14) As expected, AQP4 immunostaining (Figure 4.14, b) was predominantly localised at the cerebrovasculature, yet image analysis revealed that neither amyloid nor hypoperfusion affected the vascular AQP4 coverage at both time points analysed (Figure 4.14, d, e).

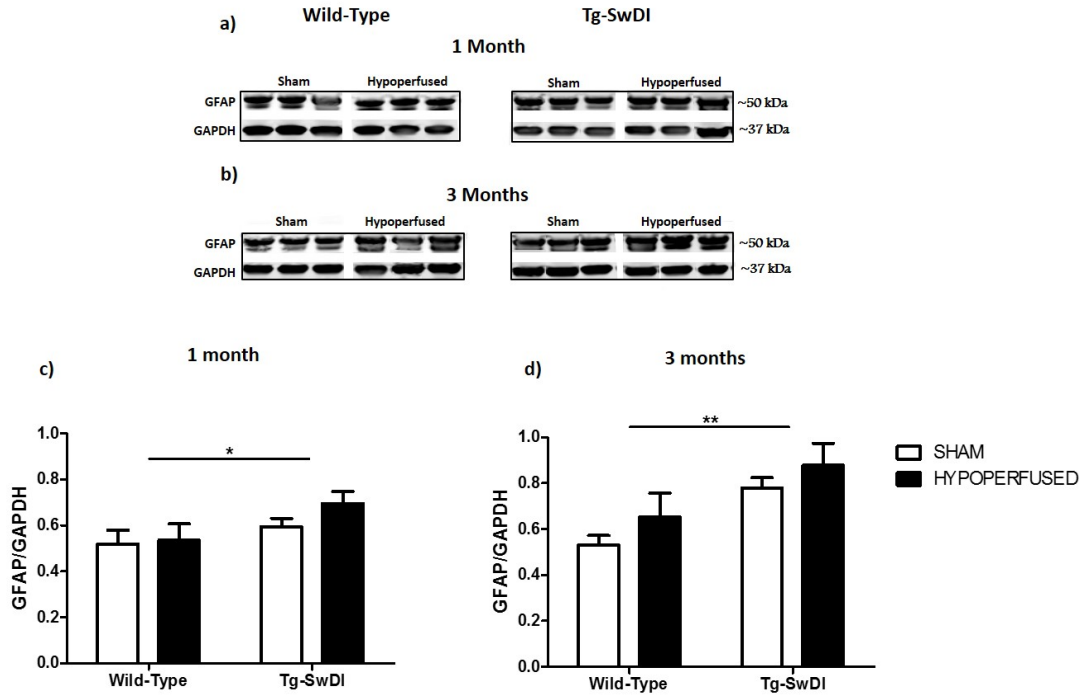

Figure 4.12. Increased astrocyte activation in the Tg-SwDI mouse model. Western blot analysis of protein extracts from brain homogenates after 1 (a) and 3 (b) months of hypoperfusion was performed to determine the expression levels of GFAP, represented in the graphs; GAPDH was used as loading control. The data presented are the means ± S.E.M., two-way ANOVA: 1 month: significant effect of genotype ($F_{(1,29)}$ = 4.786, *p = 0.0369); 3 months: significant effect of genotype ($F_{(1,23)}$ = 9.814, **p = 0.0047).

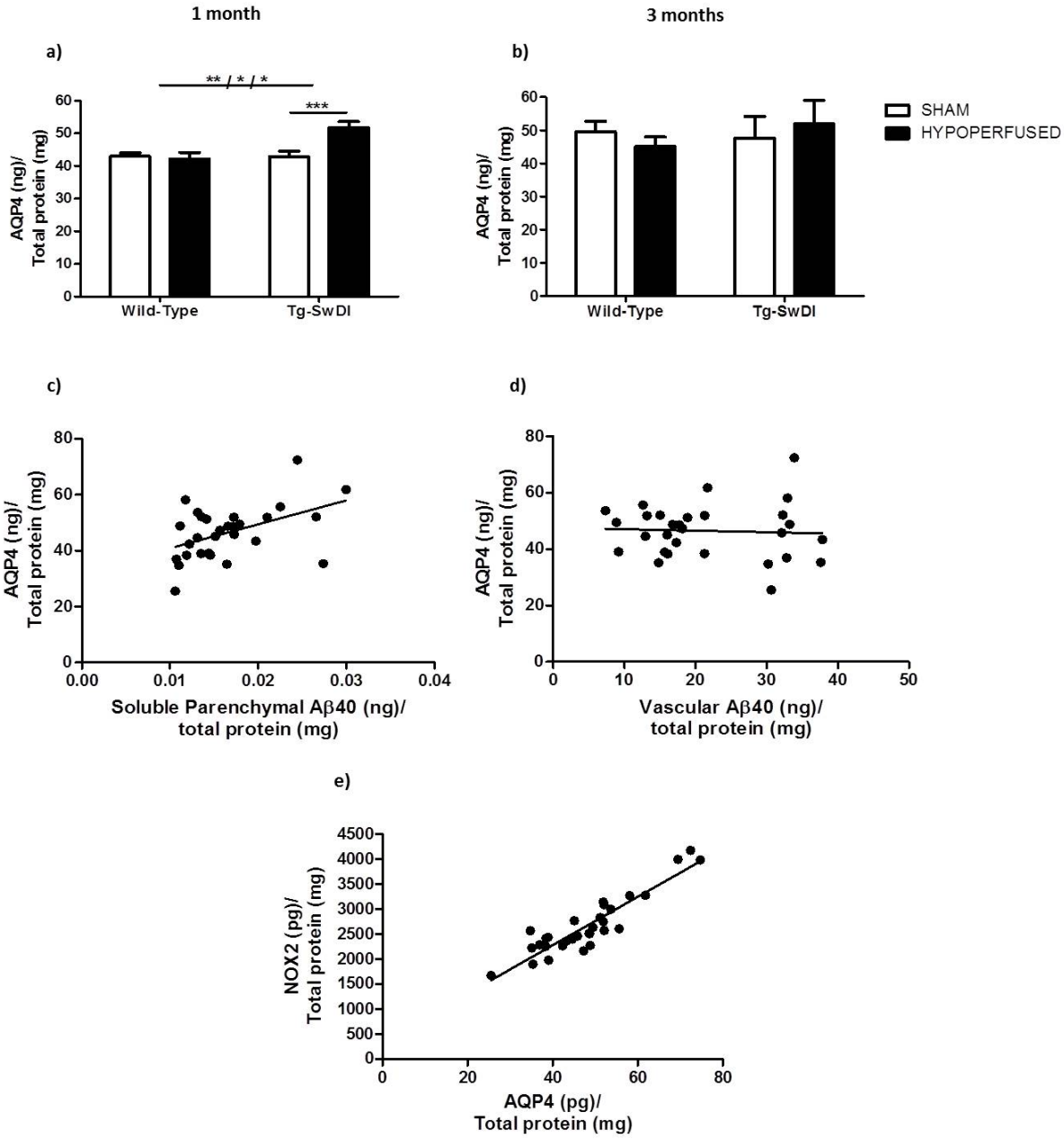

Figure 4.13. Hypoperfusion increases AQP4 levels, which correlates with levels of Aβ and NOX2. AQP4 levels were quantified in brain protein extracts using ELISA after 1 (a) and 3 (b) months of hypoperfusion. Graphs represent the levels of the protein normalised to total protein concentration, the data presented are the means ± S.E.M., two-way ANOVA: significant effect of genotype ($F_{(1,29)}$ = 7.976, *p = 0.0101), significant effect of surgery ($F_{(1,29)}$ = 5.605, *p = 0.0248), significant interaction ($F_{(1,29)}$ = 7.584, **p = 0.0085), Bonferroni post-test (***p < 0.001). Pearson correlation: Scatter plots show a positive correlation between soluble parenchymal Aβ40 and AQP4 levels (**p = 0.0095, r = 0.4735) (c) no correlation between vascular Aβ40 and AQP4 levels (p = 0.7866, r = -0.05255) (d) and positive correlation between NOX2 and AQP4 levels (***p < 0.0001, r = 0.9133) (e).

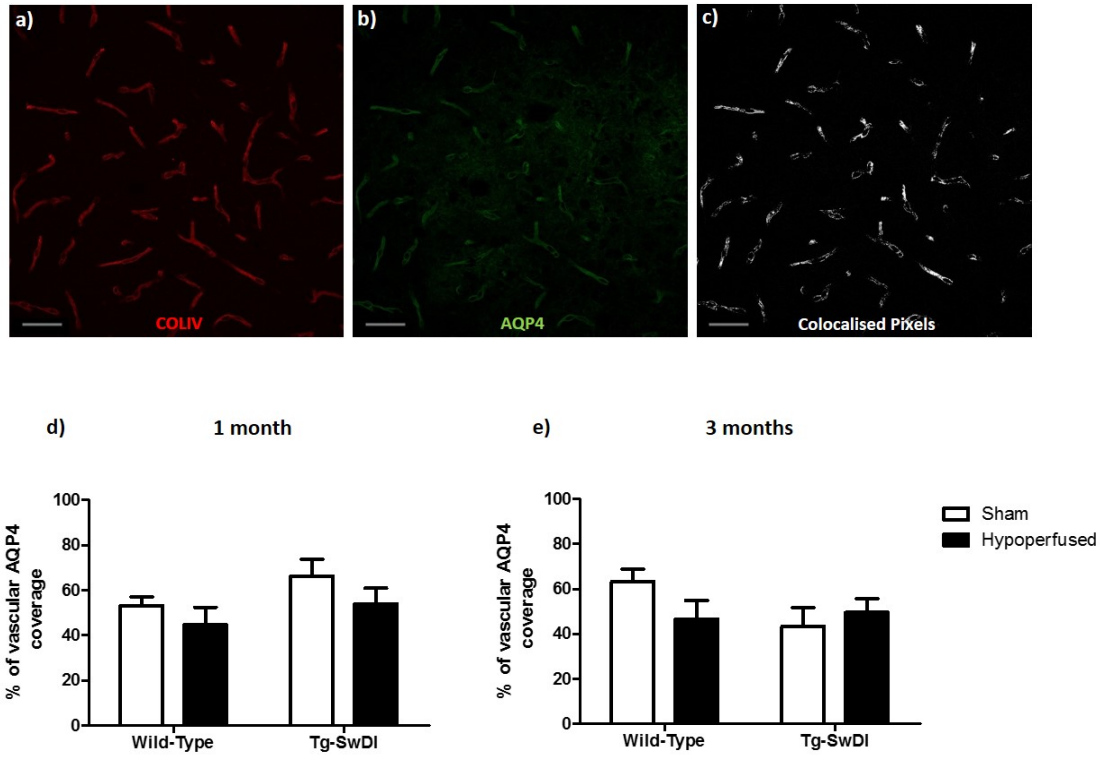

Figure 4.14. AQP4/vasculature colocalisation. Double immunostaining was performed using markers of collagen (a) and AQP4 (b), colocalising pixels of the merged images are shown in white (c) (scale bar= 50 µm). The proportion of vessels covered by AQP4 after 1 (d) and 3 (e) months of hypoperfusion is represented in the graphs. The data presented are the means ± S.E.M. two-way ANOVA, $p > 0.05$ (1 month n=42, 3 months n= 38).

4.3.9. Effect of both chronic cerebral hypoperfusion and Aβ on tight junction levels.

The levels of claudin-5, one of the main proteins comprising the TJs, were investigated in response to chronic cerebral hypoperfusion and the potential contribution of Aβ to this change was determined by studying Tg-SwDI and wild-type hypoperfused mice and compared to sham animals. Western blot analysis of protein extracts from vessel enriched fractions was performed to quantify the levels of the protein.

As shown in Figure 4.15, claudin-5 levels were significantly higher in the Tg-SwDI mice compared to the wild-type controls at the 2 time-points analysed, and this was exacerbated following 1 month of hypoperfusion in the transgenic model. In contrast, no significant changes between sham and hypoperfused animals were found after 3 months. Notably, association analyses showed positive correlation between claudin-5 and vascular Aβ levels, and no correlation between claudin-5 and soluble parenchymal Aβ levels was found (Figure 4.15, a, b).

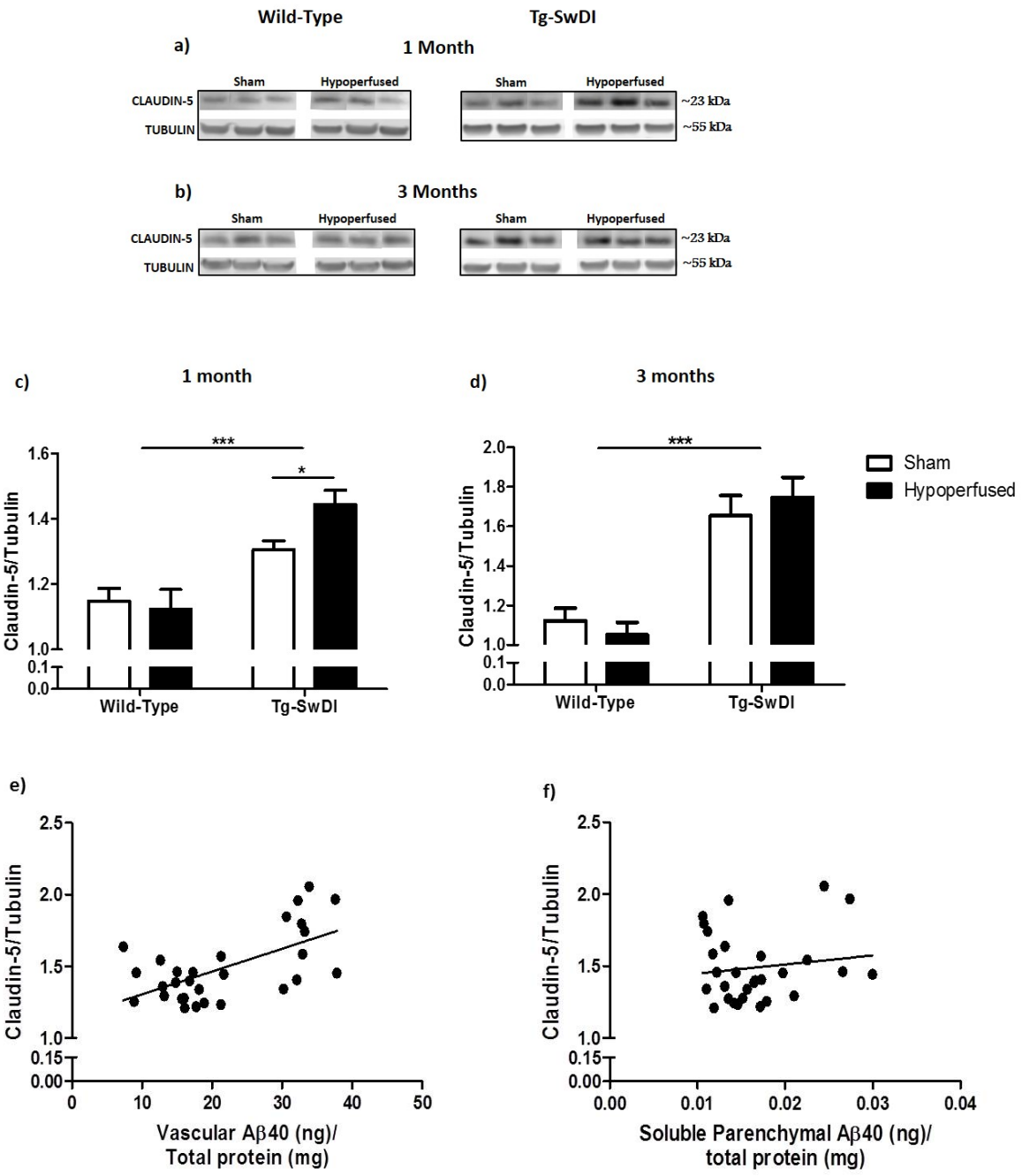

Figure 4.15. Increased claudin-5 levels in Tg-SwDI mice are exacerbated by hypoperfusion. Western blot analysis of protein extracts from vessel enriched fractions after 1 (a) and 3 (b) months of hypoperfusion was performed to determine the expression levels of claudin-5. Specific bands were quantified by densitometric analysis and expressed relative to total tubulin protein, represented in the graphs. The data presented are the means ± S.E.M., two-way ANOVA: significant effect of genotype ($F_{(1,29)}$ = 33.47, ***p < 0.0001), Bonferroni post-test (*p < 0.05) (c); significant effect of genotype ($F_{(1,23)}$ = 56.33, ***p < 0.0001) (d). Pearson correlation: Scatter plots show a positive correlation between claudin-5 and vascular Aβ40 levels (r = 0.6113, ***p = 0.0004) (e) and no correlation between claudin-5 and soluble parenchymal Aβ40 levels (r = 0.1367, p = 0.4797) (f).

4.4. Discussion.

The present study sought to test the hypothesis that chronic cerebral hypoperfusion leads to the accumulation of parenchymal and vascular Aβ, triggering the development of MIs and haemorrhages and altering the NVU integrity. The results support the hypothesis and demonstrate that chronic cerebral hypoperfusion results in a significant increase in APP levels and processing, leading to accelerated Aβ40/42 production and deposition in the parenchyma followed by aggregation in the cerebrovasculature. Notably, vascular Aβ deposition occurred predominantly in the microvasculature. Subsequent assessment of the neurovascular integrity revealed that amyloid load promotes the development of MIs and interestingly, specific pools of Aβ were associated with the alteration of different structures of the NVU. These alterations were exacerbated by hypoperfusion and associated with oxidative stress.

4.4.1. Parenchymal and vascular Aβ accumulation in response to hypoperfusion.

In the present study, it was demonstrated that hypoperfusion modified Aβ metabolism in the Tg-SwDI mice, triggering an early increase in the levels of soluble Aβ in the parenchyma followed by aggregation of the protein into insoluble fibrils and subsequently the build-up of aggregates in the cerebrovasculature. Aβ aggregation follows a seeding-nucleation mechanism, where the limiting step is the formation of small oligomeric intermediates that act as seeds to catalyse the polymerisation process. Thus, the increased levels of insoluble Aβ observed in the parenchyma after 3 months of hypoperfusion, were likely the result of the polymerisation of soluble Aβ, which started to increase following 1 month of hypoperfusion. We hypothesise that the amount of Aβ being produced in the brain of these mice was too high to be effectively eliminated by the clearance system at the BBB, therefore Aβ also started to accumulate in the vessel walls, at the clearance site. Indeed, previous studies in the Tg-SwDI model revealed that Dutch/Iowa mutant Aβ is poorly cleared from the brain into the circulation contributing to its accumulation (Davis et al., 2004). The results presented in this study demonstrate that hypoperfusion potentiated this process. Thereafter, every new Aβ molecule

synthesised was rapidly added to the growing fibrils at the parenchyma and vasculature.

It has been shown that vascular smooth cells express APP and vessels isolated from the brain are able to produce Aβ (Kalaria et al., 1996; Burgermeister et al., 2000), and thus it has been suggested that vascular amyloid originates in the cerebral vasculature. CAA is present in brain capillaries, which lack smooth muscle cells, therefore the single contribution of this type of cell to the amyloid build-up, is unlikely. However, it has been demonstrated that Aβ can also be produced by endothelial cells (Kitazume et al., 2010). In contrast, compelling evidence points towards a mechanism in which vascular amyloid is originated in the parenchyma, from neuronal production and drained along the perivascular lymphatic fluid where, under pathologic conditions, starts to accumulate in the vessel walls (Weller et al., 1998; Burgermeister et al., 2000; Van Dorpe et al., 2000; Herzig et al., 2004; Jucker, 2006; Weller et al., 2008; Vidal et al., 2009). These data support our previous assumption that following hypoperfusion, a combination of enhanced Aβ production along with altered clearance of the protein across the BBB in the Tg-SwDI model might have contributed to its accumulation in the vasculature. Furthermore, our results support previous studies showing that CAA is preceded by higher levels of soluble amyloid suggesting that soluble Aβ is a marker of potential CAA (Suzuki et al., 1994b; Shinkai et al., 1995).

Interestingly, in the wild-type group a significant increase in levels of parenchymal Aβ42 was found in the hypoperfused mice compared to the sham controls after 1 month (Figure A1), however no vascular accumulation of the protein was detected (data not shown). Unlike the Tg-SwDI mice, in which both murine and the mutant human APP proteins are expressed, wild-type mice only express murine APP. Therefore, considering the substantially lower levels of the protein being produced and the fact that rodent Aβ is not amyloidogenic *in vivo* (Selkoe, 1989; Hilbich et al., 1991; Otvos et al., 1993), it is likely that the protein was eventually effectively cleared instead of being accumulated and aggregated into insoluble fibrils as it happened in the Tg-SwDI mice. This could explain why the protein was not

detectable in those samples, which was not surprising as vascular Aβ corresponds mainly to fibrillar amyloid.

4.4.2. Aβ accumulation in microvessels.

Vascular accumulation of Aβ is present in the majority of AD patients and constitutes a risk factor for dementia (MRC-CFAS, 2001; Greenberg et al., 2002; Pfeifer et al., 2002a; Weller and Nicoll, 2003; Greenberg et al., 2004). In humans, different patterns of vascular amyloid have been described, which define different histopathological phenotypes in AD (Allen et al., 2014).

Interestingly, the results presented in this study demonstrate that following 3 months of hypoperfusion, vascular amyloid accumulated predominantly in smaller blood vessels, lacking SMA, suggesting that hypoperfusion triggered Aβ accumulation in the capillaries. However, it is important to note that the width of the majority (78.2 %) of the vessels was found to be between 0.6 and 6 μm, which were considered as small vessels, and only 21.8 % of vessels had a width over 6 μm. This sampling issue might have influenced the results, favouring statistical power due to the larger n in the small vessels group.

One of the major clearance mechanisms of Aβ in the brain is vascular transport across the BBB, which is mediated primarily by the cell surface receptor LRP1 (Shibata et al., 2000; Deane et al., 2004). Hence, according to what we suggested previously, it is likely that as Aβ levels started to increase in response to the reduced CBF, the protein was not successfully cleared through the capillary network at the BBB, therefore it started to accumulate in smaller vessels, at the clearance site. Yet it is possible that the accumulation of the protein eventually occurs within larger blood vessels. Additional studies, using later time-points would be required to confirm this.

4.4.3. Potential mechanisms underlying the Aβ increase in response to hypoperfusion.

Increased parenchymal Aβ levels might be the result of either overproduction or altered clearance of the protein, or the combination of both. In the current study, enhanced APP synthesis and processing, triggered at early stages during chronic cerebral hypoperfusion, are shown. This suggests that the increased Aβ levels observed might be the result of a general increase in APP metabolism, where both amyloidogenic and non-amyloidogenic pathways were enhanced. The latter can be concluded by the observation of increased levels of both CTF-β and CTF-α respectively. It is possible, that the time-dependant increase in basal APP levels that this model undergoes, might have masked the effect of hypoperfusion, explaining why no changes were observed following 3 months.

Although the physiological function of APP is not completely understood, there is well documented evidence of a neuroprotective and synaptogenic role of the full-length protein as well as the soluble fragments released during its processing including Aβ (Caillé et al., 2004; Han et al., 2005; Leyssen et al., 2005; Chasseigneaux and Allinquant, 2012). Indeed, there are number of studies showing that different types of brain injury including traumatic brain injury (TBI) (Itoh et al., 2009; Corrigan et al., 2011) and also ischemic injury (Stephenson et al., 1992; Bennett et al., 2000; Lee et al., 2006; Zhang et al., 2007; Koike et al., 2010), both constituting risk factors for AD (Pluta et al., 2009; Sivanandam and Thakur, 2012) induce intra-axonal upregulation of APP or increase its processing. Hence, the explanation for the hypoperfusion-induced upregulation of APP and increased metabolism of the protein observed can be directly linked to its neuroprotective role. However, in the long term, this response may have deleterious consequences due to the overproduction of Aβ. In contrast, no changes in APP were found between sham and hypoperfused mice in the wild-type group (Figure A2). We suggest that similar to changes in the Tg-SwDI group, the increased Aβ levels observed might be a neuroprotective response to hypoperfusion. However, as basal APP levels in wild-type mice are considerably lower, a much more sensitive method would be required

to detect this subtle change. Indeed, CTF-β levels were undetectable by western blot in those samples probably because the amyloidogenic pathway is less common in wild-type mice therefore a more sensitive detection assay would be needed.

To further investigate whether cerebral hypoperfusion may have altered Aβ clearance contributing to its accumulation, this study first focused on LRP-1, the main receptor involved in the active outward transport of the protein across the BBB. Previous studies of the role of this receptor in the pathogenesis of AD have revealed a positive correlation between decreased levels of LRP and AD pathology (Kang et al., 1997; Jaeger et al., 2009; Cuzzo et al., 2011). Thus, it was hypothesised that the increased Aβ levels observed following hypoperfusion might be in part due to altered LRP levels; however the results showed no such changes. Notably, the receptor was upregulated following 3 months of hypoperfusion in the wild-type mice (Figure A3), likely in response to the increased Aβ levels, supporting the previous speculation that the protein was effectively cleared in this group.

Another key player involved in Aβ clearance in the brain is microglia, which constitutes the first line of immune defence in the CNS and is in continuous surveillance for any potential injurious stimuli. In AD brains and in transgenic mouse models, as demonstrated in the previous chapter, microglia becomes activated in response to Aβ deposition and migrates into sites containing Aβ plaques (Morgan et al., 2005; Chung et al., 2011; Zabel et al., 2013; Baron et al., 2014). It is well established that cerebral hypoperfusion triggers proliferation and activation of microglial cells (Shibata et al., 2004; Farkas et al., 2004); however, the effect of hypoperfusion on microglial-dependant Aβ clearance has not been established. Microglia can bind amyloid through interaction with different receptors, however their role in the progression of AD is yet unknown. Previous research suggest that microglial cells expressing the chemokine receptor CCR2 are recruited to sites of cerebral amyloidosis, acting at the perivascular compartment to clear Aβ. Interestingly, deficiency of CC-chemokine ligand 2 (Ccl2), the main CCR2 ligand, induced accelerated β-amyloidosis and cognitive dysfunction in CCL2-deficient APP/PS1 mice (Kiyota et al., 2013). Moreover, APP-Ccr2$^{-/-}$ mice showed decreased

microglial recruitment and accelerated Aβ deposition, specially associated to the vasculature (El Khoury et al., 2007; Mildner et al., 2011). Despite the ability of microglia to be attracted by Aβ and clear the aggregates, which might delay the progression of AD pathology at early stages, during ageing and as AD progress, amyloid pathology continue to develop and the apparent dysfunction that microglia undergoe has been focus of interesting research. Importantly, isolated monocytes from AD patients show poor macrophage differentiation and Aβ phagocytosis as well as higher expression of intracellular cytokines compared to age-matched controls (Fiala et al., 2005). Furthermore, there is evidence indicating that microglia from old transgenic animals that develop increasing Aβ accumulation with age, shows downregulation of the Aβ-binding receptors scara1 and CD36, compared to young animals (Hickman et al., 2008). Thus, the phenotype of microglia changes as AD pathology develops, showing upregulation of the proinflammatory cytokines interleukin-1β (IL-1β) and tumor necrosis factor α (TNF-α) but decreasing their Aβ-clearing abilities, contributing that way to the development of the disease (Hickman et al., 2008). In addition, based on previous studies showing that class A scavenger receptors mediate adhesion of microglia to Aβ fibrils (El Khoury et al., 1996), a more recent study performed by the same group in PS1-APP mice, has found that scara1 is a major microglial receptor for soluble Aβ and that its deficiency triggers reduced Aβ uptake and increased mortality in these mouse line (Frenkel et al., 2013). Therefore, we asked the question whether hypoperfusion could have altered scara1 levels contributing to Aβ accumulation. However, the results indicate that the hypoperfusion-induced increase in Aβ levels observed was not mediated by this change. Nevertheless, although hypoperfusion had no effects in the expression levels of scara1, it might induce functional alterations of the receptor and affect its binding to Aβ. Also, the potential alteration of other receptors involved in microglial-mediated Aβ clearance such as CCR2 and CD36 cannot be ruled out. Further studies would be needed to determine this. It would also be interesting to investigate the effects of hypoperfusion on amyloid clearance through alternate mechanisms such as perivascualar drainage.

4.4.4. Development of MIs and haemorrhages in response to Aβ and hypoperfusion.

Cerebral MIs are frequently observed in AD brains (Brundel, 2012; van Rooden et al., 2014) and, as shown by several studies, the load of MIs correlates with impaired cognitive performance (Kövari et al., 2007; Troncoso et al., 2008; Arvanitakis et al., 2011). The results of this study show that the development of MIs associated with microglial proliferation, can be precipitated by chronic cerebral hypoperfusion, suggesting microinfarction as a linkage between hypoperfusion and the development of degenerative processes. Additionally, there is a large *in vitro* and *in vivo* body of evidence demonstrating Aβ toxicity and its role in the pathoetiology of AD (Canevari et al., 1999; Hardy and Selkoe, 2002; Lin et al., 2001, Atwood et al., 2003; Rosales-Corral et al., 2004; Butterfield et al., 2007; Parameshwaran et al., 2008; Wang et al., 2013). Interestingly, vascular accumulation of Aβ, which is present in almost all cases of AD, has been linked with the development of MIs; however, correlation studies have shown inconsistent results (Olichney et al., 1995; Haglund et al., 2006; Launer et al., 2008; Okamoto et al., 2009; Soontornniyomkij et al., 2010; Kövari et al., 2013; van Rooden et al., 2014).

As demonstrated in the present chapter, chronic cerebral hypoperfusion induced a significant increase in parenchymal and cerebrovascular Aβ production and deposition. To further examine the link between MIs and Aβ deposition, association analyses were performed using the Pearson correlation test, which revealed no correlation between MI load and vascular or parenchymal amyloid levels (Figure A5). However, the effect of hypoperfusion on the appearance of MIs was exacerbated in the Tg-SwDI mice compared to the wild-type group, suggesting an underlying influence of amyloid on the development of these lesions. One explanation to this result might be attributable to the fact that the association analyses were done using the quantification of the immunostaining, which does not distinguish between the different pools of Aβ. Therefore, it is possible that rather than insoluble aggregates, soluble Aβ oligomers, which constitute the most cytotoxic species of Aβ, might be involved on the development of MIs. This could also explain

the inconsistencies between the previously published studies mentioned above, showing inconsistent MI/amyloid correlation results, where no differentiation was made between the different pools of amyloid. Indeed, compelling evidence support the oligomer hypothesis, which states that soluble Aβ oligomers are the main etiologic agent that participates in the initiation of the neurodegenerative process in AD, by triggering a cascade of pathogenic events involving inflammation and oxidative injury (Klein et al., 2004; Glabe and Kayed., 2006; Haass and Selkoe, 2007; Walsh and Selkoe, 2007; Maezawa et al., 2011). Since different cohorts were used in the present study to perform the pathology and biochemistry analyses, additional studies using the same cohort would be required in order to test the specific association between Aβ oligomers and microinfarction.

Notably, although the mechanisms leading to MI formation remain unknown, oxidative stress and inflammation, as the result of cerebrovascular alterations, have been suggested as possible contributors (Miklossy, 2003; Damasceno, 2012; Chen et al., 2011b; Smith et al., 2012; Shih et al., 2013). NOX2 constitutes the main ROS source in the brain and it has a critical role in cell death following ischemic insults (Brennan-Minnella et al., 2014). For example, mice lacking a functional NOX2 presented significantly reduced infarct volume following transient cerebral ischemia (Walder et al., 1997; Tang et al., 2008; Jackman et al., 2009). Moreover, NOX2 has shown to be involved in post-ischemic brain inflammation, which exacerbates the progression of brain injury (Chen et al., 2011b). Furthermore, increasing evidence demonstrates an association between Aβ-induced neuronal damage and oxidative stress, wish has shown to involve microglial activation (Bianca et al., 1999; Coraci et al., 2002; Abramov et al., 2004; Qin et al., 2006; Wilkinson and Landreth, 2006; Narayan et al., 2014). Notably, Aβ is able to increase the processing of IL-1β into mature IL-1β in microglia via ROS (Parajuli et al., 2013). In addition, Tg2576 mice lacking NOX2 showed improved cerebrovascular function and behavioral performance through reduction of oxidative stress independently of Aβ accumulation (Park et al., 2008) suggesting that the neurovascular alterations observed in this mouse model are the result of the oxidative stress induced by the accumulation of Aβ**.** Consequently, to further investigate the potential mechanistic basis of the current

finding of increased microinfarction following chronic cerebral hypoperfusion, the levels of NOX2 were assessed. Higher levels of this protein were found in the Tg-SwDI mice compared to the wild-type controls, and this was exacerbated by hypoperfusion in the transgenic model, suggesting a synergistic effect, where both amyloid and hypoperfusion contributed to NOX2 upregulation. Thus, it is possible that NOX2-derived radicals may have contributed to the development of MIs. Interestingly, soluble parenchymal Aβ, but not vascular Aβ, correlated with increased NOX2 levels, supporting the previous speculation of the potential participation of oligomeric species in the pathoetiology of MIs.

Cerebral haemorrhages constitute another common finding in AD brains (Nakata et al., 2002; Cordonnier et al., 2006) and have been proposed to participate in the pathophysiology of the disease (Cordonier and van der Flier, 2011). Hence, the possible contribution of hypoperfusion and amyloid to the appearance of haemorrhages was also explored in the present study. Although the development of this type of lesions was minor, it was possible to observe a higher proportion of animals with haemorrhages in the transgenic group exposed to a longer period of hypoperfusion. It can be possible that a stronger stimulus such as longer exposure time to reduced CBF or higher Aβ levels (i.e. older mice) might be needed to induce a significant increase in haemorrhagic lesions. Indeed, sustained hypoperfusion over six months has been shown to induce widespread vascular disruption and BBB breakdown, leading to the development of haemorrhages in mice (Holland et al., 2015).

4.4.5. NVU alterations in response to Aβ and hypoperfusion.

The close interaction between the cells comprising the NVU controls the permeability of the BBB, regulates CBF and effective communication within the NVU is critical for normal cognitive function (Lok et al., 2007). As demonstrated in the present chapter, chronic cerebral hypoperfusion triggered the accumulation of Aβ in brain parenchyma and in the cerebrovasculature. This may contribute to perpetuate NVU alterations and accelerate the neurodegenerative process in AD. In order to test

this, the independent and combined effect of hypoperfusion and amyloid on astrocyte and TJ integrity was examined. The results of this study revealed significant differences between transgenic and control mice suggesting the involvement of Aβ deposition on these changes. Furthermore, it was demonstrated that slight reductions of CBF were able to exacerbate some of these changes, unveiling a synergistic contribution of both hypoperfusion and amyloid to the development of these alterations.

Interestingly, although behaviour was not assessed in the present study, there have been reports demonstrating that the behavioural performance of transgenic mouse models of AD is worsened following cerebral hypoperfusion. Reduced CBF induced by the occlusion of one common carotid artery aggravated the memory deficits in Tg2576 mice (Lee et al., 2011b). Similarly, BCAS triggered cognitive alterations in J20 mice (Yamada et al., 2011). In another study, where permanent occlusion of the right common carotid artery was performed in APPSWE/PS1 mice, learning deficits were also observed (Pimentel-Coelho et al., 2013). Notably, in all these studies, the behavioural alterations observed were the result of a synergistic effect of both hypoperfusion and the underlying Aβ pathology of the mice, as the effect was either not observed in the wild-type controls or it was the exacerbation of a pre-existent deficit in the transgenic mice. Nevertheless, there is a lack of studies, where the combination of hypoperfusion and AD models is explored in order to identify possible cellular or molecular targets involved in the pathways that lead to the cognitive alterations. This is of particular importance for the development of potential novel strategies for the prevention of AD.

4.4.6. Astrocyte alterations.

The function of astrocytes under physiological conditions is relatively well characterised, with increasing evidence suggesting an active role of this type of cells in several brain functions. However, their participation in the diseased brain remains poorly understood. The study of this has been particularly difficult since astrocytic reaction in response to brain injury can be diverse and potentially protective as well

as detrimental (Kölker et al., 2001; Chen and Swanson, 2003; Sofroniew, 2005; Barreto et al., 2011). There are also very few markers for the different pools of astrocytes and most studies focus on GFAP as a marker of astrocytes.

As demonstrated in previous reports, severe reduction of CBF induced by permanent BCCAO, has shown to induce upregulation of GFAP in the hippocampus of hypoperfused rats (Vicente et al., 2009). Similarly, most modest reductions of cerebral perfusion have shown astrogliosis in several WM areas of the brain in mice (Shibata et al., 2004). In contrast, the results of the present study showed no significant changes in GFAP levels following chronic cerebral hypoperfusion in wild-type mice. However, it is important to note that this discrepancy might relate to the different approaches used in these studies. For instance, in the present study, GFAP levels were determined in total brain homogenates and differently, in the previous studies above mentioned specific brain regions were analysed. Thus, although no general changes were observed in the current study, it is possible that potential regional changes might have been masked. Another explanation might be the differences in severity of CBF reductions and the extent of pathology caused.

Interestingly, it has been shown that in transgenic models of AD, astrocytic reaction is not homogeneous and, on the contrary, astrogliosis occurs in parallel to glial dystrophy as AD pathology progress, and this response is spatially different depending on the proximity of astrocytes to amyloid deposits (Rodríguez et al., 2009; Olabarria et al., 2010). The current study revealed an overall increase in astrocyte activation in the Tg-SwDI mice compared to the wild-type controls, suggesting the underlying involvement of Aβ pathology on this response. This data is in line with previously reported findings, where reactive astrogliosis has been found to be associated with Aβ aggregates in cell cultures (DeWitt et al., 1998), transgenic models of AD (Benzing et al., 1999) and in human AD brains (Nagele et al., 2004).

One of the key functions of astrocytes is the control of the ionic/osmotic balance in the brain through the water channel AQP4, which plays a central role in astrocyte plasticity in response to different types of brain of injury or stimuli. However, AQP4

also participates in pathophysiological conditions, as demonstrated by the reduced edema formation and improved neurological recovery following ischemic stroke in AQP4-knockout mice (Manley et al., 2000). Furthermore, there are conflicting reports showing either redistribution (Yang et al., 2011), downregulation (Wilcock et al., 2009) or upregulation (Moftakhar et al., 2010) of AQP4 associated to Aβ in transgenic mouse models of AD and in AD patients. However, these discrepancies may relate to differences in the particular experimental conditions of each study but more importantly to the stage of the disease or the severity of the pathology. Similar differences in AQP4 expression, in response to brain injury, have been shown by several reports. For example, increased AQP4 mRNA has been described following mechanical brain trauma (Vizuete et al., 1999) or focal cerebral ischemia (Taniguchi et al., 2000) in rats. However, a heterogeneous, time-dependent response was demonstrated following TBI, where a decreased AQP4 expression level was found followed by increased levels at later time points post injury (Ke et al., 2001). Hence, the, yet unknown, detrimental or beneficial role of AQP4 depends not only on the injury model but also on the time point studied.

The results presented in the current study showed increased AQP4 levels following chronic cerebral hypoperfusion in the Tg-SwDI mice, yet this difference was not observed in the wild–type group, suggesting a synergistic effect, where both amyloid and hypoperfusion contributed to the upregulation of the receptor. A dynamic, early and transient response can be presumed, as interestingly, this change was not observed at the later time point studied (3 months post-surgery). As mentioned above, differences on AQP4 dynamics might be time-dependant and determined by the extent of the injury. Hence, one explanation to this result could be that, as demonstrated before, following BCAS, CBF began to recover over time (Shibata et al., 2004), therefore the degree of the stimuli changes over time. Thus, although Aβ pathology is higher at the later time point, the synergistic effect might be lost.

A previous study showed compensatory AQP4 upregulation in response to oxidative damage in an AD mouse model and notably, deficiency of AQP4 in the same model resulted in higher oxidative stress and grater cognitive deficits (Liu et al., 2012). As

demonstrated in the previous chapter of the present thesis, NOX2 levels were also found to be upregulated in the Tg-SwDI model following 1 month of hypoperfusion, thus it is possible that the increased AQP4 levels observed might be a compensatory response to the increased oxidative stress induced by both hypoperfusion and Aβ. Indeed, there was a positive correlation between AQP4 and NOX2 levels. Interestingly, according to the association analyses performed, soluble parenchymal Aβ correlated with the higher AQP4 levels observed, suggesting the participation of this toxic amyloid species in the pathways that triggered this dynamic astrocytic reaction.

Astrocytes interact with the cerebrovasculature and neurons through their specialised foot processes, where AQP4 is highly expressed. This contact is crucial for the correct supply of metabolites to neurons, to maintain osmotic balance, and to regulate the local CBF in response to neuronal activity. Dissociation between astrocytic end-feet and capillaries has been shown to occur following ischemic insults resulting in a neurodegenerative inflammatory response (del Zoppo and Hallenbeck, 2000; Milner et al., 2008). After ischemia, increased ion and neurotransmitter uptake lead to enhanced water entry to the astrocyte, resulting in swelling of the end-feet (Kimelberg, 1995). Thus, astrocyte swelling triggered by AQP4 upregulation might be a possible mechanism by which loss of end-feet-capillary contact occurs in response to ischemic injury. Hence, given the increased AQP4 levels observed in the Tg-SwDI mice following hypoperfusion, it was hypothesised that this could lead to astrocyte-vasculature detachment. However, the results revealed no significant changes in the vascular AQP4 coverage, suggesting that the contact between end-feet and blood vessels was not altered neither by hypoperfusion nor by amyloid pathology. It is likely that the study was performed in an early stage, and such alterations were not present yet. Indeed, loss of AQP4 polarisation has been reported following six months of hypoperfusion in mice (Holland et al., 2015).

4.4.7. Tight junction alterations.

TJ proteins constitute an important structural component of the BBB. Alterations of the expression and distribution of these proteins can lead to altered brain homeostasis and contribute to neurodegenerative processes. Although TJ protein alteration is known to contribute to BBB dysregulation, previous reports on TJ protein levels in response to injury have shown conflicting data. For instance, a study demonstrated that Aβ induces enhanced endothelial permeability, however its effect on the expression of different TJ proteins was variable, showing downregulation of occludin but no changes in claudin-5 or ZO-1 (Tai et al., 2010). Other studies have shown decreased expression of occludin, claudin-5 and ZO-1 associated with vascular amyloid (Carrano et al., 2011). Conversely, Aβ treatment of isolated microvessels showed reductions of claudin-5 but no changes in occludin and ZO-1 levels (Hartz et al., 2012).

Additionally, chronic cerebral hypoperfusion has been linked with dysregulation of the BBB (Ueno et al., 2002, Wu et al., 2006), however, the specific effect of hypoperfusion on TJ integrity remains unclear. Interestingly, claudin-3 was shown to be upregulated following hypoperfusion induced by BCCAO (Shin et al., 2008). Altered levels of this protein have been associated with disrupted BBB permeability (Coyne et al., 2003; Wolburg et al., 2003; Brooks et al., 2005). Furthermore, *in vitro* studies performed to evaluate TJ integrity in oxidative environment have revealed contrasting results, with evidence of decreased claudin-5 and occludin expression (Schreibelt et al., 2007) but also enhanced occludin levels (Lee et al., 2004) induced by oxidative stress. Yet, BBB impairment was observed in both cases, regardless the outcome of the experiment.

Claudin-5 is one of the main components of the TJs, therefore it was used in the current study as a marker of NVU physical integrity. The results revealed significantly higher levels of claudin-5 in the Tg-SwDI mice compared to the wild-type controls and this was exacerbated following 1 month of hypoperfusion in the transgenic mice, suggesting an underlying influence of amyloid on the development

of this change and a synergistic effect when both injuries (Aβ and hypoperfusion) were present. Interestingly, the increased levels of claudin-5 positively correlated with the levels of cerebrovascular Aβ and no correlation was observed with levels of soluble parenchymal Aβ, suggesting that the accumulation of amyloid in blood vessel walls was likely the triggering factor that induced the altered expression of the protein.

Both cerebral hypoperfusion and vascular amyloid, which are associated with inflammation, constitute features of the AD and normal ageing brain. A number of studies have reported that with increased ageing, altered TJ protein expression leads to a "leaky" BBB condition (Mooradian et al., 2003; Sandoval and Witt, 2011; Blau et al., 2012). Notably, inflammation has also been shown to induce alterations in TJ protein levels, with increased expression of claudin-3 and claudin-5 (Brooks et al., 2005) and reduced occludin levels (Huber et al., 2001), leading to increased BBB permeability. Thus, an inflammatory response triggered by hypoperfusion and Aβ could be a possible explanation for the increased claudin-5 expression levels observed in the current study. Future studies are required to determine the mechanisms by which this response occurs. It would also be interesting to complement this study by looking at other components of the TJ such as ZO-1 and occludin.

It is important to mention that, rather than static structures, TJ complexes correspond to dynamic assemblies that are able to change in response to injury or stimuli in order to adapt to the conditions and that way maintain cerebral homeostasis. Hence, the dynamic properties of TJ should be taken into account when considering all the contradictory data observed in the literature, as subtle changes in experimental conditions including different time points studied, might result in different TJ reorganisation.

It is well known that astrocytes participate in the regulation of TJ proteins expression and therefore have a key role in the maintenance of the BBB (Janzer and Raff, 1987; Abbott et al., 2006). Hence, considering the previous finding of a similar response of

the astrocytes, where a synergistic effect of amyloid and hypoperfusion was found to contribute to AQP4 upregulation, following 1 month of hypoperfusion, it is possible to speculate that the changes observed at the TJ level, were likely a synchronised compensatory response where different structures of the NVU interacted in order to maintain or re-establish brain homeostasis following injury.

In the present study, the analysis of NVU alterations focussed on structural changes, and although these changes imply functional alterations it would be important to study this, for example by studying functional hyperaemia.

4.4.8. Summary and conclusions.

It is well documented that chronic cerebral hypoperfusion, an early feature of human AD, can alter Aβ metabolism, and this has been largely demonstrated in animal models of the disease (Kitaguchi et al., 2009; Okamoto et al., 2012; ElAli et al., 2013). In the present study, by investigating amyloid levels in parenchyma and vasculature at different time points, we have gained insights into the kinetics of aggregation of Aβ in the Tg-SwDI model and how this is altered by chronic cerebral hypoperfusion. In this model, Aβ is produced and rapidly aggregates to form insoluble fibrils. Hypoperfusion exacerbated this process. Similarly, in humans affected with AD, the misfolding and accumulation of Aβ in brain parenchyma and blood vessel walls are major hallmarks and constitute critical phases for the pathogenesis of the disease (Terry, 1994; Trojanowski and Lee, 2000). However, if amyloid accumulation constitutes a cause or a consequence of chronic hypoperfusion in humans, it remains currently unknown.

Critically, the results of this chapter demonstrate that chronic cerebral hypoperfusion induced a transient upregulation of APP that may have led to the increased Aβ levels and aggregation of the protein in the parenchyma followed by vascular accumulation. In the case of human AD this is not completely understood and whether increased APP levels, as a consequence of chronic cerebral hypoperfusion, constitutes the

source of the high amounts of Aβ in the brain of AD patients, has not been demonstrated.

Furthermore, the findings presented in this chapter provide evidence of a detrimental interaction between reduced CBF and Aβ pathology that contributed to the development of cerebrovascular alterations including MIs and changes in astrocytes and TJs, where specific pools of Aβ were differentially involved. Although the existence of a similar sinergistic interaction that may contribute to the progress of the disease in humans remains unknown, the independent involvement of hypoperfusion and amyloid accumulation on the development of degenerative processes has been shown to occur. Specifically, similar to what was found in this study, changes in specific components of the NVU have been demonstrated in the brains of patients with amyloid accumulation (Moftakhar et al., 2010; Hartz et al, 2012). Moreover, comparable with our findings, microinfarction has been shown to occur in areas of brain hypoperfusion in AD patients (Suter et al., 2002).

Altogether, these data support the importance of the role that Aβ plays in the pathoetiology of neurovascular deterioration, which may have implications on the development of AD. In addition, this evidence highlights the idea of an overlap between both the vascular and amyloid hypotheses of AD.

The next set of studies sought to explore whether modulation of amyloid levels by passive amyloid immunotherapy would impact on the degenerative processes found in the Tg-SwDI mice. As shown above Tg-SwDI mice exhibited, even in the absence of hypoperfusion, subcortical MIs associated with an inflammatory response.

Chapter 5. Effects of passive Aβ immunotherapy on amyloid levels and MIs in the Tg-SwDI mouse model.

5.1. Introduction.

Aggregation of Aβ peptide into soluble oligomers or amyloid plaques in brain parenchyma and cerebral blood vessels constitute a critical process in the pathogenesis of AD (Hardy and Selkoe, 2002), and suggests Aβ as an obvious therapeutic target. Thus, several approaches based on targeting Aβ in order to decrease brain levels of the protein, started to be developed (Panza et al., 2009), with Aβ immunotherapy being one of the most promising strategies for disease modifying treatment (Panza et al., 2012; Li et al., 2013; Sarazin et al., 2013). Importantly, data from clinical trials indicates that Aβ immunotherapy constitutes a potential treatment for AD patients (see section 1.1.10).

Although active immunisation with various Aβ peptide antigens failed to stimulate Aβ clearance in transgenic mouse models of AD due to impairment of the antibodies to cross the BBB (Vasilevko et al., 2007), passive peripheral administration of several antibodies including 10D5 and 3D6 has shown to reduce Aβ pathology (Bard et al., 2000; Bard et al., 2003). However, numerous reports demonstrating increased incidence of degenerative processes including haemorrhages in different transgenic mice following passive immunisation, have generated some concern (Pfeifer et al., 2002b; Wilcock et al., 2004; Racke et al., 2005; Wilcock et al., 2006; Burbach et al., 2007; Karlnoski et al., 2008; Schroeter et al., 2008). Hence, more research is needed before this approach can safely and successfully be applied in humans.

CAA is present in almost all cases of AD (Weller et al., 2009) and, as discussed in the previous chapter of the present thesis, leads to the deterioration of the cerebrovascular system, which constitutes a risk factor for cognitive decline and may contribute to neurodegenerative processes in AD. The Tg-SwDI mouse model accumulates Aβ in the brain parenchyma and predominantly in the cerebrovasculature as the animals age, modelling this key pathology associated with AD (Davis et al., 2004). The results of the previous chapter also demonstrated that MIs are present subcortically in these mice thus providing a link between amyloid aggregation and degenerative processes.

Hence, although passive immunisation has proven successful in reducing parenchymal and vascular Aβ in transgenic mouse models of AD, its efficacy in a model with robust vascular amyloid, at a stage when amyloid load is relatively low has not been tested.

5.1.1. Hypothesis and aim of study.

It was hypothesised that treatment with 10D5 and 3D6 antibodies decreases Aβ accumulation, reducing the MI load and improving the cognitive performance of the Tg-SwDI mouse model.

The specific aim of this study was to investigate the effects of passive immunisation with both 10D5 and 3D6 antibodies on Aβ40/42 levels in the parenchyma and cerebrovasculature of young heterozygous Tg-SwDI mice, at a time when amyloid burden is low, following 3 months of weekly intraperitoneal injections. Microglial burden in response to the therapy was also studied. A further aim was to determine whether treatment with these antibodies induces changes in the number of MIs and haemorrhages and whether the treatment is associated with improved cognitive performance.

5.2. Methods.

5.2.1. Animals.

Young male Tg-SwDI mice, on a heterozygous background were used. Controls, n = 8 (age = 5 ± 0.2 months); 10D5, n = 9 (age = 4.7 ± 0.2 months) and 3D6, n = 10 (age = 4.3 ± 0.05).

5.2.2. Injections.

The antibodies were obtained from Janssen Pharmaceutical Companies. Antibody solutions were diluted with sterile PBS and intraperitoneal injections were done as described in section 2.3.

5.2.3. Barnes maze.

Upon completion of the treatment, spatial learning and memory performance were tested by using the Barnes maze, as described in section 2.13.

5.2.4. Perfusion and tissue processing.

Following 3 months of treatment, animals underwent saline perfusion as described in section 2.4.1. The left hemi-brain was divided into 4 mm thick coronal sections and then processed for paraffin embedding. Coronal sections were produced as described in section 2.5.2. The right hemi-brain was used to generate parenchymal and vessel enriched fractions as described in section 2.9. Guanidine protein extraction (second step of sequential protein extraction) and quantification were performed as described in section 2.10.

5.2.5. Immunohistochemistry.

Immunohistochemistry was carried out as described in section 2.6. Tissue sections at anatomical level corresponding to -1.70 mm from bregma (Franklin and Paxinos, 1997) were used. Iba1 immunostaining was performed using immunoperoxidase labelling.

5.2.6. Histological detection of MIs and haemorrhages.

The detection of MIs was done by using H&E staining, which was performed as previously described in section 2.7.1. The detection of haemorrhages was done by using Prussian blue staining as described in section 2.7.2. Tissue sections at anatomical level corresponding to -1.70 and -2.18 mm from bregma (Franklin and Paxinos, 1997) were used.

5.2.7. Image analysis.

For the analysis of microglial load one image from the thalamus was acquired as described in section 2.8, at 4x magnification. Quantitative measurement of the staining was assessed by quantifying the number of positive Iba1 cells in the total area.

For the study of MIs, two sections per brain were analysed and one image of the thalamus per section was acquired as described in section 2.8, at 10x magnification. MIs were defined as sharply delimited areas of tissue pallor that were accompanied by microglial proliferation identified by Iba1 immunostaining in adjacent sections. The area covered by infarcted tissue was measured.

For the analysis of haemorrhages, two sections per brain were scanned. Haemorrhages were identified by the presence of ferric iron deposits on Perls stained sections. The presence or absence of haemorrhages in each mouse was recorded.

5.2.8. Enzyme-linked immunosorbent assay.

Levels of both Aβ1-40 and Aβ1-42 were determined by ELISA (Invitrogen) in protein samples extracted from the parenchymal and the vessel enriched fractions. In all experiments, manufacturer's instructions were used to perform the assays.

5.2.9. Statistical analysis.

The data obtained from the ELISA, Iba1 immunostaining and MI studies, were analysed for statistical significance using one-way ANOVA followed by the Bonferroni post-test. For the behaviour study statistical comparison was carried out using two-way repeated measures ANOVA (with training and treatment as factors), followed by the Bonferroni post-test.

5.3. Results.

5.3.1. Effects of 10D5 and 3D6 treatment on Aβ levels in the parenchyma and cerebrovasculature of Tg-SwDI mice.

To investigate whether administration of 10D5 or 3D6 antibodies may have had an effect on Aβ40/42 levels within the parenchyma and cerebrovasculature, amyloid levels were quantified by ELISA. Although lower levels of the protein were observed in the 10D5 and 3D6 treated groups, this was not significantly different from the control mice either in the parenchyma ($p = 0.20$ Aβ40, $p = 0.26$ Aβ42; Figure 5.1, a, c) or in the vasculature ($p = 0.08$ Aβ40, $p = 0.09$ Aβ42; Figure 5.1, b, d).

5.3.2. Treatment with 10D5 and 3D6 does not affect microglial burden.

In order to assess the microglial load following Aβ immunotherapy, Iba1 immunostaining was used to visualise microglial proliferation, and the number of microglial cells was quantified with ImageJ (Figure 5.2). As shown in the graph, no significant differences were observed between control and treated groups (Figure 5.3, 2).

5.3.3. Effects of 10D5 and 3D6 treatment on the development of MIs and haemorrhages.

The effect of Aβ immunotherapy on the development of MIs was studied by histological examination of tissue sections using H&E staining, and quantitative analysis of the area covered by MIs was done. Representative images of infarcted tissue in control, 10D5 and 3D6 groups are shown (Figure 5.3, a, b, c, respectively). Although the area covered by MIs in the 10D5/3D6 treated mice was not significantly different from the control group, it was noted that overall there was a tendency for the area of tissue damage to be reduced. The area of MIs was 0.0064 ± 0.0032 mm^2 (10D5 group) and 0.012 ± 0.0039 mm^2 (3D6 group) as compared to the control group ($0.017 \pm 0.0038 mm^2$) ($p = 0.15$; Figure 5.3, d).

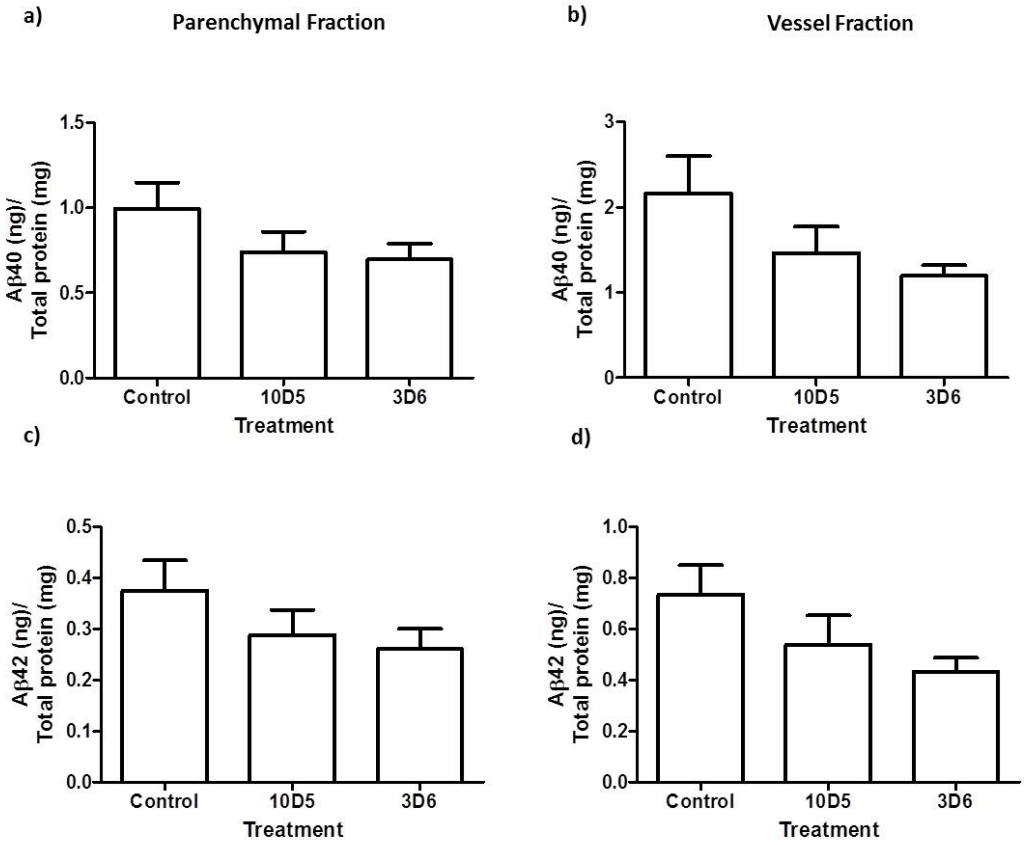

Figure 5.1. Effects of passive Aβ immunotherapy on cerebrovascular and parenchymal Aβ levels. Tg-SwDI animals were injected for 3 months with control, 10D5 or 3D6 antibodies and sacrificed 1 week after the last injection. Following protein extraction, the levels of Aβ40/42 were quantified in the parenchymal (a, c) and vessel enriched (b, d) fractions by ELISA. Graphs represent the levels of the protein normalised to total protein concentration. The data presented are the means ± S.E.M. There were no statistical differences determined using one-way ANOVA, $p > 0.05$ (control: $n = 8$, 10D5: $n = 9$ and 3D6: $n = 10$).

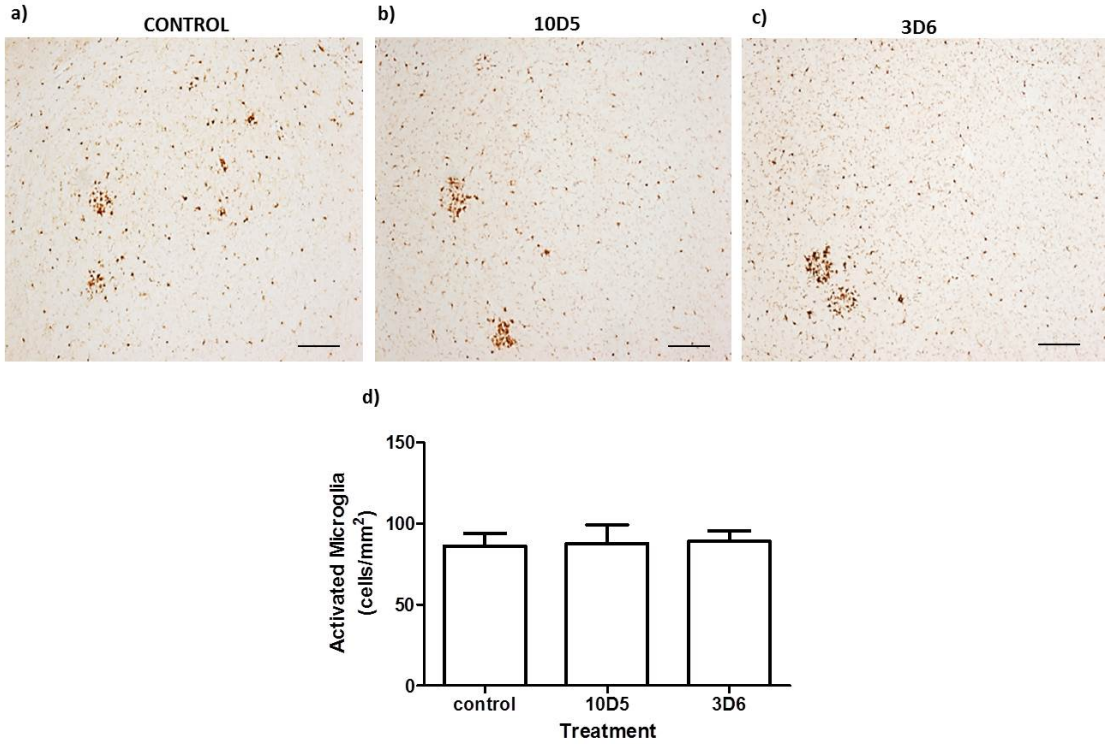

Figure 5.2. Microglia burden following Aβ immunotherapy. Representative images showing Iba1 staining, which was used to visualise microglial proliferation in controls (a), 10D5 (b) and 3D6 (c) treated mice (scale bar = 100 μm). The number of microglial cells was quantified with ImageJ and is represented in the graph (d). The data presented are the means ± S.E.M. There were no statistical differences determined using one-way ANOVA, $p > 0.05$ (control: n = 8, 10D5: n = 9 and 3D6: n = 10).

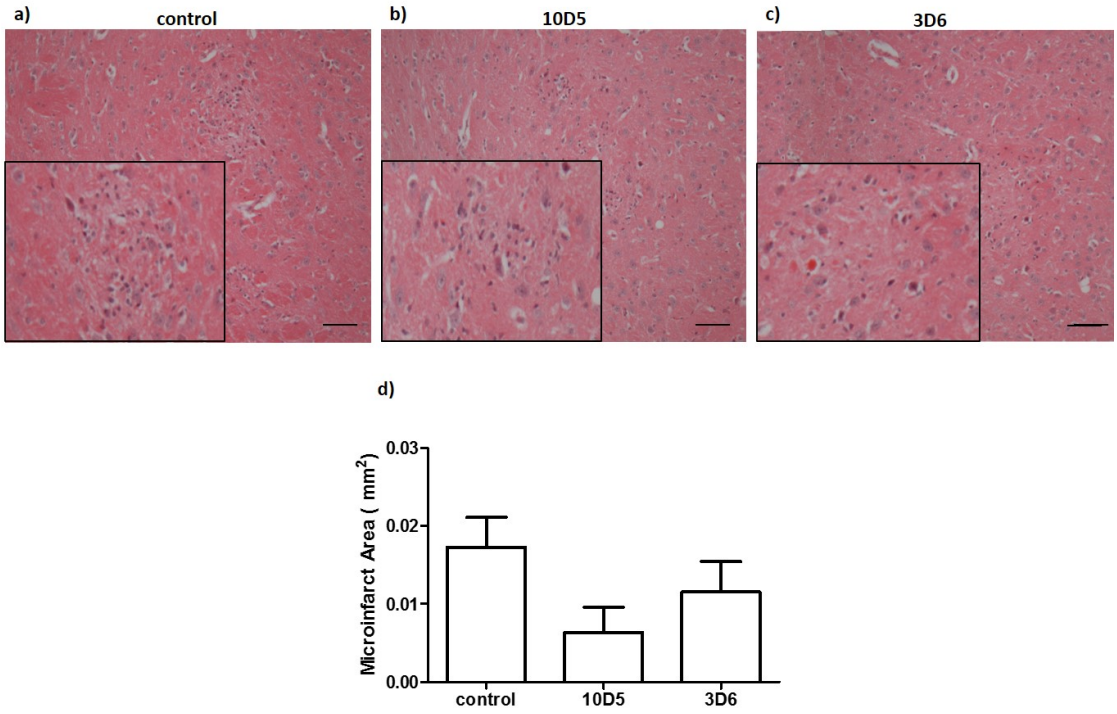

Figure 5.3. Microinfarct load following Aβ immunotherapy. Representative images showing infarcted tissue in controls (a), 10D5 (b) and 3D6 (c) treated mice (scale bar = 100 µm). Histopathological analysis was performed using H&E staining, the area covered by infarcted tissue was measured with ImageJ and is represented in the graphs. The data presented are the means ± S.E.M. There were no statistical differences determined using one-way ANOVA, $p > 0.05$ (control: n = 8, 10D5: n = 9 and 3D6: n = 10).

The analysis revealed no haemorrhages either in control or treated mice.

5.3.4. Assessment of spatial learning and memory performance following Aβ immunotherapy.

The impact of 10D5 and 3D6 administration on cognitive performance was explored using the Barnes maze, as described in section 2.13. Mice were trained over a period of 5 days, where they had to learn the relationship between distal cues to find the pathway to the escape box. 48 hours after the last training trial, animals were tested in a 90 seconds probe trial to assess long-term spatial memory.

Firstly, in order to define whether administration of 10D5 or 3D6 antibodies may have had an effect on the locomotor activity of the mice, the speed, distance travelled and the time that the mice spent immobile during the training were determined (Figure 5.4, a, b and c, respectively). As shown in the graphs, no significant differences were observed between control and 10D5 or 3D6 groups. This result indicates that if any changes in cognitive performance were to be found, this would not be influenced by locomotor alterations that the treatment might have potentially induced.

As shown in Figure 5.5, the mice in the three groups learnt the task, as it took less time to all of them to locate and enter the escape box as the training progressed. Accordingly, the graphs show a decreased numbers of primary and total errors the last training day, compared to the first day, in the three groups (Figure 5.5, c and d, respectively). However, statistical analysis revealed that neither the 10D5 nor 3D6 groups differed significantly from the control group, in terms of primary latency, latency to escape, primary errors and total errors, at all the time points analysed (all training days).

Assessment of long term spatial memory showed no significant changes in the number of primary and total errors between the controls and treated mice (Figure 5.6, a and b respectively). Additionally, the surface area of the maze was divided into

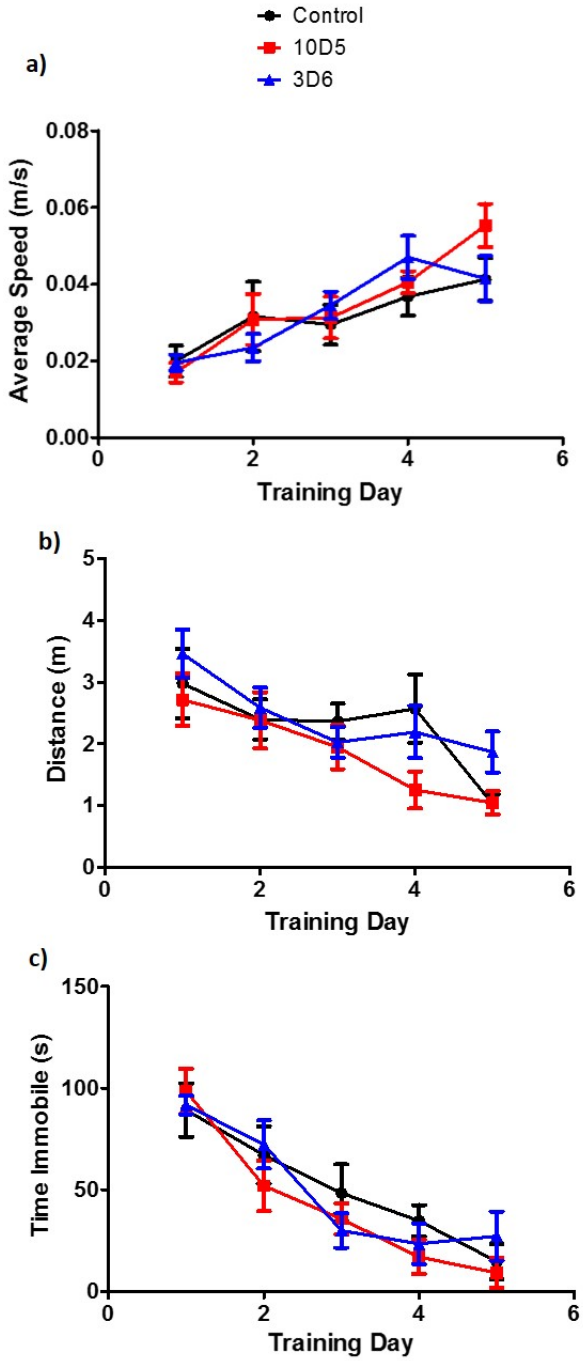

Figure 5.4. Locomotor activity following Aβ immunotherapy. The locomotor performance of Tg-SwDI mice following treatment, was assessed by using the Barnes maze. Graphs represent the speed (a), distance travelled (b) and time immobile (c) during the training. The data presented are the means ± S.E.M., two-way repeated measures ANOVA: significant effect of training ($F_{(4,96)} = 23.36$, ***$p < 0.0001$) (a); significant effect of training ($F_{(4,96)} = 9.492$, ***$p < 0.0001$) (b); significant effect of training ($F_{(4,96)} = 48.20$, ***$p < 0.0001$) (c).

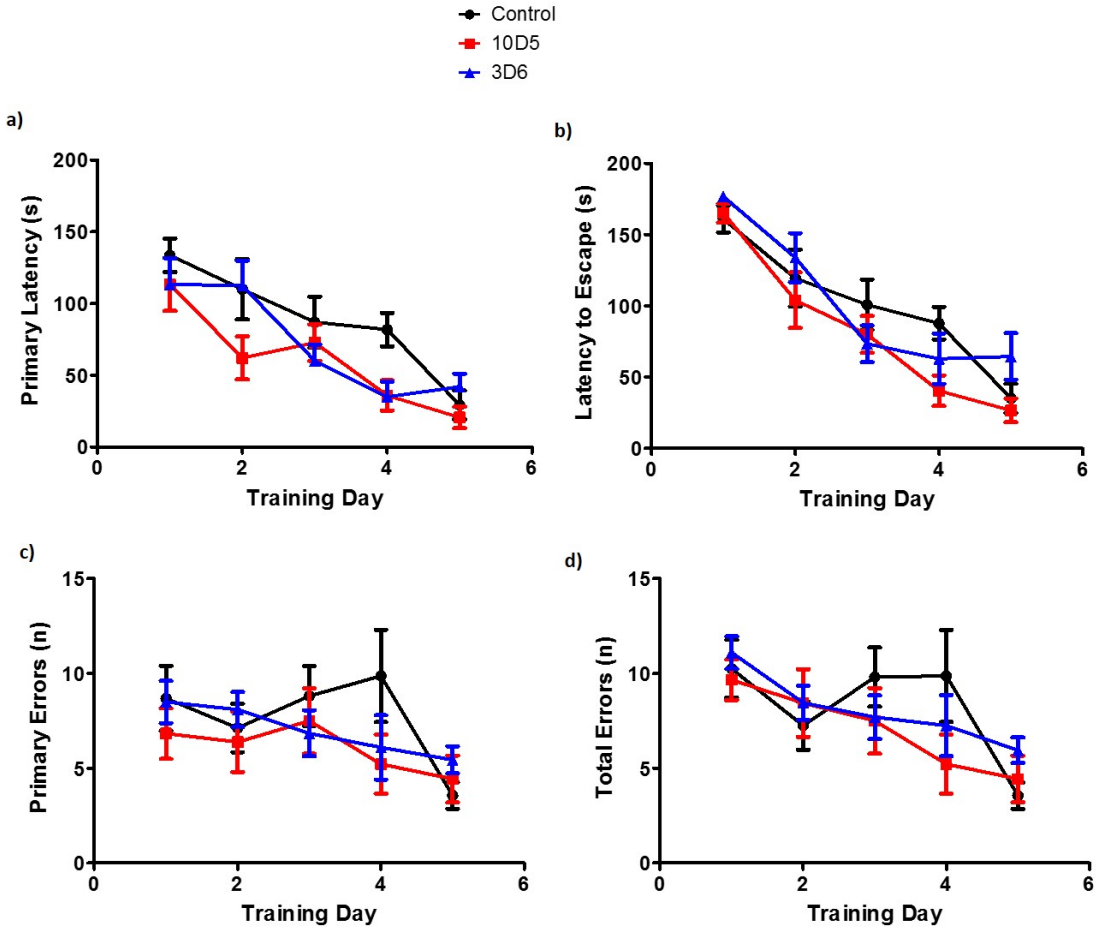

Figure 5.5. Spatial learning performance following Aβ immunotherapy. The learning performance following treatment was tested using the Barnes maze. Graphs represent the primary latency (a), latency to escape (b) primary errors (c) and total errors (d) recorded during the training. The data presented are the means ± S.E.M., two-way repeated measures ANOVA: significant effect of training ($F_{(4,96)}$ = 29.52, ***p < 0.0001) (a); significant effect of training ($F_{(4,96)}$ = 55.59, ***p < 0.0001) (b); significant effect of training ($F_{(4,96)}$ = 3.978, ***p = 0.005) (c); significant effect of training ($F_{(4,96)}$ = 7.968, ***p < 0.0001) (d).

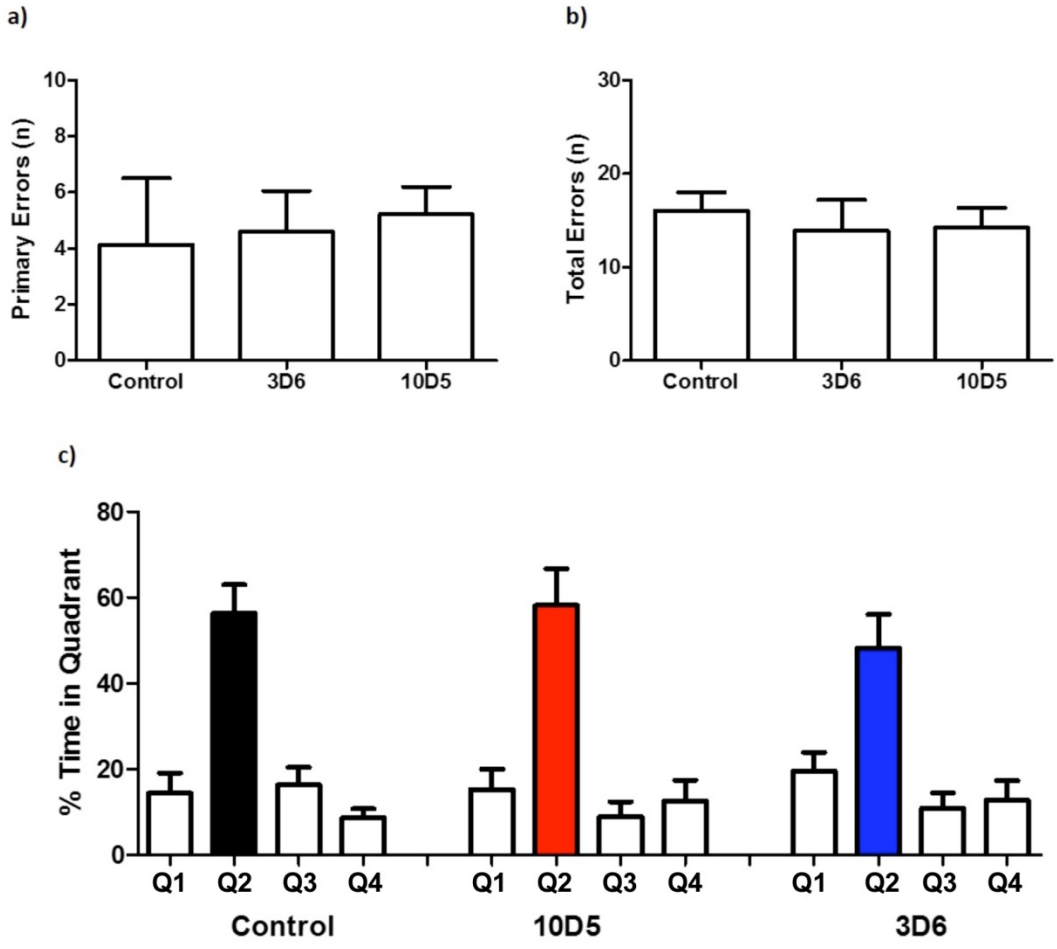

Figure 5.6. Long term spatial memory following Aβ immunotherapy. The memory performance following treatment was tested using the Barnes maze. Graphs represent the primary errors (a), total errors (b), and % of time spent on each quadrant, where Q2 correspond to the target quadrant (c) recorded during the probe trial. The data presented are the means ± S.E.M. There were no statistical differences between control and 10D5/3D6 groups determined using one-way ANOVA, $p > 0.05$ (control: n = 8, 10D5: n = 9 and 3D6: n = 10).

four zones containing five holes each, and the time spent exploring the zones was determined. As shown in the graph, all groups spent higher percent time exploring the target zone compared to the other zones (Figure 5.6, c). However, no significant differences were observed between the controls and treated mice.

5.4. Discussion.

To date, the majority of studies have focussed on clearing amyloid at stages when amyloid load is considerable and this has led to exacerbation of degenerative processes including haemorrhages. This study sought to examine the effects of passive amyloid immunisation at the early stages when amyloid burden is low.

Although there were no significant changes between control and 10D5/3D6 treated mice in amyloid levels, appearance of MIs and cognitive performance, it was noted that there was a trend towards a reduction in amyloid levels and MI area in the 10D5/3D6 treated mice compared to the control animals. Furthermore, there was no evidence of microhaemorrhages in response to the immunisation.

5.4.1. Immunotherapy mediated Aβ clearance.

The outcome of different passive amyloid immunotherapy studies on transgenic mice has shown variable results depending on different factors including the age of the animal when treatment was started, the amyloid load and the antibody used. The first passive Aβ immunotherapy experiments were performed in 2000 using PDAPP mice, which develop extensive accumulation of extracellular Aβ plaques. The results demonstrated that peripheral administration of 10D5 and 3D6 antibodies, which were able to reach the CNS, promoted Aβ clearance through Fc-dependant phagocytosis by microglia (Bard et al., 2000). Following studies performed in young PDAPP mice treated with m266 antibody, which recognises Aβ13–28, showed a decrease in soluble and insoluble amyloid levels, and the treatment also prevented the formation of plaques (DeMattos et al., 2001). However, studies in older PDAPP mice, demonstrated that only antibodies directed to n-terminal epitopes of the protein including 10D5 (which recognises Aβ3-7) and 3D6 (which recognises Aβ1-5), were able to clear the pre-existent amyloid deposits (Bard et al., 2003).

In the present study, although no significant differences were determined between control and treated groups, a trend towards decreased Aβ40 and Aβ42 levels in

parenchyma and in the cerebrovasculature of young Tg-SwDI mice was found following treatment with both 3D6 and 10D5 antibodies, markedly in the vessel fraction. In contrast, several studies have shown that although reduced parenchymal Aβ levels were found following immunisation, increased vascular amyloid was observed (Wilcock et al., 2004; Wilcock et al., 2006; Karlnoski et al., 2008). For example, it was reported that in Tg-SwDI mice, intracranial injection anti-Aβ antibodies purified from previously immunised mice with Aβ, efficiently cleared diffuse parenchymal plaques, but did not clear vascular amyloid (Vasilevko et al., 2007). Considering the intracranial delivery, it is unlikely that the lack of efficiency was due to inadequate concentration of the antibody in the brain. Therefore, this raised the concern that the particular biochemical or structural properties of the mutant Aβ generated in the Tg-SwDI model, which accumulates in the vasculature, makes it resistant to antibody mediated clearance. Indeed, there is evidence that suggests that vascular and parenchymal aggregates differ in composition (Herzig et al., 2004). Nevertheless, several differences can be found between the current study and the one performed by Vasilevko and colleagues, which need to be considered when comparing the results. For example, different antibodies and delivery route were used. Furthermore, the mice used in the published report were 14 months old at the moment of the injection and differently, in the present study, the first injection was performed when animals were ~4 months old, and therefore exhibited low levels of Aβ (Davis et al., 2004; Xu et al., 2007). Thus, it is possible that, in the present study, the treatment was able to induce the clearance of existent amyloid but also to prevent its accumulation in the vasculature. Future studies using an extra group of aged mice, are required to test this hypothesis.

It is important to note that the limited sample size used in the current study might have negatively influenced the sensitivity of the study; hence, by increasing the power, a more robust body of data would be obtained. Another main issue to be considered, is that, due to a delay in acquisition of the antibody and mice availability, the 3D6 group was set up later than the other two groups, and the average age of these animals was lower compared to the control mice (~3 weeks younger), which might have influenced the outcome of the experiment. For instance, as 3D6 was

injected in a younger cohort, it is not possible to rule out the fact that the overall reduction of Aβ observed in this group may be the result of the already lower levels of amyloid at the initiation of the experiment. Nonetheless, the 10D5 group was matched to the control group and this also showed a tendency towards a reduction in amyloid levels.

5.4.2. Microhaemorrhages and MIs following Aβ immunotherapy.

The development of cerebral microhaemorrhages has been described in numerous preclinical studies of Aβ immunotherapy (Pfeifer et al., 2002; Wilcock et al., 2004; Racke et al., 2005; Wilcock et al., 2006; Burbach et al., 2007; Karlnoski et al., 2008; Luo et al., 2010). Due to the observation of increased CAA in some of these mice, it has been suggested that clearance of parenchymal amyloid may increase vascular accumulation of the protein, which could be linked to the development of microhaemorrhages (Wilcock and Colton, 2009). It has also been suggested that the mechanism by which these lesions occurs is related to the removal of vascular amyloid from the vessel wall, which may expose the pre-existing vascular pathology associated with CAA and contribute to the leakage of the vasculature and the appearance of microbleeds (Zago et al., 2013). Indeed, a 3D6 dose-response study performed in 12 months old PDAPP mice revealed evidence of microhaemorrhage in a subset of vessels, specifically at sites where Aβ was partially or completely removed (Schroeter et al., 2008). Interestingly, in the current study no microbleeds were observed following 3 months of treatment. As previously mentioned, vascular Aβ levels in the mice used in the present study were low when the treatment was initialised, therefore it is likely that rather than removal of vascular amyloid deposits, immunisation with 3D6 and 10D5 antibodies prevented further accumulation of the protein in the vasculature. Consequently, this might have also prevented the development of vascular alterations associated either with the accumulation or removal of Aβ in the vessel wall. The vessel integrity in Tg-SwDI mice at this age of immunisation is also likely to be intact and thus be more resistant to the effects of amyloid trafficking across the BBB or build-up of CAA than at later ages.

As demonstrated in a previous chapter of the present thesis, accumulation of amyloid in the brain is associated with the development of MIs. Hence, it seems logical to hypothesise that decreased Aβ levels induced by amyloid immunisation would reduce the development of this type of lesions. However, some reports have shown evidence of microinfarction as part of the secondary effects of Aβ immunotherapy in AD patients and have attributed this to the exacerbation of CAA post treatment (Uro-Coste el at., 2010; Sakai and Yamada, 2013). Interestingly, although the data presented in the current study did not achieve statistical significance, there was a tendency for MI load to be reduced in the mice receiving the 10D5 and 3D6 antibodies as compared to the control animals. A possible explanation for this finding may relate to the decreased levels of Aβ with no further build-up of deposits in the vasculature following the treatment, as lower amyloid levels in the immunised mice might have prevented an oxidative as well as an inflammatory response that could have contributed to the development of MIs. However future studies would be required to clarify this premise.

5.4.3. Cognitive performance following Aβ immunotherapy.

Both active and passive amyloid immunotherapy strategies have proven to attenuate cognitive deficits in transgenic models (Janus et al., 2000; Dodart et al., 2002; Hartman et al., 2005; Wilcock et al., 2006). However this has not been reflected in humans and therefore, with a limited effect in clinical trials, the approach has not been translated into a treatment for AD (see section 1.1.10).

As demonstrated in previous reports, the Barnes maze task has been successfully used to determine cognitive deficits in the Tg-SwDI mice (Xu et al., 2007; Xu et al., 2014). Therefore, in the current study, this test was used to determine spatial learning and memory performance in Tg-SwDI mice following treatment with 3D6 and 10D5 antibodies. All mice learnt the task and showed a marked preference for exploring the target quadrant during the probe trial. However, no significant differences were found between control and 10D5/3D6 treated groups. A possible explanation for this result may be attributable to the minimal differences observed between control and

treated groups in amyloid burden following the therapy, as it might be possible that a certain threshold of amyloid levels needs to be reached in order for this to be translated into cognitive changes. Indeed, in the previously mentioned study by Xu and colleagues, where behavioural alterations were detected with the Barnes maze even in very young mice compared to wild-type controls, the animals used were homozygous, which develop more extensive Aβ pathology and at an earlier age than heterozygous mice. Hence, considering the heterozygous background of the animals used in the current study, and the low reduction in Aβ levels post-treatment, it is not surprising that no behavioural changes were found.

An important weakness of this study is the lack of a wild-type group as comparative controls. This would have allowed to determine whether there are behavioural alterations in the Tg-SwDI mice compared to the wild-type mice that could be reversed following the immunotherapy.

As shown previously in the present thesis, amyloid deposition is associated with microglial activation. Moreover, amyloid related cognitive alterations in Tg-SwDI mice have been shown to be associated with microglial activation and neuroinflammation (Xu et al., 2007). Therefore considering the trend towards reduced Aβ observed in the present study, it was reasonable to expect a similar trend of decreased microglial burden. However, no change in microglial cell number was found. This result supports the idea that the reduction in amyloid levels induced by the treatment was probably not sufficient to reduce the underlying inflammation that could have been reflected in a cognitive improvement.

Interestingly, a study looking at synapsis integrity in Tg2576 mice following immunotherapy with 6G1 and A-887755 antibodies, showed improved synaptic pathology even when no effect on fibrillar amyloid load was observed (Dorostkar et al., 2014). Furthermore, there is evidence of reduced memory impairment without lowering Aβ burden following immunotherapy with the m266 antibody in PDAPP mice (Dodart et al., 2002). In this study, it is discussed that reversal of memory impairment was probably associated to reductions in soluble Aβ species. Indeed, it

has been suggested that the failure to reach clinical endpoint in human trials of Aβ immunotherapy is probably due to clearance of the non-pathological Aβ species, instead of using conformational antibodies directed to the most cytotoxic amyloid pools (Murakami, 2014).

5.4.4. Summary and conclusions.

The results presented in the current chapter demonstrate that Aβ immunotherapy with the antibodies 3D6 and 10D5 may potentially decrease parenchymal and vascular amyloid accumulation, reducing the appearance of MIs and notably without triggering the development of microhaemorrhages. Further studies are needed to confirm this evidence. This is of particular importance, as Bapineuzumab, which constitutes the humanised form of the 3D6 antibody, was the first antibody tested in humans, as a potential strategy to reverse the cognitive impairment in AD patients. The treatment showed decreased Aβ burden, but it was associated with high incidence of amyloid related imaging abnormalities, and therefore the program was ended in phase III due to failure of the treatment to reach clinical endpoint (Panza et al., 2011; Tayeb et al., 2013).

Aβ aggregation constitutes a slow process that takes decades to develop. An effective treatment before the symptoms are visible seems to be a more reasonable strategy than attempting to reverse the pathology when the damage is already present and irreversible due the complexity of the pathological pathways triggered. Hence, the use of Aβ immunotherapy in the early stages of disease, as a preventive measure, might be more effective. This might also prevent further development of vascular alterations associated either with the accumulation or removal of Aβ in the vessel wall. For this reason, we aimed to carry out the intervention studies in young mice, before Aβ starts to accumulate. In contrast, as no diagnostic method has been successfully developed in order to allow the early detection of the disease in humans, clinical trials have been designed to test Aβ immunotherapy in AD patients when the clinical symptoms are present and amyloid burden is very high, and this is likely the

reason of the high incidence of degenerative processes such as haemorrhages post-treatment.

The results presented here are relevant not only for the implications in AD but also has ramifications for CAA, as no treatment is currently available for this pathology and amyloid immunisation strategies constitute a potential therapy.

Chapter 6. Overview and conclusions.

6.1. Summary.

The findings presented in this thesis provide insights into the events that are initiated by chronic cerebral hypoperfusion and culminate with degenerative processes that may lead to cognitive decline in AD. Initially, Aβ pathology was temporally characterised in the transgenic mouse model of amyloidosis Tg-SwDI. In this model, mild cerebral hypoperfusion modified APP metabolism, triggering an early increase in the levels of soluble Aβ in the parenchyma followed by aggregation of the protein into insoluble fibrils, with the subsequent build-up of aggregates in the cerebrovasculature. Furthermore, a model of mixed injury was studied by inducing chronic cerebral hypoperfusion in Tg-SwDI mice, in order to explore the contribution of both hypoperfusion and Aβ deposition to cerebrovascular alterations. It was demonstrated that Aβ pathology is associated with the development of MIs and the alteration of specific elements of the NVU, and that hypoperfusion exacerbated these changes. Finally amyloid immunotherapy showed a trend towards decreased Aβ accumulation without further development of the commonly seen associated pathological processes, supporting the view of this therapy as a potential treatment for AD.

Collectively, these findings provide evidence of a detrimental interaction between chronic cerebral hypoperfusion and Aβ pathology that contributed to the onset of the observed alterations. Thus, a mechanistic pathway is proposed, in which the cascade of events including inflammation and oxidative stress, triggered synergistically by chronic cerebral hypoperfusion and Aβ, results in the disruption of the NVU and the widespread development of MIs which may further induce the alteration of cognition networks. In parallel, vascular Aβ accumulation may contribute to perpetuate cerebrovascular dysfunction and accelerate the cognitive decline (Figure 6.1.)

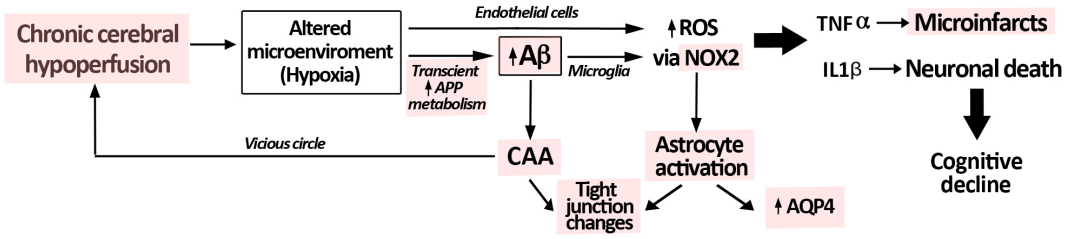

Figure 6.1. Proposed mechanistic pathway leading to cognitive decline in AD. Vascular risk factors promote cardiovascular alterations that lead to reduced cerebral perfusion, which in turn triggers metabolic changes in the cerebrovasculature. These changes increases amyloid production leading to inflammation and oxidative stress, promoting degenerative processes including MIs and NVU disruption, which may contribute to cognitive deterioration in AD. The findings of this thesis are highlighted in the figure.

6.2. Clinical implications and future studies.

It is likely that in a healthy individual, the brain is able to react following different types of injuries, by inducing compensatory responses such as changes in APP metabolism to induce neuroprotection or adaptive NVU modifications to maintain or re-establish brain homeostasis. However, in the context of pathological conditions induced by VRFs, such as ageing-related cerebrovascular deterioration, it is possible that the system loses its capability of adaptation. In this case, the changes that initially occurred as part of a transient compensatory response, such as the increased APP metabolism, turn into permanent alterations that contribute to the damage and act to self-perpetuate the degenerative processes, for instance, by inducing Aβ accumulation due to faulty clearance of the protein.

As demonstrated in the current thesis, enhanced APP and APP cleavage occurred following chronic cerebral hypoperfusion in the Tg-SwDI mice, probably as part of an adaptive response triggered in order to induce neuroprotection or recovery. Yet, considering the pathological environment of this model (Davis et al., 2004; Searcy et al, 2014), which display underlying genetic predisposition to develop amyloidosis, it cannot be ruled out that this might have influenced the results, potentiating the induction of metabolic and tissue damage.

The events leading to chronic cerebral hypoperfusion during the normal ageing process may take decades. The evidence has shown a reduction of the CBF of approximately 20% at 60 years of age as compared to age 20, and a continuous rate of dropping of 0.5% per year until age 80 (Leenders et al., 1990; Zou et al., 2009; Chen et al., 2011a). Previous characterisation of the mouse model of chronic cerebral hypoperfusion induced by BCAS used in the present thesis, has shown an initial reduction of CBF of about 30%, which is gradually recovered to approximately 10% following 1 month (Shibata et al., 2004). Therefore, although it represents an extremely useful model to study the implications of modest reductions of CBF on different aspects related to the aetiology and treatment of cognitive decline, the

model does not recapitulate the gradual and progressive process that occurs with increasing ageing in humans.

Similarly, it is widely accepted that pathological changes such as Aβ misfolding and oligomerisation constitute a slow process and may initiate decades before clinical symptoms are evident in AD patients (Braak et al., 1999; Buchhave et al., 2012). This represents another limitation of the model used in the present study, as the genetic mutations in APP predispose these mice to early and robust amyloid accumulation (Davis et al., 2004).

Considering the issues addressed above, it would be interesting to perform a similar study as the one presented in this thesis, using a different model that could replicate more closely the conditions that occurs in the context of the human pathology. This could be achieved by inducing a more gradual reduction of CBF (Kitamura et al., 2012), in a mouse model expressing the human APP without any mutations (Mucke et al., 2000). Thus, the gradual reduction of CBF would prevent the initial acute hypoxic condition and inflammatory response triggered by the severe blood flow drop. On the other hand, the use of a model expressing the wild-type human APP would avoid the genetic predisposition to develop Aβ aggregates spontaneously, although maintaining the possibility of studying experimentally-induced Aβ aggregation (which is not possible by using wild-type mice that expresses non amyloidogenic Aβ).

The experimental design of the present thesis was aimed at modelling the early events that may contribute to degenerative processes that occur in AD, therefore young mice were subjected to chronic brain hypoperfusion. However, it would be interesting to carry out a similar study using aged mice in an attempt to determine the repercussion that reduced CBF would have in the aging brain. This would mirror more closely the course of the pathology in humans. Interestingly, age has been previously demonstrated to be an important factor when studying the effects of hypoperfusion on metabolic and cognitive changes in rats (de la Torre et al., 1992).

As research in the AD field progresses, it becomes evident that when the disease is clinically manifested, a complex combination of molecular and cellular alterations has already occurred (McGeer et al., 1989; Delacourte et al., 1999; Smith et al., 2000; Cordonnier and van der Flier, 2011; van Rooden et al., 2014). For this reason, many potential targets have been the focus of different studies in an attempt of finding a successful treatment or cure for the disease (McGeer and McGeer, 1995; Sadowski et al., 2006; Greig et al., 2001; Corona et al., 2011; Deane et al., 2012; Herrmann and Spires-Jones, 2014; Hook et al., 2014; Iqbal et al., 2014).

However, considering some key aspects that were studied in the present thesis, it becomes reasonable to focus on a mixed intervention targeting brain hypoperfusion and Aβ. The key findings supporting this premise include: the evidence reinforcing the view of chronic cerebral hypoperfusion as the initial triggering factor that leads to AD pathology; the fact that Aβ represents a key contributor to the onset and progression of the disease; and that the independent or combined presence of hypoperfusion and Aβ can lead to most of the molecular, cellular and structural disturbances present in the AD brain, amongst them WM alterations, axon-gial disruption, microinfarction, microbleeds, tau hyperphosphorylation, NVU changes, CAA, neurodegeneration and synapse loss, some of which were addressed in this thesis (Shankar et al., 2007; Palop and Mucke, 2010; Coltman et al., 2011; Cordonnier and van der Flier, 2011; Reimer et al., 2011; Okamoto et al., 2012; Zhao et al; 2014).

As previously discussed, the events leading to chronic cerebral hypoperfusion, as well as the initial steps in Aβ aggregation, constitute slow processes that take decades to develop. Therefore, early diagnosis has become crucial and considerable efforts have been made to address this matter. Indeed, the detection of Aβ oligomers in biological fluids of AD patients constitutes a promising tool for the early diagnosis of AD (Salvadores et al., 2014). Of similar importance is the early identification of VRFs that could potentially lead to cerebral hypoperfusion, to stop the progression of underlying disease (Solomon et al., 2009). Thus, early diagnosis, in order to allow effective treatment before the symptoms become obvious seems to be more

reasonable than attempting to reverse the pathology when the damage is already present and irreversible due the complexity of the pathological pathways triggered.

The findings described in this thesis highlight the importance of vascular care in midlife, which means to have a healthy life that could be achieved by having a healthy diet, exercising regularly, avoiding smoking, alcohol, and all vascular risk factors (hypercholesterolemia, hypertension, etc.) that could lead to damage of the cardiovascular system. This could potentially prevent reduced cerebral perfusion during the ageing process and this in turn would prevent the initiation of Aβ pathology. Additionally, amyloid immunisation aimed at preventing Aβ accumulation by clearing any excess of the protein before the process of oligomerisation is initiated, would also decrease the likelihood of developing AD in later life. A combined, early intervention targeting hypoperfusion and amyloid appears to be crucial, as both pathologies have shown to be able to self-perpetuate and also to interact to potentiate each other.

6.3. Conclusion.

By 2050, the number of cases of AD will triple and at present there is no effective treatment for the disease. Even more devastating is that it seems that there is no consensus regarding the aetiology of the disease. The present thesis builds on the discovery of the close resemblance between VaD and AD, and further finding of chronic cerebral hypoperfusion as a potential contributor to cognitive decline. Together, the results outlined in this study add to the role of reduced cerebral perfusion as a trigger in the initial steps of the chain of events leading to degenerative processes that may lead to cognitive deterioration. Moreover, the participation of Aβ is emphasised. These findings could be extended by future studies aiming at the investigation of a combined intervention strategy for the prevention of AD progression before the damage is irreversible.

References

Aaslid R, Lindegaard KF, Sorteberg W, Nornes H. (1989) Cerebral autoregulation dynamics in humans. Stroke. 20(1):45-52.

Abbott NJ, Patabendige AA, Dolman DE, Yusof SR, Begley DJ. (2010) Structure and function of the blood-brain barrier. Neurobiol Dis. 37(1):13-25.

Abbott NJ, Rönnbäck L, Hansson E. (2006) Astrocyte-endothelial interactions at the blood-brain barrier. Nat Rev Neurosci. 7(1):41-53.

Abramov AY, Canevari L, Duchen MR. (2004) Beta-amyloid peptides induce mitochondrial dysfunction and oxidative stress in astrocytes and death of neurons through activation of NADPH oxidase. J Neurosci. 24(2):565-575.

Ainslie PN, Tzeng YC. (2010) On the regulation of the blood supply to the brain: old age concepts and new age ideas. J Appl Physiol. 108(6):1447-1449.

Akiyama H, Barger S, Barnum S, Bradt B, Bauer J, Cole GM, Cooper NR, Eikelenboom P, Emmerling M, Fiebich BL, Finch CE, Frautschy S, Griffin WS, Hampel H, Hull M, Landreth G, Lue L, Mrak R, Mackenzie IR, McGeer PL, O'Banion MK, Pachter J, Pasinetti G, Plata-Salaman C, Rogers J, Rydel R, Shen Y, Streit W, Strohmeyer R, Tooyoma I, Van Muiswinkel FL, Veerhuis R, Walker D, Webster S, Wegrzyniak B, Wenk G, Wyss-Coray T. (2000) Inflammation and Alzheimer's disease. Neurobiol Aging. 21(3):383-421.

Alsop DC, Dai W, Grossman M, Detre JA. (2010) Arterial spin labeling blood flow MRI: it's role in the early characterization of Alzheimer's disease. J Alzheimers Dis. 20(3):871-880.

Allen N, Robinson AC, Snowden J, Davidson YS, Mann DM. (2014) Patterns of cerebral amyloid angiopathy define histopathological phenotypes in Alzheimer's disease. Neuropathol Appl Neurobiol. 40(2):136-148.

Alvarez JI, Cayrol R, Prat A. (2011a) Disruption of central nervous system barriers in multiple sclerosis. Biochim Biophys Acta. 1812(2):252-264.

Alvarez JI, Dodelet-Devillers A, Kebir H, Ifergan I, Fabre PJ, Terouz S, Sabbagh M, Wosik K, Bourbonnière L, Bernard M, van Horssen J, de Vries HE, Charron F, Prat A. (2011b) The Hedgehog pathway promotes blood-brain barrier integrity and CNS immune quiescence. Science. 334(6063):1727-1731.

Alzheimer A. (1907) Ueber eine eigenartige erkrankung der hirnrinde. Z Gesamte Neurol Psychiatr. 18:177–179.

Alzheimer's Association. (2014). Alzheimer's Disease Facts and Figures. Alzheimer's and dementia. 10(2):1-80.

Amin J, Paquet C, Baker A, Asuni AA, Love S, Holmes C, Hugon J, Nicoll JA, Boche D. (2014) Effect of Aβ immunisation on hyperphosphorylated tau: a potential role for GSK-3β Neuropathol Appl Neurobiol. 2014 Dec 9. doi: 10.1111/nan.12205. [Epub ahead of print]

Applegate WB, Pressel S, Wittes J, Luhr J, Shekelle RB, Camel GH, Greenlick MR, Hadley E, Moye L, Perry HM Jr, Schron E, Wegener V. (1994) Impact of the treatment of isolated systolic hypertension on behavioral variables. Results from the systolic hypertension in the elderly program. Arch Intern Med. 154(19):2154-2160.

Arriagada PV, Growdon JH, Hedley-Whyte ET, Hyman BT. (1992) Neurofibrillary tangles but not senile plaques parallel duration and severity of Alzheimer's disease. Neurology. 42(3 Pt 1):631-639.

Arvanitakis Z, Leurgans SE, Barnes LL, Bennett DA, Schneider JA. (2011) Microinfarct pathology, dementia, and cognitive systems. Stroke. 42(3):722-727.

Asahina M, Yoshiyama Y, Hattori T. (2001) Expression of matrix metalloproteinase-9 and urinary-type plasminogen activator in Alzheimer's disease brain. Clin Neuropathol. 20(2):60-63.

Asuni AA, Boutajangout A, Quartermain D, Sigurdsson EM. (2007) Immunotherapy targeting pathological tau conformers in a tangle mouse model reduces brain pathology with associated functional improvements. J Neurosci. 27(34):9115-29.

Attems J. (2005) Sporadic cerebral amyloid angiopathy: pathology, clinical implications, and possible pathomechanisms. Acta Neuropathol. 110(4):345-359.

Attems J, Jellinger KA. (2004) Only cerebral capillary amyloid angiopathy correlates with Alzheimer pathology-a pilot study. Acta Neuropathol. 107(2):83-90.

Attems J, Jellinger KA. (2014) The overlap between vascular disease and Alzheimer's disease--lessons from pathology. BMC Med. 12:206.

Atwood CS, Obrenovich ME, Liu T, Chan H, Perry G, Smith MA, Martins RN. (2003) Amyloid-beta: a chameleon walking in two worlds: a review of the trophic and toxic properties of amyloid-beta. Brain Res Brain Res Rev. 43(1):1-16.

Auriel E, Greenberg SM. (2012) The pathophysiology and clinical presentation of cerebral amyloid angiopathy. Curr Atheroscler Rep. 14(4):343-350.

Ballabh P, Braun A, Nedergaard M. (2004) The blood-brain barrier: an overview: structure, regulation, and clinical implications. Neurobiol Dis. 16(1):1-13.

Bandopadhyay R, Orte C, Lawrenson JG, Reid AR, De Silva S, Allt G. (2001) Contractile proteins in pericytes at the blood-brain and blood-retinal barriers. J Neurocytol. 30(1):35-44.

Bard F, Barbour R, Cannon C, Carretto R, Fox M, Games D, Guido T, Hoenow K, Hu K, Johnson-Wood K, Khan K, Kholodenko D, Lee C, Lee M, Motter R, Nguyen M, Reed A, Schenk D, Tang P, Vasquez N, Seubert P, Yednock T. (2003) Epitope and isotype specificities of antibodies to beta -amyloid peptide for protection against Alzheimer's disease-like neuropathology. Proc Natl Acad Sci U S A. 100(4):2023-2038.

Bard F, Cannon C, Barbour R, Burke RL, Games D, Grajeda H, Guido T, Hu K, Huang J, Johnson-Wood K, Khan K, Kholodenko D, Lee M, Lieberburg I, Motter R, Nguyen M, Soriano F, Vasquez N, Weiss K, Welch B, Seubert P, Schenk D, Yednock T. (2000) Peripherally administered antibodies against amyloid beta-peptide enter the central nervous system and reduce pathology in a mouse model of Alzheimer disease. Nat Med. 6(8):916-919.

Baron JC, Bousser MG, Rey A, Guillard A, Comar D, Castaigne P. (1981) Reversal of focal "misery-perfusion syndrome" by extra-intracranial arterial bypass in hemodynamic cerebralischemia. A case study with 15O positron emission tomography. Stroke. 12(4):454-459.

Baron R, Babcock AA, Nemirovsky A, Finsen B, Monsonego A. (2014) Accelerated microglial pathology is associated with Aβ plaques in mouse models of Alzheimer's disease. Aging Cell. 13(4):584-595.

Barreto G, White RE, Ouyang Y, Xu L, Giffard RG. (2011) Astrocytes: targets for neuroprotection in stroke. Cent Nerv Syst Agents Med Chem. 11(2):164-173.

Barten DM, Meredith JE Jr, Zaczek R, Houston JG, Albright CF. (2006) Gamma-secretase inhibitors for Alzheimer's disease: balancing efficacy and toxicity. Drugs R D. 7(2):87-97.

Battistin L, Cagnin A. (2010) Vascular cognitive disorder. A biological and clinical overview. Neurochem Res. 35(12):1933-1938.

Beason-Held LL, Moghekar A, Zonderman AB, Kraut MA, Resnick SM. (2007) Longitudinal changes in cerebral blood flow in the older hypertensive brain. Stroke. 38(6):1766-1773.

Bell RD, Winkler EA, Sagare AP, Singh I, LaRue B, Deane R, Zlokovic BV. (2010) Pericytes control key neurovascular functions and neuronal phenotype in the adult brain and during brain aging. Neuron. 68(3):409-427.

Bell RD, Zlokovic BV. (2009) Neurovascular mechanisms and blood-brain barrier disorder in Alzheimer's disease. Acta Neuropathol.118(1):103-113.

Bennett SA, Pappas BA, Stevens WD, Davidson CM, Fortin T, Chen J. (2000) Cleavage of amyloid precursor protein elicited by chronic cerebral hypoperfusion. Neurobiol Aging. 21(2):207-214.

Benzing WC, Wujek JR, Ward EK, Shaffer D, Ashe KH, Younkin SG, Brunden KR. (1999) Evidence for glial-mediated inflammation in aged APP(SW) transgenic mice. Neurobiol Aging. 20(6):581-589.

Bi M, Ittner A, Ke YD, Götz J, Ittner LM. (2011) Tau-targeted immunization impedes progression of neurofibrillary histopathology in aged P301L tau transgenic mice. PLoS One. 6(12):e26860.

Bianca VD, Dusi S, Bianchini E, Dal Prà I, Rossi F. (1999) beta-amyloid activates the O-2 forming NADPH oxidase in microglia, monocytes, and neutrophils. A possible inflammatory mechanism of neuronal damage in Alzheimer's disease. J Biol Chem. 274(22):15493-15499.

Bierer LM, Hof PR, Purohit DP, Carlin L, Schmeidler J, Davis KL, Perl DP. (1995) Neocortical neurofibrillary tangles correlate with dementia severity in Alzheimer's disease. Arch Neurol. 52(1):81-88.

Blau CW, Cowley TR, O'Sullivan J, Grehan B, Browne TC, Kelly L, Birch A, Murphy N, Kelly AM, Kerskens CM, Lynch MA. (2012) The age-related deficit in LTP is associated with changes in perfusion and blood-brain barrier permeability. Neurobiol Aging. 33(5):1005.e23-35.

Boche D, Donald J, Love S, Harris S, Neal JW, Holmes C, Nicoll JA. (2010) Reduction of aggregated Tau in neuronal processes but not in the cell bodies after Abeta42 immunisation in Alzheimer's disease. Acta Neuropathol. 120(1):13-20.

Boimel M, Grigoriadis N, Lourbopoulos A, Haber E, Abramsky O, Rosenmann H. (2010) Efficacy and safety of immunization with phosphorylated tau against neurofibrillary tangles in mice. Exp Neurol. 224(2):472-85.

Boutajangout A, Ingadottir J, Davies P, Sigurdsson EM. (2011) Passive immunization targeting pathological phospho-tau protein in a mouse model reduces functional decline and clears tau aggregates from the brain. J Neurochem. 118(4):658-667.

Boutajangout A, Quartermain D, Sigurdsson EM. (2010) Immunotherapy targeting pathological tau prevents cognitive decline in a new tangle mouse model.
J Neurosci. 30(49):16559-16566.

Braak E, Griffing K, Arai K, Bohl J, Bratzke H, Braak H. (1999) Neuropathology of Alzheimer's disease: what is new since A. Alzheimer? Eur Arch Psychiatry Clin Neurosci. 249 Suppl 3:14-22.

Braak H, Braak E. (1991) Neuropathological stageing of Alzheimer-related changes. Acta Neuropathol. 82(4):239-259.

Braak H, Braak E, Strothjohann M. (1994) Abnormally phosphorylated tau protein related to the formation of neurofibrillary tangles and neuropil threads in the cerebral cortex of sheep and goat. Neurosci Lett. 171(1-2):1-4.

Brennan-Minnella AM, Won SJ, Swanson RA. (2014) NADPH Oxidase-2: Linking Glucose, Acidosis, and Excitotoxicity in Stroke. Antioxid Redox Signal. [Epub ahead of print].

Breteler MM. (2000) Vascular risk factors for Alzheimer's disease: an epidemiological study. Neurobiol Aging. 21:153–160.

Brooks TA, Hawkins BT, Huber JD, Egleton RD, Davis TP. (2005) Chronic inflammatory pain leads to increased blood-brain barrier permeability and tight junction proteinalterations. Am J Physiol Heart Circ Physiol. 289(2):H738-743.

Brundel M, de Bresser J, van Dillen JJ, Kappelle LJ, Biessels GJ. (2012) Cerebral microinfarcts: a systematic review of neuropathological studies. J Cereb Blood Flow Metab. 32(3):425-436.

Buchhave P, Minthon L, Zetterberg H, Wallin AK, Blennow K, Hansson O. (2012) Cerebrospinal fluid levels of β-amyloid 1-42, but not of tau, are fully changed already 5 to 10 years before the onset of Alzheimer dementia. Arch Gen Psychiatry. 69(1):98-106.

Burgermeister P, Calhoun ME, Winkler DT, Jucker M. (2000) Mechanisms of cerebrovascular amyloid deposition. Lessons from mouse models. Ann N Y Acad Sci. 903:307-316.

Burbach GJ, Vlachos A, Ghebremedhin E, Del Turco D, Coomaraswamy J, Staufenbiel M, Jucker M, Deller T. (2007) Vessel ultrastructure in APP23 transgenic mice after passive anti-Abeta immunotherapy and subsequent intracerebral hemorrhage. Neurobiol Aging. 28(2):202-212.

Butterfield DA, Reed T, Newman SF, Sultana R. (2007) Roles of amyloid beta-peptide-associated oxidative stress and brain protein modifications in the pathogenesis of Alzheimer's disease and mild cognitive impairment. Free Radic Biol Med. 43(5):658-677.

Caillé I, Allinquant B, Dupont E, Bouillot C, Langer A, Müller U, Prochiantz A. (2004) Soluble form of amyloid precursor protein regulates proliferation of progenitors in the adult subventricular zone. Development. 131(9):2173-2181.

Calhoun ME, Burgermeister P, Phinney AL, Stalder M, Tolnay M, Wiederhold KH, Abramowski D, Sturchler-Pierrat C, Sommer B, Staufenbiel M, Jucker M. (1999) Neuronal overexpression of mutant amyloid precursor protein results in prominent deposition of cerebrovascular amyloid. Proc Natl Acad Sci USA. 96(24):14088-14093.

Canevari L, Clark JB, Bates TE. (1999) beta-Amyloid fragment 25-35 selectively decreases complex IV activity in isolated mitochondria. FEBS Lett. 457(1):131-134.

Carlson C, Estergard W, Oh J, Suhy J, Jack CR Jr, Siemers E, Barakos J. (2011). Prevalence of asymptomatic vasogenic edema in pretreatment Alzheimer's disease study cohorts from phase 3 trials of semagacestat and solanezumab. Alzheimers Dement. 7(4):396-401.

Carrano A, Hoozemans JJ, van der Vies SM, van Horssen J, de Vries HE, Rozemuller AJ. (2012) Neuroinflammation and blood-brain barrier changes in capillary amyloid angiopathy. Neurodegener Dis. 10(1-4):329-331.

Carrano A, Hoozemans JJ, van der Vies SM, Rozemuller AJ, van Horssen J, de Vries HE. (2011) Amyloid Beta induces oxidative stress-mediated blood-brain barrier changes in capillary amyloid angiopathy. Antioxid Redox Signal. 15(5):1167-1178.

Castillo-Carranza DL, Sengupta U, Guerrero-Muñoz MJ, Lasagna-Reeves CA, Gerson JE, Singh G, Estes DM, Barrett AD, Dineley KT, Jackson GR, Kayed R. (2014) Passive immunization with Tau oligomer monoclonal antibody reverses tauopathy phenotypes without affecting hyperphosphorylated neurofibrillary tangles. J Neurosci. 34(12):4260-4272.

Chai X, Wu S, Murray TK, Kinley R, Cella CV, Sims H, Buckner N, Hanmer J, Davies P, O'Neill MJ, Hutton ML, Citron M. (2011) Passive immunization with anti-Tau antibodies in two transgenic models: reduction of Tau pathology and delay of disease progression. J Biol Chem. 286(39):34457-34467.

Chao LL, Buckley ST, Kornak J, Schuff N, Madison C, Yaffe K, Miller BL, Kramer JH, Weiner MW. (2010) ASL perfusion MRI predicts cognitive decline and conversion from MCI to dementia. Alzheimer Dis Assoc Disord. 24(1):19-27.

Charidimou A, Gang Q, Werring DJ. (2012) Sporadic cerebral amyloid angiopathy revisited: recent insights into pathophysiology and clinical spectrum. J Neurol Neurosurg Psychiatry. 83(2):124-137.

Chasseigneaux S, Allinquant B. (2012) Functions of Aβ, sAPPα and sAPPβ: similarities and differences. J Neurochem. 120(1):99-108.

Chen CC, Chen YC, Hsiao HY, Chang C, Chern Y. (2013) Neurovascular abnormalities in brain disorders: highlights with angiogenesis and magnetic resonance imaging studies. J Biomed Sci. 20:47.

Chen Y, Wolk DA, Reddin JS, Korczykowski M, Martinez PM, Musiek ES, Newberg AB, Julin P, Arnold SE, Greenberg JH, Detre JA. (2011a) Voxel-level comparison of arterial spin-labeled perfusion MRI and FDG-PET in Alzheimer disease. Neurology. 77(22):1977-1985.

Chen H, Kim GS, Okami N, Narasimhan P, Chan PH. (2011b) NADPH oxidase is involved in post-ischemic brain inflammation. Neurobiol Dis. 42(3):341-348.

Chen Y, Swanson RA. (2003) Astrocytes and brain injury. J Cereb Blood Flow Metab. 23(2):137-149.

Cheng T, Petraglia AL, Li Z, Thiyagarajan M, Zhong Z, Wu Z, Liu D, Maggirwar SB, Deane R, Fernández JA, LaRue B, Griffin JH, Chopp M, Zlokovic BV. (2006) Activated protein C inhibits tissue plasminogen activator-induced brain hemorrhage. Nat Med. 12(11):1278-85.

Cherubini A, Lowenthal DT, Paran E, Mecocci P, Williams LS, Senin U. (2010) Hypertension and cognitive function in the elderly. Dis Mon. 56(3):106-147.

Chui DH, Tanahashi H, Ozawa K, Ikeda S, Checler F, Ueda O, Suzuki H, Araki W, Inoue H, Shirotani K, Takahashi K, Gallyas F, Tabira T. (1999) Transgenic mice with Alzheimer presenilin 1 mutations show accelerated neurodegeneration without amyloid plaque formation. Nat Med. 5(5):560-564.

Chung KK, Anderson NE, Hutchinson D, Synek B, Barber PA. (2011) Cerebral amyloid angiopathy related inflammation: three case reports and a review. J Neurol Neurosurg Psychiatry. 82(1):20-26.

Chung YC, Ko HW, Bok E, Park ES, Huh SH, Nam JH, Jin BK. (2010) The role of neuroinflammation on the pathogenesis of Parkinson's disease. BMB Rep. 43(4):225-232.

Citron M. (2010) Alzheimer's disease: strategies for disease modification. Nat Rev Drug Discov. 9(5):387-398.

Citron M, Oltersdorf T, Haass C, McConlogue L, Hung AY, Seubert P, Vigo-Pelfrey C, Lieberburg I, Selkoe DJ. (1992) Mutation of the beta-amyloid precursor protein in familial Alzheimer's disease increases beta-protein production. Nature 360(6405):672-674.

Cole SL, Vassar R. (2007) The Alzheimer's disease beta-secretase enzyme, BACE1. Mol Neurodegener. 2:22.

Coltman R, Spain A, Tsenkina Y, Fowler JH, Smith J, Scullion G, Allerhand M, Scott F, Kalaria RN, Ihara M, Daumas S, Deary IJ, Wood E, McCulloch J,Horsburgh K. (2011) Selective white matter pathology induces a specific impairment in spatial working memory. Neurobiol Aging. 32(12):2324.e7-12.

Combs CK, Karlo JC, Kao SC, Landreth GE. (2001) beta-Amyloid stimulation of microglia and monocytes results in TNFalpha-dependent expression of inducible nitric oxide synthase and neuronal apoptosis. J Neurosci. 21(4):1179-1188.

Coraci IS, Husemann J, Berman JW, Hulette C, Dufour JH, Campanella GK, Luster AD, Silverstein SC, El-Khoury JB. (2002) CD36, a class B scavenger receptor, is expressed on microglia in Alzheimer's disease brains and can mediate production of reactive oxygen species in response to beta-amyloid fibrils. Am J Pathol. 160(1):101-112.

Cordonnier C, van der Flier WM. (2011) Brain microbleeds and Alzheimer's disease: innocent observation or key player?. Brain. 134(Pt 2):335-344.

Cordonnier C, van der Flier WM, Sluimer JD, Leys D, Barkhof F, Scheltens P. (2006) Prevalence and severity of microbleeds in a memory clinic setting. Neurology. 66(9):1356-60.

Corona C, Pensalfini A, Frazzini V, Sensi SL. (2011) New therapeutic targets in Alzheimer's disease: brain deregulation of calcium and zinc. Cell Death Dis. 2:e176.

Corrigan F, Pham CL, Vink R, Blumbergs PC, Masters CL, van den Heuvel C, Cappai R. (2011) The neuroprotective domains of the amyloid precursor protein, in traumatic brain injury, are located in the two growth factor domains. Brain Res.1378:137-143.

Coyne CB, Gambling TM, Boucher RC, Carson JL, Johnson LG. (2003) Role of claudin interactions in airway tight junctional permeability. Am J Physiol Lung Cell Mol Physiol. 285(5):1166-1178.

Cummings JL, Morstorf T, Zhong K. (2014) Alzheimer's disease drug-development pipeline: few candidates, frequent failures. Alzheimers Res Ther. 6(4):37.

Cuzzo LM, Ross-Cisneros FN, Yee KM, Wang MY, Sadun AA. (2011) Low-density lipoprotein receptor-related protein is decreased in optic neuropathy of Alzheimer disease. J Neuroophthalmol. 31(2):139-146.

d'Abramo C, Acker CM, Jimenez HT, Davies P. (2013) Tau passive immunotherapy in mutant P301L mice: antibody affinity versus specificity. PLoS One. 8(4):e62402.

Dahlgren KN, Manelli AM, Stine WB Jr, Baker LK, Krafft GA, LaDu MJ. (2002) Oligomeric and fibrillar species of amyloid-beta peptides differentially affect neuronal viability. J Biol Chem. 277(35):32046-32053.

Damasceno B. (2012) Relationship between cortical microinfarcts and cognitive impairment in Alzheimer’s disease. Dement Neuropsychol. 6(3):131-136.

Davis J, Xu F, Deane R, Romanov G, Previti ML, Zeigler K, Zlokovic BV, Van Nostrand WE. (2004) Early-onset and robust cerebral microvascular accumulation of amyloid beta-protein in transgenic mice expressing low levels of a vasculotropic Dutch/Iowa mutant form of amyloid beta-protein precursor. J Biol Chem. 279(19):20296-20306.

De Jong GI, Farkas E, Stienstra CM, Plass JR, Keijser JN, de la Torre JC, Luiten PG. (1999) Cerebral hypoperfusion yields capillary damage in the hippocampal CA1 area that correlates with spatial memory impairment. Neuroscience. 91(1):203-210.

de la Torre JC. (2012) Cardiovascular risk factors promote brain hypoperfusion leading to cognitive decline and dementia. Cardiovasc Psychiatry Neurol. 2012:367516.

de la Torre JC. (2008) Pathophysiology of neuronal energy crisis in Alzheimer's disease. Neurodegener Dis. 5(3-4):126-132

de la Torre JC. (2004) Is Alzheimer's disease a neurodegenerative or a vascular disorder? Data, dogma, and dialectics. Lancet Neurol. 3(3):184-190.

de la Torre JC. (2002) Alzheimer disease as a vascular disorder: nosological evidence. Stroke. 33(4):1152-1162.

de la Torre JC. (2000a) Cerebral hypoperfusion, capillary degeneration, and development of Alzheimer disease. Alzheimer Dis Assoc Disord. 14 Suppl 1:S72-81.

de la Torre JC. (2000b) Critically attained threshold of cerebral hypoperfusion: the CATCH hypothesis of Alzheimer's pathogenesis. Neurobiol Aging. 21(2):331-342.

de la Torre JC. (1999) Critical threshold cerebral hypoperfusion causes Alzheimer's disease? Acta Neuropathol. 98(1):1-8.

de la Torre JC, Cada A, Nelson N, Davis G, Sutherland RJ, Gonzalez-Lima F. (1997) Reduced cytochrome oxidase and memory dysfunction after chronic brain ischemia in aged rats. Neurosci Lett. 223(3):165-168.

de la Torre JC, Mussivand T. (1993) Can disturbed brain microcirculation cause Alzheimer's disease? Neurol Res. 15(3):146-153

de la Torre JC, Fortin T, Park GA, Butler KS, Kozlowski P, Pappas BA, de Socarraz H, Saunders JK, Richard M. (1992a) Chronic cerebrovascular insufficiency induces dementia-like deficits in aged rats. Brain Res. 582(2):186-195.

de la Torre JC, Fortin T, Park GA, Saunders JK, Kozlowski P, Butler K, de Socarraz H, Pappas B, Richard M. (1992b) Aged but not young rats develop metabolic, memory deficits after chronic brain ischaemia. Neurol Res. 14(2):177-180.

de Leeuw FE, Korf E, Barkhof F, Scheltens P. (2006) White matter lesions are associated with progression of medial temporal lobe atrophy in Alzheimer disease. Stroke. 37(9):2248-2252.

de Leon MJ, Golomb J, George AE, Convit A, Tarshish CY, McRae T, De Santi S, Smith G, Ferris SH, Noz M, et al. (1993) The radiologic prediction of Alzheimer

disease: the atrophic hippocampal formation. AJNR Am J Neuroradiol. 14(4):897-906.

De Strooper B. (2014) Lessons from a failed γ-secretase Alzheimer trial. Cell. 159(4):721-6.

Deb S, Wenjun Zhang J, Gottschall PE. (2003) Beta-amyloid induces the production of active, matrix-degrading proteases in cultured rat astrocytes. Brain Res. 970(1-2):205-213.

del Zoppo GJ. (2009) Relationship of neurovascular elements to neuron injury during ischemia. Cerebrovasc Dis. 27(1):65–76.

del Zoppo GJ. (2006) Stroke and neurovascular protection. N Engl J Med. 354(6):553-555.

del Zoppo GJ, Mabuchi T. (2003) Cerebral microvessel responses to focal ischemia. J Cereb Blood Flow Metab. 23(8):879-894.

del Zoppo GJ, Hallenbeck JM. (2000) Advances in the vascular pathophysiology of ischemic stroke. Thromb Res. 98(3):73-81.

Deane R, Singh I, Sagare AP, Bell RD, Ross NT, LaRue B, Love R, Perry S, Paquette N, Deane RJ, Thiyagarajan M, Zarcone T, Fritz G, Friedman AE, Miller BL,Zlokovic BV. (2012) A multimodal RAGE-specific inhibitor reduces amyloid β-mediated brain disorder in a mouse model of Alzheimer disease. J Clin Invest. 122(4):1377-1392.

Deane R, Wu Z, Sagare A, Davis J, Du Yan S, Hamm K, Xu F, Parisi M, LaRue B, Hu HW, Spijkers P, Guo H, Song X, Lenting PJ, Van Nostrand WE, Zlokovic BV. (2004) LRP/amyloid beta-peptide interaction mediates differential brain efflux of Abeta isoforms. Neuron. 43(3):333-344.

Delacourte A, David JP, Sergeant N, Buée L, Wattez A, Vermersch P, Ghozali F, Fallet-Bianco C, Pasquier F, Lebert F, Petit H, Di Menza C. (1999) The biochemical pathway of neurofibrillary degeneration in aging and Alzheimer's disease. Neurology. 52(6):1158-1165.

DeMattos RB, Bales KR, Cummins DJ, Dodart JC, Paul SM, Holtzman DM. (2001) Peripheral anti-A beta antibody alters CNS and plasma A beta clearance and decreases brain A beta burden in a mouse model of Alzheimer's disease. Proc Natl Acad Sci U S A. 98(15):8850-8855.

Desikan RS, Cabral HJ, Hess CP, Dillon WP, Glastonbury CM, Weiner MW, Schmansky NJ, Greve DN, Salat DH, Buckner RL, Fischl B; Alzheimer's Disease Neuroimaging Initiative. (2009) Automated MRI measures identify individuals with mild cognitive impairment and Alzheimer's disease. Brain. 132(Pt 8):2048-50.

Devi G, Quitschke W. (1999) Alois Alzheimer, neuroscientist (1864-1915) Alzheimer Dis Assoc Disord. 13(3):132-7.

DeWitt DA, Perry G, Cohen M, Doller C, Silver J. (1998) Astrocytes regulate microglial phagocytosis of senile plaque cores of Alzheimer's disease. Exp Neurol. 149(2):329-340.

Dodart JC, Bales KR, Gannon KS, Greene SJ, DeMattos RB, Mathis C, DeLong CA, Wu S, Wu X, Holtzman DM, Paul SM. (2002) Immunization reverses memory deficits without reducing brain Abeta burden in Alzheimer's disease model. Nat Neurosci. 5(5):452-457.

Dorostkar MM, Burgold S, Filser S, Barghorn S, Schmidt B, Anumala UR, Hillen H, Klein C, Herms J. (2014) Immunotherapy alleviates amyloid-associated synaptic pathology in an Alzheimer's disease mouse model. Brain. 137(Pt 12):3319-3326.

Duff K, Eckman C, Zehr C, Yu X, Prada CM, Perez-tur J, Hutton M, Buee L, Harigaya Y, Yager D, Morgan D, Gordon MN, Holcomb L, Refolo L, Zenk B, Hardy J, Younkin S. (1996) Increased amyloid-beta42(43) in brains of mice expressing mutant presenilin 1. Nature. 383(6602):710-713.

El Khoury J, Hickman SE, Thomas CA, Cao L, Silverstein SC, Loike JD. (1996) Scavenger receptor-mediated adhesion of microglia to beta-amyloid fibrils. Nature. 382(6593):716-719.

El Khoury J, Toft M, Hickman SE, Means TK, Terada K, Geula C, Luster AD. (2007). Ccr2 deficiency impairs microglial accumulation and accelerates progression of Alzheimer-like disease. Nat Med. 13(4):432-438.

ElAli A, Thériault P, Préfontaine P, Rivest S. (2013) Mild chronic cerebral hypoperfusion induces neurovascular dysfunction, triggering peripheral beta-amyloid brain entry and aggregation. Acta Neuropathol Commun. 1(1):75.

ElAli A, Hermann DM. (2011) ATP-binding cassette transporters and their roles in protecting the brain. Neuroscientist. 17(4):423-436.

Elder GA, Gama Sosa MA, De Gasperi R. (2010) Transgenic mouse models of Alzheimer's disease. Mt Sinai J Med. 77(1):69-81.

Ellis RJ, Olichney JM, Thal LJ, Mirra SS, Morris JC, Beekly D, Heyman A. (1996) Cerebral amyloid angiopathy in the brains of patients with Alzheimer's disease: the CERAD experience, Part XV. Neurology. 46(6):1592-1596.

Eng JA, Frosch MP, Choi K, Rebeck GW, Greenberg SM. (2004) Clinical manifestations of cerebral amyloid angiopathy-related inflammation. Ann Neurol. 55(2):250-256.

Eriksen JL, Sagi SA, Smith TE, Weggen S, Das P, McLendon DC, Ozols VV, Jessing KW, Zavitz KH, Koo EH, Golde TE. (2003) NSAIDs and enantiomers of flurbiprofen target gamma-secretase and lower Abeta 42 in vivo. J Clin Invest. 112(3):440-449.

Fan R, Xu F, Previti ML, Davis J, Grande AM, Robinson JK, Van Nostrand WE. (2007) Minocycline reduces microglial activation and improves behavioral deficits in a transgenic model of cerebral microvascular amyloid. J Neurosci. 27(12):3057-3063.

Farkas E, Donka G, de Vos RA, Mihály A, Bari F, Luiten PG. (2004). Experimental cerebral hypoperfusion induces white matter injury and microglial activation in the rat brain. Acta Neuropathol. 108(1):57-64.

Farkas E, Luiten PG, Bari F. (2007) Permanent, bilateral common carotid artery occlusion in the rat: a model for chronic cerebral hypoperfusion-related neurodegenerative diseases. Brain Res Rev. 54(1):162-180.

Farkas E, Luiten PG. (2001) Cerebral microvascular pathology in aging and Alzheimer's disease. Prog Neurobiol. 64(6):575-611.

Farrer LA, Cupples LA, Haines JL, Hyman B, Kukull WA, Mayeux R, Myers RH, Pericak-Vance MA, Risch N, van Duijn CM. (1997) Effects of age, sex, and ethnicity on the association between apolipoprotein E genotype and Alzheimer disease. A meta-analysis. APOE and Alzheimer Disease Meta Analysis Consortium. JAMA 278(16):1349-1356.

Farris W, Mansourian S, Chang Y, Lindsley L, Eckman EA, Frosch MP, Eckman CB, Tanzi RE, Selkoe DJ, Guenette S. (2003) Insulin-degrading enzyme regulates the levels of insulin, amyloid beta-protein, and the beta-amyloid precursor protein intracellular domain in vivo. Proc Natl Acad Sci U S A. 100(7):4162-4167.

Fernandez-Madrid I, Levy E, Marder K, Frangione B. (1991) Codon 618 variant of Alzheimer amyloid gene associated with inherited cerebral hemorrhage. Ann Neurol. 30(5):730-733.

Fernando MS, Simpson JE, Matthews F, Brayne C, Lewis CE, Barber R, Kalaria RN, Forster G, Esteves F, Wharton SB, Shaw PJ, O'Brien JT, Ince PG; MRC Cognitive Function and Ageing Neuropathology Study Group. (2006) White matter lesions in an unselected cohort of the elderly: molecular pathology suggests origin from chronic hypoperfusion injury. Stroke. 37(6):1391-1398.

Fiala M, Lin J, Ringman J, Kermani-Arab V, Tsao G, Patel A, Lossinsky AS, Graves MC, Gustavson A, Sayre J, Sofroni E, Suarez T, Chiappelli F, Bernard G. (2005). Ineffective phagocytosis of amyloid-beta by macrophages of Alzheimer's disease patients. J Alzheimers Dis. 7(3):221-232.

Forette F, Seux ML, Staessen JA, Thijs L, Birkenhäger WH, Babarskiene MR, Babeanu S, Bossini A, Gil-Extremera B, Girerd X, Laks T, Lilov E, Moisseyev V,Tuomilehto J, Vanhanen H, Webster J, Yodfat Y, Fagard R. (1998) Prevention of dementia in randomised double-blind placebo-controlled Systolic Hypertension in Europe (Syst-Eur) trial. Lancet. 352(9137):1347-1351.

Forette F, Seux ML, Staessen JA, Thijs L, Babarskiene MR, Babeanu S, Bossini A, Fagard R, Gil-Extremera B, Laks T, Kobalava Z, Sarti C, Tuomilehto J,Vanhanen H, Webster J, Yodfat Y, Birkenhäger WH; Systolic Hypertension in Europe Investigators. (2002) The prevention of dementia with antihypertensive treatment: new evidence from the Systolic Hypertension in Europe (Syst-Eur) study. Arch Intern Med. 162(18):2046-2052.

Franceschi M, Alberoni M, Bressi S, Canal N, Comi G, Fazio F, Grassi F, Perani D, Volonté MA. (1995) Correlations between cognitive impairment, middle cerebral artery flow velocity and cortical glucose metabolism in the early phase of Alzheimer's disease. Dementia. 6(1):32-38.

Francis PT, Palmer AM, Snape M, Wilcock GK. (1999) The cholinergic hypothesis of Alzheimer's disease: a review of progress. J Neurol Neurosurg Psychiatry. 66(2):137-147.

Frank S, Burbach GJ, Bonin M, Walter M, Streit W, Bechmann I, Deller T. (2008) TREM2 is upregulated in amyloid plaque-associated microglia in aged APP23 transgenic mice. Glia. 56(13):1438-1447.

Franklin W, Paxinos G. (1997) The mouse brain in stereotaxic coordinates. Academic Press, New York.

Frenkel D, Wilkinson K, Zhao L, Hickman SE, Means TK, Puckett L, Farfara D, Kingery ND, Weiner HL, El Khoury J. (2013) Scara1 deficiency impairs clearance of soluble amyloid-β by mononuclear phagocytes and accelerates Alzheimer's-like disease progression. Nat Commun. 4:2030.

Fukuda AM, Badaut J. (2012) Aquaporin 4: a player in cerebral edema and neuroinflammation. J Neuroinflammation.9:279.

Games D, Adams D, Alessandrini R, Barbour R, Berthelette P, Blackwell C, Carr T, Clemens J, Donaldson T, Gillespie F, et al. (1995) Alzheimer-type neuropathology in transgenic mice overexpressing V717F beta-amyloid precursor protein. Nature.373(6514):523-527.

Garbuzova-Davis S, Sanberg PR. (2014) Blood-CNS Barrier Impairment in ALS patients versus an animal model. Front Cell Neurosci. 8:21.

Garcia-Alloza M, Gregory J, Kuchibhotla KV, Fine S, Wei Y, Ayata C, Frosch MP, Greenberg SM, Bacskai BJ. (2011) Cerebrovascular lesions induce transient β-amyloid deposition. Brain. 134(12):3697-3707.

Gearing M, Mori H, Mirra SS. (1996) Abeta-peptide length and apolipoprotein E genotype in Alzheimer's disease. Ann Neurol. 39(3):395-399.

Geller LN, Potter H. (1999) Chromosome missegregation and trisomy 21 mosaicism in Alzheimer's disease. Neurobiol Dis. 6(3):167-179.

Giannakopoulos P, Herrmann FR, Bussière T, Bouras C, Kövari E, Perl DP, Morrison JH, Gold G, Hof PR. (2003) Tangle and neuron numbers, but not amyloid load, predict cognitive status in Alzheimer's disease. Neurology. 60(9):1495-1500.

Gilman S, Koller M, Black RS, Jenkins L, Griffith SG, Fox NC, Eisner L, Kirby L, Rovira MB, Forette F, Orgogozo JM, AN1792(QS-21)-201 Study Team. (2005) Clinical effects of Abeta immunization (AN1792) in patients with AD in an interrupted trial. Neurology. 64(9):1553-1562.

Glabe C, Kayed R. (2006). Common structure and toxic function of amyloid oligomers implies a common mechanism of pathogenesis. Neurology. 66(2, Suppl 1), S74–S78.

Glenner GG, Wong CW. (1984) Alzheimer's disease: initial report of the purification and characterization of a novel cerebrovascular amyloid protein. Biochem Biophys Res Commun. 120(3):885-890.

Glenner GG, Wong CW, Quaranta V, Eanes ED. (1984) The amyloid deposits in Alzheimer's disease: their nature and pathogenesis. Appl Pathol. 2(6):357-369.

Goate A, Chartier-Harlin MC, Mullan M, Brown J, Crawford F, Fidani L, Giuffra L, Haynes A, Irving N, James L, Manti R, Newton P, Rooke K, Roques P, Talbot C, Pericak-Vance M, Roses A, Williamson R, Rossor M, Owen M, Hardy J. (1991) Segregation of a missense mutation in the amyloid precursor protein gene with familial Alzheimer's disease. Nature. 349(6311):704-706.

Gordon GR, Choi HB, Rungta RL, Ellis-Davies GC, MacVicar BA. (2008) Brain metabolism dictates the polarity of astrocyte control over arterioles. Nature. 456(7223):745-749.

Grabowski TJ, Cho HS, Vonsattel JP, Rebeck GW, Greenberg SM. (2001) Novel amyloid precursor protein mutation in an Iowa family with dementia and severe cerebral amyloid angiopathy. Ann Neurol. 49(6):697-705.

Gralle M, Ferreira ST. (2007) Structure and functions of the human amyloid precursor protein: the whole is more than the sum of its parts. Prog Neurobiol. 82(1):11-32.

Green RC, Schneider LS, Amato DA, Beelen AP, Wilcock G, Swabb EA, Zavitz KH; Tarenflurbil Phase 3 Study Group. (2009) Effect of tarenflurbil on cognitive decline and activities of daily living in patients with mild Alzheimer disease: a randomized controlled trial. JAMA. 302(23):2557-2564.

Greenberg SM, Vernooij MW, Cordonnier C, Viswanathan A, Al-Shahi Salman R, Warach S, Launer LJ, Van Buchem MA, Breteler MM; Microbleed Study Group. (2009) Cerebral microbleeds: a guide to detection and interpretation. Lancet Neurol. 8(2):165-174.

Greenberg SM, Gurol ME, Rosand J, Smith EE. (2004) Amyloid angiopathy-related vascular cognitive impairment. Stroke 35(11 Suppl 1):2616-2619.

Greenberg SM. (2002) Cerebral amyloid angiopathy and dementia: Two amyloids are worse than one. Neurology. (11):1587-1588.

Greenberg SM, Rebeck GW, Vonsattel JP, Gomez-Isla T, Hyman BT. (1995) Apolipoprotein E epsilon 4 and cerebral hemorrhage associated with amyloid angiopathy. Ann Neurol. 38(2):254-259.

Greig NH, Utsuki T, Yu Q, Zhu X, Holloway HW, Perry T, Lee B, Ingram DK, Lahiri DK. (2001) A new therapeutic target in Alzheimer's disease treatment: attention to butyrylcholinesterase. Curr Med Res Opin. 17(3):159-165.

Gold CA, Budson AE (2008) Memory loss in Alzheimer's disease: implications for development of therapeutics. Expert Rev Neurother. 8(12):1879-91.

Goñi F, Herline K, Peyser D, Wong K, Ji Y, Sun Y, Mehta P, Wisniewski T. (2013) Immunomodulation targeting of both Aβ and tau pathological conformers ameliorates Alzheimer's diseasepathology in TgSwDI and 3xTg mouse models. J Neuroinflammation. 10:150.

Guerreiro R, Wojtas A, Bras J, Carrasquillo M, Rogaeva E, Majounie E, Cruchaga C, Sassi C, Kauwe JS, Younkin S, Hazrati L, Collinge J, Pocock J, Lashley T,Williams J, Lambert JC, Amouyel P, Goate A, Rademakers R, Morgan K, Powell J, St George-Hyslop P, Singleton A, Hardy J; Alzheimer Genetic Analysis Group. (2013) TREM2 variants in Alzheimer's disease. N Engl J Med. 368(2):117-27.

Guerreiro R, Hardy J. (2014) Genetics of Alzheimer's disease. Neurotherapeutics. 11(4):732-737.

Haass C, Selkoe DJ. (2007) Soluble protein oligomers in neurodegeneration: lessons from the Alzheimer’s amyloid beta-peptide. Nat.Rev.Mol.Cell Biol. 8, 101–112.

Haass C, Hung AY, Selkoe DJ. (1991) Processing of beta-amyloid precursor protein in microglia and astrocytes favors an internal localization over constitutive secretion. J Neurosci. 11(12):3783-3793.

Hachinski V. (2011) Stroke and Alzheimer disease: fellow travelers or partners in crime? Arch Neurol. 68(6):797-798.

Haglund M, Passant U, Sjöbeck M, Ghebremedhin E, Englund E. (2006) Cerebral amyloid angiopathy and cortical microinfarcts as putative substrates of vascular dementia. Int J Geriatr Psychiatry. 21(7):681-687.

Han P, Dou F, Li F, Zhang X, Zhang YW, Zheng H, Lipton SA, Xu H, Liao FF. (2005) Suppression of cyclin-dependent kinase 5 activation by amyloid precursor protein: a novel excitoprotective mechanism involving modulation of tau phosphorylation. J Neurosci. 25(50):11542-11552.

Hardy J. (2009) The amyloid hypothesis for Alzheimer's disease: a critical reappraisal. J Neurochem. 110(4):1129-1134.

Hardy J. Allsop D. (1991) Amyloid deposition as the central event in the aetiology of Alzheimer's disease. Trends Pharmacol Sci. 12(10):383-388.

Hardy J, Selkoe DJ. (2002) The amyloid hypothesis of Alzheimer's disease: progress and problems on the road to therapeutics. Science. 297(5580):353-356.

Hardy J, Higgins G. (1992) Alzheimer's disease: the amyloid cascade hypothesis. Science. 256(5054):184-185

Hartman RE, Izumi Y, Bales KR, Paul SM, Wozniak DF, Holtzman DM. (2005) Treatment with an amyloid-beta antibody ameliorates plaque load, learning deficits, and hippocampal long-term potentiation in a mouse model of Alzheimer's disease. J Neurosci. 25(26):6213-6220.

Hartmann T, Bieger SC, Brühl B, Tienari PJ, Ida N, Allsop D, Roberts GW, Masters CL, Dotti CG, Unsicker K, Beyreuther K. (1997) Distinct sites of intracellular production for Alzheimer's disease A beta40/42 amyloid peptides. Nat Med. 3(9):1016-1020.

Hartz AM, Bauer B, Soldner EL, Wolf A, Boy S, Backhaus R, Mihaljevic I, Bogdahn U, Klünemann HH, Schuierer G, Schlachetzki F. (2012) Amyloid-β contributes to blood-brain barrier leakage in transgenic human amyloid precursor protein mice and in humans with cerebral amyloid angiopathy. Stroke. 43(2):514-523.

Harvey RJ, Skelton-Robinson M, Rossor MN. (2003) The prevalence and causes of dementia in people under the age of 65 years. J Neurol Neurosurg Psychiatry 74(9):1206-1209.

Hauser PS, Ryan RO. (2013) Impact of apolipoprotein E on Alzheimer's disease. Curr Alzheimer Res. 10(8):809-17.

Hayashi Y, Nomura M, Yamagishi S, Harada S, Yamashita J, Yamamoto H. (1997) Induction of various blood-brain barrier properties in non-neural endothelial cells by close apposition to co-cultured astrocytes. Glia. 19(1):13-26.

Haydon PG, Carmignoto G. (2006) Astrocyte control of synaptic transmission and neurovascular coupling. Physiol Rev. 86(3):1009-1031.

Hendriks L, van Duijn CM, Cras P, Cruts M, Van Hul W, van Harskamp F, Warren A, McInnis MG, Antonarakis SE, Martin JJ, Hofman A, Van Broeckhoven C. (1992) Presenile dementia and cerebral haemorrhage linked to a mutation at codon 692 of the beta-amyloid precursor protein gene. Nat Genet. 1(3):218-221.

Henkel JS, Beers DR, Wen S, Bowser R, Appel SH. (2009) Decreased mRNA expression of tight junction proteins in lumbar spinal cords of patients with ALS. Neurology. 72(18):1614-1616.

Herrmann A, Spires-Jones T. (2014) Clearing the way for tau immunotherapy in Alzheimer's disease. J Neurochem. [Epub ahead of print].

Herzig MC, Van Nostrand WE, Jucker M. (2006) Mechanism of cerebral beta-amyloid angiopathy: murine and cellular models. Brain Pathol. 16(1):40-54.

Herzig MC, Winkler DT, Burgermeister P, Pfeifer M, Kohler E, Schmidt SD, Danner S, Abramowski D, Stürchler-Pierrat C, Bürki K, van Duinen SG, Maat-Schieman ML, Staufenbiel M, Mathews PM, Jucker M. (2004) Abeta is targeted to the vasculature in a mouse model of hereditary cerebral hemorrhage with amyloidosis. Nat Neurosci. 7(9):954-960.

Heuer E, Rosen RF, Cintron A, Walker LC. (2012) Nonhuman primate models of Alzheimer-like cerebral proteopathy. Curr Pharm Des. 18(8):1159-1169.

Hickman SE, Allison EK, El Khoury J. (2008). Microglial dysfunction and defective beta-amyloid clearance pathways in aging Alzheimer's disease mice. J Neurosci. 28(33):8354-8360.

Hilbich C, Kisters-Woike B, Reed J, Masters CL, Beyreuther K. (1991) Human and rodent sequence analogs of Alzheimer's amyloid beta A4 share similar properties and can be solubilized in buffers of pH 7.4. Eur J Biochem. 201(1):61-69.

Hiltunen M, Mäkinen P, Peräniemi S, Sivenius J, van Groen T, Soininen H, olkkonen J. (2009) Focal cerebral ischemia in rats alters APP processing and expression of Abeta peptide degrading enzymes in the thalamus. Neurobiol Dis. 35(1):103-113.

Hirao K, Ohnishi T, Hirata Y, Yamashita F, Mori T, Moriguchi Y, Matsuda H, Nemoto K, Imabayashi E, Yamada M, Iwamoto T, Arima K, Asada T (2005) The prediction of rapid conversion to Alzheimer's disease in mild cognitive impairment using regional cerebral blood flow SPECT. NeuroImage 28:1014-1021

Holland PR, Searcy JL, Salvadores N, Scullion G, Chen G, Lawson G, Scott F, Bastin ME, Ihara M, Kalaria R, Wood ER, Smith C, Wardlaw JM,Horsburgh K. (2015) Gliovascular disruption and cognitive deficits in a mouse model with features

of small vessel disease. J Cereb Blood Flow Metab. Feb 11. doi: 10.1038/jcbfm.2015.12. [Epub ahead of print]

Holmes C, Boche D, Wilkinson D, Yadegarfar G, Hopkins V, Bayer A, Jones RW, Bullock R, Love S, Neal JW, Zotova E, Nicoll JA. (2008) Long-term effects of Abeta42 immunisation in Alzheimer's disease: follow-up of a randomised, placebo-controlled phase I trial. Lancet.372(9634):216-23.

Hook G, Yu J, Toneff T, Kindy M, Hook V. (2014) Brain pyroglutamate amyloid-β is produced by cathepsin B and is reduced by the cysteine protease inhibitor E64d, representing a potential Alzheimer's disease therapeutic. J Alzheimers Dis. 41(1):129-149

Horstmann S, Budig L, Gardner H, Koziol J, Deuschle M, Schilling C, Wagner S. (2010) Matrix metalloproteinases in peripheral blood and cerebrospinal fluid in patients with Alzheimer's disease. Int Psychogeriatr. 22(6):966-972.

Howard R, McShane R, Lindesay J, Ritchie C, Baldwin A, Barber R, Burns A, Dening T, Findlay D, Holmes C, Hughes A, Jacoby R, Jones R, Jones R, McKeith I,Macharouthu A, O'Brien J, Passmore P, Sheehan B, Juszczak E, Katona C, Hills R, Knapp M, Ballard C, Brown R, Banerjee S, Onions C, Griffin M, Adams J,Gray R, Johnson T, Bentham P, Phillips P. (2012) Donepezil and memantine for moderate-to-severe Alzheimer's disease. N Engl J Med. 366(10):893-903.

Hsiao K, Chapman P, Nilsen S, Eckman C, Harigaya Y, Younkin S, Yang F, Cole G. (1996) Correlative memory deficits, Abeta elevation, and amyloid plaques in transgenic mice. Science. 274(5284):99-102.

Huang C, Wahlund LO, Svensson L, Winblad B, Julin P. (2002) Cingulate cortex hypoperfusion predicts Alzheimer's disease in mild cognitive impairment. BMC Neurol. 2:9.

Huang Y, Mucke L. (2012) Alzheimer mechanisms and therapeutic strategies. Cell. 148(6):1204-1222.

Huber JD, Witt KA, Hom S, Egleton RD, Mark KS, Davis TP. (2001) Inflammatory pain alters blood-brain barrier permeability and tight junctional protein expression. Am J Physiol Heart Circ Physiol. 280(3):H1241-1248.

Hultman K, Strickland S, Norris EH. (2013) The APOE ε4/ε4 genotype potentiates vascular fibrin(ogen) deposition in amyloid-laden vessels in the brains of Alzheimer's disease patients. J Cereb Blood Flow Metab. 33(8):1251-1258.

Hurtado-Alvarado G, Cabañas-Morales AM, Gómez-Gónzalez B. (2014) Pericytes: brain-immune interface modulators. Front Integr Neurosci. 7:80.

Hyde C, Peters J, Bond M, Rogers G, Hoyle M, Anderson R, Jeffreys M, Davis S, Thokala P, Moxham T. (2013) Evolution of the evidence on the effectiveness and

cost-effectiveness of acetylcholinesterase inhibitors and memantine for Alzheimer's disease: systematic review and economic model. Age Ageing. 42(1):14-20.

Iadecola C. (2004) Neurovascular regulation in the normal brain and in Alzheimer's disease. Nat Rev Neurosci. 5(5):347–360.

Inestrosa NC, Reyes AE, Chacón MA, Cerpa W, Villalón A, Montiel J, Merabachvili G, Aldunate R, Bozinovic F, Aboitiz F. (2005) Human-like rodent amyloid-beta-peptide determines Alzheimer pathology in aged wild-type Octodon degu. Neurobiol Aging. 26(7):1023-1028.

Iqbal K, Gong CX, Liu F. (2014) Microtubule-associated protein tau as a therapeutic target in Alzheimer's disease. Expert Opin Ther Targets. 18(3):307-318.

Irizarry MC, Soriano F, McNamara M, Page KJ, Schenk D, Games D, Hyman BT. (1997) Abeta deposition is associated with neuropil changes, but not with overt neuronal loss in the human amyloid precursor protein V717F (PDAPP) transgenic mouse. J Neurosci. 17(18):7053-7059.

Ishibashi K, Tanaka K, Nakabayashi T, Nakamura M, Uchiyama M, Okawa M. (1998) Latent cerebral artery stenoses on magnetic resonance angiography in a patient diagnosed as probable Alzheimer disease. Psychiatry Clin Neurosci. 52(1):93-96.

Ito, D., Y. Imai, K. Ohsawa, K. Nakajima, Y. Fukuuchi, and S. Kohsaka. 1998. Microglia-specific localisation of a novel calcium binding protein, Iba1. Brain Res. Mol. Brain Res. 57:1-9

Itoh T, Satou T, Nishida S, Tsubaki M, Hashimoto S, Ito H. (2009) Expression of amyloid precursor protein after rat traumatic brain injury. Neurol Res. 31(1):103-109.

Iwata N, Tsubuki S, Takaki Y, Shirotani K, Lu B, Gerard NP, Gerard C, Hama E, Lee HJ, Saido TC. (2001) Metabolic regulation of brain Abeta by neprilysin. Science. 292(5521):1550-1552.

Jackman KA, Miller AA, De Silva TM, Crack PJ, Drummond GR, Sobey CG. (2009) Reduction of cerebral infarct volume by apocynin requires pretreatment and is absent in Nox2-deficient mice. Br J Pharmacol. 156(4):680-688.

Jaeger LB, Dohgu S, Hwang MC, Farr SA, Murphy MP, Fleegal-DeMotta MA, Lynch JL, Robinson SM, Niehoff ML, Johnson SN, Kumar VB, Banks WA. (2009) Testing the neurovascular hypothesis of Alzheimer's disease: LRP-1 antisense reduces blood-brain barrier clearance, increases brain levels of amyloid-beta protein, and impairs cognition. J Alzheimers Dis. 17(3):553-570.

Janus C, Pearson J, McLaurin J, Mathews PM, Jiang Y, Schmidt SD, Chishti MA, Horne P, Heslin D, French J, Mount HT, Nixon RA, Mercken M, Bergeron C,Fraser

PE, St George-Hyslop P, Westaway D. (2000) A beta peptide immunization reduces behavioural impairment and plaques in a model of Alzheimer's disease. Nature. 408(6815):979-982.

Janzer RC, Raff MC. (1987) Astrocytes induce blood-brain barrier properties in endothelial cells. Nature. 325(6101):253-257.

Jarrett JT, Berger EP, Lansbury PT Jr. (1993) The carboxy terminus of the beta amyloid protein is critical for the seeding of amyloid formation: implications for the pathogenesis of Alzheimer's disease. Biochemistry. 32(18):4693-4697.

Jellinger KA. (2007) The enigma of vascular cognitive disorder and vascular dementia. Acta Neuropathol. 113: 349–388.

Jendroska K, Poewe W, Daniel SE, Pluess J, Iwerssen-Schmidt H, Paulsen J, Barthel S, Schelosky L, Cervós-Navarro J, DeArmond SJ. (1995) Ischemic stress induces deposition of amyloid beta immunoreactivity in human brain. Acta Neuropathol. 90(5):461-466.

Johnson KA, Jones K, Holman BL, Becker JA, Spiers PA, Satlin A, Albert MS. (1998) Preclinical prediction of Alzheimer's disease using SPECT. Neurology. 50(6):1563-1571.

Johnson NA, Jahng GH, Weiner MW, Miller BL, Chui HC, Jagust WJ, Gorno-Tempini ML, Schuff N. (2005) Pattern of cerebral hypoperfusion in Alzheimer disease and mild cognitive impairment measured with arterial spin-labeling MR imaging: initial experience. Radiology. 234(3):851-859.

Jonsson T, Stefansson H, Steinberg S, Jonsdottir I, Jonsson PV, Snaedal J, Bjornsson S, Huttenlocher J, Levey AI, Lah JJ, Rujescu D, Hampel H, Giegling I,Andreassen OA, Engedal K, Ulstein I, Djurovic S, Ibrahim-Verbaas C, Hofman A, Ikram MA, van Duijn CM, Thorsteinsdottir U, Kong A, Stefansson K. (2013). Variant of TREM2 associated with the risk of Alzheimer's disease. N Engl J Med. 368(2):107-116.

Jucker, M. (2006) The neuronal origini hypothesis of cerebral amyloid angiopathy. In Alzheimer:100 years and beyond. First Edition. Springer.

Kalaria RN. (2000) The role of cerebral ischemia in Alzheimer's disease. Neurobiol Aging. 21(2):321-330.

Kalaria RN, Ince P. (2000) Vascular factors in Alzheimer’s disease. Ann NY Acad Sci. 903:1–552.

Kalaria RN, Ballard C. (1999) Overlap between pathology of Alzheimer disease and vascular dementia. Alzheimer Dis Assoc Disord. 13 Suppl 3:S115-123.

Kalaria RN, Premkumar DR, Pax AB, Cohen DL, Lieberburg I. (1996) Production and increased detection of amyloid beta protein and amyloidogenic fragments in brain microvessels, meningeal vessels and choroid plexus in Alzheimer's disease. Brain Res Mol Brain Res. 35:58-68.

Kalaria RN, Bhatti SU, Lust WD, Perry G. (1993) The amyloid precursor protein in ischemic brain injury and chronic hypoperfusion. Ann N Y Acad Sci. 695:190-193.

Kang DE, Saitoh T, Chen X, Xia Y, Masliah E, Hansen LA, Thomas RG, Thal LJ, Katzman R. (1997) Genetic association of the low-density lipoprotein receptor-related protein gene (LRP), an apolipoprotein E receptor, with late-onset Alzheimer's disease. Neurology. 49(1):56-61.

Kang J, Lemaire HG, Unterbeck A, Salbaum JM, Masters CL, Grzeschik KH, Multhaup G, Beyreuther K, Müller-Hill B. (1987) The precursor of Alzheimer's disease amyloid A4 protein resembles a cell-surface receptor. Nature. 325(6106):733-736.

Karlnoski RA, Rosenthal A, Alamed J, Ronan V, Gordon MN, Gottschall PE, Grimm J, Pons J, Morgan D. (2008) Deglycosylated anti-Abeta antibody dose-response effects on pathology and memory in APP transgenic mice. J Neuroimmune Pharmacol. 3(3):187-197.

Ke C, Poon WS, Ng HK, Pang JC, Chan Y. (2001) Heterogeneous responses of aquaporin-4 in edema formation in a replicated severe traumatic brain injury model in rats. Neurosci Lett. 301(1):21-24.

Kimelberg H. (1995) Brain edema. In Neuroglia (Kettenmann H, Ransom BR, eds), Oxford University.

Kitagawa K. (2010) Cerebral blood flow measurement by PET in hypertensive subjects as a marker of cognitive decline. J Alzheimers Dis. 20(3):855-859.

Kitaguchi H, Tomimoto H, Ihara M, Shibata M, Uemura K, Kalaria RN, Kihara T, Asada-Utsugi M, Kinoshita A, Takahashi R. (2009) Chronic cerebral hypoperfusion accelerates amyloid beta deposition in APPSwInd transgenic mice. Brain Res. 1294:202-210.

Kitamura A, Fujita Y, Oishi N, Kalaria RN, Washida K, Maki T, Okamoto Y, Hase Y, Yamada M, Takahashi J, Ito H, Tomimoto H, Fukuyama H, Takahashi R,Ihara M. (2012) Selective white matter abnormalities in a novel rat model of vascular dementia. Neurobiol Aging. 33(5):1012.e25-35.

Kitazume S, Tachida Y, Kato M, Yamaguchi Y, Honda T, Hashimoto Y, Wada Y, Saito T, Iwata N, Saido T, Taniguchi N. (2010) Brain endothelial cells produce amyloid beta from amyloid precursor protein 770 and preferentially secrete the O-glycosylated form. J Biol Chem. 285(51):40097-103.

Kiyota T, Gendelman HE, Weir RA, Higgins EE, Zhang G, Jain M. (2013). CCL2 affects β-amyloidosis and progressive neurocognitive dysfunction in a mouse model of Alzheimer's disease. Neurobiol Aging. 34(4):1060-8.

Klein WL, Stine WB Jr, Teplow DB. (2004) Small assemblies of unmodified amyloid beta-protein are the proximate neurotoxin in Alzheimer's disease. Neurobiol Aging. 25(5):569-580.

Koike MA, Green KN, Blurton-Jones M, Laferla FM. (2010) Oligemic hypoperfusion differentially affects tau and amyloid-beta. Am J Pathol. 177(1):300-310.

Koistinaho M, Ort M, Cimadevilla JM, Vondrous R, Cordell B, Koistinaho J, Bures J, Higgins LS. (2001) Specific spatial learning deficits become severe with age in beta -amyloid precursor protein transgenic mice that harbor diffuse beta-amyloid deposits but do not form plaques. Proc Natl Acad Sci U S A. 98(25):14675-14680.

Kokmen E, Whisnant JP, O'Fallon WM, Chu CP, Beard CM. (1996) Dementia after ischemic stroke: a population-based study in Rochester, Minnesota (1960-1984). Neurology. 46(1):154-159.

Kölker S, Ahlemeyer B, Hühne R, Mayatepek E, Krieglstein J, Hoffmann GF. (2001) Potentiation of 3-hydroxyglutarate neurotoxicity following induction of astrocytic iNOS in neonatal rat hippocampal cultures. Eur J Neurosci.13(11):2115-2122.

Kosunen O, Soininen H, Paljärvi L, Heinonen O, Talasniemi S, Riekkinen PJ Sr. (1996) Diagnostic accuracy of Alzheimer's disease: a neuropathological study. Acta Neuropathol. 91(2):185-193.

Kövari E, Herrmann FR, Hof PR, Bouras C. (2013) The relationship between cerebral amyloid angiopathy and cortical microinfarcts in brain ageing and Alzheimer's disease. Neuropathol Appl Neurobiol. 39(5):498-509.

Kövari E, Gold G, Herrmann FR, Canuto A, Hof PR, Bouras C, Giannakopoulos P. (2007) Cortical microinfarcts and demyelination affect cognition in cases at high risk for dementia. Neurology. 68(12):927-931.

Kukar T, Prescott S, Eriksen JL, Holloway V, Murphy MP, Koo EH, Golde TE, Nicolle MM. (2007) Chronic administration of R-flurbiprofen attenuates learning impairments in transgenic amyloid precursor protein mice. BMC Neurosci. 8:54.

Kurumatani T, Kudo T, Ikura Y, Takeda M. (1998) White matter changes in the gerbil brain under chronic cerebral hypoperfusion. Stroke. 29(5):1058-1062.

Lannfelt L, Relkin NR, Siemers ER. (2014) Amyloid-ß-directed immunotherapy for Alzheimer's disease. J Intern Med. 275(3):284-295.

Lambert JC, Ibrahim-Verbaas CA, Harold D, Naj AC, Sims R, Bellenguez C, DeStafano AL, Bis JC, Beecham GW, Grenier-Boley B, et al. (2013) Meta-analysis of 74,046 individuals identifies 11 new susceptibility loci for Alzheimer's disease. Nat Genet. 45(12):1452-8.

Launer LJ, Petrovitch H, Ross GW, Markesbery W, White LR. (2008) AD brain pathology: vascular origins? Results from the HAAS autopsy study. Neurobiol Aging. 29(10):1587-1590.

Leake A, Morris CM, Whateley J. (2000) Brain matrix metalloproteinase 1 levels are elevated in Alzheimer's disease. Neurosci Lett. 291(3):201-3.

Lee JH, Kim SH, Kim GH, Seo SW, Park HK, Oh SJ, Kim JS, Cheong HK, Na DL. (2011a) Identification of pure subcortical vascular dementia using 11C-Pittsburgh compound B. Neurology. 77(1):18-25.

Lee JS, Im DS, An YS, Hong JM, Gwag BJ, Joo IS (2011b) Chronic cerebral hypoperfusion in a mouse model of Alzheimer's disease: an additional contributing factor of cognitive impairment. Neurosci Lett. 489(2):84-88.

Lee HS, Namkoong K, Kim DH, Kim KJ, Cheong YH, Kim SS, Lee WB, Kim KY. (2004) Hydrogen peroxide-induced alterations of tight junction proteins in bovine brain microvascular endothelial cells. Microvasc Res. 68(3):231-238.

Lee PH, Hwang EM, Hong HS, Boo JH, Mook-Jung I, Huh K. (2006) Effect of ischemic neuronal insults on amyloid precursor protein processing. Neurochem Res. 31(6):821-827.

Lee PH, Bang OY, Hwang EM, Lee JS, Joo US, Mook-Jung I, Huh K. (2005) Circulating beta amyloid protein is elevated in patients with acute ischemic stroke. J Neural Transm. 112(10):1371-1379.

Lee SW, Kim WJ, Choi YK, Song HS, Son MJ, Gelman IH, Kim YJ, Kim KW. (2003) SSeCKS regulates angiogenesis and tight junction formation in blood-brain barrier. Nat Med. 9(7):900-906.

Leenders KL, Perani D, Lammertsma AA, Heather JD, Buckingham P, Healy MJ, Gibbs JM, Wise RJ, Hatazawa J, Herold S, Beaney RP, Brooks DJ, Spinks T, Rhodes C, Frackowiack, RS. (1990) Cerebral blood flow, blood volume and oxygen utilization. Normal values and effect of age. Brain. 113 (1):27-47.

Lemere CA, Maron R, Spooner ET, Grenfell TJ, Mori C, Desai R, Hancock WW, Weiner HL, Selkoe DJ (2000) Nasal A beta treatment induces anti-A beta antibody production and decreases cerebral amyloid burden in PD-APP mice. Ann N Y Acad Sci. 920:328-331.

Lemere CA, Masliah E. (2010) Can Alzheimer disease be prevented by amyloid-beta immunotherapy? Nat Rev Neurol. 6(2):108-119.

Levy E, Carman MD, Fernandez-Madrid IJ, Power MD, Lieberburg I, van Duinen SG, Bots GT, Luyendijk W, Frangione B. (1990) Mutation of the Alzheimer's disease amyloid gene in hereditary cerebral hemorrhage, Dutch type. Science. 248(4959):1124-1126.

Leybaert L. (2005) Neurobarrier coupling in the brain: a partner of neurovascular and neurometabolic coupling? J Cereb Blood Flow Metab. 25(1):2-16.

Leyssen M, Ayaz D, Hébert SS, Reeve S, De Strooper B, Hassan BA. (2005) Amyloid precursor protein promotes post-developmental neurite arborization in the Drosophila brain. EMBO J. 24(16):2944-2955.

Li J, Kanekiyo T, Shinohara M, Zhang Y, LaDu MJ, Xu H, Bu G. (2012) . Differential regulation of amyloid-β endocytic trafficking and lysosomal degradation by apolipoprotein E isoforms. J Biol Chem. 287(53):44593-44601.

Li Y, Liu Y, Wang Z, Jiang Y. (2013) Clinical trials of amyloid-based immunotherapy for Alzheimer's disease: end of beginning or beginning of end? Expert Opin Biol Ther. 13(11):1515-1522.

Lin H, Bhatia R, Lal R. (2001) Amyloid beta protein forms ion channels: implications for Alzheimer's disease pathophysiology. FASEB J. 15(13):2433-2444.

Liu H, Zhang J. (2012) Cerebral hypoperfusion and cognitive impairment: the pathogenic role of vascular oxidative stress. Int J Neurosci. 122(9):494-499.

Liu L, Lu Y, Kong H, Li L, Marshall C, Xiao M, Ding J, Gao J, Hu G. (2012) Aquaporin-4 deficiency exacerbates brain oxidative damage and memory deficits induced by long-term ovarian hormone deprivation and D-galactose injection. Int J Neuropsychopharmacol. 15(1):55-68.

Lok J, Gupta P, Guo S, Kim WJ, Whalen MJ, van Leyen K, Lo EH. (2007) Cell-cell signaling in the neurovascular unit. Neurochem Res. 32(12):2032-2045.

Longa EZ, Weinstein PR, Carlson S, Cummins R. (1989) Reversible middle cerebral artery occlusion without craniectomy in rats. Stroke. 20(1):84-91.

Lorenzl S, Albers DS, Relkin N, Ngyuen T, Hilgenberg SL, Chirichigno J, Cudkowicz ME, Beal MF. (2003) Increased plasma levels of matrix metalloproteinase-9 in patients with Alzheimer's disease. Neurochem Int. 43(3):191-196.

Love S, Miners S, Palmer J, Chalmers K, Kehoe P. (2009) Insights into the pathogenesis and pathogenicity of cerebral amyloid angiopathy. Front Biosci. 14:4778-4792.

Lue LF, Kuo YM, Roher AE, Brachova L, Shen Y, Sue L, Beach T, Kurth JH, Rydel RE, Rogers J. (1999) Soluble amyloid beta peptide concentration as a predictor of synaptic change in Alzheimer's disease. Am J Pathol. 155(3):853-862.

Lucarelli P, Piciullo A, Palmarino M, Verdecchia M, Saccucci P, Arpino C, Curatolo P. (2004) Association between presenilin-1 -48C/T polymorphism and Down's syndrome. Neurosci Lett. 367(1):88-91.

Luo F, Rustay NR, Seifert T, Roesner B, Hradil V, Hillen H, Ebert U, Severin JM, Cox BF, Llano DA, Day M, Fox GB. (2010) Magnetic resonance imaging detection and time course of cerebral microhemorrhages during passiveimmunotherapy in living amyloid precursor protein transgenic mice. J Pharmacol Exp Ther. 335(3):580-588.

Maeda A, Yamada M, Itoh Y, Otomo E, Hayakawa M, Miyatake T. (1993) Computer-assisted three-dimensional image analysis of cerebral amyloid angiopathy. Stroke. 24(12):1857-1864.

Maezawa I, Zimin PI, Wulff H, Jin LW. (2011) Amyloid-beta protein oligomer at low nanomolar concentrations activates microglia and induces microglial neurotoxicity. J Biol Chem. 286(5):3693-3706.

Maier M, Seabrook TJ, Lazo ND, Jiang L, Das P, Janus C, Lemere CA. (2006) Short amyloid-beta (Abeta) immunogens reduce cerebral Abeta load and learning deficits in an Alzheimer's disease mouse model in the absence of an Abeta-specific cellular immune response. J Neurosci.26(18):4717-28.

Mangialasche F, Solomon A, Winblad B, Mecocci P, Kivipelto M. (2010) Alzheimer's disease: clinical trials and drug development. Lancet Neurol. 9(7):702-716.

Manley GT, Fujimura M, Ma T, Noshita N, Filiz F, Bollen AW, Chan P, Verkman AS. (2000) Aquaporin-4 deletion in mice reduces brain edema after acute water intoxication and ischemic stroke. Nat Med. 6(2):159-163.

Marco S, Skaper SD. (2006) Amyloid beta-peptide1-42 alters tight junction protein distribution and expression in brain microvessel endothelial cells. Neurosci Lett. 401(3):219-224.

Matsuda H (2007) Role of Neuroimaging in Alzheimer's Disease, with Emphasis on Brain Perfusion SPECT. J Nucl Med 48:1289-1300.

Masters CL, Simms G, Weinman NA, Multhaup G, McDonald BL, Beyreuther K. (1985) Amyloid plaque core protein in Alzheimer disease and Down syndrome. Proc Natl Acad Sci USA. 82(12):4245-4249.

Mazza M, Marano G, Traversi G, Bria P, Mazza S. (2011) Primary cerebral blood flow deficiency and Alzheimer's disease: shadows and lights. J Alzheimers Dis. 23(3):375-389.

McCarran WJ, Goldberg MP. (2007) White matter axon vulnerability to AMPA/kainate receptor-mediated ischemic injury is developmentally regulated. J Neurosci. 27(15):4220-4229.

McCarron MO, Nicoll JA, Stewart J, Cole GM, Yang F, Ironside JW, Mann DM, Love S, Graham DI. (2000) Amyloid beta-protein length and cerebral amyloid angiopathy-related haemorrhage. Neuroreport. 11(5):937-940.

McGeer PL, McGeer EG. (1995) The inflammatory response system of brain: implications for therapy of Alzheimer and other neurodegenerative diseases. Brain Res Brain Res Rev. 21(2):195-218.

McGeer PL, Akiyama H, Itagaki S, McGeer EG. (1989) Activation of the classical complement pathway in brain tissue of Alzheimer patients. Neurosci Lett. 107(1-3):341-346.

McLean CA, Cherny RA, Fraser FW, Fuller SJ, Smith MJ, Beyreuther K, Bush AI, Masters CL. (1999) Soluble pool of Abeta amyloid as a determinant of severity of neurodegeneration in Alzheimer's disease. Ann Neurol. 46(6):860-866.

Melchior B, Garcia AE, Hsiung BK, Lo KM, Doose JM, Thrash JC, Stalder AK, Staufenbiel M, Neumann H, Carson MJ. (2010) Dual induction of TREM2 and tolerance-related transcript, Tmem176b, in amyloid transgenic mice: implications for vaccine-based therapies for Alzheimer's disease. ASN Neuro. 2(3):e00037.

Merlini M, Meyer EP, Ulmann-Schuler A, Nitsch RM. (2011) Vascular β-amyloid and early astrocyte alterations impair cerebrovascular function and cerebral metabolism in transgenic arcAβ mice. Acta Neuropathol. 122(3):293-311.

Miao J, Vitek MP, Xu F, Previti ML, Davis J, Van Nostrand WE. (2005) Reducing cerebral microvascular amyloid-beta protein deposition diminishes regional neuroinflammation in vasculotropic mutant amyloid precursor protein transgenic mice. J Neurosci. 25(27):6271-6277.

Miklossy J. (2003) Cerebral hypoperfusion induces cortical watershed microinfarcts which may further aggravate cognitive decline in Alzheimer's disease. Neurol Res. 25(6):605-610.

Mildner A, Schlevogt B, Kierdorf K, Böttcher C, Erny D, Kummer MP, Quinn M, Brück W, Bechmann I, Heneka MT, Priller J, Prinz M. (2011). Distinct and non-redundant roles of microglia and myeloid subsets in mouse models of Alzheimer's disease. J Neurosci.31(31):11159-11171.

Millan Sanchez M, Heyn SN, Das D, Moghadam S, Martin KJ, Salehi A. (2012) Neurobiological elements of cognitive dysfunction in down syndrome: exploring the role of APP. Biol Psychiatry. 71(5):403-409.

Milner R, Hung S, Wang X, Spatz M, del Zoppo GJ. (2008) The rapid decrease in astrocyte-associated dystroglycan expression by focal cerebral ischemia is protease-dependent. J Cereb Blood Flow Metab. 28(4):812-823.

Milone M. (2012) Mitochondria, Diabetes, and Alzheime's Disease. Diabetes. 61(5) 991- 992.

Mizoguchi H, Takuma K, Fukuzaki E, Ibi D, Someya E, Akazawa KH, Alkam T, Tsunekawa H, Mouri A, Noda Y, Nabeshima T, Yamada K. (2009) Matrix metalloprotease-9 inhibition improves amyloid beta-mediated cognitive impairment and neurotoxicity in mice. J Pharmacol Exp Ther. 331(1):14-22.

Moftakhar P, Lynch MD, Pomakian JL, Vinters HV. (2010) Aquaporin expression in the brains of patients with or without cerebral amyloid angiopathy. J Neuropathol Exp Neurol. 69(12):1201-1209.

Mooradian AD, Haas MJ, Chehade JM. (2003) Age-related changes in rat cerebral occludin and zonula occludens-1 (ZO-1). Mech Ageing Dev. 124(2):143-146.

Morgan D, Gordon MN, Tan J, Wilcock D, Rojiani AM. (2005) Dynamic Complexity of the Microglial Activation Response in Transgenic Models of Amyloid Deposition: Implications for Alzheimer Therapeutics. J Neuropathol Exp Neurol. 64(9):743-753.

Morris JC, Cummings J. (2005) Mild cognitive impairment (MCI) represents early-stage Alzheimer's disease. J Alzheimers Dis. 7(3):235-239.

Morris JC, Storandt M, McKeel DW Jr, Rubin EH, Price JL, Grant EA, Berg L. (1996) Cerebral amyloid deposition and diffuse plaques in "normal" aging: Evidence for presymptomatic and very mild Alzheimer's disease. Neurology. 46(3):707-719.

Mrak RE, Griffinbc WS. (2001) The role of activated astrocytes and of the neurotrophic cytokine S100B in the pathogenesis of Alzheimer's disease. Neurobiol Aging. 22(6):915-22.

MRC-CFAS. (2001) Pathological correlates of late-onset dementia in a multicentre, community-based population in England and Wales. Neuropathology Group of the Medical Research Council Cognitive Function and Ageing Study (MRC CFAS). Lancet. 357(9251):169-175.

Mucke L, Masliah E, Yu GQ, Mallory M, Rockenstein EM, Tatsuno G, Hu K, Kholodenko D, Johnson-Wood K, McConlogue L. (2000) High-level neuronal expression of abeta 1-42 in wild-type human amyloid protein precursor transgenic mice: synaptotoxicity without plaque formation. J Neurosci. 20(11):4050-4058.

Mullan M, Crawford F, Axelman K, Houlden H, Lilius L, Winblad B, Lannfelt L. (1992) A pathogenic mutation for probable Alzheimer's disease in the APP gene at the N-terminus of beta-amyloid. Nat Genet. 1(5):345-347.

Mulligan SJ, MacVicar BA. (2004) Calcium transients in astrocyte endfeet cause cerebrovascular constrictions. Nature. 431(7005):195-199.

Murakami K. (2014) Conformation-specific antibodies to target amyloid β oligomers and their application to immunotherapy for Alzheimer's disease. Biosci Biotechnol Biochem. 78(8):1293-1305.

Muresanu DF, Popa-Wagner A, Stan A, Buga AM, Popescu BO. (2014) The vascular component of Alzheimer's disease. Curr Neurovasc Res. 11(2):168-176.

Nagele RG, Wegiel J, Venkataraman V, Imaki H, Wang KC, Wegiel J. (2004) Contribution of glial cells to the development of amyloid plaques in Alzheimer's disease. Neurobiol Aging. 25(5):663-674.

Nakata Y, Shiga K, Yoshikawa K, Mizuno T, Mori S, Yamada K, Nakajima K. (2002) Subclinical brain hemorrhages in Alzheimer's disease: evaluation by magnetic resonance T2*-weighted images. Ann N Y Acad Sci. 977:169-172.

Narayan P, Holmström KM, Kim DH, Whitcomb DJ, Wilson MR, St George-Hyslop P, Wood NW, Dobson CM, Cho K, Abramov AY, Klenerman D. (2014) Rare individual amyloid-β oligomers act on astrocytes to initiate neuronal damage. Biochemistry. 53(15):2442-2453.

Naruse S, Igarashi S, Kobayashi H, Aoki K, Inuzuka T, Kaneko K, Shimizu T, Iihara K, Kojima T, Miyatake T, et al. (1991) Mis-sense mutation Val----Ile in exon 17 of amyloid precursor protein gene in Japanese familial Alzheimer's disease. Lancet. 337(8747):978-979.

Neuwelt EA, Bauer B, Fahlke C, Fricker G, Iadecola C, Janigro D, Leybaert L, Molnár Z, O'Donnell ME, Povlishock JT, Saunders NR, Sharp F, Stanimirovic D,Watts RJ, Drewes LR. (2011) Engaging neuroscience to advance translational research in brain barrier biology. Nat Rev Neurosci. 12(3):169-182.

Nicoll JA, Wilkinson D, Holmes C, Steart P, Markham H, Weller RO. (2003) Neuropathology of human Alzheimer disease after immunization with amyloid-beta peptide: a case report. Nat Med. 9(4):448-452.

Nihashi T, Inao S, Kajita Y, Kawai T, Sugimoto T, Niwa M, Kabeya R, Hata N, Hayashi S, Yoshida J. (2001) Expression and distribution of beta amyloid precursor protein and beta amyloid peptide in reactive astrocytes after transient middle cerebral artery occlusion. Acta Neurochir (Wien). 143(3):287-295.

Novak V, Last D, Alsop DC, Abduljalil AM, Hu K, Lepicovsky L, Cavallerano J, Lipsitz LA. (2006) Cerebral blood flow velocity and periventricular white matter hyperintensities in type 2 diabetes. Diabetes Care. 29(7):1529-1534.

O'Brien JT, Erkinjuntti T, Reisberg B, Roman G, Sawada T, Pantoni L, Bowler JV, Ballard C, DeCarli C, Gorelick PB, Rockwood K, Burns A, Gauthier S, DeKosky ST. (2003) Vascular cognitive impairment. Lancet Neurol. 2(2):89-98.

Obermeier B, Daneman R, Ransohoff RM. (2013) Development, maintenance and disruption of the blood-brain barrier. Nat Med. 19(12):1584-1596.

Oddo S, Caccamo A, Shepherd JD, Murphy MP, Golde TE, Kayed R, Metherate R, Mattson MP, Akbari Y, LaFerla FM. (2003) Triple-transgenic model of Alzheimer's disease with plaques and tangles: intracellular Abeta and synaptic dysfunction. Neuron. 39(3):409-421.

Ohtaki H, Fujimoto T, Sato T, Kishimoto K, Fujimoto M, Moriya M, Shioda S. (2006) Progressive expression of vascular endothelial growth factor (VEGF) and angiogenesis after chronic ischemic hypoperfusion in rat. Acta Neurochir.96:283-287.

Ohtsuki S, Terasaki T. (2007) Contribution of carrier-mediated transport systems to the blood-brain barrier as a supporting and protecting interface for the brain; importance for CNS drug discovery and development. Pharm Res. 24(9):1745-1758.

Okamoto Y, Yamamoto T, Kalaria RN, Senzaki H, Maki T, Hase Y, Kitamura A, Washida K, Yamada M, Ito H, Tomimoto H, Takahashi R, Ihara M. (2012) Cerebral hypoperfusion accelerates cerebral amyloid angiopathy and promotes cortical microinfarcts. Acta Neuropathol. 123(3):381-394.

Okamoto Y, Ihara M, Fujita Y, Ito H, Takahashi R, Tomimoto H. (2009) Cortical microinfarcts in Alzheimer's disease and subcortical vascular dementia. Neuroreport. 20(11):990-996.

Olabarria M, Noristani HN, Verkhratsky A, Rodríguez JJ. (2010) Concomitant astroglial atrophy and astrogliosis in a triple transgenic animal model of Alzheimer's disease. Glia. 58(7):831-838.

Olichney JM, Hansen LA, Hofstetter CR, Grundman M, Katzman R, Thal LJ. (1995) Cerebral infarction in Alzheimer's disease is associated with severe amyloid angiopathy and hypertension. Arch Neurol. 52(7):702-708.

Otvos L Jr, Szendrei GI, Lee VM, Mantsch HH. (1993) Human and rodent Alzheimer beta-amyloid peptides acquire distinct conformations in membrane-mimicking solvents. Eur J Biochem. 211(1-2):249-257.

Palop JJ, Mucke L. (2010) Amyloid-beta-induced neuronal dysfunction in Alzheimer's disease: from synapses toward neural networks. Nat Neurosci. 13(7):812-818.

Panza F, Logroscino G, Imbimbo BP, Solfrizzi V. (2014) Is there still any hope for amyloid-based immunotherapy for Alzheimer's disease? Curr Opin Psychiatry. 27(2):128-137.

Panza F, Frisardi V, Solfrizzi V, Imbimbo BP, Logroscino G, Santamato A, Greco A, Seripa D, Pilotto A. (2012) Immunotherapy for Alzheimer's disease: from anti-β-amyloid to tau-based immunization strategies. Immunotherapy. 4(2):213-238.

Panza F, Frisardi V, Imbimbo BP, Seripa D, Paris F, Santamato A, D'Onofrio G, Logroscino G, Pilotto A, Solfrizzi V. (2011) Anti-β-amyloid immunotherapy for Alzheimer's disease: focus on bapineuzumab. Curr Alzheimer Res. 8(8):808-817.

Panza F, Solfrizzi V, Frisardi V, Capurso C, D'Introno A, Colacicco AM, Vendemiale G, Capurso A, Imbimbo BP. (2009) Disease-modifying approach to the treatment of Alzheimer's disease: from alpha-secretase activators to gamma-secretase inhibitors and modulators. Drugs Aging. 26(7):537-555.

Pappas BA, Davidson CM, Bennett SA, de la Torre JC, Fortin T, Tenniswood MP. (1997) Chronic ischemia: memory impairment and neural pathology in the rat. Ann N Y Acad Sci. 826:498-501.

Parajuli B, Sonobe Y, Horiuchi H, Takeuchi H, Mizuno T, Suzumura A. (2013) Oligomeric amyloid β induces IL-1β processing via production of ROS: implication in Alzheimer's disease. Cell Death Dis. 4:e975.

Parameshwaran K, Dhanasekaran M, Suppiramaniam V. (2008) Amyloid beta peptides and glutamatergic synaptic dysregulation. Exp Neurol. 210(1):7-13.

Park L, Koizumi K, El Jamal S, Zhou P, Previti ML, Van Nostrand WE, Carlson G, Iadecola C. (2014) Age-dependent neurovascular dysfunction and damage in a mouse model of cerebral amyloid angiopathy. Stroke.45(6):1815-21.

Park L, Zhou P, Koizumi K, El Jamal S, Previti ML, Van Nostrand WE, Carlson G, Iadecola C. (2013) Brain and circulating levels of Aβ1-40 differentially contribute to vasomotor dysfunction in the mouse brain. Stroke. 44(1):198-204.

Park L, Zhou P, Pitstick R, Capone C, Anrather J, Norris EH, Younkin L, Younkin S, Carlson G, McEwen BS, Iadecola C. (2008) Nox2 derived radicals contribute to neurovascular and behavioral dysfunction in mice overexpressing the amyloid precursor protein. Proc Natl Acad Sci U S A. 105(4):1347-1352.

Patel NS, Paris D, Mathura V, Quadros AN, Crawford FC, Mullan MJ. (2005) Inflammatory cytokine levels correlate with amyloid load in transgenic mouse models of Alzheimer's disease. J Neuroinflammation. 2(1):9.

Pauwels K, Williams TL, Morris KL, Jonckheere W, Vandersteen A, Kelly G, Schymkowitz J, Rousseau F, Pastore A, Serpell LC, Broersen K. (2012) Structural basis for increased toxicity of pathological aβ42:aβ40 ratios in Alzheimer disease. J Biol Chem. 287(8):5650-5660.

Pfeifer LA, White LR, Ross GW, Petrovitch H, Launer LJ. (2002a) Cerebral amyloid angiopathy and cognitive function: the HAAS autopsy study. Neurology. 58(11):1629-1634.

Pfeifer M, Boncristiano S, Bondolfi L, Stalder A, Deller T, Staufenbiel M, Mathews PM, Jucker M. (2002b) Cerebral hemorrhage after passive anti-Abeta immunotherapy. Science. 298(5597):1379.

Pimentel-Coelho PM, Michaud JP, Rivest S. (2013) Effects of mild chronic cerebral hypoperfusion and early amyloid pathology on spatial learning and the cellular innate immune response in mice. Neurobiol Aging. 34(3):679-693.

Pluta R, Ułamek M, Jabłoński M. (2009) Alzheimer's mechanisms in ischemic brain degeneration. Anat Rec (Hoboken). 292(12):1863-1881.

Pluta R. (2000) The role of apolipoprotein E in the deposition of beta-amyloid peptide during ischemia-reperfusion brain injury. A model of early Alzheimer's disease. Ann N Y Acad Sci. 903:324-334.

Pluta R, Barcikowska M, Mossakowski MJ, Zelman I. (1998) Cerebral accumulation of beta-amyloid following ischemic brain injury with long-term survival. Acta Neurochir Suppl. 71:206-208.

Popa-Wagner A, Schröder E, Walker LC, Kessler C. (1998) beta-Amyloid precursor protein and ss-amyloid peptide immunoreactivity in the rat brain after middle cerebral artery occlusion: effect of age. Stroke. 29(10):2196-2202.

Prohovnik I, Mayeux R, Sackeim HA, Smith G, Stern Y, Alderson PO. (1988) Cerebral perfusion as a diagnostic marker of early Alzheimer's disease. Neurology. 38(6):931-7.

Qi JP, Wu H, Yang Y, Wang DD, Chen YX, Gu YH, Liu T. (2007) Cerebral ischemia and Alzheimer's disease: the expression of amyloid-beta and apolipoprotein E in human hippocampus. J Alzheimers Dis. 12(4):335-341.

Qin B, Cartier L, Dubois-Dauphin M, Li B, Serrander L, Krause KH. (2006) A key role for the microglial NADPH oxidase in APP-dependent killing of neurons. Neurobiol Aging. 27(11):1577-1587.

Qiu C, Kivipelto M, von Strauss E. (2009) Epidemiology of Alzheimer's disease: occurrence, determinants, and strategies toward intervention. Dialogues Clin Neurosci 11(2):11-28.

Qiu C, von Strauss E, Fastbom J, Winblad B, Fratiglioni L. (2003) Low blood pressure and risk of dementia in the Kungsholmen project: a 6-year follow-up study. Arch Neurol. 60(2):223-228.

Racke MM, Boone LI, Hepburn DL, Parsadainian M, Bryan MT, Ness DK, Piroozi KS, Jordan WH, Brown DD, Hoffman WP, Holtzman DM, Bales KR, Gitter BD,May PC, Paul SM, DeMattos RB. (2005) Exacerbation of cerebral amyloid angiopathy-associated microhemorrhage in amyloid precursor protein transgenic mice by immunotherapy is dependent on antibody recognition of deposited forms of amyloid beta. J Neurosci. 25(3):629-636.

Rapoport M, Dawson HN, Binder LI, Vitek MP, Ferreira A. (2002) Tau is essential to beta -amyloid-induced neurotoxicity. Proc Natl Acad Sci U S A. 99(9):6364-6369.

Rebeck GW, Reiter JS, Strickland DK, Hyman BT. (1993) Apolipoprotein E in sporadic Alzheimer's disease: allelic variation and receptor interactions. Neuron. 11(4):575-580.

Reimer MM, McQueen J, Searcy L, Scullion G, Zonta B, Desmazieres A, Holland PR, Smith J, Gliddon C, Wood ER, Herzyk P, Brophy PJ, McCulloch J, Horsburgh K. (2011) Rapid disruption of axon-glial integrity in response to mild cerebral hypoperfusion. J Neurosci. 31(49):18185-18194.

Richard E, Gouw AA, Scheltens P, van Gool WA. (2010) Vascular care in patients with Alzheimer disease with cerebrovascular lesions slows progression of white matterlesions on MRI: the evaluation of vascular care in Alzheimer's disease (EVA) study. Stroke. 41(3):554-556.

Richard E, Kuiper R, Dijkgraaf MG, Van Gool WA; Evaluation of Vascular care in Alzheimer's disease. (2009) Vascular care in patients with Alzheimer's disease with cerebrovascular lesions-a randomized clinical trial. J Am Geriatr Soc. 57(5):797-805.

Rodríguez JJ, Olabarria M, Chvatal A, Verkhratsky A. (2009) Astroglia in dementia and Alzheimer's disease. Cell Death Differ. 16(3):378-385.

Roberson ED, Scearce-Levie K, Palop JJ, Yan F, Cheng IH, Wu T, Gerstein H, Yu GQ, Mucke L. (2007) Reducing endogenous tau ameliorates amyloid beta-induced deficits in an Alzheimer's disease mouse model. Science. 316(5825):750-754.

Rosales-Corral S, Tan DX, Reiter RJ, Valdivia-Velázquez M, Acosta-Martínez JP, Ortiz GG. (2004) Kinetics of the neuroinflammation-oxidative stress correlation in rat brain following the injection of fibrillar amyloid-beta onto the hippocampus in vivo. J Neuroimmunol. 150(1-2):20-28.

Rosand J, Hylek EM, O'Donnell HC, Greenberg SM. (2000) Warfarin-associated hemorrhage and cerebral amyloid angiopathy: a genetic and pathologic study. Neurology.55(7):947-951.

Rosenberg GA. (2009) Matrix metalloproteinases and their multiple roles in neurodegenerative diseases. Lancet Neurol. 8(2):205-216.

Rosendorff C, Beeri MS, Silverman JM. (2007) Cardiovascular risk factors for Alzheimer's disease. Am J Geriatr Cardiol.16(3):143-149.

Ruitenberg A, den Heijer T, Bakker SL, van Swieten JC, Koudstaal PJ, Hofman A, Breteler MM. (2005) Cerebral hypoperfusion and clinical onset of dementia: the Rotterdam Study. Ann Neurol. 57(6):789-794.

Rusinek H, De Santi S, Frid D, Tsui WH, Tarshish CY, Convit A, de Leon MJ. (2003) Regional brain atrophy rate predicts future cognitive decline: 6-year longitudinal MR imaging study of normal aging. Radiology. 229(3):691-696.

Sadowski MJ, Pankiewicz J, Scholtzova H, Mehta PD, Prelli F, Quartermain D, Wisniewski T. (2006) Blocking the apolipoprotein E/amyloid-beta interaction as a potential therapeutic approach for Alzheimer's disease. Proc Natl Acad Sci U S A. 103(49):18787-18792.

Sagare AP, Bell RD, Zlokovic BV. (2013) Neurovascular defects and faulty amyloid-β vascular clearance in Alzheimer's disease. J Alzheimers Dis. 33(1):S87-100.

Sakai K, Yamada M. (2013) Aβ immunotherapy for Alzheimer's disease. Brain Nerve. 65(4):461-468.

Salvadores N, Shahnawaz M, Scarpini E, Tagliavini F, Soto C. (2014) Detection of misfolded Aβ oligomers for sensitive biochemical diagnosis of Alzheimer's disease. Cell Rep. 7(1):261-268.

Sandoval KE, Witt KA. (2011) Age and 17β-estradiol effects on blood-brain barrier tight junction and estrogen receptor proteins in ovariectomized rats. Microvasc Res. 81(2):198-205.

Santacruz K, Lewis J, Spires T, Paulson J, Kotilinek L, Ingelsson M, Guimaraes A, DeTure M, Ramsden M, McGowan E, Forster C, Yue M, Orne J, Janus C, Mariash A, Kuskowski M, Hyman B, Hutton M, Ashe KH. (2005) Tau suppression in a neurodegenerative mouse model improves memory function. Science. 309(5733):476-481.

Sarazin M, Dorothée G, de Souza LC, Aucouturier P. (2013) Immunotherapy in Alzheimer's disease: do we have all the pieces of the puzzle? Biol Psychiatry. 74(5):329-332.

Schenk D, Barbour R, Dunn W, Gordon G, Grajeda H, Guido T, Hu K, Huang J, Johnson-Wood K, Khan K, Kholodenko D, Lee M, Liao Z, Lieberburg I, Motter R,Mutter L, Soriano F, Shopp G, Vasqsuez N, Vandevert C, Walker S, Wogulis M,

Yednock T, Games D, Seubert P. (1999) Immunization with amyloid-beta attenuates Alzheimer-disease-like pathology in the PDAPP mouse. Nature. 400(6740):173-177.

Schmechel DE, Saunders AM, Strittmatter WJ, Crain BJ, Hulette CM, Joo SH, Pericak-Vance MA, Goldgaber D, Roses AD. (1993) Increased amyloid beta-peptide deposition in cerebral cortex as a consequence of apolipoprotein E genotype in late-onset Alzheimer disease. Proc Natl Acad Sci U S A. 90(20):9649-9653.

Schneider LS, Mangialasche F, Andreasen N, Feldman H, Giacobini E, Jones R, Mantua V, Mecocci P, Pani L, Winblad B, Kivipelto M. (2014) Clinical trials and late-stage drug development for Alzheimer's disease: an appraisal from 1984 to 2014. J Intern Med. 275(3):251-283.

Schrag M, McAuley G, Pomakian J, Jiffry A, Tung S, Mueller C, Vinters HV, Haacke EM, Holshouser B, Kido D, Kirsch WM. (2010) Correlation of hypointensities in susceptibility-weighted images to tissue histology in dementia patients with cerebral amyloid angiopathy: a postmortem MRI study. Acta Neuropathol. 119(3):291-302.

Schor NF. (2011) What the halted phase III γ-secretase inhibitor trial may (or may not) be telling us. Ann Neurol. 69(2):237-239.

Schreibelt G, Kooij G, Reijerkerk A, van Doorn R, Gringhuis SI, van der Pol S, Weksler BB, Romero IA, Couraud PO, Piontek J, Blasig IE, Dijkstra CD, Ronken E, de Vries HE. (2007) Reactive oxygen species alter brain endothelial tight junction dynamics via RhoA, PI3 kinase, and PKB signaling. FASEB J. 21(13):3666-3676.

Schroeter S, Khan K, Barbour R, Doan M, Chen M, Guido T, Gill D, Basi G, Schenk D, Seubert P, Games D. (2008) Immunotherapy reduces vascular amyloid-beta in PDAPP mice. J Neurosci. 28(27):6787-6793.

Searcy JL, Le Bihan T, Salvadores N, McCulloch J, Horsburgh K. (2014) Impact of age on the cerebrovascular proteomes of wild-type and Tg-SwDI mice. PLoS One. 9(2):e89970.

Selkoe DJ. (1991) The molecular pathology of Alzheimer's disease. Neuron. 6(4):487-498.

Selkoe DJ. (1989) Biochemistry of altered brain proteins in Alzheimer's disease. Annu Rev. Neurosci. 12:463-490.

Semenza GL. (2011) Oxygen sensing, homeostasis, and disease. N Engl J Med. 365(6):537-547

Serrano-Pozo A, Frosch MP, Masliah E, Hyman BT. (2011) Neuropathological alterations in Alzheimer disease. Cold Spring Harb Perspect Med. 1(1):a006189.

Shankar GM, Bloodgood BL, Townsend M, Walsh DM, Selkoe DJ, Sabatini BL. (2007) Natural oligomers of the Alzheimer amyloid-beta protein induce reversible synapse loss by modulating an NMDA-type glutamate receptor-dependent signaling pathway. J Neurosci. 27(11):2866-2875.

Sharp ES, Gatz M. (2011) Relationship between education and dementia: an updated systematic review. Alzheimer Dis Assoc Disord. 25(4):289-304.

Shepherd J, Blauw GJ, Murphy MB, Bollen EL, Buckley BM, Cobbe SM, Ford I, Gaw A, Hyland M, Jukema JW, Kamper AM, Macfarlane PW, Meinders AE, Norrie J, Packard CJ, Perry IJ, Stott DJ, Sweeney BJ, Twomey C, Westendorp RG; PROSPER study group. PROspective Study of Pravastatin in the Elderly at Risk. (2002) Pravastatin in elderly individuals at risk of vascular disease (PROSPER): a randomised controlled trial. Lancet. 360(9346):1623-1630.

Shi J, Yang SH, Stubley L, Day AL, Simpkins JW. (2000) Hypoperfusion induces overexpression of beta-amyloid precursor protein mRNA in a focal ischemic rodent model. Brain Res. 853(1):1-4.

Shibata M, Yamasaki N, Miyakawa T, Kalaria RN, Fujita Y, Ohtani R, Ihara M, Takahashi R, Tomimoto H. (2007) Selective impairment of working memory in a mouse model of chronic cerebral hypoperfusion. Stroke. 38(10):2826-2832.

Shibata M, Ohtani R, Ihara M, Tomimoto H. (2004) White matter lesions and glial activation in a novel mouse model of chronic cerebral hypoperfusion. Stroke. 35(11):2598-2603.

Shibata M, Yamada S, Kumar SR, Calero M, Bading J, Frangione B, Holtzman DM, Miller CA, Strickland DK, Ghiso J, Zlokovic BV. (2000) Clearance of Alzheimer's amyloid-ss(1-40) peptide from brain by LDL receptor-related protein-1 at the blood-brain barrier. J Clin Invest. 106(12):1489-1499.

Shih AY, Blinder P, Tsai PS, Friedman B, Stanley G, Lyden PD, Kleinfeld D. (2013) The smallest stroke: occlusion of one penetrating vessel leads to infarction and a cognitive deficit. Nat Neurosci. 16(1):55-63.

Shinkai Y, Yoshimura M, Ito Y, Odaka A, Suzuki N, Yanagisawa K, Ihara Y. (1995) Amyloid beta-proteins 1-40 and 1-42(43) in the soluble fraction of extra- and intracranial blood vessels. Ann Neurol. 38(3):421-428.

Shin JS, Hyun SY, Kim DH, Lee S, Jung JW, Choi JW, Ko KH, Kim JM, Ryu JH. (2008) Chronic hypoperfusion increases claudin-3 immunoreactivity in rat brain. Neurosci Lett. 445(2):144-148.

Singh-Manoux A, Sabia S, Kivimaki M, Shipley MJ, Ferrie JE, Marmot MG. (2009) Cognition and incident coronary heart disease in late midlife: The Whitehall II study. Intelligence. 37(6):529-534.

Sivanandam TM, Thakur MK. (2012) Traumatic brain injury: a risk factor for Alzheimer's disease. Neurosci Biobehav Rev. 36(5):1376-1381.

Sofroniew MV. (2005) Reactive astrocytes in neural repair and protection. Neuroscientist. 11(5):400-407.

Solomon A, Kivipelto M, Wolozin B, Zhou J, Whitmer RA. (2009) Midlife serum cholesterol and increased risk of Alzheimer's and vascular dementia three decades later. Dement Geriatr Cogn Disord. 28(1):75-80.

Solomon, B., Koppel, R., Hanan, E. & Katzav, T. (1996) Monoclonal antibodies inhibit in vitro fibrillar aggregation of the Alzheimer β-amyloid peptide. Proc. Natl Acad. Sci. USA 93, 452–455.

Solomon, B., Koppel, R., Frenkel, D. & Hanan-Aharon, E. (1997) Disaggregation of Alzheimer β-amyloid by site-directed mAb. Proc. Natl Acad. Sci. USA 94, 4109–4112.

Soontornniyomkij V, Lynch MD, Mermash S, Pomakian J, Badkoobehi H, Clare R, Vinters HV. (2010) Cerebral microinfarcts associated with severe cerebral beta-amyloid angiopathy. Brain Pathol. 20(2):459-467.

Smith EE, Schneider JA, Wardlaw JM, Greenberg SM. (2012) Cerebral microinfarcts: the invisible lesions. Lancet Neurol. 11(3):272-282.

Smith MA, Rottkamp CA, Nunomura A, Raina AK, Perry G. (2000) Oxidative stress in Alzheimer's disease. Biochim Biophys Acta. 1502(1):139-144.

Spires-Jones TL, Mielke ML, Rozkalne A, Meyer-Luehmann M, de Calignon A, Bacskai BJ, Schenk D, Hyman BT. (2009) Passive immunotherapy rapidly increases structural plasticity in a mouse model of Alzheimer disease. Neurobiol Dis. 33(2):213-220.

Stanimirovic DB, Friedman A. (2012) Pathophysiology of the neurovascular unit: disease cause or consequence? J Cereb Blood Flow Metab. 32(7):1207-1221.

Stephenson DT, Rash K, Clemens JA. (1992) Amyloid precursor protein accumulates in regions of neurodegeneration following focal cerebral ischemia in the rat. Brain Res. 593(1):128-135.

Streit WJ. (2004) Microglia and Alzheimer's disease pathogenesis. J Neurosci Res. 77(1):1-8.

Sun X, He G, Qing H, Zhou W, Dobie F, Cai F, Staufenbiel M, Huang LE, Song W. (2006) Hypoxia facilitates Alzheimer's disease pathogenesis by up-regulating BACE1 gene expression. Proc Natl Acad Sci U S A. 103(49):18727-18732.

Suter OC, Sunthorn T, Kraftsik R, Straubel J, Darekar P, Khalili K, Miklossy J. (2002) Cerebral hypoperfusion generates cortical watershed microinfarcts in Alzheimer disease. Stroke. 33(8):1986-1992.

Suzuki N, Cheung TT, Cai XD, Odaka A, Otvos L Jr, Eckman C, Golde TE, Younkin SG. (1994a) An increased percentage of long amyloid beta protein secreted by familial amyloid beta protein precursor (beta APP717) mutants. Science 264(5163):1336-1340.

Suzuki N, Iwatsubo T, Odaka A, Ishibashi Y, Kitada C, Ihara Y. (1994b) High tissue content of soluble beta 1-40 is linked to cerebral amyloid angiopathy. Am J Pathol. 145(2):452-460.

Tai LM, Holloway KA, Male DK, Loughlin AJ, Romero IA. (2010) Amyloid-beta-induced occludin down-regulation and increased permeability in human brain endothelial cells is mediated by MAPK activation. J Cell Mol Med. 14(5):1101-1112.

Takahashi K, Rochford CD, Neumann H. (2005) Clearance of apoptotic neurons without inflammation by microglial triggering receptor expressed on myeloidcells-2. J Exp Med. 201(4):647-657.

Tamura A, Graham DI, McCulloch J, Teasdale GM. (1981) Focal cerebral ischaemia in the rat: 1. Description of technique and early neuropathological consequences following middle cerebral artery occlusion. J Cereb Blood Flow Metab. 1(1):53-60.

Taniguchi M, Yamashita T, Kumura E, Tamatani M, Kobayashi A, Yokawa T, Maruno M, Kato A, Ohnishi T, Kohmura E, Tohyama M, Yoshimine T. (2000) Induction of aquaporin-4 water channel mRNA after focal cerebral ischemia in rat. Brain Res Mol Brain Res. 78(1-2):131-137.

Tang XN, Cairns B, Cairns N, Yenari MA. (2008) Apocynin improves outcome in experimental stroke with a narrow dose range. Neuroscience. 154(2):556-562.

Tayeb HO, Murray ED, Price BH, Tarazi FI. (2013) Bapineuzumab and solanezumab for Alzheimer's disease: is the 'amyloid cascade hypothesis' still alive? Expert Opin Biol Ther. 13(7):1075-1084.

Teller JK, Russo C, DeBusk LM, Angelini G, Zaccheo D, Dagna-Bricarelli F, Scartezzini P, Bertolini S, Mann DM, Tabaton M, Gambetti P. (1996) Presence of soluble amyloid beta-peptide precedes amyloid plaque formation in Down's syndrome. Nat Med. 2(1):93-95.

Terry RD. (1994) Neuropathological changes in Alzheimer disease. Prog Brain Res 101:383-390.

Terry RD, Masliah E, Salmon DP, Butters N, DeTeresa R, Hill R, Hansen LA, Katzman R. (1991) Physical basis of cognitive alterations in Alzheimer's disease:

synapse loss is the major correlate of cognitiveimpairment. Ann Neurol. 30(4):572-580.

Thal DR, Capetillo-Zarate E, Larionov S, Staufenbiel M, Zurbruegg S, Beckmann N. (2009) Capillary cerebral amyloid angiopathy is associated with vessel occlusion and cerebral blood flow disturbances. Neurobiol Aging. 30(12):1936-1948.

Thal DR, Griffin WS, de Vos RA, Ghebremedhin E. (2008) Cerebral amyloid angiopathy and its relationship to Alzheimer's disease. Acta Neuropathol. 115(6):599-609.

Tolppanen AM, Lavikainen P, Solomon A, Kivipelto M, Soininen H, Hartikainen S. (2013) Incidence of stroke in people with Alzheimer disease: a national register-based approach. Neurology. 80(4):353-358.

Tout S, Chan-Ling T, Holländer H, Stone J. (1993) The role of Müller cells in the formation of the blood-retinal barrier. Neuroscience. 55(1):291-301.

Trojanowski JQ, Lee VM. (2000) "Fatal attractions" of proteins. A comprehensive hypothetical mechanism underlying Alzheimer's disease and other neurodegenerative disorders. Ann N Y Acad Sci. 924:62-7.

Troncoso JC, Zonderman AB, Resnick SM, Crain B, Pletnikova O, O'Brien RJ. (2008) Effect of infarcts on dementia in the Baltimore longitudinal study of aging. Ann Neurol. 64(2):168-176.

Troquier L, Caillierez R, Burnouf S, Fernandez-Gomez FJ, Grosjean ME, Zommer N, Sergeant N, Schraen-Maschke S, Blum D, Buee L. (2012) Targeting phospho-Ser422 by active Tau Immunotherapy in the THYTau22 mouse model: a suitable therapeutic approach. Curr Alzheimer Res. 9(4):397-405.

Tzourio C, Anderson C, Chapman N, Woodward M, Neal B, MacMahon S, Chalmers J; PROGRESS Collaborative Group. (2003) Effects of blood pressure lowering with perindopril and indapamide therapy on dementia and cognitive decline in patients with cerebrovascular disease. Arch Intern Med. 163(9):1069-1075.

Ueno M, Tomimoto H, Akiguchi I, Wakita H, Sakamoto H. (2002) Blood-brain barrier disruption in white matter lesions in a rat model of chronic cerebral hypoperfusion. J Cereb Blood Flow Metab. 22(1):97-104.

Underhill SM, Goldberg MP. (2007) Hypoxic injury of isolated axons is independent of ionotropic glutamate receptors. Neurobiol Dis 25(2):284-290.

Urbanelli L, Magini A, Ciccarone V, Trivelli F, Polidoro M, Tancini B, Emiliani C. (2009) New perspectives for the diagnosis of Alzheimer's disease. Recent Pat CNS Drug Discov 4(3):160-181.

Uro-Coste E, Russano de Paiva G, Guilbeau-Frugier C, Sastre N, Ousset PJ, da Silva NA, Lavialle-Guillotreau V, Vellas B, Delisle MB. (2010) Cerebral amyloid angiopathy and microhemorrhages after amyloid beta vaccination: case report and brief review. Clin Neuropathol. 29(4):209-216.

Van Broeckhoven C, Haan J, Bakker E, Hardy JA, Van Hul W, Wehnert A, Vegter-Van der Vlis M, Roos RA. (1990) Amyloid beta protein precursor gene and hereditary cerebral hemorrhage with amyloidosis (Dutch). Science. 248(4959):1120-1122.

Van Den Heuvel C, Thornton E, Vink R. (2007) Traumatic brain injury and Alzheimer's disease: a review. Prog Brain Res. 161:303-316.

Van Dorpe J, Smeijers L, Dewachter I, Nuyens D, Spittaels K, Van Den Haute C, Mercken M, Moechars D, Laenen I, Kuiperi C, Bruynseels K, Tesseur I, Loos R, Vanderstichele H, Sciot R, Van Leuven F. (2000) Prominent cerebral amyloid angiopathy in transgenic mice overexpressing the london mutant of human APP in neurons. Am J Pathol. 157:1283-1298.

van Groen T, Puurunen K, Mäki HM, Sivenius J, Jolkkonen J. (2005) Transformation of diffuse beta-amyloid precursor protein and beta-amyloid deposits to plaques in the thalamusafter transient occlusion of the middle cerebral artery in rats. Stroke. 36(7):1551-1556.

van Norden AG, van Dijk EJ, de Laat KF, Scheltens P, Olderikkert MG, de Leeuw FE. (2012) Dementia: Alzheimer pathology and vascular factors: from mutually exclusive to interaction. Biochim Biophys Acta. 1822(3):340-349.

van Rooden S, Goos JD, van Opstal AM, Versluis MJ, Webb AG, Blauw GJ, van der Flier WM, Scheltens P, Barkhof F, van Buchem MA, van der Grond J. (2014) Increased number of microinfarcts in Alzheimer disease at 7-T MR imaging. Radiology. 270(1):205-211.

Vasilevko V, Xu F, Previti ML, Van Nostrand WE, Cribbs DH. (2007) Experimental investigation of antibody-mediated clearance mechanisms of amyloid-beta in CNS of Tg-SwDI transgenic mice. J Neurosci. 27(49):13376-13383.

Vellas B, Black R, Thal LJ, Fox NC, Daniels M, McLennan G, Tompkins C, Leibman C, Pomfret M, Grundman M; AN1792 (QS-21)-251 Study Team. (2009) Long-term follow-up of patients immunized with AN1792: reduced functional decline in antibody responders. Curr Alzheimer Res. 6(2):144-151.

Vermeer SE, Prins ND, den Heijer T, Hofman A, Koudstaal PJ, Breteler MM. (2003) Silent brain infarcts and the risk of dementia and cognitive decline. N Engl J Med. 348(13):1215-1222.

Vicente E, Degerone D, Bohn L, Scornavaca F, Pimentel A, Leite MC, Swarowsky A, Rodrigues L, Nardin P, de Almeida LM, Gottfried C, Souza DO, Netto CA,

Gonçalves CA. (2009) Astroglial and cognitive effects of chronic cerebral hypoperfusion in the rat. Brain Res.1251:204-212.

Vidal R, Barbeito AG, Miravalle L, Ghetti B. (2009) Cerebral amyloid angiopathy and parenchymal amyloid deposition in transgenic mice expressing the Danish mutant form of human BRI2. Brain Pathol. 19:58-68.

Vingtdeux V, Sergeant N, Buée L. (2012) Potential contribution of exosomes to the prion-like propagation of lesions in Alzheimer's disease. Front Physiol. 3:229.

Vinters HV. (1987) Cerebral amyloid angiopathy. A critical review. Stroke. 18(2):311-324.

Vite CH, Head E. (2014) Aging in the canine and feline brain. Vet Clin North Am Small Anim Pract. 44(6):1113-29.

Vizuete ML, Venero JL, Vargas C, Ilundáin AA, Echevarría M, Machado A, Cano J. (1999) Differential upregulation of aquaporin-4 mRNA expression in reactive astrocytes after brain injury: potential role in brain edema. Neurobiol Dis. 6(4):245-258.

Volterra A, Meldolesi J. (2005) Astrocytes, from brain glue to communication elements: the revolution continues. Nat Rev Neurosci. 6(8):626-640.

Vonsattel JP, Myers RH, Hedley-Whyte ET, Ropper AH, Bird ED, Richardson EP Jr. (1991) Cerebral amyloid angiopathy without and with cerebral hemorrhages: a comparative histological study. Ann Neurol. 30(5):637-649.

Wakita H, Tomimoto H, Akiguchi I, Matsuo A, Lin JX, Ihara M, McGeer PL. (2002) Axonal damage and demyelination in the white matter after chronic cerebral hypoperfusion in the rat. Brain Res 924:63-70

Walder CE, Green SP, Darbonne WC, Mathias J, Rae J, Dinauer MC, Curnutte JT, Thomas GR. (1997) Ischemic stroke injury is reduced in mice lacking a functional NADPH oxidase. Stroke. 28(11):2252-2258.

Walsh DM, Selkoe DJ. (2007) A beta oligomers - a decade of discovery. J Neurochem. 101(5):1172-1184.

Wang X, Xing A, Xu C, Cai Q, Liu H, Li L. (2010) Cerebrovascular hypoperfusion induces spatial memory impairment, synaptic changes, and amyloid-β oligomerization in rats. J Alzheimers Dis. 21(3):813

Wang Y, Zhou TH, Zhi Z, Barakat A, Hlatky L, Querfurth H. (2013) Multiple effects of β-amyloid on single excitatory synaptic connections in the PFC. Front Cell Neurosci. 7:129.

Wang YJ, Zhou HD, Zhou XF. (2006) Clearance of amyloid-beta in Alzheimer's disease: progress, problems and perspectives. Drug Discov Today. 11(19-20):931-938.

Wardlaw JM, Allerhand M, Doubal FN, Valdes Hernandez M, Morris Z, Gow AJ, Bastin M, Starr JM, Dennis MS, Deary IJ. (2014) Vascular risk factors, large-artery atheroma, and brain white matter hyperintensities. Neurology. 82(15):1331-1338.

Waubant E. (2006) Biomarkers indicative of blood-brain barrier disruption in multiple sclerosis. Dis Markers. 22(4):235-244.

Weiner HL, Lemere CA, Maron R, Spooner ET, Grenfell TJ, Mori C, Issazadeh S, Hancock WW, Selkoe DJ. (2000) Nasal administration of amyloid-beta peptide decreases cerebral amyloid burden in a mouse model of Alzheimer's disease. Ann Neurol. 48(4):567-79.

Weintraub S, Wicklund AH, Salmon DP. (2012) The neuropsychological profile of Alzheimer disease. Cold Spring Harb Perspect Med. 2(4):a006171.

Weller RO, Preston SD, Subash M, Carare RO. (2009) Cerebral amyloid angiopathy in the aetiology and immunotherapy of Alzheimer disease. Alzheimers Res Ther. 1(2):6.

Weller RO, Subash M, Preston SD, Mazanti I, Carare RO. (2008) Perivascular drainage of amyloid-beta peptides from the brain and its failure in cerebral amyloid angiopathy and Alzheimer's disease. Brain Pathol. 18(2):253-266.

Weller RO, Nicoll JA. (2003) Cerebral amyloid angiopathy: pathogenesis and effects on the ageing and Alzheimer brain. Neurol Res. 25(6):611-616.

Weller RO, Massey A, Newman TA, Hutchings M, Kuo YM, Roher AE. (1998) Cerebral amyloid angiopathy: amyloid beta accumulates in putative interstitial fluid drainage pathways in Alzheimer’s disease. Am J Pathol. 153:725-733.

Wilcock DM, Vitek MP, Colton CA. (2009) Vascular amyloid alters astrocytic water and potassium channels in mouse models and humans with Alzheimer's disease. Neuroscience. 159(3):1055-1069.

Wilcock DM, Colton CA. (2009) Immunotherapy, vascular pathology, and microhemorrhages in transgenic mice. CNS Neurol Disord Drug Targets. 8(1):50-64.

Wilcock DM, Alamed J, Gottschall PE, Grimm J, Rosenthal A, Pons J, Ronan V, Symmonds K, Gordon MN, Morgan D. (2006) Deglycosylated anti-amyloid-beta antibodies eliminate cognitive deficits and reduce parenchymal amyloid with minimal vascular consequences in aged amyloid precursor protein transgenic mice. J Neurosci. 26(20):5340-5346.

Wilcock GK, Black SE, Hendrix SB, Zavitz KH, Swabb EA, Laughlin MA; Tarenflurbil Phase II Study investigators. (2008) Efficacy and safety of tarenflurbil in mild to moderate Alzheimer's disease: a randomised phase II trial. Lancet Neurol. 7(6):483-493.

Wilcock DM, Rojiani A, Rosenthal A, Subbarao S, Freeman MJ, Gordon MN, Morgan D. (2004) Passive immunotherapy against Abeta in aged APP-transgenic mice reverses cognitive deficits and depletesparenchymal amyloid deposits in spite of increased vascular amyloid and microhemorrhage. J Neuroinflammation. 1(1):24.

Wilkinson BL, Landreth GE. (2006) The microglial NADPH oxidase complex as a source of oxidative stress in Alzheimer's disease. J Neuroinflammation. 3:30.

Wimo A, Winblad B, Jönsson L. (2010) The worldwide societal costs of dementia: Estimates for 2009. Alzheimers Dement. 6(2):98-103.

Wimo, A, Prince, M. (2010) World Alzheimer report 2010. In The global economic impact of dementia. Alzheimer’s disease international.

Wischik CM, Edwards PC, Lai RY, Roth M, Harrington CR. (1996) Selective inhibition of Alzheimer disease-like tau aggregation by phenothiazines. Proc Natl Acad Sci U S A. 93(20):11213-11218.

Wischik CM, Staff RT, Wischik DJ, Bentham P, Murray AD, Storey JM, Kook KA, Harrington CR. (2015) Tau aggregation inhibitor therapy: an exploratory phase 2 study in mild or moderate Alzheimer's disease. J Alzheimers Dis. 44(2):705-720.

Wisniewski HM, Wegiel J. (1994) Beta-amyloid formation by myocytes of leptomeningeal vessels. Acta Neuropathol. 87(3):233-241.

Wolburg H, Wolburg-Buchholz K, Kraus J, Rascher-Eggstein G, Liebner S, Hamm S, Duffner F, Grote EH, Risau W, Engelhardt B. (2003) Localization of claudin-3 in tight junctions of the blood-brain barrier is selectively lost during experimental autoimmune encephalomyelitis and human glioblastoma multiforme. Acta Neuropathol. 105(6):586-592.

Wu JS, Chen XC, Chen H, Shi YQ. (2006) A study on blood-brain barrier ultrastructural changes induced by cerebral hypoperfusion of different stages. Neurol Res. 28(1):50-58.

Xu F, Grande AM, Robinson JK, Previti ML, Vasek M, Davis J, Van Nostrand WE. (2007) Early-onset subicular microvascular amyloid and neuroinflammation correlate with behavioral deficits in vasculotropic mutant amyloid beta-protein precursor transgenic mice. Neuroscience. 146(1):98-107.

Xu W, Xu F, Anderson ME, Kotarba AE, Davis J, Robinson JK, Van Nostrand WE. (2014) Cerebral microvascular rather than parenchymal amyloid-β protein pathology

promotes early cognitive impairment in transgenic mice. J Alzheimers Dis. 38(3):621-632.

Yam PS, Takasago T, Dewar D, Graham DI, McCulloch J. (1997) Amyloid precursor protein accumulates in white matter at the margin of a focal ischaemic lesion. Brain Res. 760(1-2):150-157.

Yamada M, Ihara M, Okamoto Y, Maki T, Washida K, Kitamura A, Hase Y, Ito H, Takao K, Miyakawa T, Kalaria RN, Tomimoto H, Takahashi R. (2011) The influence of chronic cerebral hypoperfusion on cognitive function and amyloid β metabolism in APP overexpressing mice. PLoS One. 6(1):e16567.

Yang J, Lunde LK, Nuntagij P, Oguchi T, Camassa LM, Nilsson LN, Lannfelt L, Xu Y, Amiry-Moghaddam M, Ottersen OP, Torp R. (2011) Loss of astrocyte polarization in the tg-ArcSwe mouse model of Alzheimer's disease. J Alzheimers Dis. 27(4):711-722.

Yang Y, Estrada EY, Thompson JF, Liu W, Rosenberg GA. (2007) Matrix metalloproteinase-mediated disruption of tight junction proteins in cerebral vessels is reversed by synthetic matrix metalloproteinase inhibitor in focal ischemia in rat. J Cereb Blood Flow Metab. 27(4):697-709. Epub 2006 Jul 19.

Yoon HJ, Park KW, Jeong YJ, Kang DY. (2012) Significant correlation between cerebral hypoperfusion and neuropsychological assessment scores of patients with mild cognitive impairment. Nucl Med Commun. 33(8):848-858.

Younkin SG. (1995) Evidence that A beta 42 is the real culprit in Alzheimer's disease. Ann Neurol. 37(3):287-288.

Zabel M, Schrag M, Crofton A, Tung S, Beaufond P, Van Ornam J, Dininni A, Vinters HV, Coppola G, Kirsch WM. (2013) A shift in microglial β-amyloid binding in Alzheimer's disease is associated with cerebral amyloid angiopathy. Brain Pathol. 23(4):390-401.

Zago W, Schroeter S, Guido T, Khan K, Seubert P, Yednock T, Schenk D, Gregg KM, Games D, Bard F, Kinney GG. (2013) Vascular alterations in PDAPP mice after anti-Aβ immunotherapy: Implications for amyloid-related imaging abnormalities. Alzheimers Dement. 9(5 Suppl):S105-115.

Zarow C, Zaias B, Lyness SA, Chui H. (1999) Cerebral amyloid angiopathy in Alzheimer’s disease is associated with apolipoprotein E4 and cortical neuron loss. Alzheimer Dis Assoc Disord. 13(1):1-8.

Zekry D, Duyckaerts C, Belmin J, Geoffre C, Moulias R, Hauw JJ. (2003) Cerebral amyloid angiopathy in the elderly: vessel walls changes and relationship with dementia. Acta Neuropathol. 106(4):367-373.

Zhao Y, Gu JH, Dai CL, Liu Q, Iqbal K, Liu F, Gong CX. (2014) Chronic cerebral hypoperfusion causes decrease of O-GlcNAcylation, hyperphosphorylation of tau and behavioral deficits in mice. Front Aging Neurosci. 6:10.

Zhang X, Zhou K, Wang R, Cui J, Lipton SA, Liao FF, Xu H, Zhang YW. (2007) Hypoxia-inducible factor 1alpha (HIF-1alpha)-mediated hypoxia increases BACE1 expression and beta-amyloid generation. J Biol Chem. 282(15):10873-10880.

Zhiyou C, Yong Y, Shanquan S, Jun Z, Liangguo H, Ling Y, Jieying L. (2009) Upregulation of BACE1 and beta-amyloid protein mediated by chronic cerebral hypoperfusion contributes to cognitive impairment and pathogenesis of Alzheimer's disease. Neurochem Res. 34(7):1226-1235

Zlokovic BV. (2011) Neurovascular pathways to neurodegeneration in Alzheimer's disease and other disorders. Nat Rev Neurosci. 12(12):723-738.

Zlokovic BV. (2008) The blood-brain barrier in health and chronic neurodegenerative disorders. Neuron. 57(2):178-201.

Zlokovic BV. (2004) Clearing amyloid through the blood-brain barrier. J Neurochem. 89(4):807-811.

Zou Q, Wu CW, Stein EA, Zang Y, Yang Y. (2009) Static and dynamic characteristics of cerebral blood flow during the resting state. Neuroimage. 48(3):515-524.

Zuccalà G, Onder G, Marzetti E, Monaco MR, Cesari M, Cocchi A, Carbonin P, Bernabei R; GIFA Study Group. (2005) Use of angiotensin-converting enzyme inhibitors and variations in cognitive performance among patients with heart failure. Eur Heart J. 26(3):226-233.

Appendices

Appendix 1. Aβ levels in wild-type mice.

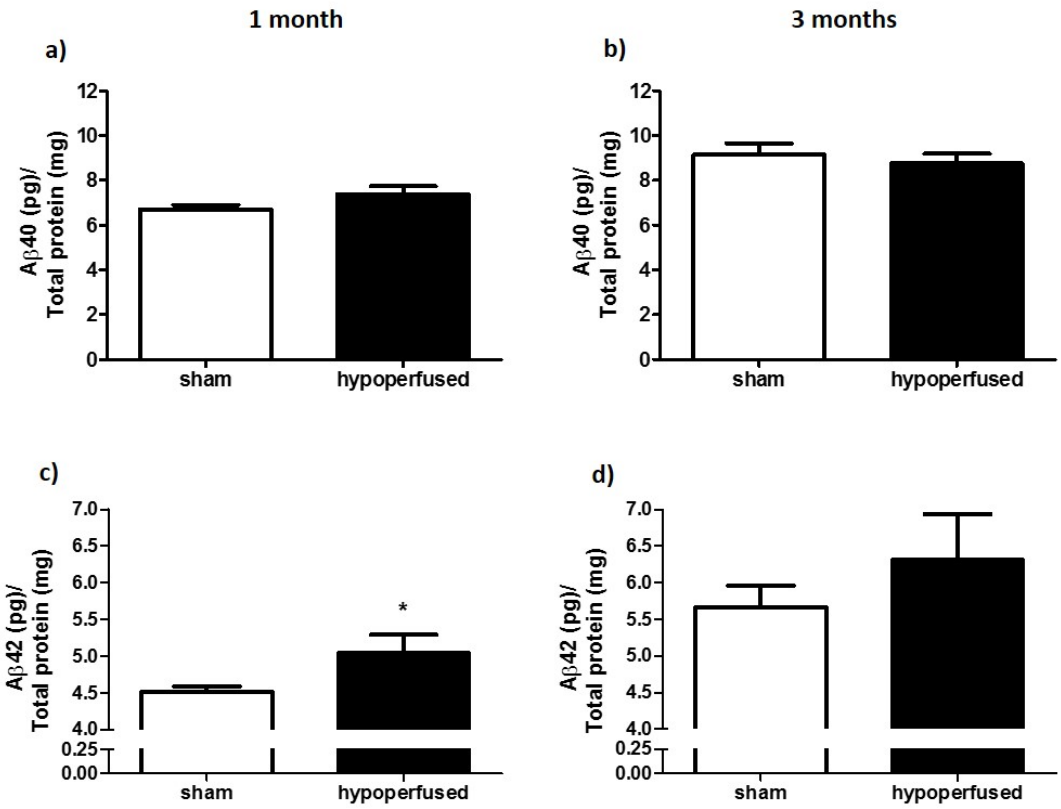

Figure A1. Aβ levels are increased after chronic cerebral hypoperfusion in wild-type mice. Animals were sacrificed after 1 (a, c) and 3 (b, d) months of chronic cerebral hypoperfusion. Following protein extraction, the levels of Aβ40/42 were quantified in the parenchymal fraction by ELISA. Graphs represent the levels of the protein normalised to total protein concentration. The data presented are the means ± S.E.M., $p<0.05$.

Appendix 2. APP levels in wild-type mice.

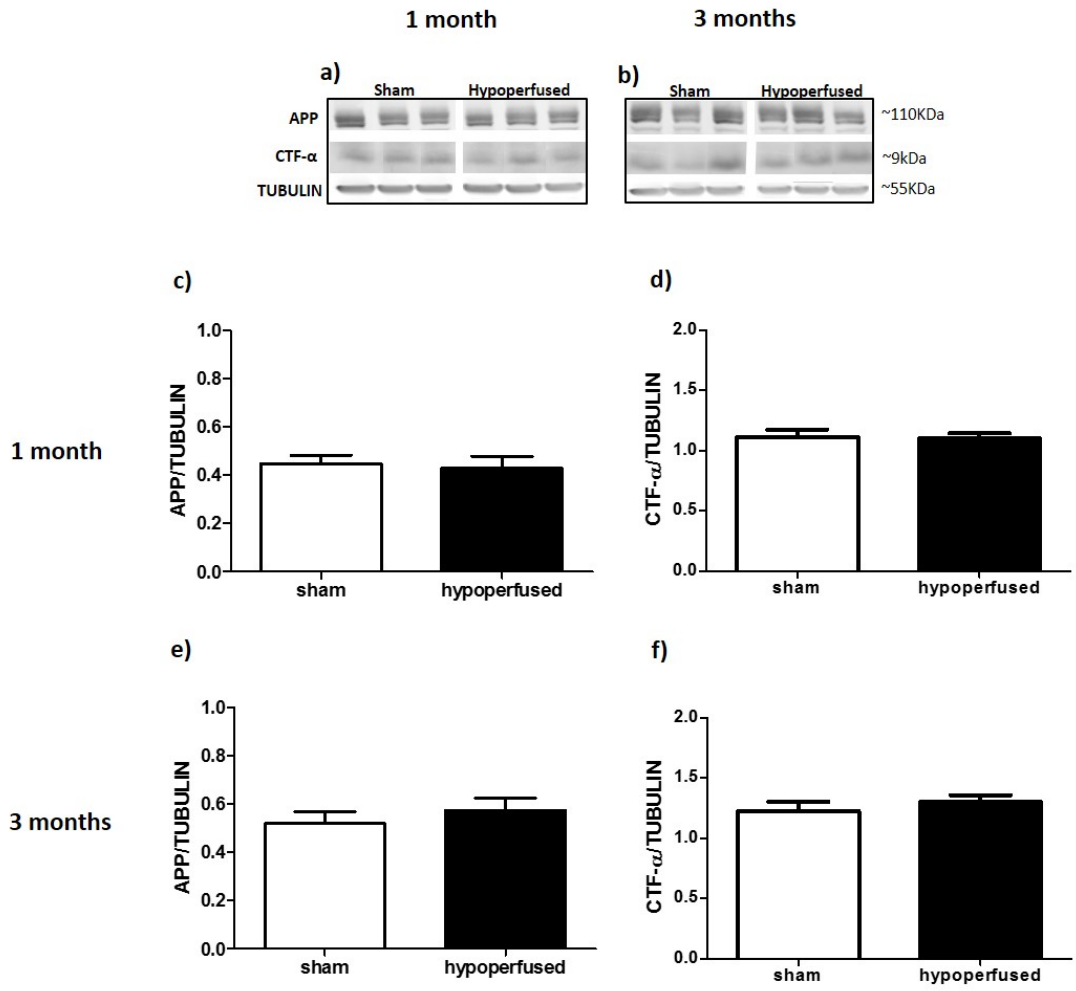

Figure A2. Chronic cerebral hypoperfusion does not affect APP metabolism in wild type animals. Western blot analysis of brain protein extracts after 1 (a, c, d) and 3 (b, e, f) months of hypoperfusion was performed to determine the expression levels of APP and CTFα. Specific bands were quantified by densitometric analysis and expressed relative to total tubulin protein, represented in the graphs. The data presented are the means ± S.E.M.

Appendix 3. LRP levels in wild-type mice.

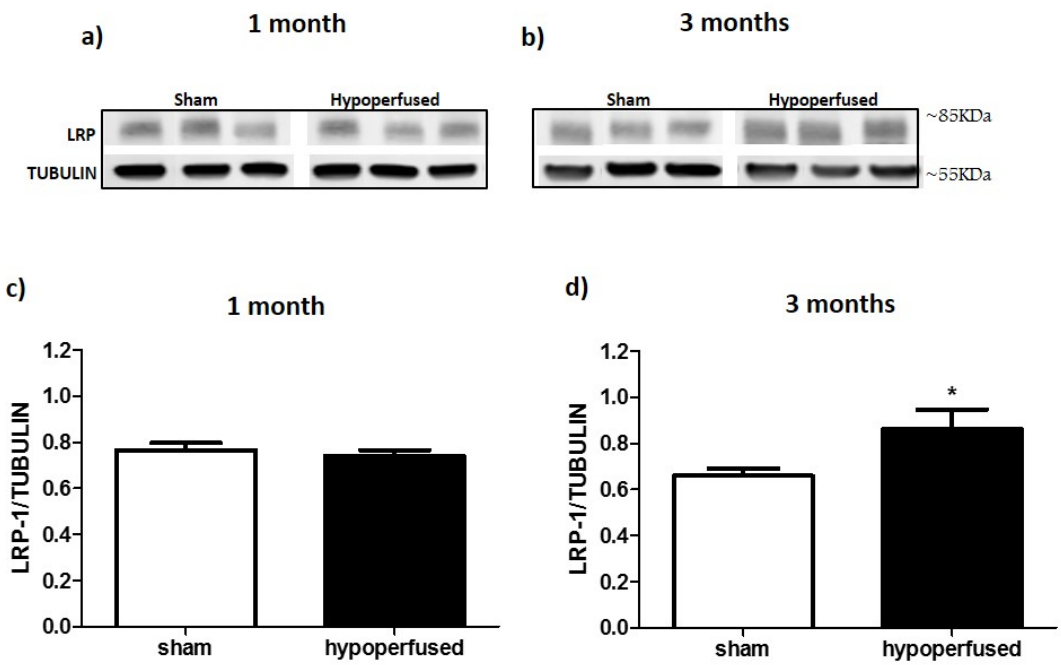

Figure A3. Cerebral hypoperfusion increases vascular LRP-1 levels in wild-type animals. Western blot analysis of proteins extracts from vessels enriched fractions after 1 (a, c) or 3 (b, d) months of hypoperfusion was performed to determine the expression levels of LRP in wild-type mice; specific bands were quantified by densitometric analysis and expressed relative to total tubulin protein, represented in the graphs. The data presented are the means ± S.E.M., $p < 0.05$.

Appendix 4. Association analyses between MI load and amyloid levels.

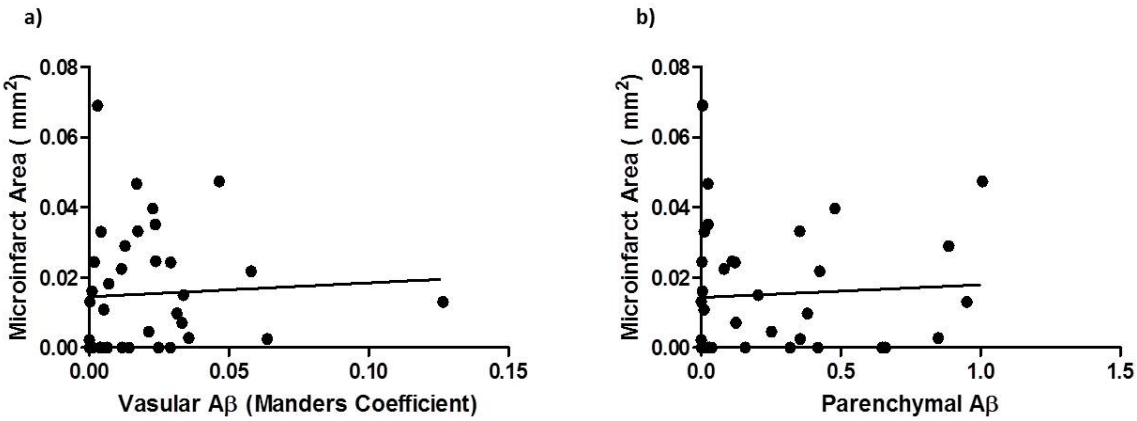

Figure A4. MI load does not correlate either with vascular or with parenchymal Aβ. Scatter plot show no correlation between MI area and vascular (r = 0.05611, p = 0.7415) (a) or parenchymal (r = 0.06368, p = 0.7122) (b) amyloid.